

The Rational Design of Dermatological Formulations

By

Rebecca Mary Watkinson

A thesis submitted in partial fulfilment of the requirements of
the University of Greenwich for the Degree of Doctor of
Philosophy



June 2005

ACKNOWLEDGEMENTS

Firstly I would like to acknowledge the financial support given to me by Leo Pharma (Denmark) and for kindly allowing me to spend time working in their organisation.

I would like to thank my supervisor Jon Hadgraft for his unending patience, support and encouragement throughout my PhD. I would also like to thank John Mitchell and Tony Beezer for their words of wisdom and guidance over the past five years. Also, a big thanks to all the members of Medway Sciences, past and present for their valuable suggestions when it all seemed too much.

Thanks to Lakshmi Raghavan for teaching me the ways of an ageing HPLC.

Finally, I reserve the biggest thanks for Moomin and Adam, for their constant love, understanding and support. The cups of tea and glasses of wine always made things better...

ABSTRACT

In order to understand the role of the formulation components in topical drug delivery it is necessary to separate the various contributing factors, these include thermodynamic activity effects, changes in the ionisation state of the permeant and alteration of the membrane properties. Three model permeants, ibuprofen, salicylic acid and acetaminophen were selected to represent a range of physicochemical properties. Solubility and distribution behaviour of ibuprofen and salicylic acid was determined and demonstrated how the addition of cosolvent could impact upon the permeation of the two weak acids by altering the ionisation state of the permeants. The cosolvents, (typical formulation excipients) were water, propylene glycol ethanol, mineral oil, miglyol and Transcutol™. To begin with binary combinations were tested, moving on to ternary combinations more representative of an actual formulation.

Silicone membranes were used to investigate the diffusional properties of the model permeants. Similarities in the behaviour of the permeants in the selected solvents were observed. Ibuprofen was found to have a higher permeation rate than salicylic acid possibly because of the hydrophobic nature of the silicone membrane. Analysis of diffusion profiles using a non-linear curve fitting procedure revealed that the selected vehicles enhanced the permeation of ibuprofen and salicylic acid by increasing partitioning into the membrane. Acetaminophen was found to oxidise in the presence of hydrogen bonding solvents, and for this reason was eliminated from the study.

Diffusion experiments were conducted using an established ATR-FTIR approach but the data interpreted using sophisticated chemometric

approaches which allowed the deconvolution of the IR signals of all permeating species and the membrane. Using this approach it was possible to examine the individual profiles from multi-component formulations. Using data from traditional diffusion experiments alongside information obtained from ATR-FTIR diffusion experiments using a new method of analysis allowed a deeper insight into the role of the solvent in the permeation process. Data from ATR-FTIR experiments revealed that ethanol permeated silicone membrane at a faster rate than the other solvents studied. This finding was in line with evidence from Franz-type diffusion experiments in which flux was consistently higher from formulations containing ethanol. Where possible, the effect of the same vehicles on the permeability properties of human skin was examined. The vehicles selected were predominantly influencing the partition of the drug into the skin rather than the diffusion coefficient.

CONTENTS

Declaration	ii
Acknowledgements	iii
Abstract	iv
Contents	iv
Abbreviations	vi
Dedication	xii

Chapter One

Introduction

1.1. Introduction	2
1.2. Background	4
1.3. Skin structure and function	5
1.4. Routes of penetration	11
1.5. The mathematics of the diffusion process	15
1.6. Techniques used to study skin permeation	19
1.6.1. In vitro techniques	19
1.6.1.1. Diffusion experiments using Franz-type cells	19
1.6.1.2. Diffusion experiments using ATR-FTIR spectroscopy	25
1.6.1.3. Tape stripping	28
1.6.2. In vivo techniques	29
1.6.2.1. Measurement of drug levels	29
1.6.2.2. Measurement of residual material	30
1.6.2.3. Measurement of physiological effects	31
1.6.3. Models	32
1.6.3.1. Animal models	32
1.6.3.2. Model membranes	32
1.7. Topical drug delivery and bioavailability	36
1.8. Methods for assessing bioavailability of topical products	39
1.9. Role of vehicle in skin permeation	41
1.10. Conclusions	46
1.11. Research objectives	47
1.12. References	48

Chapter Two

Non-Steroidal Anti-inflammatory Drugs

2.1. Non-steroidal ant-inflammatory drugs: an overview	60
2.2. Mode of action	63
2.2.1. Physiological effects of NSAIDs	63
2.3. Model permeants	69
2.3.1. Acetaminophen	69
2.3.2. Ibuprofen	70
2.3.3. Salicylic acid	72
2.4. Model formulations	74
2.4.1. Formulation of dermatological vehicles	74
2.4.2. Model formulations	79
2.4.3. Background information about model vehicles	80
2.5. Physicochemical characterisation of model permeants	82
2.5.1. Theoretical background: pH, pK_a and Sirius GlpK_a	82
2.6. Methods	89
2.6.1. Solubility study	89
2.6.1.1. Saturated solubility in pH controlled conditions	89
2.6.1.2. Buffer solutions for pH controlled experiments	90
2.6.2. Sirius GlpK_a	90
2.7. Results	94
2.7.1. Solubility study	94
2.7.2. pK_a determination	104
2.7.3. Partitioning experiments	114
2.8. Prediction of physicochemical properties	118
2.9. Summary	121
2.10. References	122

Chapter Three

Materials and Methods

3.1. Introduction	126
3.2. Materials used	127
3.2.1. Chemicals used	127
3.2.2 Apparatus	128
3.3. Methods	130
3.3.1. Diffusion cell studies	130
3.3.2. Preparation of isolated human epidermis	131
3.3.3. ATR-FTIR studies	132
3.4. Analysis	136
3.4.1. UV Spectroscopy	136
3.4.2. Preparation of calibration standards	138
3.4.3. High performance liquid chromatography (HPLC)	144
3.5. Solvent uptake studies	148
3.6. References	150

Chapter Four

Diffusion Studies Through Silicone Membrane

4.1. Introduction	152
4.2. Mathematical analysis using Fick's second law of diffusion	153
4.3. Methods	159
4.4. Experimental	160
4.5. Results and discussion	162
4.5.1. Single-phase studies	162
4.5.1.1. Ibuprofen	162
4.5.1.2. Salicylic acid	166
4.5.1.3. Acetaminophen	168
4.5.1.4. Summary	169
4.5.2. Binary solvent vehicles	170
4.5.2.1. Ibuprofen	170
4.5.2.2. Salicylic acid	195
4.5.2.3. Acetaminophen	206
4.5.2.4. Summary	208
4.5.3. Ternary solvent vehicles	211
4.6. Conclusions	233
4.7. References	234

Chapter Five

Diffusion Studies Through Silicone Membrane: ATR-FTIR Spectroscopy

5.1. Introduction	236
5.2. Methods	237
5.3. Experimental	237
5.4. Results	238
5.4.1. Infrared spectra of model permeants	238
5.4.2. Infrared spectra of solvents	242
5.4.3. Results of ATR-FTIR diffusion experiments	243
5.4.3.1. Salicylic acid	243
5.4.3.2. Ibuprofen	248
5.4.3.3. Ibuprofen in ternary solvent formulations	257
5.5. Conclusions	278
5.6. References	279

Chapter Six

Diffusion Studies Through Human Skin

6.1. Introduction	281
6.2. Methods	282
6.3. Experimental	282
6.4. Results	283
6.4.1. Mineral oil and miglyol formulations	283
6.4.2. Propylene glycol and water formulations	288
6.4.3. Ethanol and water formulations	292
6.4.4. Ternary solvent formulations	296
6.5. Conclusions	301
6.6. References	303

Chapter Seven
General Discussion

7.1. Overall discussion	305
7.2. Future Work	310
Appendix I	312
Appendix II	313
Appendix III	315

ABBREVIATIONS

α and β	K_h and D/h^2 respectively
AM	Acetaminophen
ATR-FTIR	Attenuated Total Reflectance Fourier Transform Infrared
B_e	Base equivalents
CV	Coefficient of Variation
C_v	Drug concentration in the vehicle
COX	Cyclooxygenase (exists in two forms COX-1 and COX-2)
D	Diffusion coefficient
DMSO	Dimethylsulphoxide
DS	Degree of saturation
EtOH	Ethanol
GI	Gastro-intestinal
h	diffusional pathlength
HPLC	High Performance Liquid Chromatography
IBU	Ibuprofen
IL-1	Interleukin
J	Flux ($\mu\text{g}/\text{cm}^2/\text{hr}$)
KCl	Potassium chloride
K_{ow}	Octanol/Water partition coefficient
k_p	Permeability coefficient
L	Lag time
LC-MS	Liquid Chromatography - Mass Spectrometry
LogD	Distribution coefficient at a particular pH
LogP	Octanol/water partition coefficient
MeOH	Methanol
MG	Miglyol
MO	Mineral Oil

MW	Molecular weight
NMR	Nuclear Magnetic Resonance
NSAID	Non-Steroidal Anti-Inflammatory Drug
ODS	Octadecylsiloxane
PBS	Phosphate Buffered Saline
PCA	Principal Component Analysis
PDMS	Polydimethylsiloxane
PG	Propylene Glycol
PGDP	Propylene Glycol Dipelargonate
pK_a	Aqueous ionisation constant
pK_w	Ionisation constant of water
p_sK_a	Apparent ionisation constant (in presence of solvent)
p_oK_a	Apparent ionisation constant derived from octanol segment of a difference plot
PGE	E-type Prostaglandin
SA	Salicylic Acid
SC	Stratum Corneum
SD	Standard Deviation
t	Time
TC	Transcutol™
THF	Tetrahydrofuran
TFA	Target Factor Analysis
UV	Ultraviolet

To my family

- Chapter One -

Introduction

1.1. Introduction

It is estimated that up to 15% of a GP's caseload is for dermatological diseases. These disorders have a considerable impact upon people's lives. Those who suffer from chronic diseases such as eczema, psoriasis and acne will be all too aware of how crippling these complaints can be. The physical effects include the discomfort caused by the disease, or the limitations it places upon the sufferer. In extreme cases simple tasks like bathing, household chores or writing can become difficult. But perhaps as damaging is the emotional aspect of having a skin disorder, and skin diseases can have a damaging effect upon the sufferer's social interactions. The sufferer may feel embarrassed by their disease, particularly if it is manifested in a visible part of the body such as the face, or hands. They may also feel isolated by their disease or depressed and it is often found that sufferers of skin disorders exhibit depression scores higher than that of the general population. Because it is on display the skin is an organ by which we are all judged, whether we are aware of it or not. In a revealing and rather poignant study Finlay (1996) investigated the quality of life of patients and found that those with skin disorders would rather suffer from a potentially life threatening disease such as hypertension, diabetes or bronchitis.

Current topical therapy for skin diseases is poor because of the low bioavailability of topically applied drugs. Treatment and quality of life would be far better if bioavailability could be improved, but the skin is a formidable barrier to the passage of substances and unwilling to share its secrets. Despite this, interest in the permeability of the skin has been sustained throughout the last century. A reason for this is that the skin does permit absorption of a wide variety of chemicals, though the degree

of absorption is dependent on the molecule, with several orders of magnitude difference in permeability coefficients observed for chemicals at either end of the spectrum (Barry, 1983; Scheuplein and Bronaugh, 1983).

During the last century, considerable progress was made towards elucidating mechanisms by which this selective permeability is achieved. A major breakthrough was the confirmation of the role of the stratum corneum in forming the major barrier to absorption (Monash, 1957; Scheuplein and Blank, 1971). Further to this was the understanding of the importance of physicochemical attributes in governing absorption across epithelial membranes such as the skin (Rothman, 1955; Higuchi, 1960; Katz and Shaikh, 1965).

From the initial discovery of the selective permeability of the skin, the absorption of a variety of chemicals has been investigated. It is this accumulated data, along with increasingly advanced biophysical techniques, that have contributed to our current understanding of the mechanisms of skin permeation. This chapter provides a review of the basic principles governing the process of percutaneous absorption, and outlines the objectives of the research discussed in succeeding chapters.

1.2. Background

With a surface area of around 2m² in the average adult, and accounting for approximately 10% of the body mass (Bowman and Rand, 1978), the skin is the largest, and one of the most versatile organs in the body. It was widely believed that intact skin was completely impermeable to all substances. However, during the last century, many studies have demonstrated that the skin is not a perfect barrier and it will allow the passage of some chemicals, though in small quantities.

While entry of foreign chemicals is usually restricted, water and essential chemicals are retained within the body. As the skin forms a major point of contact of the body with the environment, the potential for exposure to chemicals (e.g. therapeutic substances, household chemicals, cosmetics) via this route is great. In most cases however, only a small proportion of the total surface area will be exposed.

The term **percutaneous absorption** covers the entire process by which a chemical applied to the outer surface of the skin is taken up into the systemic circulation. This requires **penetration** into the layers of the skin with subsequent **permeation** across each layer, and finally uptake into the capillary blood vessels in the upper region of the dermis.

To determine the physical and chemical factors which assist or hinder the process, it is necessary to consider both the structure of the membrane and the interactions of the three components – membrane, penetrant and vehicle.

1.3. Skin structure and function

The skin is a multi-layered membrane, which can be divided into two main regions; the epidermis and the dermis. The former is a dynamic tissue in which new cells are continually being formed to replace those lost at the surface. The thickness of this layer varies, and may be an order of magnitude larger in areas such as the palm of the hand and the soles of the feet, areas of the body associated with the physical environment (Walters and Roberts, 2002). Within the epidermis, four separate layers of cells may be identified:

1. Basal layer (Stratum Germinativum)
2. Prickle cell layer (Stratum Spinosum)
3. Granular layer (Stratum Granulosum)
4. Horny layer (Stratum Cornuem)

The first three layers are termed collectively the viable epidermis. In the plantar surfaces of the palms and the soles of the feet, a further layer known as the stratum lucidum has been described.

Continual replacement of epidermal cells is brought about by mitosis of the basal layer epithelium. As a cell proceeds from the basal layer to the stratum corneum it undergoes a series of morphological and biochemical changes, which convert the columnar epithelial cells of the basal cell into the flattened, dead, keratin-packed cells of the highly organised stratum corneum. In normal, healthy skin the average turnover time (i.e. the time taken from formation of the cell in the basal layer to shedding at the skin surface) is approximately 28 days. In psoriasis, a skin disease characterised by hyper-keratinisation, epidermal proliferation is much

more rapid. This may be shortened to only four days, causing 'scales' at the skin surface which are itchy and irritating to the sufferer.

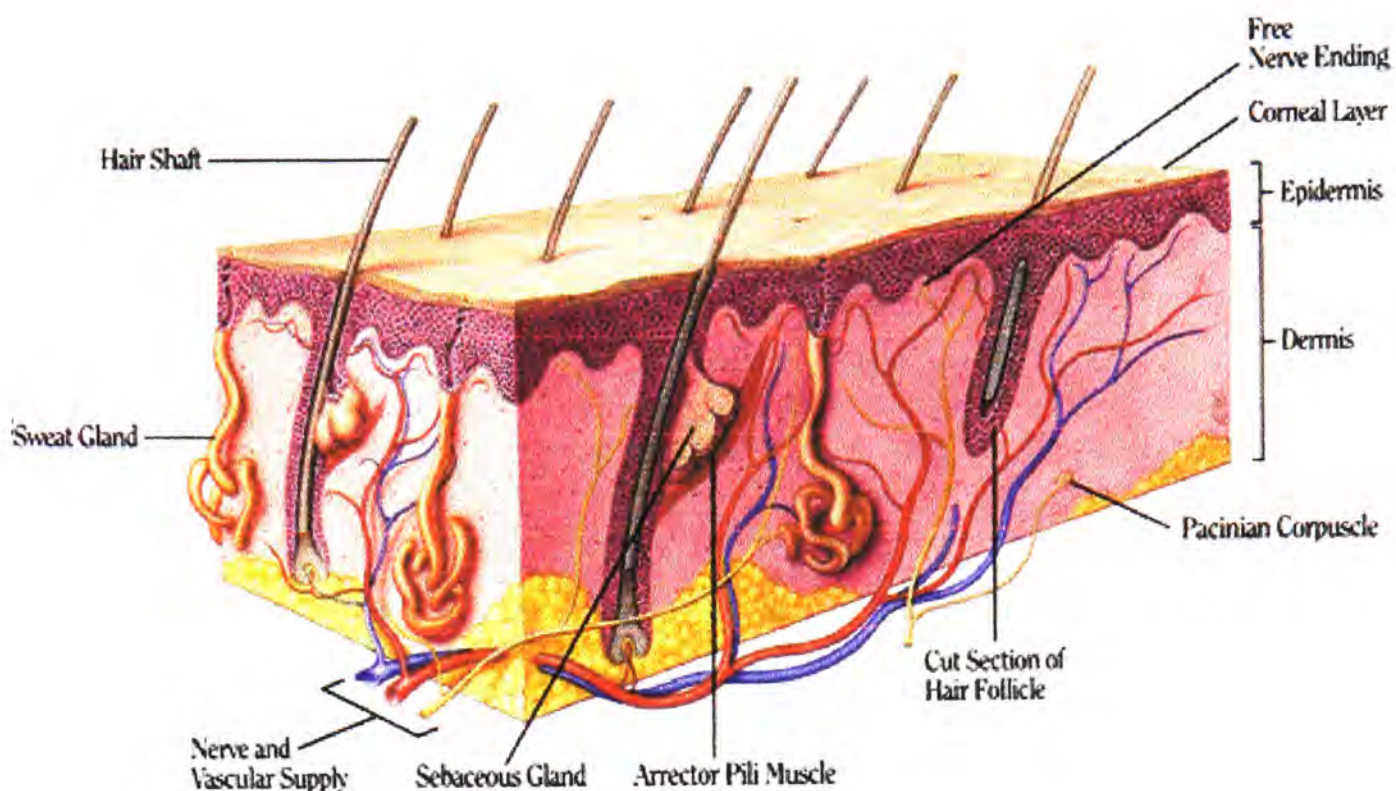


Figure 1.1. Diagrammatic representation of the skin (Adapted from and image on the website: <http://www.AOCD.org/skin/>)

The stratum corneum forms the major barrier to absorption of chemicals in intact skin. This layer is ca 10 μ m thick when dry but can swell to several times this on prolonged contact with water. It is composed of 10-15 layers of dead, keratinised cells embedded in a lipid-protein matrix. The lipids in the intercellular spaces are extruded from the epithelial cells at the base of the epidermis, and from into bilayers, which are tightly packed between the cells, as the layers progress towards the outer surface (Fartasch et al. 1993; Winkleman, 1969).

The cells are arranged with long axes lying parallel to the skin surface in cohesive layers, which may be removed by stripping with adhesive tape (Feldman and Maibach, 1965; Dupuis et al. 1986, Rougier et al. 1983). This arrangement of the corneocytes within the lipid-protein matrix has

been likened to a brick wall (Michaels et al. 1975; Elias, 1983), with the corneocytes being the bricks and the lipid-protein matrix the mortar. It is this 'bricks and mortar' structure of the stratum corneum that is responsible for the pronounced barrier properties of intact skin.

Epidermal appendages – hair follicles and their associated sebaceous glands; apocrine and eccrine sweat glands – penetrate the stratum corneum at intervals. The distribution of these structures varies depending upon anatomical location. The appendages are derived embryonically from the ectoderm along with the epidermis (Bucks, 1984), but are located mainly in the dermis, thus providing a possible route for absorption, bypassing the stratum corneum (see section 'routes of absorption').

Hair follicles

Hairs are keratin structures produced by hair follicles, which are themselves formed by the downward growth of epidermal cells into the dermis. Hair follicles develop everywhere within the skin, except the red part of the lips, the palms, soles of the feet and external genitalia. Each follicle is anchored to the surrounding connective tissue by an individual strand of smooth muscle and the arrector pilorum and has one or more sebaceous glands that are open into the follicle.

Sebaceous glands

The sebaceous glands are responsible for the secretion of sebum, of which the components are; glycerides, free fatty acids, cholesterol, cholesterol esters, wax esters and squalene. The ducts of these glands open into the hair follicles where the oily sebum keeps the hair soft and pliable. Sebum also provides some waterproofing of the skin and prevents drying on exposure to heat.

Sweat glands

The two types of sweat glands in the skin, as mentioned previously, are the eccrine and apocrine glands. The eccrine glands are found all over the body, their most important function being the regulation of body temperature by secretion of dilute saline solution with a pH of about 5. This secretion accounts for 80% of water loss via the skin. The eccrine gland itself is an epidermal structure arising from the lower dermis with a coiled ball of about 100µm in diameter that emerges at the surface. Even though the total number of eccrine glands is 2-5 million, they represent less than 0.001% of the total surface area. The apocrine glands are found predominantly on the palms, soles of the feet, axillae and genital areas and produce a milky fluid rich in lipids, proteins and saccharides in response to emotion and stress.

Other types of cell found in the epidermis are melanocytes, which produce the pigment melanin, and Langerhans cells which are thought to be involved in the organisation of the epidermis and, possibly, the immune response within the membrane. Metabolism of chemicals may occur within this layer, which possesses drug-metabolising enzymes involved in both the primary oxidation and/or reduction reactions, in complex conjugation reactions (Pannatier et al. 1978; Tauber and Rost, 1987). Assessment of absorption may, therefore, require consideration of the likely production of metabolites during the passage through the skin (Bronaugh et al. 1989).

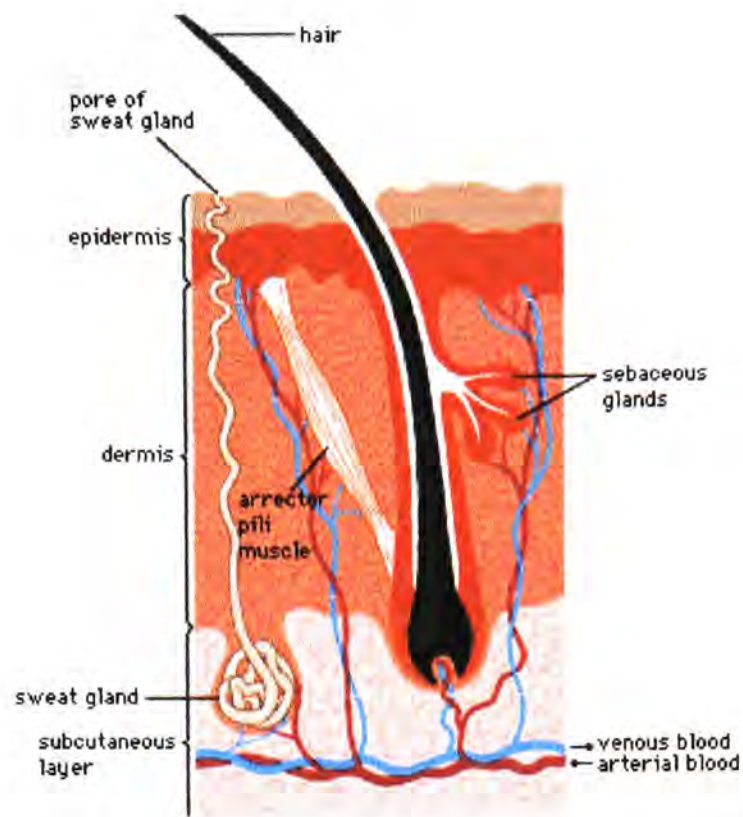


Figure 1.2. Cross sectional view of a hair follicle and related appendages
 (Adapted from and image on the website: <http://www.AOCD.org/skin/>)

Where the epidermis and dermis meet there is a specialised region known as the dermo-epidermal junction. This is composed of the basal cell plasma membranes, the lamina lucida, the basal lamina and fibrous material. Sections of the dermis project upwards into the epidermis into the epidermis forming a ridged boundary layer rather than a flat structure running parallel to the skin surface. These ridges produce the unique 'fingerprint' patterns of humans. The functions of the dermo-epidermal junction are those of mechanical support for the epidermis, adherence of the two major layers of the skin and the control of movement of cells and very large molecules (Barry, 1983). For other, small molecules this region does not form an additional barrier to penetration.

Below the dermo-epidermal junction lies the vascular, aqueous dermis. In contrast to the relatively thin epidermis, this layer is 3-5mm thick and is a matrix of connective tissue embedded in a ground substance. The connective tissue is composed of fibrous proteins – collagen and elastin;

while the ground substance is formed from mucopolysaccharides, including hyalauronic acid and dermatan sulphate, lipids and proteins (Barry, 1983; Bucks, 1984). Cell components – fibroblasts and mast cells are also found in this layer.

There is a rich network of blood vessels, lymphatic channels and nerve terminals within the dermis. The blood supply to this tissue delivers all nutrients to, and removes waste products from the entire skin membrane, as the epidermis is devoid of blood vessels. Fine capillaries penetrate into the ridges of the dermo-epidermal junction to supply the epidermis by diffusion of nutrients outwards. Waste material diffuses inwards and is removed by the same vessels. Chemicals that penetrate the barrier layer are taken up into the systemic circulation at this level; therefore the thickness of the dermis does not generally influence the absorption process *in vivo*.

1.4. Routes of penetration

As previously stated, the major barrier to percutaneous absorption resides in the outer horny layer, which must be crossed for absorption to proceed.

There are two main routes of permeation through this layer:

1. Transappendageal
2. Transepidermal

Transappendageal

The first involves transport via skin appendages – hair follicles, sebaceous glands or sweat glands – with absorption through the squamous epithelial cells lining these structures into the deeper layers of the skin. At the base of both the hair follicles and the sweat glands there is a dense network of capillary blood vessels, thus any substance permeating by these routes will be rapidly removed into the systemic circulation. While this route would appear to provide an easy passage for topically applied chemicals into the circulation, the surface area covered by skin appendages is small compared with the area available for transepidermal absorption. This route has generally been considered of limited importance, except in the very early stages of penetration, before steady state absorption through the membranous stratum corneum is achieved, and for chemicals which have a very slow rate of diffusion through the membrane, where 'shunt' diffusion dominates for a longer period. (Scheuplein et al. 1969; Heuber et al. 1992).

Transepidermal

There are two possibilities for transepidermal permeation. The intercellular route is via the lipid matrix surrounding the cells. Alternatively, the

penetrant may use the transcellular route, through the corneocytes. Within the lamellar matrix, the lipids are arranged in tightly packed lipid lamellae, which originate in the lamellar bodies secreted by cells in the granular layer (Abraham and Downing 1991; Fartasch et al. 1993). The extracellular lipids are composed mainly of ceramides, cholesterol, free fatty acids and cholesterol sulphate. Abraham and Downing demonstrated that the acyl- and acylglucosyl- ceramides produced fusion of adjacent lipids bilayers in vitro. They suggested that these long molecules might have a role in maintaining the cohesion of the multiple lipid lamellae by spanning adjacent layers. Additionally, interactions between the extracellular lipids and the corneocyte membrane were demonstrated, which would serve to enhance further the cohesion within the stratum corneum.

The highly ordered nature of the intercellular lipid is generally considered to be responsible for the barrier function of the stratum corneum. The arrangement of adjacent cells and lipid lamellae produces a tortuous route as a means of passage through the membrane. Thus, the pathlength for absorption is very long, compared with the lateral thickness of the membrane, contributing to the slow permeation observed for most molecules.

In transcellular absorption, the chemical takes a more direct route through the membrane; passing through the intercellular lipid, and the more hydrophilic interiors of the corneocytes. The latter are densely packed with keratin, which possesses a large proportion of amino acids with polar functional groups (-COOH or -NH₂). These polar groups interact with water molecules and are responsible for the uptake of water by the stratum corneum upon hydration (Flynn, 1985).

Experimental evidence indicates that the lipids of the stratum corneum provide the main barrier to absorption. Removal of the lipids using chemicals severely reduces the barrier's efficiency, while keratolytic agents cause relatively little increase in permeability (Matoltsy et al. 1968; Elias et al. 1981; Menczel, 1985). This serves to emphasise the importance of the intercellular route in absorption even though this occupies only 5-30% of the volume of the stratum corneum (Matoltsy et al. 1968; Michaels et al. 1975; Dugard and Scott, 1984; Menczel, 1985). Further support for the intercellular route comes from analysis of published data that suggested that for a wide range of chemicals, it was the properties of the stratum corneum lipids which could explain the observed permeability (Potts and Guy, 1992).

Perhaps the most convincing evidence for intercellular transport is that concerning the length of this route compared with that which would be observed for transcellular transport. As mentioned before, the stratum corneum is approximately 10-20 μm thick, therefore one would naturally assume a pathlength equal to that. However, research in vivo, on the skin absorption of methyl nicotinate was analysed using solutions to Fick's laws of diffusion and the best fit to the data was found for a diffusional pathlength of 350 μm (Albery and Hadgraft, 1979). This is 20 times the actual thickness of the stratum corneum and suggests the intercellular route is important. Further to this is the finding of Potts and Francoeur (1991). Their work on the diffusion of water suggested that even a small polar molecule transferred along a tortuous pathway. In this case the pathlength for the diffusion of water was quoted as 500 μm .

Once across the stratum corneum, the chemical must penetrate into the viable epidermis. This, like the initial step of penetration into the stratum

corneum, is a partitioning process. Diffusion through the viable epidermis is more rapid than that through the stratum corneum because of the absence of the tightly packed lipid/protein layers. Chemicals diffusing through this tissue are transported via the intercellular fluid. Upon reaching the dermo-epidermal junction, the chemical must then partition into the dermis. Once in this layer, it is rapidly taken up into capillaries located close to the junction, and hence into the systemic circulation. The capillary network acts as a sink for penetrating chemicals by carrying them away from the site of absorption. This, in turn, promotes further absorption by maintaining a concentration gradient across the membrane. As the dermis is a very aqueous, hydrophilic medium, it may provide an additional barrier to the passage of very lipophilic compounds, which will not partition readily from the stratum corneum. Diffusion coefficients in the dermis are considerably greater than those in the stratum corneum (Blank and Scheuplin, 1969), and are indicative of movement through large, aqueous pores (Treherne, 1956).

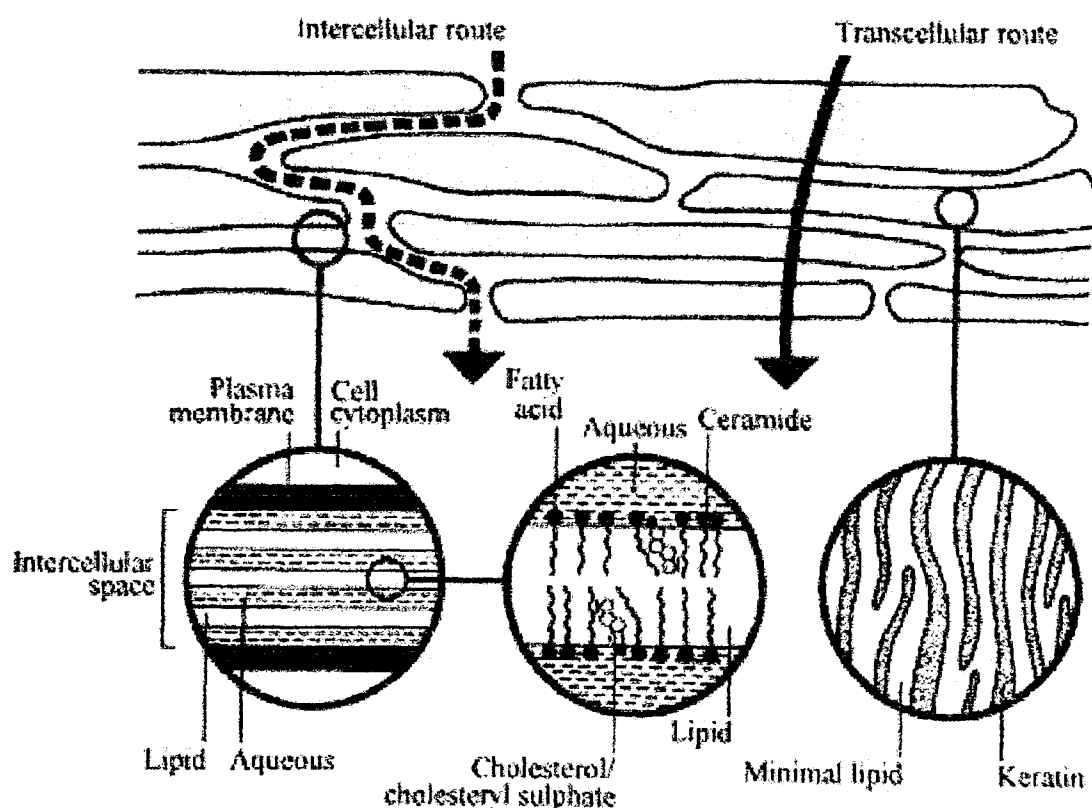


Figure 1.4. Schematic illustration of the two principal routes of permeation.

Taken from Elias (1992).

1.5. The Mathematics of the Diffusion Process

Absorption through the skin is a passive process driven by the concentration gradient from the application site on the external surface into the capillary network 'sink'. Below is a brief introduction to the mathematical principles of this process.

In passive diffusion, matter moves from one region of a system to another following random molecular motions. The basic hypothesis underlying the mathematical theory for isotropic materials is that the rate of transfer of a diffusing substance per unit area is proportional to the concentration gradient. This is known as Fick's first law of diffusion;

$$J = -D(\partial C/\partial x) \quad (\text{Eqn. 1.1})$$

Where J is the rate of transfer per unit area of surface (the flux), C is the concentration of the diffusing substance, x is the space co-ordinate measured normal to the section and D is the diffusion coefficient. The negative sign indicates the flux is in the direction of decreasing concentration. Fick's first law contains three variables J, C and x. J contains two variables, dm/dt, where m is amount and t, is time. Fick's second law of diffusion reduces the number of variables and, assuming diffusion is unidirectional is,

$$\partial C/\partial t = D(\partial^2 C/\partial x^2) \quad (\text{Eqn. 1.2})$$

If the cumulative mass of diffusant, m, which passes per unit area is measured through a membrane as a function of time a typical plot (as shown on the next page) is obtained.

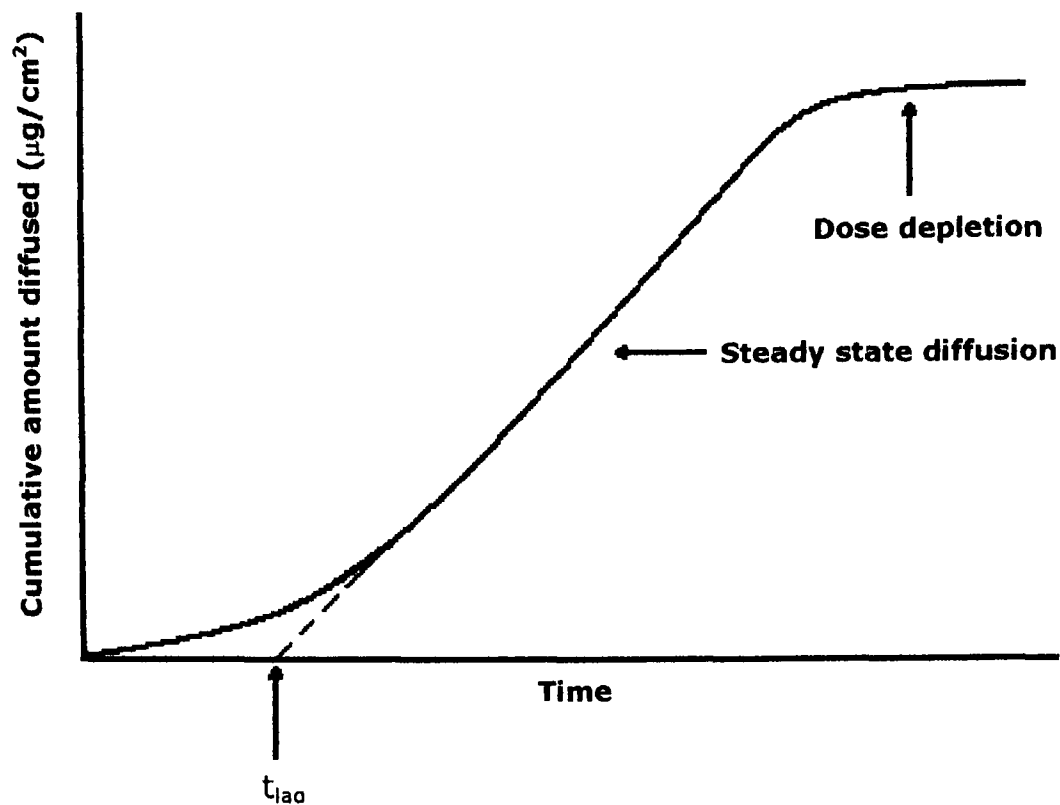


Figure 1.5. Drug-penetration time profile for an idealised drug diffusing through a membrane

After sufficient time, steady state flux exists across the membrane, which may be denoted dm/dt . The equation above can then be simplified to,

$$dm/dt = DC_0/h \quad (\text{Eqn. 1.3})$$

Where C_0 is the concentration of diffusant in the first layer of the membrane at the surface contacting the donor solution and h is the membrane thickness. However, C_0 is difficult to measure but C'_0 , the concentration of diffusant in the donor solution bathing the membrane is related to C_0 by,

$$C_0 = KC'_0 \quad (\text{Eqn. 1.4})$$

Where K is the partition coefficient of the diffusant between the membrane and the donor solution. Equation 4 can be substituted into equation 3 giving,

$$dm/dt = DC'_0K/h \quad (\text{Eqn. 1.5})$$

If a steady state plot like that shown previously is extrapolated to the time axis, the intercept obtained at $m=0$ is the lag time (L). The lag time is related to the diffusion coefficient by,

$$L = h^2/6D \quad \text{(Eqn. 1.6)}$$

Theoretically D can be estimated provided the membrane thickness, h, is known. However there are inherent problems with this estimation. Lag time values for example, obtained from permeation experiments using the extrapolation method tend to be very variable (especially through human skin because of its biological variability, i.e. stratum corneum thickness). It should be noted however that the skin appendages account for less than 0.1% of the total surface area and their contribution to permeation is negligible. When using stratum corneum in such studies the exact thickness is extremely difficult to measure. The measured thickness of the membrane does not allow for a tortuous pathway for diffusion and therefore the value obtained for D is more often than not, an apparent one.

The relationships described in both equations 1 and 2 point to the importance of penetrant concentration in determining absorption. Flux is proportional to the concentration gradient in existence across the membrane. To achieve and maintain flux, a high concentration must exist in the upper layers of the stratum corneum, and a low concentration at the site of removal into the systemic circulation or receptor medium, thus maintaining the driving force for inward movement. High concentrations of penetrant in the outer layers of the stratum corneum will be achieved if the affinity of the penetrant for the membrane is greater than that for the vehicle. As the membrane is lipophilic, this implies a requirement for lipid solubility in the penetrant. Conversely, to ensure that the diffusing

substance partitions into the viable epidermis and dermis, and from there is removed in the circulation, a reasonable degree of water solubility will be required as these tissues are more aqueous in nature. These two requirements are contradictory (except for certain molecules which are amphiphilic in nature) and hence for absorption (i.e. uptake into the circulation) to occur readily, some degree of both lipid and aqueous solubility is required. This balance has been recognised as a pre-requisite for absorption (Rothman, 1955).

1.6. Techniques used to study skin permeation

1.6.1. In Vitro techniques

In vitro techniques are often employed for the study of permeation because of the cost and ethical issues surrounding in vivo experimentation. Ethical approval for experiments is vital, yet difficult and time consuming to obtain. The only approval needed for in vitro studies is for the use of human or animal skin, which is considerably easier to achieve. Another major advantage of in vitro studies is the possibility for controlling the conditions of the experiment, in many cases the only variability arising from the skin used. In vitro studies are cost effective and relatively easy to perform, and can be conducted using model membranes, as well as animal or human skin.

1.6.1.1. Diffusion experiments using Franz-type cells

Performing diffusion experiments using purpose built diffusion cells is by far the most common method used to evaluate permeation. The permeant is applied to the donor compartment of the cell and its diffusion through the membrane is evaluated by measuring the amount of drug in the receptor compartment at pre-determined time points. When designing a diffusion experiment it is important to remember the purpose of the generated data. The most common mathematical model used, Fick's first law of diffusion makes the following assumptions:

1. The receptor phase is a perfect sink
2. Depletion of the donor phase is negligible
3. The membrane is homogenous

Of course, in practice not all of these assumptions is true, in which case a more appropriate mathematical model should be sought (see section 4.2).

However, with careful experimental design diffusion cells provide valuable information concerning the permeation behaviour of drugs.

The diffusion cell

A well-designed diffusion cell should be inert, robust and easy to handle (Brain et al. 2002). Glass is the most common construction material used, although Teflon and stainless steel (Walters et al. 1981) have also been used. The membrane is mounted as a barrier between the donor and receptor chamber, and the amount of compound permeating from the donor to the receptor side is determined as a function of time. Efficient mixing of the receptor phase is essential, and sample removal should be straightforward. Neither of these should interfere with diffusion of the permeant. Continuous agitation of the receptor medium, sampling from the bulk liquid rather than the side arm, and accurate replenishment of the receptor fluid to ensure sink conditions are all important practical considerations. It is also essential that air bubbles are not introduced below the membrane during sampling, indeed at any time during the course of the experiment. Static cells are usually upright "Franz" or side-by-side type, with receptor volumes that can range from 2-10mL and surface areas of exposed membranes of 0.2-2cm². Cell dimensions should be accurately measured, and precise values should be used in subsequent calculations, with particular attention to analyte dilution resulting from sampling and replenishment.

The main difference in the application of the two static cell types is that side-by-side cells can be used for the measurement of permeation from one stirred solution, through a membrane, and into another stirred solution. This is of particular use when examining flux from saturated solutions in the presence of excess solid if accumulation of solid on the

membrane surface must be prevented. Side-by-side cells also offer the advantage of isothermal conditions. Upright cells are particularly useful for studying absorption from semi-solid formulations spread on the membrane surface and are optimal for simulating in vivo performance. The donor compartment can be capped to provide occlusive conditions or left open, according to the objective of the study. Flow through cells can be useful when the permeant has a very low solubility in the receptor medium, and designs are continuously changing and improving. Sink conditions are maximised as the fluid is continuously replaced using a suitable pump (typically set at a rate of 1.5mL/h). However, the dilution produced by the continuous flow can raise problems with analytical sensitivity, particularly if permeation is low. Flow through and static systems have produced equivalent results (Clowes, 1994). Automated flow-through systems can allow unattended sampling and commercial systems are available.

Standard upright static diffusion cells, which offer a simple, low-cost and versatile system, can be employed on a large scale and adapted to meet the requirements of a large range of studies. In summary a well-designed diffusion cell should meet the following criteria:

- Be inert
- Be robust and easy to handle
- Allow the use of membranes of varying thickness
- Provide thorough mixing of the receptor chamber contents
- Ensure intimate contact between membrane and receptor phase
- Be maintainable at constant temperature
- Have precisely calibrated volumes and diffusional areas
- Maintain membrane integrity
- Provide easy sampling and replenishment of receptor phase
- Be available at reasonable cost

Receptor chamber and receptor medium

Receptor chamber dimensions are constrained by the conflicting requirements of guaranteeing that the receptor phase can act as a sink, while ensuring that sample dilution does not preclude analysis. A large receptor volume may ensure sink conditions, but will reduce analytical sensitivity unless large samples can be taken and subsequently concentrated. Concentration of permeant in an aqueous receptor phase may be possible by lyophilisation, or by techniques such as solid phase extraction. The ideal receptor phase provides an accurate simulation of the conditions found *in vivo* for the permeation of the test compound. To ensure sink conditions the concentration of the permeant in the receptor fluid should not be allowed to exceed approximately 10% of saturation solubility (Skelly et al. 1987). Excessive receptor phase concentration can lead to a decrease in the rate of absorption, which may result in an underestimate of the bioavailability. The most commonly used receptor fluid is pH 7.4 phosphate buffered saline (PBS), although this is not always the most appropriate material. If a compound has a water solubility of less than about 10 μ g/mL, then a wholly aqueous receptor is unsuitable, and the addition of solubilizers becomes necessary (Bronaugh, 1985).

Receptor fluids can range from pure water through to isotonic phosphate buffers containing albumin and preservatives. Albumin increases the solubility of the permeant (Dick et al. 1996), while preservatives inhibit microbial growth in the receptor fluid. Microbial growth can cause problems because the permeant may partition into, or be metabolised by the bacteria. An alternative to the use of preservatives is to use a 25% (v/v) aqueous ethanol solution. This provides a sink for most permeants by improving their solubility, whilst also having sufficient anti-microbial character to remove the need for other antimicrobial constituents.

It is also important to consider the pH of an aqueous buffered receptor solution as it may affect the apparent flux of a permeating weakly ionisable compound. The pH of the hydrophilic viable epidermal layers may be altered by the receptor solution, and this can, theoretically, result in modulation of the partitioning tendencies of the ionisable species. Kou (1993) demonstrated this effect using a weak acid and a weak base permeating through human skin into receptor solutions of varying pH. The results of this study showed clearly how a receptor fluid pH dependency on flux. Indeed, it highlights that great care should be taken when deciding upon the conditions of a diffusion experiment. For this work, a phosphate buffered saline solution (pH 7.4) was used for all diffusion experiments.

Choice of membrane

Several types of membrane have been used to study in vitro permeation. Human and animal skin as well as synthetic membranes can be chosen, though really the choice depends upon the study being performed. This is discussed in more detail in section 1.6.3.

Donor phase

The way in which a permeant is applied to the skin surface can be a determinant of its subsequent absorption, and there are several factors to consider when deciding upon a suitable application procedure. These include; the nature of the vehicle, the amount of vehicle applied, the permeant concentration, the exposure time.

a. Application method

There are two basic approaches to applying substances to the membrane; infinite dose and finite dose. Infinite dose techniques involve application of sufficient permeant to make any changes in donor concentration caused by

diffusion or evaporation of the experiment negligible (i.e. the dose is effectively infinite). This is a desirable method if the experimental objectives include calculation of diffusional parameters, such as permeability coefficients, or if the aim is to investigate penetration enhancement. It also has the advantage that data analysis and interpretation is easier.

Finite dose techniques (Franz, 1978) are designed to model in-use conditions, involve application of a dose that may show marked depletion during an experiment. Depletion occurs where the proportion of permeant entering the membrane is large, relative to the amount applied. Alternatively, the permeant may be removed from the membrane surface during, for example, the simulation of a washing or rinsing procedure. With finite dosing the permeation profile may exhibit the characteristic plateau that accompanies donor depletion. The finite dose technique may involve application of permeants or enhancers in small volumes of volatile solvent (e.g. acetone or ethanol). This allows assessment of the gross effects of enhancers but results are more difficult to interpret mechanistically. Direct comparisons of infinite and finite dose applications are relatively rare, but the predicted effects have been investigated. Franz et al. (1993) used a mathematical model to predict infinite dose flux from a finite dose equation. The results showed that this type of modelling is better suited to experiments using silicone membranes to avoid the variability associated with human skin, and the effects some solvents may have upon the barrier function of the skin.

b. Dose Level

There are several published recommendations on both the expression of dose levels and the specific quantities involved. The FDA/AAPS guidelines

suggested a universal application weight of approximately $5\text{mg}/\text{cm}^2$ of formulation (Skelly et al. 1987). COLIPA (COLIPA, 1995) proposed $5\mu\text{L}/\text{cm}^2$ for liquid formulations, and $2\text{mg}/\text{cm}^2$ for semi-solid formulations (or $5\text{mg}/\text{cm}^2$ if these are being compared with a liquid). However, these levels are almost impossible to achieve in practice.

Distribution of an even film over the surface of the membrane presents a practical challenge. Pre-treatment of the membrane before mounting in a diffusion cell may be easier than treating pre-mounted membranes. Semisolid formulations can be applied and spread with a small pre-weighed formulation coated spatula. The precise weight can be determined by difference, and the same operator should apply all test materials. Evaluation of spray-on formulations poses even more difficulty, and for this reason evaluation of the effect of enhancers is best made by their incorporation into appropriate formulations, rather than the more common strategy of pre-treatment, which does not model the in-use scenario.

Having considered the 'traditional' methods of studying permeation, the next section examines an alternative way of conducting diffusion experiments. This is the use of Attenuated Total Reflectance Fourier Transform Infrared (ATR-FTIR) Spectroscopy.

1.6.1.2. Diffusion experiments using ATR-FTIR spectroscopy.

Attenuated Total Reflectance Fourier Transform Infra-Red (ATR-FTIR) spectroscopy has found increasing use for the study of skin permeation. Partly this is because of the ease of the technique, but primarily it is because ATR-FTIR can yield considerably more information than traditional permeation experiments. The aim of any permeation experiment is to evaluate the flux of a drug across a membrane and assess whether different vehicles improve or retard permeation. There are many well-

known penetration enhancers, but the mechanism by which they act is not easy to determine. Some work by intercalating with skin lipids, disordering them and allowing diffusion of the permeant. Alternatively, the enhancer can act in a solvent capacity, improving the partitioning into the skin and the solubility of the permeant in the skin. It is also possible for both mechanisms to occur simultaneously in which case separation is even more difficult but synergy in the degree of enhancement is seen. This is why ATR-FTIR is now a popular method for deconvoluting enhancement mechanisms. The method has been described in detail in the literature (Brandt, 1985; Watkinson et al, 1995; Pellett et al 1997; Harrison et al, 1996; Dias et al, 2001) but briefly the procedure is as follows.

In this technique, radiation propagating through an optical medium of high refractive index (n_1) undergoes total internal reflection at an interface with a medium of lower refractive index (n_2) when the incident angle (θ) exceeds the critical angle (see figure 1.5). At the interface between the two media, an evanescent wave is established within the medium of lower refractive index. When energy is absorbed in this medium, the reflected beam contains information characteristic of the absorbing molecules.

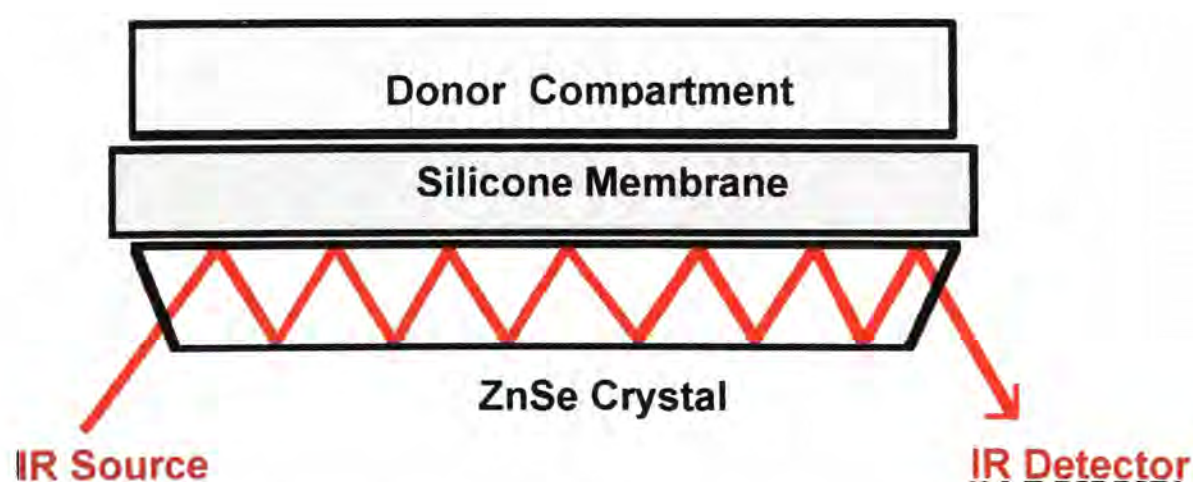


Figure 1.5. Schematic representation of ATR-FTIR.

In a typical ATR-FTIR permeation experiment, a membrane is placed on a ZnSe crystal mounted in an FTIR spectrometer. Initially the IR spectrum of the membrane is observed. A permeant is selected which has a characteristic IR band that is discrete both from the signals of the solvent into which it is dissolved and the membrane. A saturated solution of the permeant is placed in a trough on the surface of the membrane and the IR spectra observed as a function of time. As the permeant arrives at the interface between the membrane and the ATR crystal its signal will be observed and will increase with time until a plateau is reached. Since a saturated solution of the permeant is used, the signal will plateau at a level corresponding to the saturated solubility of the permeant in the membrane (A_0). The increase in signal (A) with time (t) should be sigmoidal according to the following solution of Fick's 2nd law of diffusion:

$$\frac{A}{A_0} = 1 - \frac{4}{\pi} \sum_{n=1}^{\infty} \frac{(1-n)}{2n+1} \exp\left[\frac{-D(2n+1)^2 \pi^2 t}{4h^2}\right] \quad (\text{Eqn.1.7})$$

Where D is the diffusion coefficient of the permeant through the membrane of thickness h . If the membrane is treated with an enhancer that solely alters D in the membrane the value of A will be unaltered but the time to reach the plateau will decrease. An enhancer that alters the solubility properties of the membrane, improving permeation will give an increased value of A_0 but the time to arrive at the plateau value will be unaltered.

In previous experiments (Harrison et al, 1996) this methodology has been used to determine mechanisms of action of enhancers such as Azone (which alters D) and Transcutol (alters A_0). However the only data interpretation used was to examine the change in permeant signal (A) with time. Clearly in any ATR-FTIR study the entire spectral range is captured

and the data should also encode information about other processes that are taking place in the membrane. One of the most important uses of data describing diffusion through skin pertains to the analysis of mechanisms of passive and enhanced transport. Successful solutions to such mechanistic questions require that diffusion profiles be deconvoluted to allow separate evaluation of the contributions arising from each component of the formulation, and their relative roles in diffusion and partitioning. Until now, it was the complexity of generated raw data that posed a significant problem. Interpretation was difficult because of the convoluted or overlapping nature of the spectra. A method capable of deconvoluting the data would significantly enhance data interpretation and open up the possibility of investigating more complex systems. Recently Dias (2003) reported such a method. Data were analysed using a sophisticated chemometric method which permitted deconvolution of the IR signal arising from the permeant (benzoic acid), the solvent (octanol) and the silicone membrane.

ATR-FTIR diffusion experiments require more sophisticated apparatus than traditional diffusion experiments but offer a way to monitor the mechanisms of permeation enhancement. There is however, a low-tech alternative to the ATR-FTIR approach which also provides mechanistic information, and this method is tape-stripping.

1.6.1.3. Tape-stripping and determination of drug concentration in the skin

The tape-stripping technique is commonly being used to assess the drug concentration profile across stratum corneum. In this technique, a permeant is applied to the skin surface for a fixed period of time. The permeant remaining on the skin surface is then removed (where possible)

by wiping or washing and the stratum corneum is progressively removed by serial adhesive tape-stripping. Determination of the drug amount in each tape and the thickness of stratum corneum removed by each tape-strip allow the diffusivity and solubility of the permeant within the stratum corneum to be calculated (Pellett et al, 1997; Tsai et al, 1999; Stinchcomb et al, 1999).

An appropriate solution to Fick's second law of diffusion predicts the concentration of drug (c_x) as a function of position (x) within the stratum corneum according to the following equation (Pirrot et al, 1997):

$$c_x = Kc_v \left\{ 1 - \frac{x}{L} - \frac{2}{\pi} \sum_{n=1}^{\infty} \frac{1}{n} \sin\left(n\pi \frac{x}{L}\right) \exp\left(-\frac{D}{L^2} n^2 \pi^2 t\right) \right\} \quad (\text{Eqn. 1.8})$$

The concentration of drug in the outermost layer of the stratum corneum (when $c_{x=0}$) divided by its concentration in the applied vehicle (c_v) gives the partition coefficient (K). To acquire more information it is necessary to fit experimental concentration profiles to equation 1.8 which will reveal not only K but also D/L^2 , and so provide some information concerning mode of action. What is particularly useful about this technique is its ability to be used both in vitro and in vivo (Reddy et al, 2002), provided it is combined with a suitable analytical method such as HPLC.

1.6.2. In vivo techniques

In vivo studies use various models (e.g. rat, rabbit, monkey, pig) and also humans where therapeutic substances are of interest. There are several methods by which in vivo absorption can be assessed.

1.6.2.1. Measurement of drug levels in excreta, blood or internal organs

Analysis of urinary excretion of drug related material has been used to assess percutaneous absorption in both humans and animals (Feldmann and Maibach, 1969; Wester et al, 1983). The material is applied to the skin and urine is collected over a period of time. This is then analysed for the presence of drug and metabolites and the concentration of drug equivalents determined. Using an intravenous administration of the same, the proportion excreted in urine can be measured, and a correction factor applied to calculate the absorption following application. Historically, radio-labelled drugs were used because this allowed greater sensitivity, but with advances in LC-MS technology, there is sufficient sensitivity that LC-MS-MS is more routinely used for the assessment of drug levels. Where small animals are used, radioactivity may be measured in faeces and blood as well as various organs and the carcass to determine accurately total absorption (Hotchkiss et al. 1990).

1.6.2.2. Measurement of residual material on the skin surface

Techniques that assess absorption by residual analysis or difference monitor the disappearance of material from the surface of the skin. This method's main advantage over others described is that it is non-invasive. There are two approaches to surface disappearance: single point and continuous monitoring. In a single point experiment the test material is applied for a fixed time and the residual formulation is subsequently removed from the skin surface and analysed. This approach requires only a small amount of permeant, and for this reason radiolabels are often used. The main issue with single point experiments is that it allows only one assay site per application, and it follows that if absorption kinetics are required, multiple application sites are necessary.

Following application, the disappearance of radiolabel from the skin surface is monitored spectroscopically or by using radioisotope techniques (Mak et al, 1990; Sennhenn et al, 1993). Optothermal imaging techniques (such as optothermal transient emission radiometry; OTTER) have also been used to monitor disappearance of material from the surface of the skin. Again, it is non-destructive, non-invasive and can be used for a wide variety of materials including sunscreens (Imhof et al, 1990a, 1990b). Optothermal imaging has also been used to characterize skin condition (Bindra et al, 1991).

1.6.2.3. Measurement of physiological effects

If the permeant of interest causes a physiological or pharmacological reaction when reaching deeper tissues, then this response may be used to provide the basis for investigating drug flux and the permeability of the stratum corneum. Examples of induced skin reactions are vasoconstriction, vasodilatation, activity of the sweat glands and epidermal proliferation. The skin blanching caused by topical corticosteroids is well known and often used as a response parameter (Stoughton et al, 1960; McKenzie and Stoughton, 1962; Barry and Woodford, 1976). Erythema produced by vasodilating nicotines is another example (Guy et al. 1986). The dependence of the pharmacodynamic response on the applied dose or the concentration in the vehicle is described by dose-response and concentration-response curves respectively. While this method can be used to compare the potency of different drugs or formulations, it is not capable of quantitatively measuring the amount of chemical which actually penetrate the skin. It is also limited to a small group of chemicals which produce a measurable chemical effect.

The methods described in the preceding section do not cover all of the techniques used to assess permeation in vivo. Other methods, including surface biopsy and punch biopsy can be found in section 1.8 which considers the bioavailability of topical products.

1.6.3. Models

1.6.3.1. Animal models

Many in vivo methods for studying skin permeation in vivo are based upon animal models that are used in the early stages in product development (before the availability of toxicological data). Although the relevance of animal models to humans is often questioned, studies conducted using animal models can, if well-designed provide great insight into the human situation. The most appropriate data relating to permeation are those generated in vivo in human volunteers. However, it is not always practically or ethically possible to conduct studies in humans and so animal models are often used as a substitute. There are several animal models in which percutaneous permeation has been studied such as rat, pig, hairless dog, hairless mouse, rabbit and monkey (Barteck et al, 1972; Scott, 1986; Durrheim et al, 1990; Niazy, 1996).

1.6.3.2. Model membranes

The use of an appropriate model can provide valuable information concerning the mechanisms of action of different formulation components and their contribution to permeation behaviour. Artificial membranes have considerable advantage over human or animal membrane because they are cheap, readily available and generally the experiments are less time-consuming.

Transport of a solute through a membrane that divides two aqueous solutions takes place by both partition into and diffusion through the membrane, or through the membrane via channels. Cellulose acetate and dialysis membranes fall into the latter category, as they are considered to be porous membranes. In such cases, the solute diffuses through the pores and the membrane merely provides a physical barrier to free movement of the solute. The concentration of the solute and the tortuosity of the pores, therefore determine the rate of diffusion. Although the mechanism is not representative of the diffusion process in human skin, it may be relevant for the study of damaged skin, where the dermis is the only remaining barrier.

Partitioning membranes imply that the solute partitions into, and diffuses through a phase different from the donor and receptor phase. These membranes are frequently hydrophobic and include both solids (polymers and phospholipids below their phase transition temperature) and liquids (isopropyl myristate, hydrocarbons, etc). These membranes can be utilised as mechanistic models when the lipophilic diffusion barrier of the stratum corneum determines skin transport (Houk and Guy, 1988).

Recently human skin equivalents have been used to study permeation. The technology behind the construction of human skin equivalents has been driven by research into the treatment of burns. SkinEthic was the first company to develop the technology for cultured skin and now provide a range of different models. Originally, only epidermal models were available. These skin equivalents behave like human *in vivo* epidermis when treated with pharmacologically active or irritating substances. SkinEthic have also developed a reconstituted human full-thickness model consists of living, multi-layered dermal-epidermal tissue which is

functionally equivalent to human skin. The use of artificially cultured skin in permeation experiments is still of limited application because the methodology is both expensive and not clearly predictive of in vivo results (Lotte et al. 1997; Marty et al. 1997). Human skin equivalents have been found to be approximately ten times more permeable than human skin (Dusser et al. 1996). In the past five years much work has gone into characterising the physiology of these artificial constructs, and has provided valuable insight into their potential applications (Ponec et al, 2000a; 2003; Garcia, 2002). New models are continually being developed (Hoffmann, 2005).

Among the several model membranes studied as potential membranes for human skin, one in particular has been given the most extensive consideration: polydimethylsiloxane (silicone) membrane. There are many others to choose from however, such as eggshell membranes, synthetic zeolites and multi-component synthetic membranes. For a full account of different types of model membranes refer to Houk and Guy (1988).

Silicone membrane

Polydimethylsiloxane (PDMS) is a non-polar, non-porous partitioning membrane, which behaves as a homogeneous hydrophobic barrier. Silica filler (20-30%w/w), is usually included to impart tear resistance to cast sheets of the polymer, and behaves as a dispersed phase (Twist and Zatz, 1989). It may be a relevant model for human skin because of its hydrophobic properties. Permeation through PDMS membranes consists of initial dissolution of the solute into, and then diffusion through, the polymer matrix (Higuchi and Higuchi, 1960). Silicone membranes can be used either untreated or pre-soaked in a hydrophobic vehicle (Iervolino et al. 2000; Davis et al, 1991), and the permeation of drugs through this

membrane has been extensively investigated. Flynn et al (1981) investigated the physicochemical properties of a homologous series of alcohols across PDMS membranes. A plot of the logarithm of the membrane/saline partition coefficient for each alcohol against alkyl chain length was linear, and the diffusion coefficients were shown to decrease as the molecular size of the alcohols increased. Dias et al (1999) evaluated the permeation of caffeine from an aqueous saturated solution and several cosmetic formulations through silicone membrane and human skin. The results showed that although synthetic membranes can provide reliable information in assessment of batch-to-batch variation in quality assurance, they give no indication of how a formulation will behave in skin. It was also found that the permeation was higher through the silicone membrane impregnated with IPM than through skin. However, Iervolino et al. (2000) found a correlation between the permeation of ibuprofen from supersaturated solutions through silicone membrane and human skin.

Work by Flynn (1972) and later Davis (1991) has demonstrated that PDMS membranes show a clear response to changes in thermodynamic activity. Davis used a co-solvent method to prepare supersaturated solutions of hydrocortisone acetate and found that for systems up to eight degrees of saturation flux was linearly proportional to the degree of saturation.

To conclude, the only reliable membrane for the study of percutaneous absorption is a suitable skin preparation. However, silicone membranes can be used when the aim is to understand the basic concepts concerning permeation.

1.7. Topical Drug Delivery and Bioavailability

The bioavailability of topical dosage forms is an area that is fraught with difficulties. However, before attempting to cross this minefield it is important to understand the various terms used.

The word topical derives from the Greek 'topos' meaning local, and topical dosage forms include ophthalmic, nasal preparations, urogenital preparations and dermatological preparations. These preparations act at target sites that are identical or close to the site of application and can be external (e.g. skin or eyes) or internal. The aim of topical or local delivery is the direct application of the drug to the target site to maximise efficacy, while minimizing systemic absorption, to improve safety. It is clear that in this thesis only topical systems applied to the skin are of relevance.

Topical delivery is the application of a drug-containing formulation to the skin to treat directly cutaneous disorders (e.g. acne) or the cutaneous manifestations of a general disease (e.g. psoriasis) with the intent of confining the pharmacological or other effect of the drug to the surface of the skin or within the skin. While systemic absorption may be unavoidable it is always unwelcome. It is important to understand the distinction between topical and transdermal delivery. Generally, semi-solid formulations are used, but foams, sprays, medicated powders, solutions and medicated adhesive systems are also in use.

Regional delivery involves the application of a drug to the skin for the purpose of treating diseases or alleviating disease symptoms in deep tissues beneath the application. Here the intent is to effect pharmacological actions of the drug within musculature, vasculature,

joints, and other, beneath and around the site of application. A selectivity of action over that achieved by systemic administration is sought. Regional activity requires percutaneous absorption and deposition. Systemic uptake, although unwelcome, is unavoidable. Nevertheless, regional concentrations are thought to be higher than can be achieved by systemic administration at the same total body exposure to the drug. The focusing of drugs into tissues in this manner has been difficult to prove, and thus considerable scepticism exists concerning the validity of regional therapy. Regional delivery is accomplished with traditional ointments and creams as well as large adhesive patches, plasters, poultices and cataplasms.

Transdermal delivery involves the application of a drug to the skin to treat systemic disease and is aimed at achieving systemically active levels of the drug. Although such traditional dosage forms as ointments can be employed in this kind of therapy (e.g. nitroglycerin ointments), adhesive systems of precisely defined size are the rule. Here percutaneous absorption with appreciable systemic drug accumulation is essential. Ideally, there would be no local accumulation of drug, but such accumulation is unavoidable. The drug is forced through the relatively small diffusional window defined by the contact area of the patch. Consequently, high and potentially irritating or sensitising concentrations of a drug in the viable tissues underlying the patch are preordained by the nature of the delivery process.

Current topical therapy for skin diseases is poor because of the low bioavailability of topically applied drugs. Treatment and quality of life would be far better if bioavailability could be improved. Understanding the pharmacodynamics and pharmacokinetics of a drug is essential for its safe use. A therapeutic effect of a drug and its appropriate dosage regimen are

based upon the relationship of time and drug concentration at the active site (target organ or biophase) and the resultant drug response. Correlation of drug effects and drug concentration in blood or urine are most often monitored for systemically acting agents. Three factors generally assessed are:

1. The area under serum concentration versus time curve
2. The peak serum concentration
3. The time to peak serum concentration

If analytical difficulties prevent the measurement of drug or metabolite levels in the body fluids drug effects are assessed by observing an appropriate pharmacologic response. For topical drug products bioavailability studies similar to those of orally administered drugs are often difficult to carry out. This is mainly because topical doses tend to be very small, so that concentrations in the blood and urine are undetectable. Moreover, systemic availability may not properly reflect cutaneous bioavailability for medications that are intended to treat local skin disorders since systemically injected drug is no longer at the site of action. Assessment of the bioavailability of topical formulations may be made taking one of several approaches. Bioavailability may be established through a well-controlled clinical trial or through an easily monitored pharmacological endpoint. Establishing whether the concentration of drug within the tissue correlates with clinical performance or to a relevant pharmacological endpoint is being debated. At present a well-controlled clinical trial is the only uncontested, generally accepted procedure for demonstrating bioavailability of topical drug products. It is highly desirable to develop alternative *in vivo* and *in vitro* procedures because of the high costs of conducting clinical trials. The next section describes some of the

methods used to assess bioavailability, but is not intended to be an in-depth discussion of all techniques. For a more detailed review, refer to Surber and Davis (2002).

1.8. Methods for assessing bioavailability of topical products

Suction blister technique

This method, that separates the skin strata epidermally, was first described by Kiistala et al (1968). Kiistala used a special dome-shaped cap with several small holes (of 6mm in diameter), and applied suction of 200 mmHg for a 2-3 hour period to induce blisters. After this period, 50-150mL suction blister fluid and stratum corneum-epidermal sheets can be harvested. The blister fluid corresponds to interstitial fluid. It should be noted that this technique cannot be used on diseased skin, for the reason that it is not possible to 'raise' blisters uniformly.

Related to the suction blister is the Cantharidin blister technique. Large sheets of stratum corneum and blister fluid can be obtained with this method. It is named after the substance used to induce the blisters, cantharidin which is harvested from the Spanish fly and has proved highly effective, producing blisters (up to 4cm in diameter). Clearly there will be some discomfort for the volunteer, however this method does not leave a permanent scar. The blister fluid is continuous with the intravascular fluid and the skin surface, and so an immediate representation of the tissue concentration of a drug can be assumed. The one drawback with using cantharidin is that it induces an inflammatory response which may alter the composition of the blister fluid or the morphology of the blister roof.

Skin biopsy

The most invasive and yet the most practical of all methods to access skin compartments is the excision of skin tissue. Punch and shave biopsies allow direct access into the part of the skin of interest. Removal of the stratum corneum is optional, but if not required it is removed by tape stripping. The punch biopsy will contain parts of the subcutaneous tissue, dermis and epidermis. The shave biopsy will mainly contain epidermis and some dermis. Subcutaneous tissue can be mechanically divided from the dermis, and the latter can be separated from the epidermis by heat separation. The typical amount of skin removed is around 50mg.

Tape stripping and determination of drug concentration in the skin.

As mentioned in section 1.6 skin stripping is increasingly being used to measure drug concentration, and concentration profile across the stratum corneum (Shah, 1998). In this technique the stratum corneum is progressively removed by serial stripping using adhesive tape. For each strip two things are measured:

1. The amount of drug in the strip
2. The thickness of the stratum corneum removed

Knowledge of these allows the diffusivity and the solubility of the drug within the stratum corneum to be calculated using an appropriate solution to Fick's law of diffusion. There are still a few issues to be addressed concerning tape-stripping, but as a minimally invasive, in vivo technique it certainly has an advantage.

1.9. Role of the vehicle in skin permeation

For a formulator to be able to deliver a therapeutic level of drug at the desired site of action from a simple (single or binary component) vehicle would be like finding the holy grail of dermal therapy. Needless to say, this is highly unlikely. The main reason behind this is not only the excellent barrier properties of the skin, but also the physicochemical properties of the drug. Often it is necessary to increase the amount and rate of dermal delivery to achieve the required therapeutic drug levels. In this situation, the formulator will investigate possible enhancement strategies.

It is clear from inspection of equation 1.5 that the physicochemical determinants that can be manipulated to increase permeation are D and C_0 . Barry (1983) suggested that in an ideal situation an enhancer should fulfil the majority of the following criteria:

- 1 The enhancer itself should be pharmacologically inactive
- 2 It should be well tolerated by the skin and be cosmetically acceptable
- 3 The mechanism of action of the enhancer should be known
- 4 It should be inexpensive and compatible with a large selection of adjuvant

Chemical enhancers such as laurocapram (Azone™), oleic acid, dimethyl sulfoxide (DMSO), propylene glycol, fatty acid derivatives and others are defined as vehicle components that enter the stratum corneum and increase drug diffusivity within the barrier membrane (alter D), or increase vehicle drug solubility-partitioning (C_0) or both. The majority of investigations of penetration enhancement are concerned with chemicals which penetrate the stratum corneum and interact with the intercellular

barrier lipids. Azone™ is possibly the most widely studied enhancer of this type, which has been successfully used to improve the flux of many drugs (Wotton et al, 1985, Sato et al, 1988) and has also been the subject of mechanistic studies (Hadgraft et al, 1985, Lewis and Hadgraft, 1990). Structure activity relationships with Azone analogues have revealed that the polar head groups linked to long alkyl chains are vital to its activity (see figure 1.6 for the structure of Azone™ and other chemical enhancers). Substituting the oxygen in Azone™ with sulphur produces an inactive molecule because it reduces the interaction of the -OH groups of the ceramides and as a consequence it does not 'lock' into position in the polar head regions where it is required to act. An alkyl chain length of 12 or 14 is optimum, indicating that the ring structure needs the support of the alkyl 'tail' to anchor it in position. If the alkyl chain is too short or too long it will not be able to locate the ring structure in the polar head group regions.

Another membrane disrupting enhancer, oleic acid, acts by forming pools within bilayers (Ongpipattanakul et al, 1991) rather than distributing homogeneously as Azone™. This allows a diffusing molecule to travel across the bilayer via interfacial defects between pools of oleic acid and ceramides, or by diffusing through the pools, which would be liquid at 37°C.

A mechanism by which C_0 may be increased is enhancer induced modification of the polarity of the skin, such that the drug solubility in the skin is increased. One example of this is the small molecule propylene glycol that is known to transfer through the skin. It is a commonly used solubility enhancer in formulations and its presence in the skin should improve skin permeation.

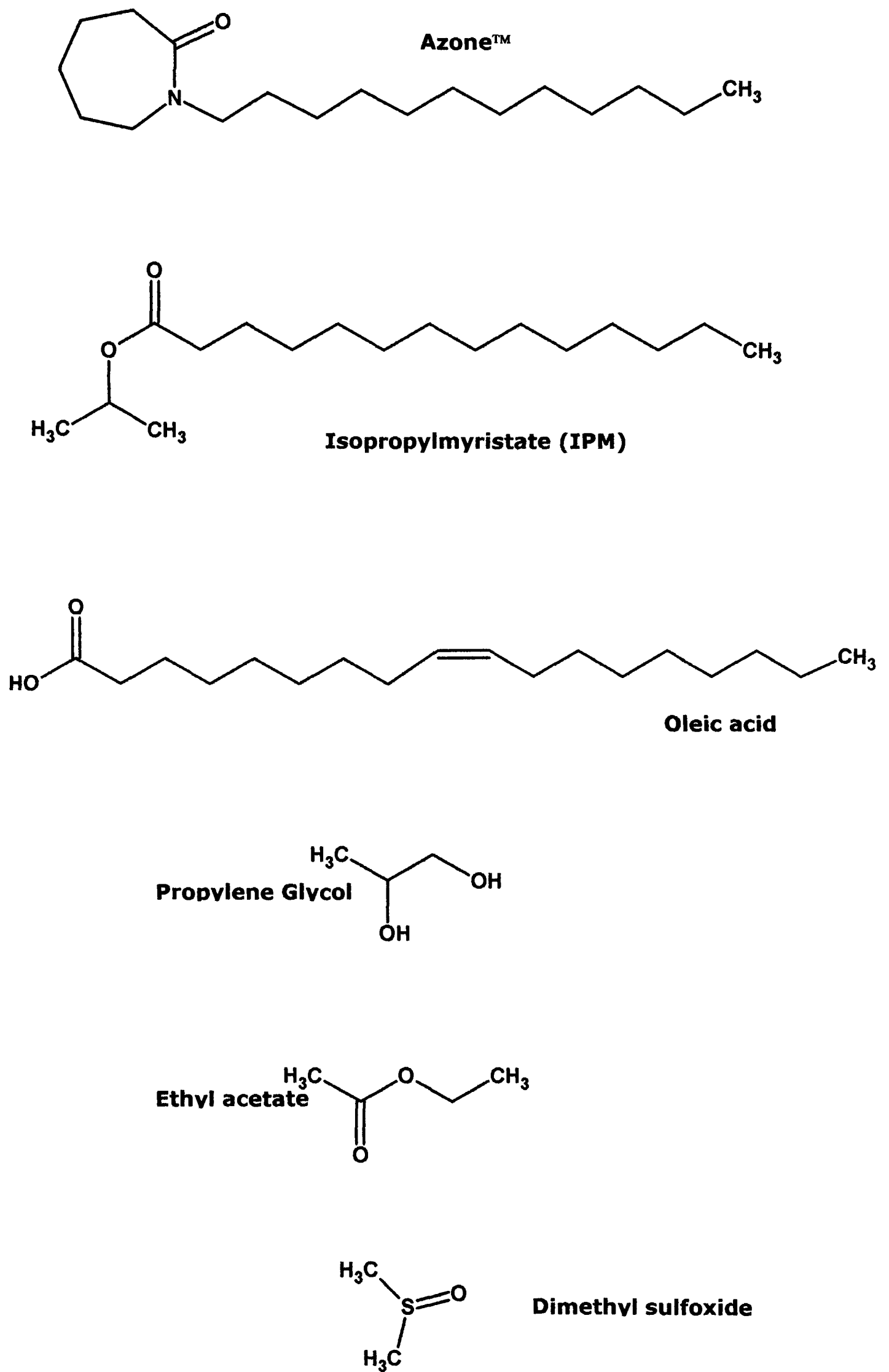


Figure 1.6. Examples of permeation enhancers

In an elegant experiment, Harrison et al (1996) demonstrated that it was possible to separate the two enhancing effects using ATR-FTIR. Permeants were selected that had IR signatures discrete from that of the membrane being used. Recall from section 1.6.1. that the profile from an ATR-FTIR experiment will increase sigmoidally with time. The reason for the shape of the profile is that there is a lag phase, a pseudo steady-state phase and then an equilibration as the skin (or other membrane) becomes saturated with the permeant. If the skin is pre-treated with an enhancer that modifies the diffusional properties of the skin the plateau reached will be the same, but it will occur earlier. If an enhancer alters the solubility properties of the skin the plateau will be affected, but the time to reach the plateau will not. This is shown schematically in figure 1.7

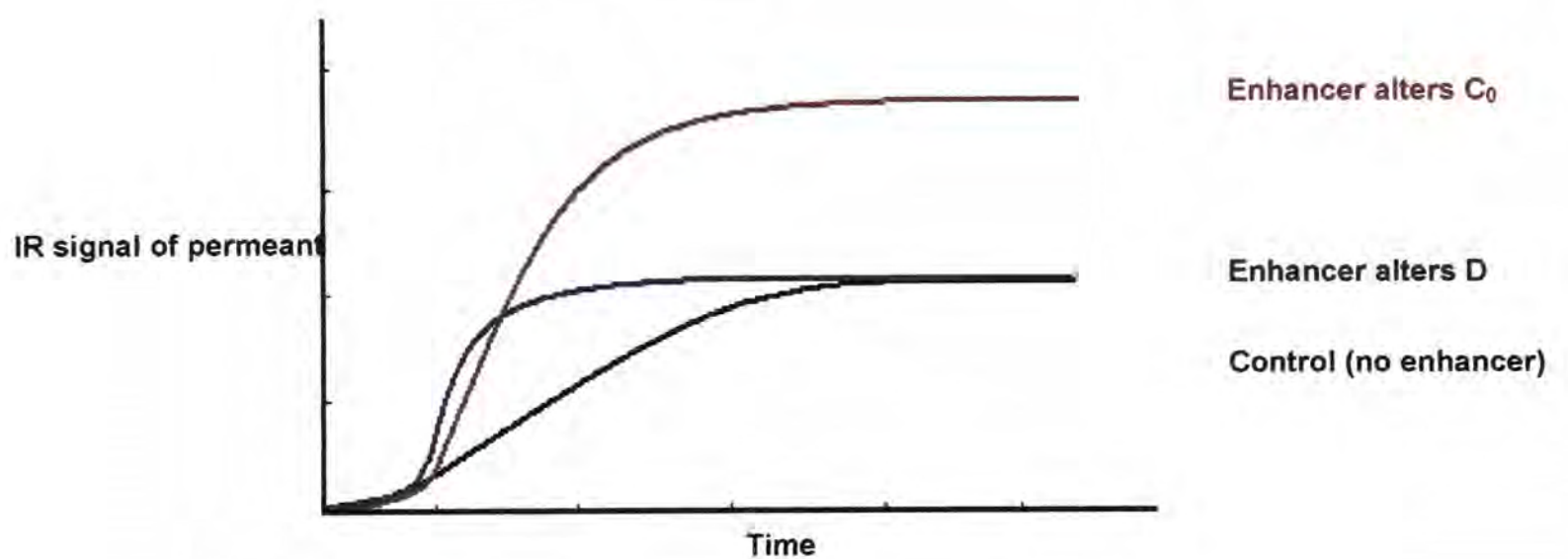


Figure. 1.7. The effect of enhancer on the ATR-FTIR diffusion profile of a permeant

Co-enhancer systems, in which two enhancers that work in different ways are brought together, are particularly effective. This is the result of a

synergistic effect by which each enhancer increases the delivery of the other as well as that of the drug, and the effect is multiplicative.

The last way in which an enhancer may act is to extract skin lipids. It has been known for some time that the skin can be treated with solvents that are able to extract stratum corneum lipids. What is interesting with this approach is that the barrier function is reduced dramatically, but can be restored if the lipids are re-introduced. It appears the skin, recognising its barrier function has been compromised, rapidly reacts and synthesises lipids to replace those lost Bommannan et al (1991). One of the most effective combinations of solvents for this purpose is methanol and chloroform, which will remove all but the lipids covalently bonded to the corneocyte envelope. Ethanol extracts some lipids, but it is much milder than the chloroform/methanol mixture.

1.10. Conclusions

It is clear that over the last century our knowledge of the skin has advanced to a point where the systems used to increase permeation are becoming increasingly sophisticated. However, despite the wealth of knowledge available, the process of designing formulations is still largely informed guesswork, guided not by insight but rather a pragmatic trial and error approach. There are very little published data about the 'rules' for choosing an optimum topical vehicle, though what is clear is that the choice will depend upon the physicochemical properties of the permeant. The rationale behind how a solvent combination is chosen is less clear. From section 1.9 it may be suggested that this is because of the complex interactions that are possible, and an inability to separate the various effects that the different components are eliciting on the barrier function of the skin. The glimmer of hope is the development of chemometric approaches to data analysis, and the rather more ambitious high-throughput screening to find suitable combinations (Karande, 2002).

The aim of this project is to examine the structural features of selected vehicles with different properties, and investigate their influence on the permeation of three model drugs (acetaminophen, ibuprofen and salicylic acid). These three drugs span a range of logP representative of those that would be used therapeutically. There is already considerable information in the literature regarding the permeation of both ibuprofen and salicylic acid and it is hoped that the studies presented in this thesis will build upon this. Solubility and permeation behaviour of the permeants will be assessed in two types of vehicle: hydrophilic and lipophilic. Both traditional diffusion experiments (Franz-type) and ATR-FTIR will be used to assess permeation.

1.11. Research objectives:

Bearing in mind the information gathered in Chapter One, a summary of the objectives of this thesis is listed below.

- To evaluate the solubility behaviour of the selected permeants in a range of hydrophilic and lipophilic vehicles.
- To investigate the effect of these vehicles upon the in vitro diffusion of the selected permeants across synthetic membranes and human skin.
- To investigate the possible interaction of vehicles with PDMS membranes using ATR-FTIR spectroscopy.
- To evaluate a chemometric approach to the analysis of data from ATR-FTIR diffusion experiments.

1.12. References

W. Abraham, and D. T. Downing. Factors affecting the formation, morphology and permeability of stratum corneum lipid bilayers in vitro. In: *Prediction of Percutaneous Penetration*, Eds R. C. Scott, R. H. Guy, and J. Hadgraft. IBC Technical Services Ltd. London. P110-112 (1991).

W. J. Albery, and J. Hadgraft. Percutaneous absorption: in vivo experiments. *J. Pharm. Sci. and Pharmacol.* **31**, 140-147 (1979).

B. W. Barry. *Dermatological Formulations: Percutaneous Absorption*. Marcel Dekker Inc. New York (1983).

B. W. Barry and R. Woodford. Proprietary hydrocortisone creams. Vasoconstrictor activities and bioavailabilities of six preparations. *Br. J. Dermatol.* **95**, 423-425 (1976).

M. J. Barteck, J. A. La Budde and H. I. Maibach. Skin permeability in vivo: comparison in rat, rabbit, pig and human. *J. Invest. Dermatol.* **58**, 114-123 (1972).

R. M. S. Bindra, G. M. Eccleston, R. E Imhof and D. J. S. Birch. Opto-thermal in vivo monitoring of human skin condition. In: *Prediction of Percutaneous Penetration*, Eds: R. C. Scott, R. H. Guy, J. Hadgraft and H. E. Boddé. Vol. 2. STS Publishing, Cardiff. pp628-635, 1991.

I. H. Blank. Cutaneous barriers. *J. Invest. Dermatol.* **45**, 249-256 (1965).

W. C. Bowman, and M. J. Rand. *Textbook of Pharmacology*, 2nd Edition. Blackwell Scientific Publications, London (1978).

K. R. Brain, K. A. Walters, and A. C. Watkinson. Methods for studying percutaneous absorption. In: *Dermatological and transdermal formulations*. Marcel Dekker Inc. New York (2002).

H. Brandt. Determination of diffusion specific parameters by means of IR-ATR spectroscopy. *Exp. Tech. Phys.* **33**, 423-431 (1985).

R. L. Bronaugh, S. W. Collier and J. E. Storm. In vitro methods for measuring skin penetration and metabolism. *J. Am. Coll. Tox.* **8**, 801-2 (1989).

R. L. Bronaugh and R. F. Stewert. Methods for in vitro percutaneous studies: IV: The flow-through diffusion cell. *J. Pharm. Sci.* **74**, 64-67 (1985).

D. A. W. Bucks. Skin structure and metabolism: relevance to the design of cutaneous therapeutics. *Pharm Res.* **4**, 148-153 (1984).

H. M. Clowes, R. C. Scott and J. R. Heylings. Skin absorption: flow-through or static diffusion cells. *Toxicol. In vitro.* **8**, 827-830 (1994).

COLIPA (European Cosmetic, Toiletry and Perfumery Association). 1995. Cosmetic ingredients: guidelines for percutaneous absorption/penetration. Brussels: COLIPA.

A. F. Davis and J. Hadgraft. Effect of supersaturation on membrane transport: 1. Hydrocortisone acetate. *Int. J. Pharm.* **76**, 1-8 (1991).

M. Dias, S. L. Raghavan and J. Hadgraft. ATR-FTIR spectroscopic investigations on the effect of solvents on the permeation of benzoic acid and salicylic acid through silicone membranes. *Int. J. Pharm.* **216**, 51-59 (2001).

M. Dias, A. Farinha, E. Faustino, J. Hadgraft, J. Pais and C. Toscano. Topical delivery of caffeine from some commercial formulations. *Int. J. Pharm.* **182**, 41-48 (1999).

I. P. Dick, P. G. Blain and F. M. Williams. Improved in vitro skin absorption for lipophilic compounds following the addition of albumin to the receptor fluid in flow-through cells. In: *Prediction of Percutaneous Penetration*, Eds. K. R. Brain, V. J. James and K. A. Walters. STS Publishing, Cardiff. pp267-270 (1996).

P. H. Dugard, and R. C. Scott. Absorption through skin. In: *Chemotherapy of Psoriasis*. Pergamon Press, Oxford, pp125-144, (1984).

H. Durrheim, G. L. Flynn, W. I. Higuchi and C. R. Behl. Permeation of hairless mouse skin I: experimental methods and comparison with human epidermal permeation by alkanols. *J. Pharm. Sci.* **69**, 781-786 (1980).

D. Dupuis, A. Rougier, R. Rouget and C. Lotte. The measurement of the stratum corneum reservoir: A simple method to predict the influence of vehicles on in vivo percutaneous absorption. *Br. J. Dermatol.* **115**, 233-238 (1986).

P. Elias. Epidermal lipids, membranes and keratinisation. *Int. J. Dermatol.* **20**, 1-19 (1981).

M. Fartasch, I. D. Bassukas and T. L. Diepgen. Structural relationship between epidermal lipid lamellae, lamellar bodies and desmosomes in human epidermis: An Ultrastructural Study. *Br. J. Dermatol.* **128**, 1-9 (1993).

R. J. Feldmann and H. I. Maibach. Percutaneous penetration of steroids in man. *J. Invest. Dermatol.* **52**, 89-94 (1969).

R. J. Feldmann and H. I. Maibach. Penetration of [¹⁴C] hydrocortisone through Normal Skin. The effect of stripping and occlusion. *Arch. Dermatol.* **91**, 661-666 (1965).

A. Y. Finlay and T. J. Ryan. *Int. J. Derm.* **35**, 305-311 (1996).

G. L. Flynn. Mechanism of percutaneous absorption from physicochemical evidence. In: *Percutaneous Absorption*. Eds. Bronaugh, R. L. and Maibach, H. I. Marcell Dekker Inc. New York. pp17-42 (1985).

G. L. Flynn and R. W. Smith. Membrane diffusion. III. Influence of solvent composition and permeant solubility on membrane transport. *J. Pharm. Sci.* **60**. 1788-1796 (1972).

T. J. Franz, P. A. Lehman, S. F. Franz, H. North-Root, J. L. Demetrulias, C. K. Kelling, S. J. Moloney and S. D. Gettings. Percutaneous penetration of N-nitrosodiethanolamine through human skin (in vitro): comparison of

finite and infinite dose applications from cosmetic vehicles. *Fundam. Appl. Toxicol.* **21**, 213-221 (1993).

T. J. Franz. The finite dose technique as a valid in vitro model for the study of percutaneous absorption. *Curr. Probl. Dermatol.* **7**, 58-68 (1978).

N. Garcia, O. Doucet, M. Bayer, D. Fouchard, L. Zastrow and J. P. Marty. Characterisation of the barrier function in a reconstructed human epidermis cultivated in chemically defined medium. *Int. J. Cosmet. Sci.* **24**, 25-34 (2002).

R. H. Guy, E. M. Carlstrom, D. A. W. Bucks, R. S. Hinz and H. I. Miabach. Percutaneous penetration of nicotines: in vivo and in vitro measurements. *J. Pharm. Sci.* **75**, 968-972 (1986).

J. E. Harrison, A. C. Watkinson, D. M. Green, J. Hadgraft and K. Brain. The relative effect of azone and transcutol on permeant diffusivity and solubility in human stratum corneum. *Pharm. Res.* **13**, 542-546 (1996).

T. Higuchi. Physical chemical analysis of percutaneous absorption process from creams and ointments. *J. Soc. Cosmet. Chem.* **11**, 85-97 (1960).

W. I. Higuchi and T. Higuchi. Theoretical analysis of diffusional movement through heterogeneous barriers. *J. Pharm. Sci.* **49**, 598-606 (1960).

J. Hoffmann, E. Heisler, S. Karpinski, J. Losse, D. Thomas, W. Skiefken, H-J. Ahr, H-W. Vohr and H. W. Fuchs. Epidermal-skin-test 1000 (EST-1000) - a new reconstructed epidermis for in vitro skin corrosivity testing. *Toxicol. In vitro*. In press.

S. A. Hotchkiss, M. A.J. Chidgey, S. Rose and J. Caldwell. Percutaneous absorption of benzyl acetate through rat skin in vitro 1. validation of an in vitro model against in vivo data. *Fd. Chem. Tox.* **28**, 443-447 (1990).

J. Houk and R. H. Guy. Membrane models for skin penetration studies. *Chem. Rev.* **88**, 455-471 (1988).

F. Hueber, J. Wepierre and H. Schaefer. Role of transepidermal and transfollicular routes in percutaneous absorption of hydrocortisone and testosterone: in vivo study in the hairless rat. *Skin Pharmacol.* **5**, 99-107 (1992).

M. Iervolino, S. L. Raghavan and J. Hadgraft. Membrane penetration enhancement of ibuprofen using supersaturation. *Int. J. Pharm.* **198**, 229-238 (2000).

R. E. Imhof, C. J. Whitters and D. J. S. Birch. Opto-thermal in vivo monitoring of sunscreens on the skin. *Phys. Med. Biol.* **35**, 95-102 (1990a).

R. E. Imhof, C. J. Whitters and D. J. S. Birch. Opto-thermal monitoring of structural breakdown of an emulsion sunscreen on skin. *Clin. Mater.* **5**, 272-278 (1990b).

P. Karande and S. Mitrogotri. High throughput screening of transdermal formulations. *Pharm. Res.* **19** (5) 655-660 (2002).

M. Katz and Z. I. Shaikh. Percutaneous corticosteroid absorption correlated to partition Coefficient. *J. Pharm. Sci.* **54**, 591-594 (1965).

U. Kiistala, K. K. Mustakallio and H. Rorsman. Suction Blister in the study of cellular dynamics of inflammation. *Acta. Derm. Venereol.* **47**, 150-153 (1967).

J. H. Kou, S. D. Roy, J. Du and J. Fujiki. Effect of receiver fluid pH on in vitro skin flux of weakly ionisable drugs. *Pharm. Res.* **10**, 986-990 (1993).

A. W. McKenzie and R. B. Stoughton. Method for comparing percutaneous absorption of steroids. *Arch. Dermatol.* **86**, 608-610 (1962).

A. G. Matoltsy, A. M. Downes and T. M. Sweeney. Studies of the epidermal water barrier. Part II. Investigation of the chemical nature of the water barrier. *J. Invest. Dermatol.* **50**, 19-26 (1968).

E. Menczel. Skin delipidization and percutaneous absorption. In: *Percutaneous Absorption*. Eds. Bronaugh, R. L. and Maibach, H. I. Marcel Dekker Inc. New York. pp133-139, (1985).

A. S. Michaels, Chandrasekaran, S. K. and Shaw, J. E. Drug permeation through human skin: theory and in vitro experimental measurement. *AIChE Journal*, **21** 985-996 (1975).

S. Monash. Location of the superficial barrier to skin penetrability. *J. Invest. Dermatol.* **29**, 367-376 (1957).

E. M. Niazy. Differences in penetration-enhancing effect of Azone through excised rabbit, rat, hairless mouse, guinea-pig and human skins. *Int. J. Pharm.* **130**, 225-230 (1986).

A. Pannatier, P. Jenner, B. Testa and J. C. Etter. The skin as a drug metabolising organ. *Drug Metab. Rev.* **8**, 319-343 (1978).

M. A. Pellett, A. C. Watkinson, J. Hadgraft and K. R. Brain. Comparison of permeability data from traditional diffusion cells and ATR-FTIR spectroscopy part I. Synthetic membranes. *Int. J. Pharm.* **154**, 205-215 (1997).

M. A. Pellett, M. S. Roberts and J. Hadgraft. Supersaturated solutions evaluated with an in vitro stratum corneum tape stripping technique. *Int. J. Pharm.* **151**, 205-214 (1997).

F. Pirot, Y. N. Kalia, A. L. Stinchcomb, G. Keating, A. Bunge and R. H. Guy. Characterisation of the permeability barrier of human skin in vivo. *Proc. Natl. Acad. Sci. USA.* **94**, 1562-1567 (1997).

M. Ponc, E. Boelsma, A. Mulder, A. Weerheim, J. Bouwstra, M. Mommaas. Lipid and ultrastructural characterisation of reconstructed skin models. *Int. J. Pharm.* **203**, 211-225 (2000a).

M. Ponc, A. Weerheim, P. Lankhorst, P. Wertz. New acylceramide in native and reconstructed epidermis. *J. Invest. Dermatol.* **120** (4), 581-588 (2003)

R. O. Potts and R. H. Guy. Predicting skin permeability. *Pharm. Res.* **9**, 663-669 (1992).

R. O. Potts and M. L. Francoeur. The influence of stratum corneum morphology on water permeability. *J invest. Dermatol.* **96** (4), 496-499 (1991).

M.B. Reddy, A.L. Stinchcomb, R.H. Guy and A.L. Bunge. Determining Dermal Absorption Parameters *In Vivo* from Tape Strip Data. *Pharm. Res.* **19**, 292-298 (2002).

S. Rothman. The mechanism of percutaneous penetration and absorption. *J. Soc. Cosmet. Chem.* **6**, 193-200 (1955).

A. Rougier, D. Dupuis, C. Lotte, R. Rouget and H. Schaefer. In vivo correlation between stratum corneum reservoir function and percutaneous absorption. *J. Invest. Dermatol.* **81**, 275-278 (1983).

R. J. Scheuplein and R. L. Bronaugh. *Percutaneous Absorption in Biochemistry and Physiology of the Skin*, Vol II. Ed. Goldsmith, L. A. Oxford University Press, New York. pp1255-1295 (1983).

R. J. Scheuplein and I. H. Blank. Permeability of the skin. *Physiol. Rev.* **51**, 702-747 (1971).

R. J. Scheuplein, I. H. Blank, G. J. Brauner and D. J. MacFarlane. Percutaneous absorption of steroids. *J. Invest. Dermatol.* **52**, 63-70 (1969).

R. C. Scott, P. H. Dugard and A. W. Doss. Permeability of abnormal rat skin. *J. Invest. Dermatol.* **86**, 200-207 (1986).

R. C. Scott, M. Walker and P. H. Dugard. A comparison of the in vitro permeability properties of human and some laboratory animals. *Int. J. Cosmet. Sci.* **8**, 189-194 (1986).

V. P. Shah, G. L. Flynn, A. Yacobi, H. I. Maibach, C. Bon, N. M. Fleischer, T. J. Franz, S. A. Kaplan, J. Kawamoto, L. J. Lesko, J-P. Marty, L. K. Pershing, H. Schaefer, J. A. Sequeira, S. P. Shrivastava, J. Wilkin and R. L. Williams. AAPS/FDA workshop report: Bioequivalence of topical dermatological dosage forms – methods of evaluation of Bioequivalence. *Pharm. Res.* **15**, 167-171 (1998).

J. P. Skelly, V. P. Shah, H. I. Maibach, R. H. Guy, R. C. Wester, G. L. Flynn and A. Yacobi. AAPS/FDA report of the workshop on principles and practices of in vitro percutaneous studies: relevance to bioavailability and Bioequivalence. *Pharm. Res.* **4**, 265-267 (1987).

A. L. Stinchcomb, F. Pirot, G. D. Touraille, A. L. Bunge and R. H. Guy. Chemical uptake into human stratum corneum in vivo from volatile and non-volatile solvents. *Pharm. Res.* **16**, 1288-1293 (1999).

R. B. Stoughton, W. E. Clendenning and D. Kruse. *J. Invest. Derm.* **35**, 52-63 (1960).

C. Surber and A. F. Davis. Bioavailability and Bioequivalence of dermatological formulations. In: *Dermatological and transdermal formulations*. Ed. Walters, K. A. Marcel Dekker Inc. New York. pp401-498 (2002).

U. Tauber and K. L. Rost. Esterase activity of the skin including species variation. *Pharmacol. Skin.* **1**, 170-183 (1987).

J. E. Treherne. The permeability of the skin to some non-electrolytes. *J. Physiol.* **133**, 171-180 (1956).

J. C. Tsai, S. A. Chaung, M. Y. Hsu and H. M. Sheu. Distribution of salicylic acid in human stratum corneum following topical application in vivo: a comparison of six different formulations. *Int. J. Pharm.* **188**, 145-153 (1999).

K. A. Walters, G. L. Flynn and J. R. Marvel. Physicochemical characterization of the human nail: I Pressure sealed apparatus for measuring nail plate permeabilities. *J. Invest. Dermatol.* **76**, 76-79 (1981).

A. C. Watkinson, H. Joubin, D. M. Green, K. R. Brain and J. Hadgraft. The influence of vehicle on permeation from saturated solutions. *Int. J. pharm.* **121**, 27-36 (1995).

R. C. Wester, P.K. Noonan, S. Smeach and L. Kosobud. Pharmacokinetics and bioavailability of intravenous and topical nitroglycerin in the rhesus monkey: estimate of first-pass metabolism. *J. Pharm. Sci.* **72**, 746-748 (1983).

R. K. Winkleman. The relationship of the structure of the epidermis to percutaneous absorption. *Br. J. Dermatol.* **81** (Suppl 4), 11-22 (1969).

Reference for Figures 1.1 and 1.2: The website of the *American Osteopathic College of Dermatology (AOCD)*, <http://www.AOCD.org/skin/>

- Chapter Two -

Non-steroidal Anti-inflammatory Drugs

2.1. Non-steroidal anti-inflammatory drugs: an overview

Non-steroidal anti-inflammatory drugs are among the most widely used of all therapeutic agents. They are frequently prescribed for rheumatic musculoskeletal complaints and are often taken without prescription for minor aches and pains. There are now over 50 NSAIDs on the market and none of these is ideal in controlling or modifying the signs and symptoms of inflammation, particularly those that occur in the common inflammatory joint diseases. Virtually all currently available NSAIDs, particularly the "classical" NSAIDs can have significant unwanted effects, especially in elderly patients. However, newer, more selective agents have fewer and less serious adverse reactions. NSAIDs include a variety of different agents of different chemical classes, but most of the drugs have three major types of effect:

- Anti-inflammatory effects: modification of the inflammation reaction
- Analgesic effect: reduction of pain
- Antipyretic effect: lowering of raised temperature

In general all of these effects are related to the primary action of the drugs – inhibition of arachidonate cyclooxygenase and thus inhibition of the production of prostaglandins and thromboxanes – though some aspects of the action of individual drugs may occur by different mechanisms. In addition, some drugs have actions other than those on inflammation. NSAID's are classified according to their chemical structure, the classifications are listed below:

- Salicylates
- Propionic acids (profens)
- Aryl and heteroarylacetic acids
- Anthranilates (fenamates)

- Oxicams ("enol acids")
- Phenylpyrazolones
- Anilides

In general, NSAID's consist of an acidic moiety (carboxylic acid or enol) attached to a planar, aromatic functionality. Some analgesics also contain a polar linking group, which attaches the planar moiety to an additional lipophilic group. Below is a representation of NSAID generic functionality:

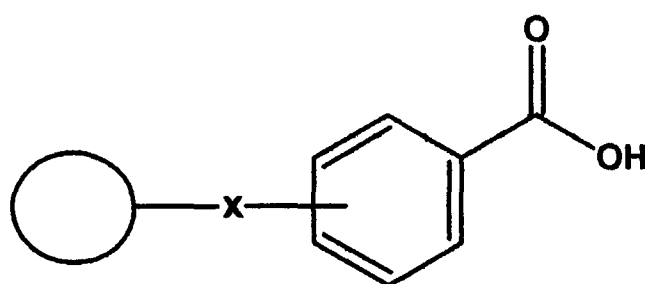


Figure 2.1. NSAID general chemical structure

As a result of their structure, the NSAID's are characterised by several chemical and pharmacologic properties. All are relatively strong organic acids with pK_a s in the 3-5 range, and most, but not all are carboxylic acids. Because of their acidic functionality, salts can be generated upon treatment with base and all NSAIDs are extensively ionised at physiological pH. Their ionisation properties are somewhat a concern when the pH of the skin is considered (approximately 5.5), as it is clear that they will be ionised at skin pH, which could affect their permeation behaviour. This is discussed in more detail later in this chapter.

NSAIDs span a range of lipophilicities, their lipophilicity is affected by the nature of the aryl groups and additional lipophilic moieties and substituents. The acidic group in all NSAIDs serves as a major binding group (ionic binding) with plasma proteins and, because of this, all are

highly bound by plasma proteins. The acidic group also serves as a major site of metabolism by conjugation, and therefore the main pathway for clearance for many NSAIDs is glucuronidation (and inactivation) followed by renal elimination.

2.2. Mode of action

As already stated, NSAIDs work by interfering with the cyclo-oxygenase pathway (figure 2.2). The normal process begins with arachidonic acid, a dietary unsaturated fatty acid obtained from animal fats, which is converted by the enzyme cyclo-oxygenase to synthesise prostaglandins. The prostaglandins go on to stimulate many other regulatory functions and reactionary responses in the body. Recent research has shown that the COX enzyme exists in two different forms; COX-1 and COX-2, and each type of cyclo-oxygenase lends itself to producing different types of prostaglandins. COX-1 enzyme is thought to mediate "housekeeping" or homeostatic functions, and COX-2 is induced in response to injury or inflammation. COX-2 inhibitors are "next generation" NSAIDs that may selectively block the COX-2 isoenzyme without affecting COX-1 function. This may result in control of pain and inflammation with a lower rate of adverse effects compared with older non-selective NSAIDs (such as those used in this project).

Expression of COX-2 is restricted under basal conditions, but it can be induced substantially during inflammation, repair and neoplasia. COX-1 is expressed constitutively and maintains normal physiologic functions of the cells in most tissues, but in a few situations COX-1 may also be induced. Both isoforms convert arachidonic acid to prostaglandin (PG). Depending on the site and circumstances of expression, the final PG product may vary.

2.2.1. Physiological effects of NSAIDs

Antipyretic effect

Normal body temperature is regulated by a centre in the hypothalamus that ensures a balance between heat loss and heat gain. Fever occurs

when there is a disturbance of this internal 'thermostat', which leads to the set-point of the body temperature being raised. NSAIDs reset the thermostat, and once the body has returned to its normal set-point, the temperature regulating mechanisms of the body (e.g. dilatation of superficial blood vessels, sweating) then operate to reduce temperature. Normal body temperature is not affected by NSAIDs. NSAIDs are thought to act as anti-pyretics through inhibition of prostaglandin production in the hypothalamus.

During an inflammation reaction, bacterial endotoxins cause the release of macrophages of a pyrogen – interleukin (IL-1) – which stimulates the generation, in the hypothalamus, of E-type prostaglandins (PGEs). These in turn cause the elevation of the set-point for temperature. It is thought that COX- has a role here since it is induced by IL-1 in blood vessel endothelium in the hypothalamus.

Analgesic effect

NSAIDs are mainly effective against pain associated with inflammation or tissue damage because they decrease production of prostaglandins that sensitise nociceptors to inflammatory mediators such as bradykinin (a vasoactive peptide, causes pain vasodilatation, spasm of smooth muscle). Because of this they are effective in arthritis, bursitis, pain of muscular and vascular origin, toothache, dysmenorrhoea, postpartum pain and the pain of metastases in bone – all conditions that are associated with increased prostaglandin synthesis. The ability of NSAIDs to alleviate headaches may be attributed to decreased prostaglandin-mediated vasodilatation.

Anti-inflammatory effects

Inflammation is a non-specific response of the immune system to damaged cells. There are many chemical mediators of the inflammatory and allergic response. Each part of the response (vasodilatation, increased vascular permeability, cell accumulation etc.) can be produced by several different mechanisms. Added to this, different mediators may be of particular importance in different inflammatory and allergic responses, and some mediators have complex interactions with others; for example, small amounts of nitric oxide (NO) stimulate cyclooxygenase, while large amounts inhibit it.

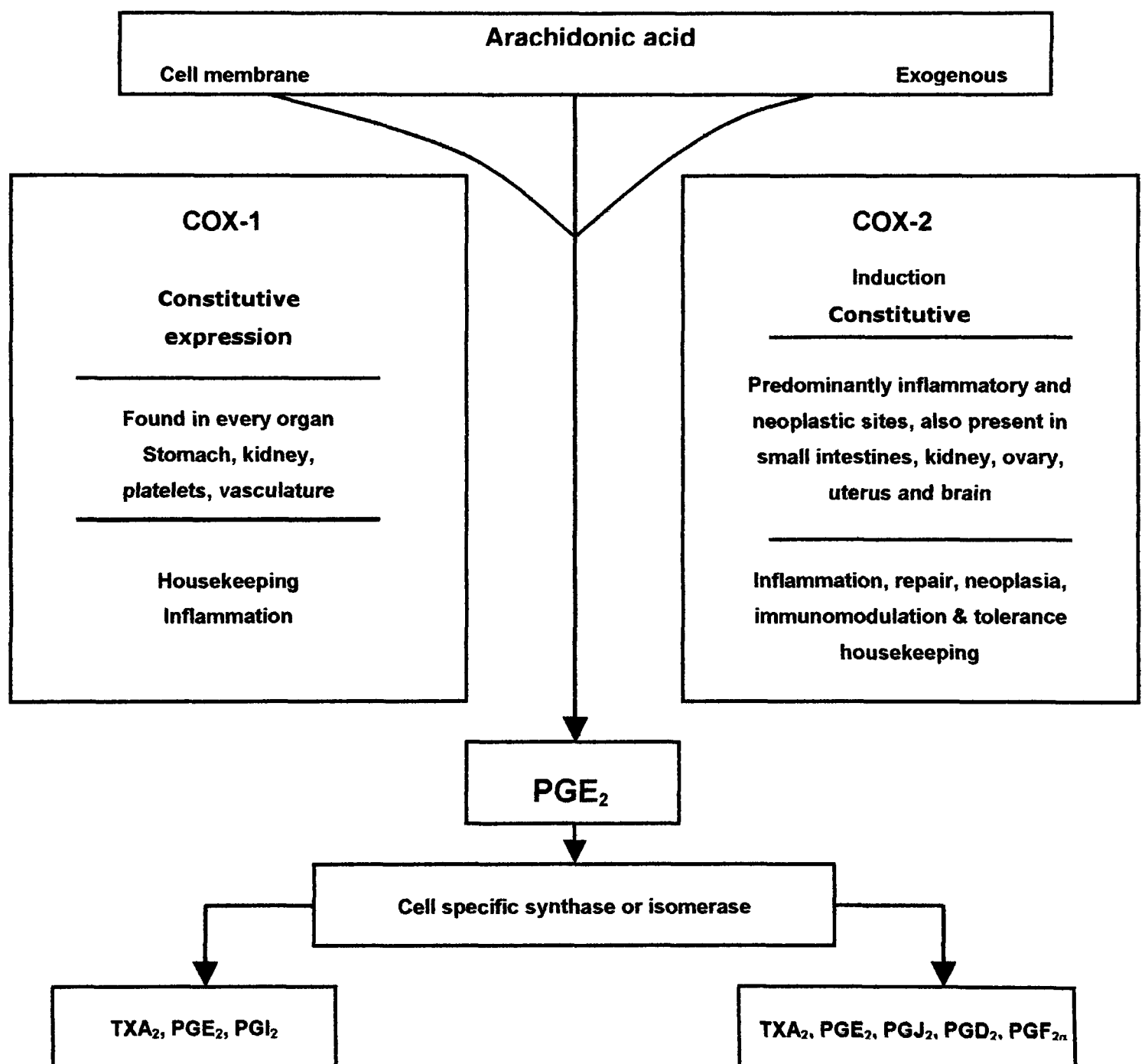


Figure 2.2. The cyclo-oxygenase pathway.

NSAIDs reduce the components of the inflammatory and immune response in which the products of COX-2 are involved; vasodilatation, oedema and pain. Prostaglandin E₂ (PGE₂) is the form of prostaglandin most associated with inflammation. It dilates blood vessels, allowing more blood to flow through the affected tissue, and the increased blood flow generates the heat and redness of inflammation. PGE₂ prolongs pain, and may also stimulate the emigration of phagocytes through capillary walls.

In an autoimmune disease, the body is inadvertently attacking its own cells through the inflammatory process as though they were foreign particles. So, by reducing the prostaglandin, swelling, heat and pain of inflammation is reduced. However, other parts of the inflammatory response, such as the destruction of healthy tissue by phagocytes, continue unabated in an autoimmune disease. X-ray crystallographic analysis has revealed that COX-1 and COX-2 are very similar enzymes consisting of a long narrow channel with a hairpin bend at the end, and having equal molecular weights. Both isoforms are membrane-associated so arachidonic acid released from damaged membranes adjacent to the opening of the enzyme channel, which is largely hydrophobic, is sucked into it. Once in the channel it is twisted around at the hairpin bend, two oxygens are inserted, and a free radical extracted, resulting in the five-carbon ring characteristic of prostaglandins (Hawkey, 1999).

Several studies have shown how and where NSAIDs act on cyclo-oxygenase to inhibit prostaglandin synthesis. Arachidonic acid is fluorescent, and quenching showed that NSAIDs block COX-1 about halfway down the channel. X-ray crystallography suggested that this blocking occurs by hydrogen bonding to the polar arginine at position 120. Arginine-120 is also present in COX-2. It is a nearby single amino acid

difference that is critical for selectivity of many drugs. This difference occurs at position 523, and is an isoleucine molecule in COX-1 and a valine (smaller by a single methyl group) in COX-2. The smaller valine molecule in COX-2 leaves a gap in the wall of the channel, giving access to a side pocket, which is thought to be the site of binding of many selective drugs. The bulkier isoleucine at 523 in COX-1 is large enough to block access to the side pocket. Most NSAIDs work by temporarily blocking the attachment site for arachidonic acid, but aspirin irreversibly acetylates the serine at position 530, completely inactivating the enzyme. It takes longer for the effects of aspirin to wear off because new enzymes must be synthesised to replace the altered enzymes. When COX-1 is acetylated by aspirin the site for arachidonic acid is blocked, however, when aspirin acetylates COX-2 the active site is still large enough to accept arachidonic acid. Acetylation also accounts for aspirin's anti-platelet effect, which helps prevent blood clots.

Table 2.1. Comparison of the properties of COX-1 and COX-2.

Function	COX-1	COX-2
Regulation	Constitutive	Inducible
Range of induced expression	2 to 4-fold	10 to 80-fold
Rate of gene activation	24 hours	0.5 to 4 hours
Effect of glucuronidation	Little or none	Inhibits expression
Relative size of active site	Smaller	Larger
Rate of arachidonic acid consumption	34nmol/min/mg	39nmol/min/mg
Effect of aspirin on COX activity	Inhibited	Not affected

Other NSAIDs also affect platelet production, but the effect is much milder. Interestingly, acetaminophen has only mild activity on COX-1 and COX-2,

yet it manages to reduce prostaglandin synthesis in the brain, relieving pain and fever, as does aspirin and the NSAIDs. It could be that acetaminophen is more specific to a third form of cyclo-oxygenase, a COX-3 which exists in the brain, accounting for the drug's analgesic or antipyretic properties (Basan and Flower, 2002).

Some NSAIDs have worse side effects than others, even though they may have the same amount of anti-inflammatory action. This is because of the specificity each drug has towards each form of COX. The classic NSAIDs have varying degrees of selectivity for COX-1 and COX-2 enzyme inhibition. Most drugs exhibit COX-1 rather than COX-2. When NSAIDs are ordered by their specificity to COX-1 those which are more selective also happen to be the drugs with the greatest side effects. A good example of this is aspirin, which is 160 times more specific to COX-1 than COX-2, and is well known for its ulcerative potential.

2.3. Model permeants

Three drugs, spanning a range of logP, were chosen to represent those that could be used therapeutically. These are acetaminophen (AM), salicylic acid (SA) and ibuprofen (IBU). All three are non-steroidal anti-inflammatory drugs (NSAID's) available OTC in Europe.

2.3.1. Acetaminophen

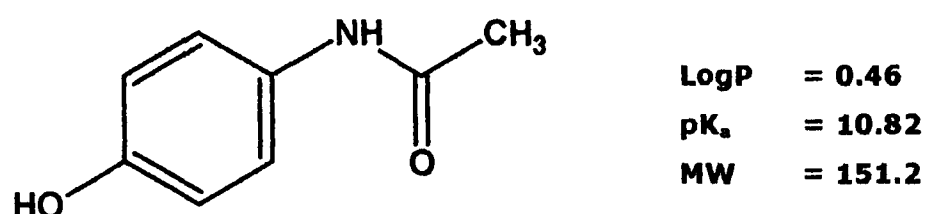


Figure 2.3. Physicochemical properties (obtained using ACD software) and chemical structure of acetaminophen

Acetaminophen belongs to the anilide class of NSAIDs. The anilides are simple acetamides of aniline which may or may not contain a 4-hydroxy or 4-alkoxy group. Acetaminophen is produced by oxidative-O-dealkylation of phenacetin. The anilides do not possess the carboxylic acid functionality and therefore they are classified as neutral drugs and possess little, if any, inhibitory activity against cyclooxygenase.

Mode of action

The anilides are a little different from other NSAIDs in their mechanism of action as they are believed to act as scavengers of hydroperoxide radicals, which are generated by invading leucocytes after injury has occurred. The hydroperoxide radicals have a stimulating effect on cyclooxygenase. In areas of high leukocyte activity (significant injury and inflammation) the high concentration of hydroperoxides are able to overcome the anilides and prostaglandins are produced. Therefore the anilides have no anti-

inflammatory action, they are only capable of suppressing cyclooxygenase activity in the anilides which imparts several advantages to these agents including limited gastric irritation and ulceration, limited cardiovascular and respiratory effects, and little effect on platelets (no increase in clotting).

One problem with the anilides is their toxicity. Because they are aromatic amines, they are capable of producing a number of problems including methemoglobinemia, anaemia, hepatotoxicity and nephrotoxicity. These toxicities are related to metabolic transformations that the anilides undergo. Under normal conditions, acetaminophen is metabolised by glucuronidation (primarily in adults) or sulfation (in children) of the hydroxyl function. Minor pathways of anilide metabolism include oxidation of the aromatic ring to the quinoneimine and hydrolysis and N-oxidation.

When acetaminophen concentrations are very high, as in overdose, formation of a toxic quinoneimine becomes significant. This is normally detoxified by conjugation with glutathione; however, if glutathione is depleted, alkylation of tissue nucleophiles may occur. Ethanol potentiates acetaminophen toxicity by a number of mechanisms.

2.3.2. Ibuprofen

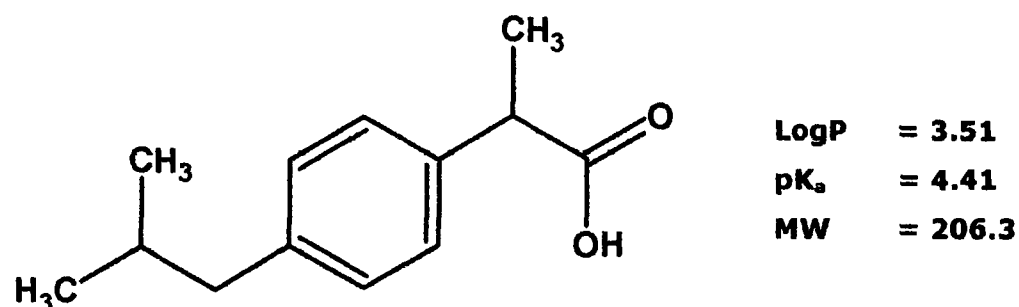


Figure 2.4. Physicochemical properties (obtained using ACD software) and chemical structure of ibuprofen

Ibuprofen belongs to a class of NSAIDs known as the propionic acid derivatives, or profens. Some of the most useful NSAIDs are structurally derived from arylacetic acids. These compounds are referred to as profens based on the suffix of the prototype member, ibuprofen. Like the salicylates, all profens are organic acids and so form water-soluble salts with alkaline reagents. The profens are predominantly ionised at physiological pH, and more lipophilic than aspirin or salicylic acid.

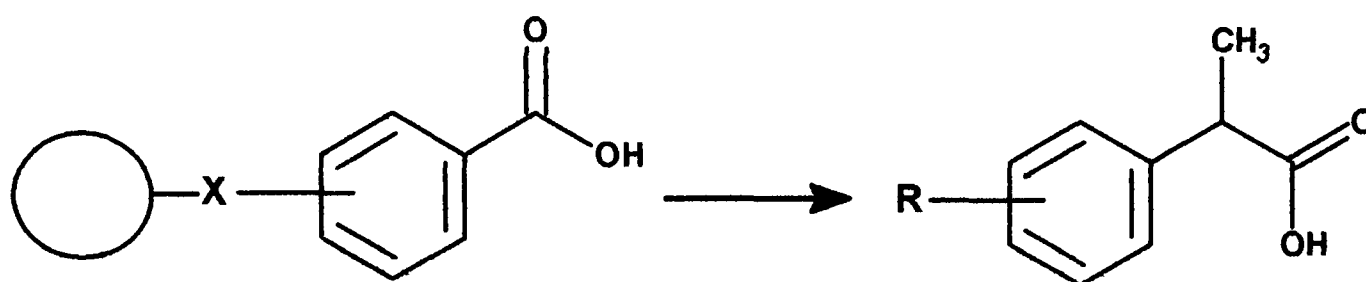


Figure 2.5. The conversion of an NSAID into a propionic acid derivative

The α -CH₃ substituent present in the profens increases the cyclooxygenase inhibitory activity and reduces toxicity. The α -carbon is chiral, the S-enantiomer being the more potent cyclooxygenase inhibitor. Most profen products (with the exception of naproxen) are marketed as racemates. This is not a matter for concern as the profens undergo metabolic inversion at the chiral carbon involving stereospecific transformation of the R-enantiomer to the active S-enantiomer. This is believed to proceed through an activated (more acidic α -carbon) thioester intermediate. Generally, only the S-enantiomer is present in plasma. Ibuprofen is formulated as tablets, sustained release tablets, suspensions, gels and creams which generally contain 5% ibuprofen. It has a half life of 2 hours.

Mode of action

Profens are anti-inflammatory agents with analgesic and antipyretic activity. The profens are considered to be slightly COX-1 selective, and are

used for treatment of rheumatoid arthritis, osteoarthritis and as analgesics and antipyretics. However, they should not be used during pregnancy or nursing as they can enter fetal circulation and breast milk. They produce considerably less GI irritation than the salicylates, but may cause thrombocytopenia, headaches, dizziness and fluid retention oedema.

2.3.3. Salicylic acid

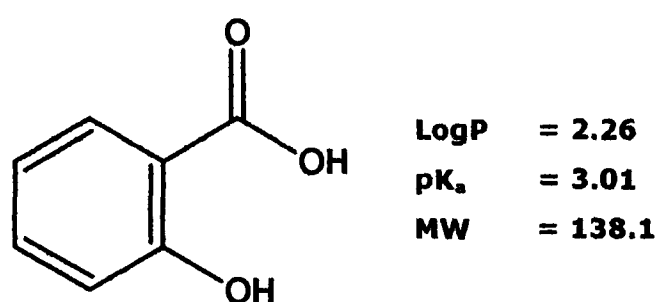


Figure 2.6. Physicochemical properties (obtained using ACD software) and chemical structure of salicylic acid.

Salicylic acid belongs to the class of NSAIDs known as salicylates, and is one of the oldest NSAIDs. It was in 1763 that Edward Stone first noticed that chewing the bark of the willow tree (*Salix Alba*) helped to relieve the chills and fever that are the symptoms of malaria but it was not until 1827 that the active ingredient, salicin was isolated. Just four years later a Swiss pharmacist, Johann Pagenstecher, distilled meadowsweet flowers (*Spirea salicifolia*) and obtained and characterised salicylaldehyde. In 1835 Karl Ludwig isolated salicylic acid from a mixture of products obtained from the alkaline hydrolysis of salicylaldehyde. After Herman Kolbe developed a convenient and inexpensive synthesis of salicylic acid in 1859 it was widely used as a medicine. However, it burned the mouth and to moderate the effects of the acidity it was administered as the sodium salt of salicylic acid, sodium salicylate. In the late 1800s it was replaced therapeutically by the acetylated derivative, acetylsalicylic acid (aspirin), which is still in use.

Salicylic is used on the skin where it exerts a slight antiseptic action and marked keratolytic action. It is this latter property which makes salicylic acid a beneficial agent in the local treatment of warts, corns and fungal infections. Tissues swell, soften and ultimately desquamate. Salicylic acid is applied in a 2 to 20% concentration in lotions or ointments and a 10 to 40% concentration in plasters.

Mode of action

The salicylates have potent anti-inflammatory activity with mild analgesic and antipyretic activities. These compounds are mainly COX-1 selective – they are bound with higher affinity by COX-1. Toxicities include GI irritation, hypersensitivity reactions, inhibition of platelet aggregation and ototoxicity (tinnitus).

2.4. Model formulations

Before describing the model formulations that were used in this work, it is important to gain an understanding of the different dermatological vehicles commonly used to treat skin diseases.

2.4.1. Formulation of dermatological vehicles

Day to day, many people apply lotions, creams, gels to their skin without a thought for their design. In this age of fighting the signs of ageing or disease, formulations are becoming increasingly sophisticated. The days of greasy ointments and sticky creams are gone, as consumers and patients demand products that not only feel good but also deliver their promise, be it relief from eczema or disappearance of wrinkles. However, formulators often develop such preparations for stability, compatibility, and patient acceptability rather than considering the influences that the components may have on drug bioavailability.

It is clear that the best way to approach the problem is to use fundamental permeation theories (Fick's Laws, alteration of K , D or h), while remembering that the treatment regimen and the state of the skin may alter the constraints of simple diffusion theory. The physician may want a topical application to provide several therapeutic effects as well as good absorption. These aims may include anti-inflammatory efficacy in acute inflammation, relief of pain and itch, protection from irritation as well as lubricant and emollient actions. Multi-component bases are generally used. A general rule for bases is that for wet lesions the patient should use an aqueous base, and for dry skin a lipophilic base is best. Most vehicles are blended from one or more of three main components; aqueous, powder and oil together with thickening and emulsifying agents, buffers, antioxidants, preservatives, colours, etc.

Liquid preparations

Liquid preparations for external application include simple soaks or baths, liniments, lotions and paints. A simple soak provides an active ingredient in aqueous solution or suspension, sometimes with water miscible solvents. Gums and gelling agents may alter the consistency from mobile liquids to stiff gels. Bath additives such as Oilatum Emollient deposit a layer of liquid paraffin on the stratum corneum in an attempt to maintain the skin's moisture content. Liniments may be oily or alcoholic solutions or emulsions which should not be applied to broken skin. Lotions are aqueous solutions or suspensions from which water evaporates to leave a thin, uniform coating of powder. Evaporation cools and soothes the skin, making lotions valuable for treating acutely inflamed areas. Alcohol enhances the cooling effect and glycerol sticks the powder to the skin. Lotions may also be dilute emulsions, usually of the oil-in-water type. Paints, varnishes and tinctures present solutions of active ingredients in volatile solvents such as water, industrial methylated spirits, acetone or ether.

Gels

Gels are two-component semisolid systems rich in liquid. Their one characteristic feature is the presence of a continuous structure, providing solid like properties. In a typical polar gel, a natural or synthetic polymer builds a three-dimensional matrix throughout a hydrophilic liquid. Typical polymers used include the natural gums tragacanth, carageenan, pectin, agar and alginic acid. Semi-synthetic materials include polymers such as methylcellulose, hydroxyethylcellulose, hydroxypropylmethylcellulose, carboxymethylcellulose, and the synthetic polymer carbopol. Provided that the active ingredient does not bind to the polymer, such gels release drugs well as the open molecular structure allows relatively rapid diffusion of small molecules.

Creams

Creams are semisolid emulsions for external application. Oil-in-water (o/w) emulsions are the most useful as water-washable bases whereas water-in-oil (w/o) emulsions are emollient and cleansing. Patients often prefer a w/o cream to an ointment because a cream spreads more readily, is less greasy and the evaporating water soothes the inflamed tissue. O/w creams ('vanishing' creams) rub into the skin; the continuous phase evaporates and increases the concentration of a water soluble drug in the adhering film. The concentration gradient across the stratum corneum therefore increases, promoting percutaneous absorption. To minimise drug precipitation a formulator may include a non-volatile, water-miscible cosolvent such as propylene glycol. An o/w cream is non-occlusive because it does not deposit a continuous film of water impervious liquid. However, such a cream can deposit lipids and other moisturisers onto and into the stratum corneum and so restore the tissues ability to hydrate, i.e. the cream has emollient properties.

It is extremely difficult to determine the role which an emulsion has in percutaneous absorption. This is because added to all the physiological and physicochemical considerations, there must also be a consideration of: the partitioning of the drug between the emulsion phases; the addition of preservatives; the determination of a true viscosity for the diffusing molecule in the vehicle and the possibility of phase inversion or cracking of the emulsion when it is applied to the skin. There may also be the possibility of the drug being trapped in micelles present in the continuous phase. Emulsions are complex systems and therefore all drugs must be considered individually with respect to emulsion design. Lastly, the nature of an emulsion changes with time as ingredients permeate and/or evaporate.

Ointments

Ointments are greasy, semisolid preparations, often anhydrous in nature and contain dissolved or dispersed drug.

Hydrocarbon bases

These usually consist of soft paraffin or mixtures with hard paraffin. Paraffins form a greasy film on the skin, inhibiting moisture loss and improving hydration of the horny layer in dry scaly skin conditions. The plastibases are a series of hydrocarbons containing polyethylene which forms a structural matrix in the systems which are fluid at the molecular scale but are typical dermatological semisolids. They are soft, smooth, homogenous, neutral, colourless, odourless, non-irritating, non-sensitising, extremely stable vehicles. Plastibases are compatible with most drugs and they maintain their consistency even at high concentrations of solids and under extremes of temperature. The bases apply easily and spread readily, adhere to the skin and impart a velvety, non-greasy feel and can be readily removed. Soap base greases may be produced by, for example, incorporating aluminium stearate in a heavy mineral oil.

Fats and fixed oil bases

Dermatological vehicles frequently contain fixed oils of vegetable origin, consisting of the mono- di- and triglycerides of mixtures of saturated and unsaturated fatty acids. The most commonly used oils include peanut, sesame, olive and almond. The problem with the use of these oils is their decomposition upon exposure to air, light and high temperature, causing them to turn rancid. Trace metal additives catalyse oxidative reactions, but this can be overcome using antioxidants such as butylated hydroxytoluene, butylated hydroxyanisole or propyl gallate, or with chelating agents such as the salts of ethylenediaminetetra-acetic acid (EDTA). However, there is

always the possibility of antioxidants being incompatible with the drug, or sensitising in patients.

Silicones

Dimethicones or dimethyl polysiloxanes have properties similar to hydrocarbon bases. They are water repellent with a low surface tension and are incorporated into barrier creams to protect the skin against water-soluble irritants. Silicones are often added to products because they have excellent cosmetic feel, which imparts the idea of luxury to a consumer.

Absorption bases

Absorption bases soak up water to form water-in-oil emulsions while retaining their semisolid consistency. Generally they are anhydrous vehicles composed of a hydrocarbon base and a miscible substance with polar groups which function as a water-in-oil emulsifier (e.g. lanolin, mono-oleate, cholesterol or other sterols). Bases such as these deposit a greasy film on the skin similar to a hydrocarbon base but they suppress less the transepidermal water loss.

Emulsifying bases

These are essentially anhydrous bases that contain oil-in-water emulsifying agents which make them miscible with water and so washable or 'self-emulsifying'. There are three types of emulsifying base: anionic, cationic and non-ionic. Because they contain certain surfactants, emulsifying bases may help to bring the drug into contact with the skin. The bases mix with aqueous secretions and readily wash off the skin, and for this reason they are particularly useful for treating the scalp.

Water soluble bases

Water soluble bases are prepared from mixtures of high and low molecular weight polyethylene glycols (macrogels, carbowaxes). Suitable combinations provide products with an ointment-like consistency which soften or melt when brought into contact with the skin. They are non-occlusive, mix readily with skin exudates and do not stain sheets or clothing. The macrogels do not hydrolyse, deteriorate, support microbial growth or irritate the skin, making them ideal formulation components. Because they are water soluble they will not take up more than 8% of an aqueous solution before losing their desirable physicochemical properties. To enable a base to incorporate more water, stearyl alcohol is often substituted for the macrogel component. Macrogel bases have been used with local anaesthetics such as lignocaine.

2.4.2. Model formulations

Bearing in mind that the three selected permeants span a range of logP, it was clear that the model formulations would need careful selection. To begin with, simple systems were chosen that would give the best chance of understanding the complex interactions that occur between solvent, solute and membrane. Taking this into account, and building on the work of Katz and Poulsen (1971), the first model formulations tested were binary solvent systems. Two sets of vehicles, one hydrophilic and one lipophilic were the starting point of this project. The solvents selected were propylene glycol (PG), water, mineral oil (MO) and miglyol (MG), with combinations of PG-water forming the basis of hydrophilic formulations and MO-MG combinations being lipophilic.

For a vehicle to be more representative of a pharmaceutical formulation it would need to contain more than two solvents, therefore a third solvent

was added to the hydrophilic vehicle. In one ternary combination a volatile solvent (ethanol) was added, whilst another system contained a 'genuine' solvent (Transcutol).

2.4.3. Background information about model vehicles

Propylene glycol

Propylene glycol is a commonly used solvent in topical formulations and an effective cosolvent for other penetration enhancers (e.g. Azone, polar lipids and terpenes). Propylene glycol fulfils several requirements for an ideal enhancer as it is non-volatile and has good solvent properties for many hydrophilic as well as lipophilic drugs. It is a small molecule that is known to transfer through the skin and thought to act by increasing the solubility of the permeant in the membrane.

Propylene glycol is a component of commercial lotions and creams and gels.

Diethylene glycol monoethyl ether (Transcutol™)

Transcutol solubilizes many very poorly-soluble drug actives, for formulation in liquid or capsule formulations. In terms of topicals and transdermal delivery it is a very effective penetration enhancer and is able to increase the solubility of the drug in the skin (Harrison et al, 1996). It can be incorporated into all types of emulsions, solutions and gels.

Mineral oil

Mineral oil is a component of a wide range of skin formulations. It is found in creams, ointments, gels, lotions and bath oils. Generally it is added to increase the emollient properties of the formulation, and to add to the 'richness' or moisturizing benefit of a product.

Fractionated coconut oil (Miglyol)

The main benefit of fractionated oil is that specific fatty acids can be separated or combined for particular applications. Its main constituents are caprylic acid, capric acid, caproic acid, lauric acid and myristic acid. Caprylic acid and capric acid are present in the greatest quantity (~50-60% and 30-45% respectively). The other acids normally make up the remaining 6-10% between them. It is water-clear, light in texture, odourless, tasteless and has an indefinite shelf life. Miglyol is a vegetable alternative to mineral oil. Fractionated coconut oil is coconut oil with the naturally occurring stearic acid removed so that it is liquid at room temperature. It is often incorporated to reduce the "greasy feel" of lotions.

2.5. Physicochemical characterisation of model permeants

2.5.1. Theoretical background: pH, pK_a and Sirius GlpKa™

Knowledge of the aqueous ionisation constant, pK_a, of a substance is very important in the pharmaceutical industry. The pK_a of a molecule predicts its degree of ionisation at a particular pH. This in turn affects the availability of a chemical to enter into physical, biological and chemical reactions. The pK_a will affect the absorption, distribution and elimination of medicinal substances. Usually it is the unionised form of an organic substance that is capable of entering and passively diffusing through lipid cell membranes of organisms. The distribution of a molecule between the organic and aqueous solution can be described by the partition coefficient, P (or K_{ow}), which is the ratio of the concentrations of a molecule dissolved at equilibrium in the two miscible phases. It is often expressed in the logarithmic form as logP. n-octanol is widely used as a model for the lipid phase in partition coefficient measurements.

Partition coefficient values have many applications in pharmacy. The logP of a substance is a critical parameter in quantitative structure activity relationships (QSAR) (Hansch 1969). It can be used to correlate and predict biological activity of drugs and the bio-concentration of substances in aquatic and terrestrial organisms. Measuring pK_as and logP can be difficult and problematic, since many new substances of interest are very poorly soluble in water. Potentiometry can be a quick technique for pK_a determination (Albert and Serjeant 1984), provided the solubility of the substance is at least 10⁻⁴M over a suitable pH range. Solutions as dilute as 10⁻⁵M can still be analysed, but special attention must be given to electrode calibration, and ambient CO₂ must be excluded (or corrections for its presence must be incorporated). If the substance is only soluble to

the extent of 10^{-6} M and possesses an analytically useful chromophore, then spectroscopic methods can be applied. If the compound is water-insoluble, then a mixed solvent approach can be tried. There are various methods for measuring pK_a values but potentiometry is widely used because it is fast, accurate and reproducible (Albert and Serjeant, 1984). Indeed, the only hindrance to the use of this technique is low water solubility of the sample. By using a good quality glass electrode and performing proper calibration, potentiometry can be applied to concentrations as low as 10^{-4} M. But, it follows that at low concentrations, accuracy and reproducibility will be compromised.

In situations where there is low water solubility, a mixed solvent approach is used. This method is based on the measurement of apparent ionisation constants (p_sK_a) in different ratios of organic solvent/water mixtures where the aqueous phase pK_a is obtained by extrapolation. The organic solvents frequently employed are methanol, ethanol, propanol, DMSO and THF. Methanol is by far the most characterised of these solvents, with much literature accumulated for MeOH/water solvent mixtures. It is also commonly accepted that methanol shows a solvation effect closest to that of water and therefore methanol is normally the organic solvent of choice (Avdeef et al., 1993).

Since many substances of interest in the pharmaceutical industry are insoluble in water, it is necessary to use mixed solvents to study them. The organic solvents of interest are of lower dielectric strength than water.

The addition of such a solvent to water affects equilibria in the following ways:

- the activity of water decreases
- the ionisation constant of water, pK_w , increases
- the activity coefficients of ions decrease because they depend on the dielectric constant of the solvent
- Equilibrium reactions leading to an increased charge are thus less favoured.

It is vital to calibrate the glass electrode to obtain good quality data from potentiometric experiments. Avdeef and co-workers (1993) have developed a "four parameter" calibration procedure, which they claim provides very reliable pK_a determination in MeOH/water (and other) solvent systems. According to the Yasuda-Shedlovsky method, a linear correlation is established in a plot of $p_sK_a + \log [H_2O]$ versus $1/\epsilon \times 1000$. The "apparent" aqueous pK_a is calculated by extrapolation to 0% co-solvent. This is explained in greater detail in the results section.

Titration with a pH electrode

In order to assess the ionisation behaviour of the weak acids, and the extent to which the formulation would affect this behaviour, pH-metric titration were carried out using the Sirius equipment. The background to this type of experiment is introduced in the following section.

The Sirius uses a pH-metric titration to determine pK_a and $\log P$. This means a volumetric analysis where precisely known volumes of a standardised strong acid or base are added to a solution of a protogenic substance. During the addition of acid or base, pH is continuously measured with a combination glass electrode within the pH interval

selected. Specifically, an alkalimetric titration uses base as a titrant, and acidimetric is the reverse. The substance being analysed is dissolved in water or in a mixed solvent consisting of either water plus an organic water-miscible solvent or water plus an organic water-immiscible solvent. An inert water-soluble salt is added to the solution to improve the measurement precision. The plot of pH against the volume of titrant added is called a potentiometric titration curve. The shape of such a curve indicates the acid-base ionisation properties of a substance. The inflection points corresponding to where the slope is at its maximum magnitude are called endpoints. The inflection points where the slope is at a minimum magnitude indicate regions of maximum buffering capacity.

Titration curves are plotted as pH vs. mL (volume added) data. Although features in the curves can be recognised, complete quantitative interpretations are not possible when volume units are used. To derive more information it is necessary to transform the volume units into "base equivalents", B_e . These are "normalised" volume units, and are defined as moles of strong base added minus moles of strong acid added, divided by moles of sample substance present. The advantage of B_e plots is that endpoint and mid-buffer points still have their original meaning but they are more easily located as the integral and $1/2$ -integral B_e respectively. Sometimes it is possible to read the approximate pK_a s directly from the pH vs. B_e plots. In the presence of a water-immiscible organic solvent, the two-phase titration can indicate the amount of substance dissolved in the organic phase at a particular pH, from which a partition coefficient can be determined.

Difference Plots

Difference plots are a way of counting the protons, detecting discrepancies and balancing the mass balance expressions, to make sure that the overall statement of ionisation is correct so that the later application of least squares refinement may be made with confidence. To estimate pK_a or p_sK_a it is often more convenient, and sometimes necessary to use the difference curve rather than the titration curve. The difference curve is a plot of η_H , the average number of bound protons (the hydrogen ion binding capacity), versus p_cH ($= -\log[H^+]$). The difference curve can also be used as a diagnostic tool, which can reveal sample concentration errors, acid/base errors, presence of unsuspected chemical impurities, electrode performance problems, or invalid assumptions in the model describing the equilibrium reactions. Difference curves were first used in the 1940's, and they are often called formation curves or Bjerrum plots. An example of a Bjerrum plot is shown in figure 2.7.

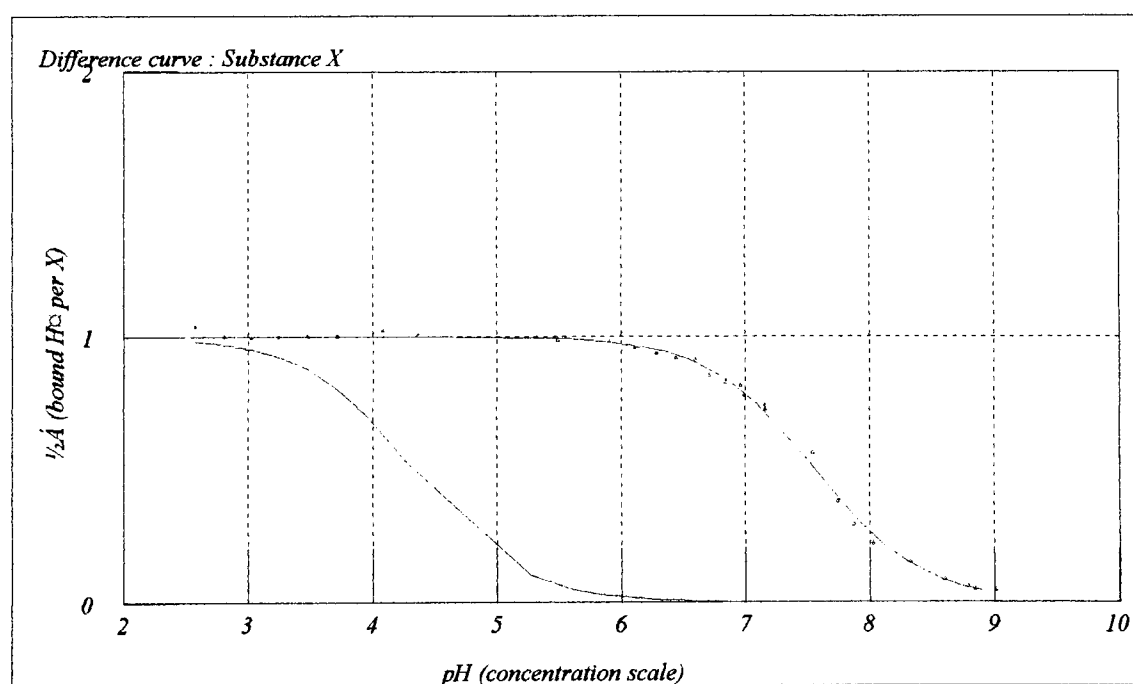


Figure 2.7. Example of a Bjerrum difference curve (STAN vol. 1, 1994).

Effect of octanol on the difference function

The pH metric technique consists of two linked titrations. Typically, a pre-acidified solution of a weak acid is alkalimetrically titrated to some appropriately high pH; octanol (or any other useful organic partition solvent that is immiscible with water) is then added, and the dual-solvent mixture is acidimetrically titrated back to the starting pH. After each titrant addition the pH is measured. If the weak acid partitions into the octanol phase, the two titrations show non-overlapping pH vs. base equivalent curves. The greatest divergence will occur in the buffer region, and since the pK_a is approximately equal to the pH at the mid-buffer inflection point, the two-part assay produces two constants: pK_a and p_oK_a , where p_oK_a is the apparent constant derived from the octanol containing segment of data. A large difference between pK_a and p_oK_a indicates a large value of $\log P$. Difference plots based on titrations of substances in octanol-water solution are valuable for developing partition equilibrium models. For multiprotic substances, it is particularly useful because the difference plots can identify neutral-species and ion-pair partitioning. For a monoprotic weak acid (such as ibuprofen), which partly dissolves in water and a water-immiscible partition solvent (e.g. octanol), the partition coefficient is defined as:

$$P_{HA} = [HA]_{org} / [HA] \quad (\text{Eqn. 2.1})$$

where $[HA]$ is the weak acid aqueous concentration and $[HA]_{org}$ is the concentration in the oil phase. For this simple system, the relation between $\log P$ and pK_a is

$$P_{HA} = (10^{+(p_oK_a - pK_a)} - 1) / r \quad (\text{Eqn. 2.2})$$

Where

$$r = \frac{Vol_o}{Vol_{aq}} \quad (\text{Eqn. 2.3})$$

If the two phases are equal in volume and the substance is lipophilic, then $\log P_{HA} \approx (p_oK_a - pK_a)$. For a weak base partitioning the corresponding equation is:

$$P_B = (10^{-(p_oK_a - pK_a)} - 1) / r \quad (\text{Eqn. 2.4})$$

Similarly, for equivolume titrations of lipophilic bases, $\log P_B \approx -(p_oK_a - pK_a)$

The effect of ionic strength on the measured logP of neutral species is usually found to be negligible under physiological conditions.

2.6. Methods

2.6.1. Solubility study

Adequate lipid and water solubility are important criteria for predicting optimal topical delivery of drugs. The drugs must be able to diffuse through the lipid-aqueous bilayers of the skin for effective topical absorption. For this reason the solubility of the three permeants in all the vehicles and vehicle combinations were determined by the method outlined below.

Excess drug was added to each solvent or co-solvent mixture and stirred with a magnetic bar for 48 hours (to attain equilibrium) in a water bath maintained at 32°C. Solutions were centrifuged for 15 minutes at 10 000rpm. The supernatant was then diluted and assayed either by HPLC or UV spectroscopy. For experiments using oily vehicles, samples had to be diluted in a solvent that would completely dissolve the mineral oil and the Miglyol. For HPLC analysis the sample was diluted 1:10 in isopropanol, followed by appropriate dilution in methanol. UV analysis was conducted using hexane. Experiments were performed in triplicate and mean values with standard deviation and coefficient of variation were calculated. The HPLC system used for this work did not have the facility for temperature modulation, therefore the system ran at ambient room temperature.

2.6.1.1. Saturated solubility in pH controlled solutions

The solubility of a drug in a vehicle is a very important factor in percutaneous penetration. The pH of the vehicle will determine the ionisation state of the permeant and may therefore control its rate of penetration, because differently ionised species will permeate at different

rates. In the lipophilic environment of the stratum corneum an ionised species would be expected to permeate at a slower rate than an un-ionised species. The solubility of ibuprofen and salicylic acid in citrate-phosphate buffer over the range pH 2-7 has been determined. The effect of ionic strength has not been investigated. Excess drug was added to 10mL of a phosphate-citrate buffer controlled solution and stirred with a magnetic bar for 48 hours in a water bath maintained at 32°C. Solutions were centrifuged for 30 minutes at 10,000 rpm. The supernatant was diluted and assayed by UV spectroscopy. Experiments were performed in triplicate and mean values with SD and CV were calculated.

2.6.1.2. Buffer solutions for pH controlled experiments

Phosphate-citrate buffer was used to control the pH of saturated solutions of drug. These were prepared using the method below.

Table 2.2. Citrate/phosphate buffer (proportions to give 100mL)

PH	0.2M Na₂HPO₄	0.1M citric acid
3.0	20.5	79.5
4.0	37.0	63.0
5.0	49.3	50.7
6.0	62.1	37.9
7.0	82.3	17.7

For experiments in which the ionic strength was to be controlled, 3M NaClO₄ was added to the buffer solutions.

2.6.2. Sirius GLpK_a

Because of the low solubility of the chosen permeants, it was necessary to use a co-solvent technique to determine pK_as. The procedure is as follows:

Blank-standardisation

An empty vial was placed in the sample holder and the automated blank standardisation procedure was initiated. This is the most common method for pH electrode standardisation. The Sirius adds water to the vial, measures pH to determine CO₂ content, it then adds acid titrant to lower the pH to 1.8 and then titrates with base. Using the dedicated software, the Four plus™ parameters that describe the pH electrode can be determined, and used as a reference for pK_a and logP determinations. An example is shown in figure 2.8.

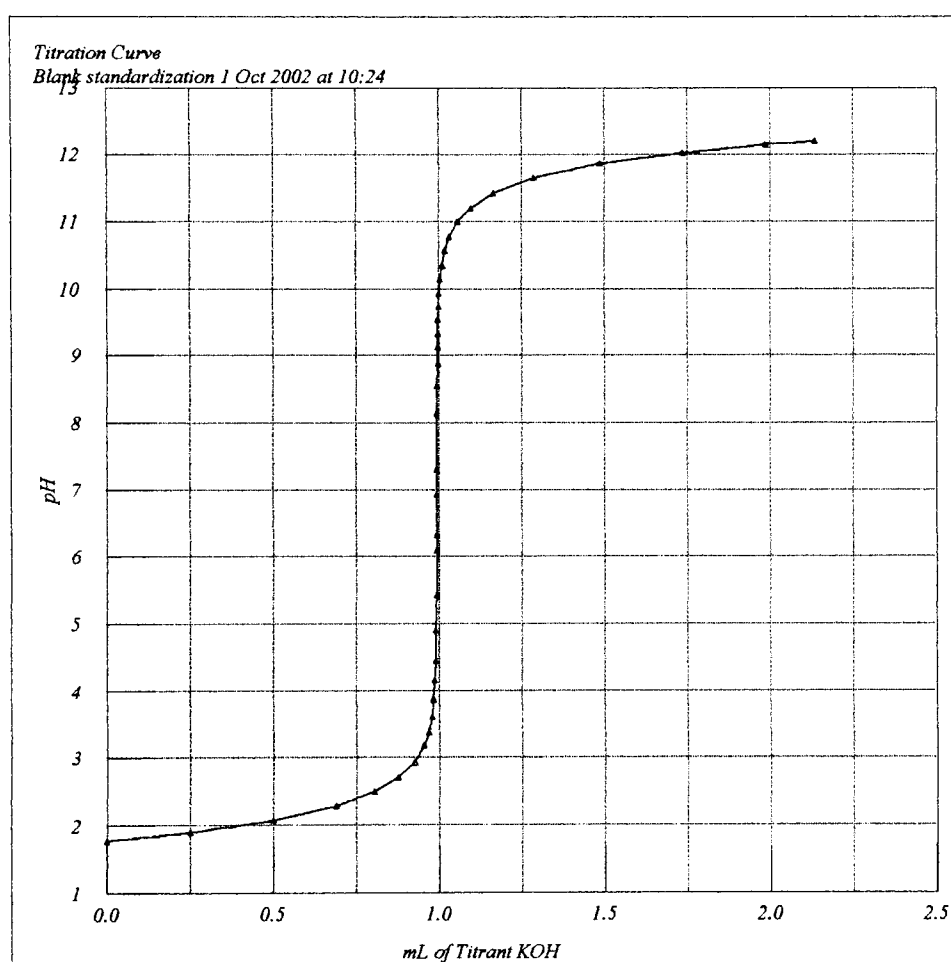


Figure 2.8. Typical blank standardisation plot (pH vs. mL data)

Mixed solvent procedures

Water insoluble samples can be titrated in solution in mixtures of water with co-solvents such as methanol. From these titrations, p_sK_a values (apparent pK_a values in the presence of co-solvent) can be calculated. The

Yasuda-Shedlovsky extrapolation procedure can be used to calculate "aqueous" pK_a values from two or more p_sK_a values determined at different water-co-solvent ratios. Where possible methanol is the co-solvent of choice because its general effect on pK_a s has been studied extensively; it is the least "error-prone" of the common co-solvents. For the correct calculation of p_sK_a values, Four plus™ pH electrode standardisation parameters valid at the same water/co-solvent ratio as the sample, titration must be used in the refinement of data.

The methanol used in this procedure must be of controlled ionic strength, using an appropriate salt dissolved and made up to the same ionic strength as the ionic-strength adjusted "water". In this case the ionic strength was set at 0.15M with KCl. A suitable water volume was chosen, along with a suitable "pre-dose" of methanol. The volume of methanol requested will be added such that the sum of the volume of methanol plus the volume of water is equal to the volume of the total aqueous phase.

Once all these parameters have been determined and recorded, an appropriate amount of sample was weighed into the vial and placed in the autosampler tray of the Sirius. The GlpK_a software contains a program that recommends a sample weight to be used in assays, for all experiments this recommended sample weight was used.

LogP determination

The sample was weighed into a vial and a measured volume of partition solvent was added. The automated assay procedure was initiated. A typical plot obtained from a logP determination is shown in figure 2.9.

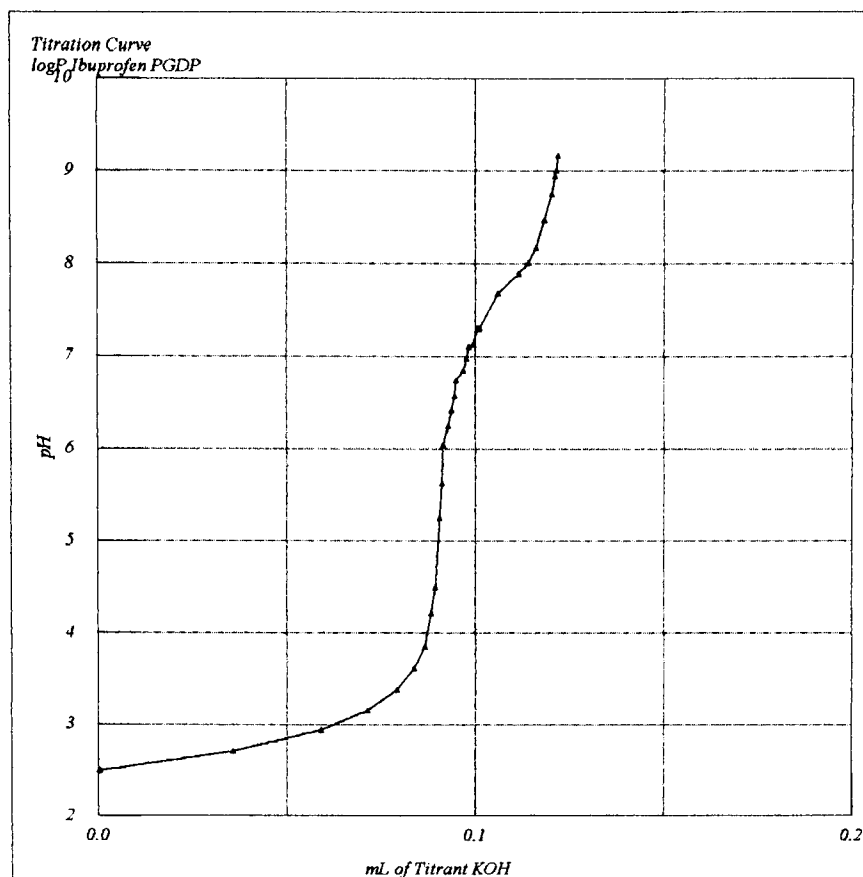


Figure 2.9. Typical plot from a partitioning experiment using ibuprofen in PGDP/buffer (pH vs. mL data).

Data refinement

Data from experiments were refined using a non-linear least-squares refinement.

2.7. Results

2.7.1. Solubility study

Ibuprofen

The solubility of ibuprofen in the solvents studied was determined as described in section 2.8.1 Tables 2.3 to 2.7 show the solubilities expressed in mg/mL, and the standard deviation associated with each experiment. The experiments were performed in triplicate.

Table 2.3. Solubility of ibuprofen in propylene glycol and water vehicles.

% Propylene glycol in vehicle (v/v)	Solubility (mg/mL)	Standard deviation (n=3)
0	0.09	0.06
10	0.06	0.02
20	0.11	0.03
30	0.16	0.04
40	0.47	0.06
50	0.92	0.78
60	3.48	0.25
70	11.24	0.42
80	36.67	10.47
90	94.96	7.41
100	157.69	26.63

The unit cell of racemic crystalline ibuprofen consists of rigid molecules paired off as hydrogen-bonded (R)-(S) dimers. From the table above it can be seen that the solubility of ibuprofen increases with increasing proportion of propylene glycol. This result is not surprising since propylene glycol is used as a solvent in pharmaceutical formulations to increase solubility. Ibuprofen molecules are able to take part in hydrogen bonding with

solvents through the carboxylic group of the molecule, and it is likely that this is where ibuprofen interacts with propylene glycol.

Table 2.4. Solubility of ibuprofen in ethanol and water vehicles.

% Ethanol in vehicle (v/v)	Solubility (mg/mL)	Standard deviation (n=3)
0	0.09	0.056
25	342.72	6.50
50	452.85	21.26
75	488.73	20.05
100	499.68	4.12

Ibuprofen shows high solubility in ethanol. Addition of just 25% ethanol increases the solubility to 342.72 mg/mL, almost 4000 fold higher than its aqueous solubility. In pure ethanol the solubility is 5500 fold higher than in water, demonstrating the incredible solvent power of ethanol.

Table 2.5. Solubility of ibuprofen in mineral oil and miglyol vehicles.

% Mineral oil in vehicle (v/v)	Solubility (mg/mL)	Standard deviation (n=3)
0	151.60	17.69
10		
20	167.63	0.43
30	125.12	25.73
40	140.19	33.76
50		
60	115.73	15.22
70	85.73	6.26
80	53.61	22.14
90	59.26	7.33
100	31.99	3.44

Ibuprofen has higher solubility in mineral oil than in miglyol. In mineral oil, it is likely that ibuprofen would self associate through intermolecular bonds to form dimers and therefore although the molecule does have some polar nature, the polar -COOH ends of the molecule will be 'protected', giving the dimer non-polar characteristics, providing a more favourable interaction with mineral oil (non-polar vehicle).

Table 2.6. Solubility of ibuprofen in Transcutol and propylene glycol vehicles.

% Transcutol in vehicle (v/v)	Solubility (mg/mL)	Standard deviation (n=3)
0	0.09	0.056
25	338.57	36.10
50	393.69	29.55
75	460.39	28.54
100	432.98	21.37

As for ethanol, ibuprofen is ~5000 fold more soluble in Transcutol than water. Like propylene glycol, Transcutol is often added to formulations to increase solubility.

Table 2.7. Solubility of ibuprofen in solutions of differing pH

pH	Solubility (mg/ml)
2.0	0.028
3.0	0.031
4.0	-
5.0	0.4
6.0	1.3

Ibuprofen has a pK_a of 4.41, and therefore pH will have a significant influence on solubility As ibuprofen is ionised, the carboxylic acid moiety is

better able to interact with water molecules, increasing the solubility. Data were only collected in the range pH 2-7, as this range is most relevant with respect to the skin physiology. Below pH 2, and above pH 8 there is the possibility that skin may become irritated and therefore topical formulations are always buffered as near to the natural pH of the skin as is possible.

Salicylic acid

The solubility of salicylic acid in the solvents studied was determined as described in section 2.8.1 Tables 2.8 and 2.9 show the solubilities expressed in mg/mL, and the standard deviation associated with each experiment. The experiments were performed in triplicate.

Table 2.8. Solubility of salicylic acid in propylene glycol and water vehicles.

% Propylene glycol in vehicle (v/v)	Solubility (mg/mL)	Standard deviation
0	0.76	0.80
10	1.67	0.44
20	3.12	0.52
30	3.31	0.21
40	6.69	0.17
50	15.57	2.31
60	16.07	1.13
70	40.78	2.37
80	81.01	6.20
90	122.74	15.77
100	168.44	7.15

Salicylic acid has relatively low water solubility, which is increased upon addition of propylene glycol as a co-solvent. There is approximately 200-

fold difference in the solubility of salicylic acid between water and pure propylene glycol.

Table 2.9. Solubility of salicylic acid in mineral oil and miglyol vehicles.

% Mineral oil in vehicle (v/v)	Solubility (mg/mL)	Standard deviation
0	41.53	2.39
10	35.8	1.34
20	33.59	0.66
30	30.78	1.33
40	21.46	4.35
50	19.72	1.90
60	13.42	3.43
70	10.45	1.35
80	4.99	0.04
90	2.24	0.05
100	0.24	0.06

Although salicylic acid is capable of intra-molecular hydrogen bonding, it does not self-associate to form dimers as ibuprofen does. Because of this, the molecule will always retain a degree of polarity, and will not interact to any great extent with non-polar solvents such as mineral oil. It is not clear why the solubility in miglyol is low, as it contains fatty acids, capable of participating in hydrogen bonding.

Table 2.10. Solubility of salicylic acid in solutions of differing pH.

PH	Solubility (mg/ml)
2.0	5.01
3.0	6.9
4.0	17.45
5.0	20.24
6.0	27.5

The pK_a of salicylic acid is ~ 3 . The data in figure 2.10 show that above pH 3 the solubility of salicylic acid increases, corresponding to the change in ionisation of the molecule. At pH 6.0 salicylic acid is almost entirely ionised and there has been a 5-fold increase in solubility.

Acetaminophen

The solubility of acetaminophen in propylene glycol, water and varying ratios of the two is shown in table 2.11. This study on the solubility characteristics of acetaminophen resulted in some interesting and unexpected findings. It was discovered that when acetaminophen is dissolved in a hydrogen bonding solvent (in this case propylene glycol, water or a mixture of the two) the solution turns a pink colour. This behaviour has been reported by Sherwood *et al.* who have extensively studied the crystallization of acetaminophen in aqueous solution. The pink colour is a result of hydrolysis of acetaminophen to *p*-aminophenol, which further oxidises to a conjugated quinoid species. If left for a sufficiently long period (~ 1 month) the solution turns a brown colour. Because of their basic nature, amines are oxidised with ease, and it is this property of the *p*-aminophenol oxidation product that causes the main problem with the use of acetaminophen. Once the oxidation reaction is underway there are many further oxidation steps, and all result in products that tend to contaminate what was once a pure batch of acetaminophen.

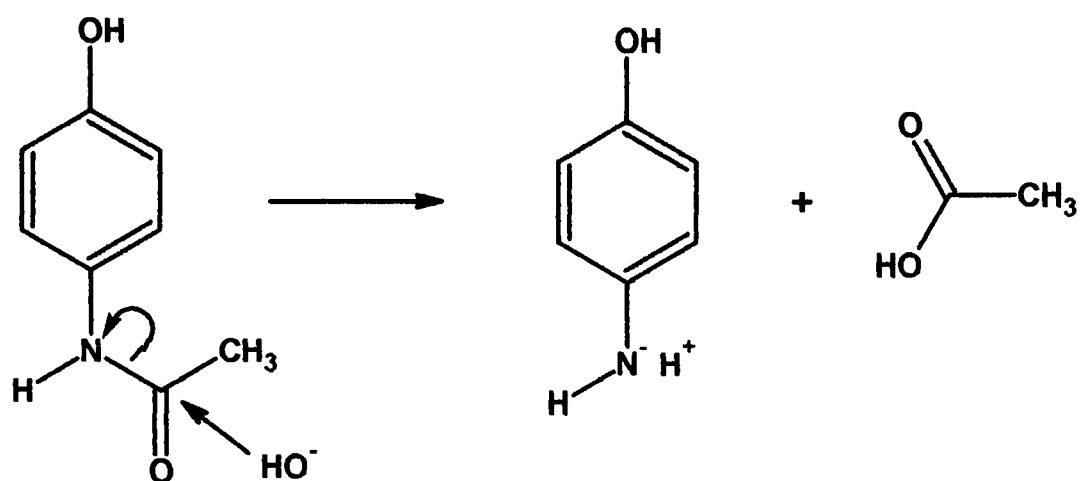


Figure 2.10. Mechanism of hydrolysis of acetaminophen.

The product can exist in a many forms, three of the most likely are shown in figure 2.11.

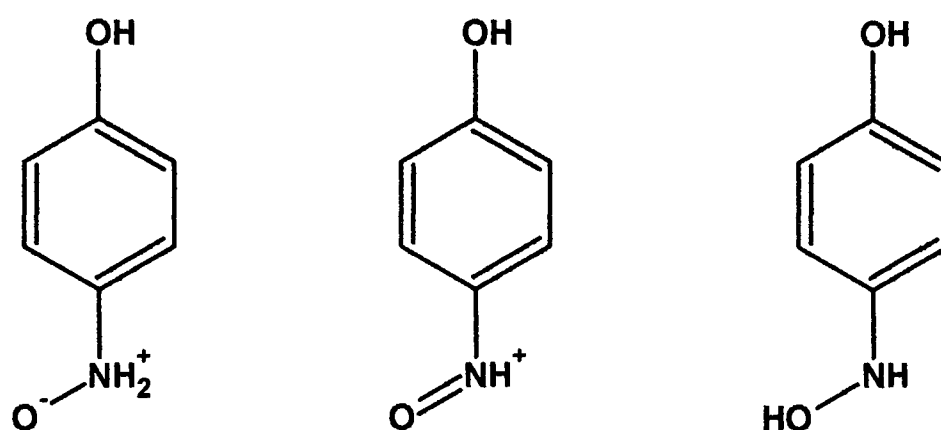


Figure 2.11. Possible oxidation products of acetaminophen

Sherwood *et al* (2001) postulated that the coloured products become incorporated into the crystal during crystallization, and that the oxidation products have a major inhibiting influence on the nucleation and growth process, significantly altering the topography of acetaminophen crystals. These findings could have considerable impact on future formulation design.

Attempts were made to avoid oxidation, by bubbling nitrogen through solutions and keeping all samples in a nitrogen atmosphere. This prevented oxidation during the period of analysis (~3 days), but after this

time it was necessary to purge the solutions with nitrogen again if they were required for further study. The change in colour was not predictable, and tended to vary greatly between apparently identically produced samples.

Table 2.11. Solubility of acetaminophen in propylene glycol and water vehicles

% Propylene glycol in vehicle (v/v)	Solubility (mg/mL)	Standard deviation
0	13.67	0.04
10	18.34	0.01
20	28.66	0.15
30	24.0	12.64
40	38.67	3.21
50	68.73	0.75
60	73.67	2.88
70	99.67	1.26
80	99.67	0.57
90	106.33	0.14
100	115.51	3.72

There is an approximately 10-fold increase in solubility in propylene glycol compared with water.

Graphical Summary of solubility data

In order to gain a clearer idea of how the three solubility of the permeants compare, the data are presented graphically in figures 2.12 and 2.13.

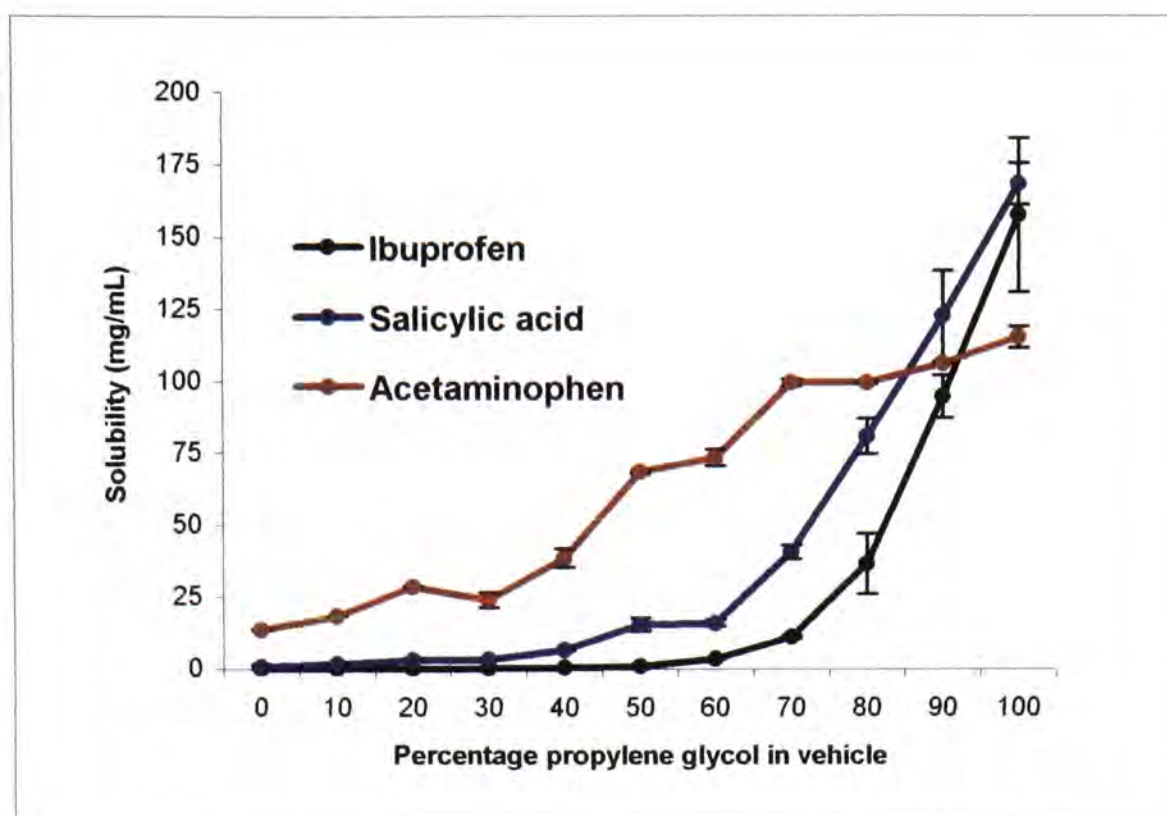


Figure 2.12. Graph comparing the solubility of IBU, SA and AM in PG/water vehicles.

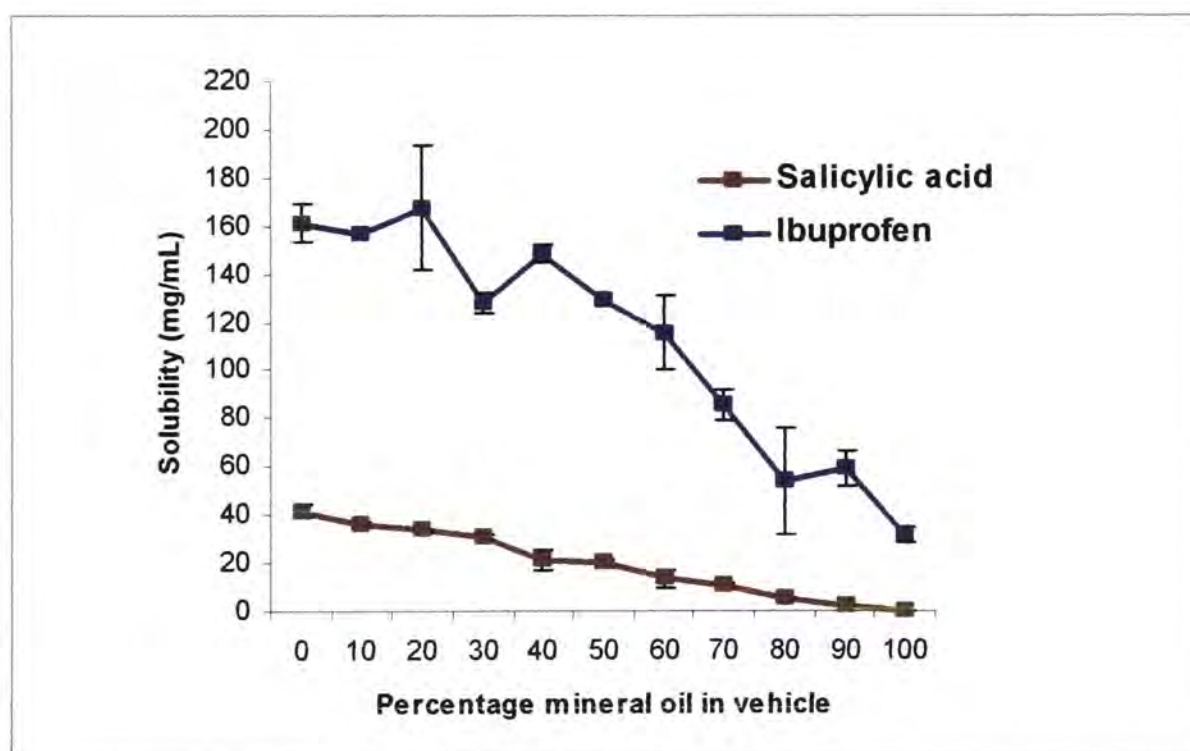


Figure 2.13. Graph comparing the solubility of IBU and SA in MO/MG vehicles

From figures 2.12 and 2.13 it is clear that although salicylic acid shows greater solubility in the hydrophilic vehicles, ibuprofen has significantly higher solubility in the lipophilic vehicles. This is consistent with the

difference in logP between the two drugs, 2.26 and 3.51 for salicylic acid and ibuprofen respectively. This does suggest that salicylic acid would be better suited to a hydrophilic formulation because for saturated solutions the total dose applied would be higher than for a lipophilic base as a result of higher solubility.

2.7.2. pK_a determination

Both salicylic acid and ibuprofen have low water solubility (~1mg/ml and ~0.1mg/ml respectively). For this reason it is not possible to determine an aqueous pK_a in the normal way, i.e. acid–base titration. It is instead necessary to use a co-solvent to increase solubility. This approach tends to produce much more reliable and better quality data for low solubility substances. For preliminary experiments methanol was used as this is considered the co-solvent of choice for pK_a determinations. This is because it is well characterised, and does not tend to pick up CO₂ at high and low pH, which can affect the results obtained.

It is known that the pK_a of weak acids is modified by the presence of co-solvent, and the experiments conducted confirmed this. Two co-solvents were studied; methanol and ethanol. It was hoped that the change in pK_a in the presence of propylene glycol could be investigated. However, Sirius do not have sufficient information (“Four Plus™” calibration parameters) about propylene glycol for these experiments to be conducted. It should also be remembered that determination of pH in non-electrolytes (mixed solvents) is extremely difficult as pH is a description of aqueous systems.

Although the original aim of these experiments was to determine the pK_as of the two weak acids, it became clear that the information regarding the change in pK_a as a result of adding a cosolvent could be of further use. Ethanol is commonly used in topical products, yet it is not entirely clear if formulators fully appreciate how the addition of any alcohol to a formulation can affect the behaviour of the active ingredients. Many drugs are weak acids or bases, and therefore what is clear is that this is an important factor to consider. Experiments were first conducted in methanol, then repeated using ethanol as a co-solvent. The rationale

behind this approach is that methanol does not lend itself to formulation design because of its toxicity. Ethanol has been well characterised by Sirius (i.e. the four-Plus parameters were available) and it can be used in model formulations therefore was a good alternative to methanol as a model co-solvent.

The experiments showed that at a given pH, the degree of ionisation changed significantly in the presence of co-solvent.

Phosphoric acid

Phosphoric acid was used as a "test" compound. The manufacturers of the Sirius suggest using this as a test and reference to ensure that the equipment is working satisfactorily. Phosphoric acid is a commonly used component of buffers for permeation experiments and its pK_a values are known. It was expected that there would be an effect on the pK_a , but that this effect would be insignificant. It can be seen from figure 2.16 that the pK_a s were affected, and to a higher degree than anticipated. Although not strictly part of the research, this goes to show that buffer components, as part of a formulation, need to be monitored carefully. It also underlines the entire premise of this project – understanding how different components of formulations affect one another, and investigating ways to manipulate these effects to our advantage.

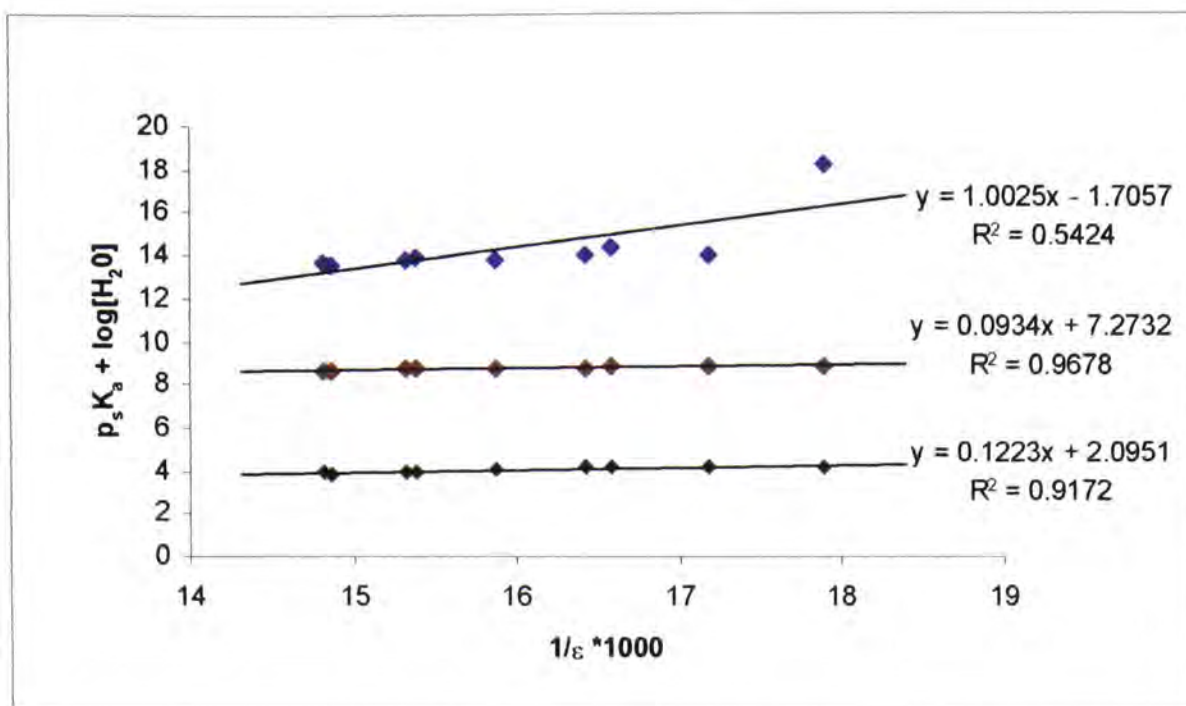


Figure 2.16. Yasuda Shedlovsky plot – phosphoric acid

Salicylic acid

Yasuda-Shedlovsky plots were constructed from the raw data generated by the Sirius. These are presented in figures 2.17 and 2.18.

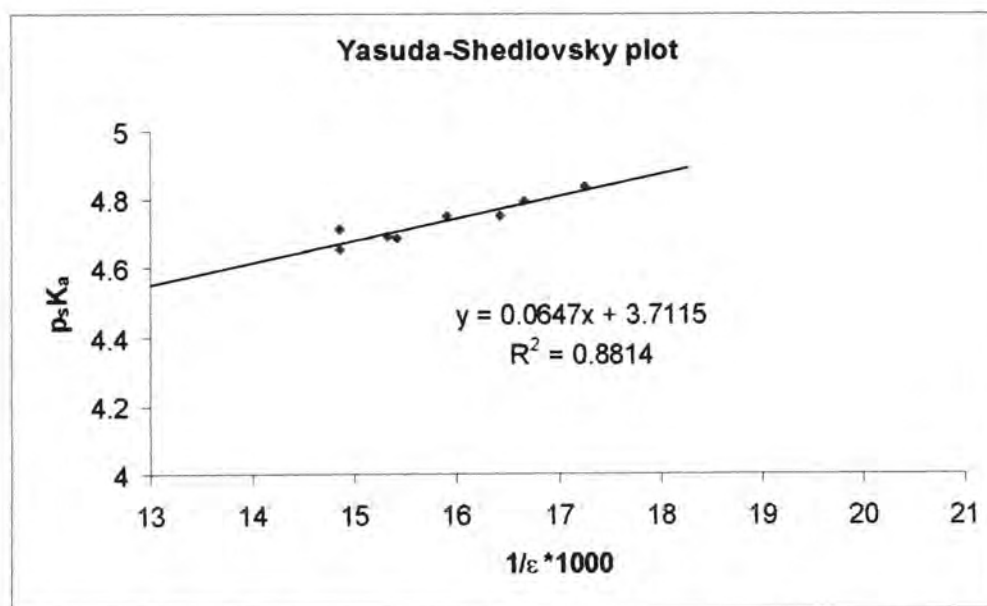


Figure 2.17. Yasuda-Shedlovsky plot of salicylic acid with methanol as a co-solvent

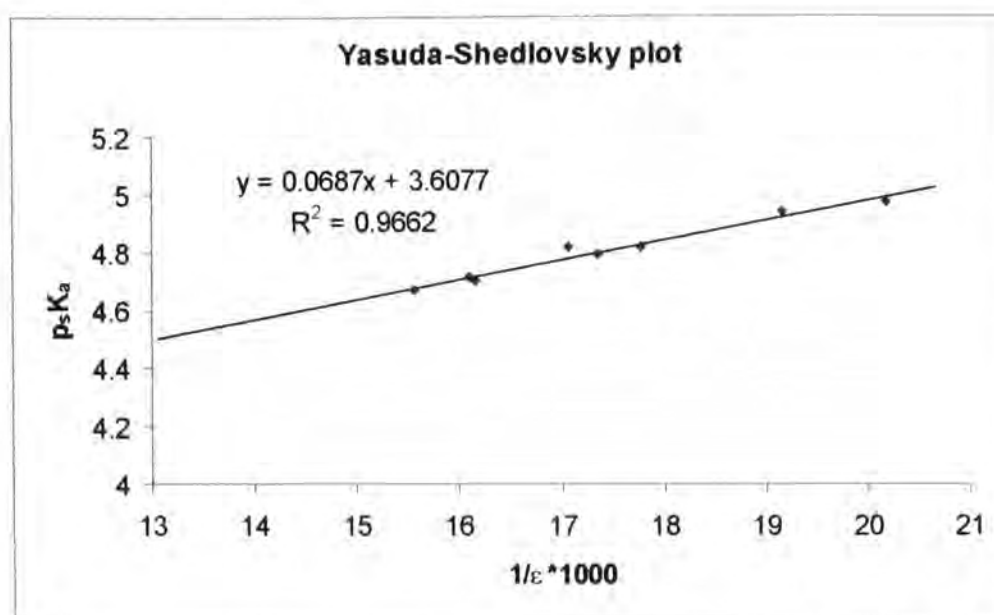


Figure 2.18. Yasuda-Shedlovsky plot of salicylic acid with ethanol as a co-solvent

If the fraction of salicylic acid ionised as a function of pH is plotted (figures 2.19-2.21), it provides a clearer picture of what is happening as the amount of methanol increases. The pK_a increases, and therefore the fraction ionised at any pH will decrease. Ethanol had the greatest effect on the pK_a , this is because it has a lower dielectric constant than methanol, therefore as the amount of ethanol is increased the dielectric constant of the medium will decrease more than for the corresponding methanol/water mixture. The plots show that at skin pH (~ 5) there is very little difference in the percentage of salicylic acid ionised upon the addition of portions of methanol or ethanol. The biggest difference in the plot is seen at pH 3 which corresponds to the pK_a of salicylic acid. The pH of the formulation would need to be kept lower than 2.7 to optimise permeation (i.e. to keep salicylic acid in its un-ionised form).

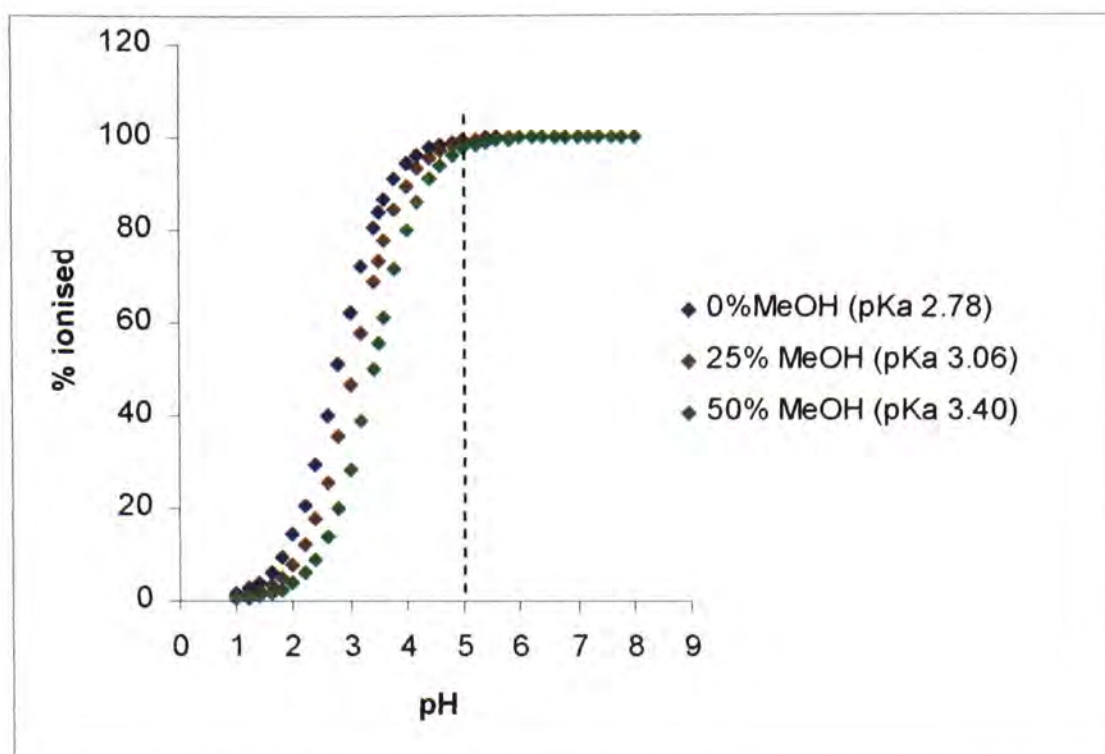


Figure 2.19. Change of pK_a with increasing % co-solvent – SA/MeOH

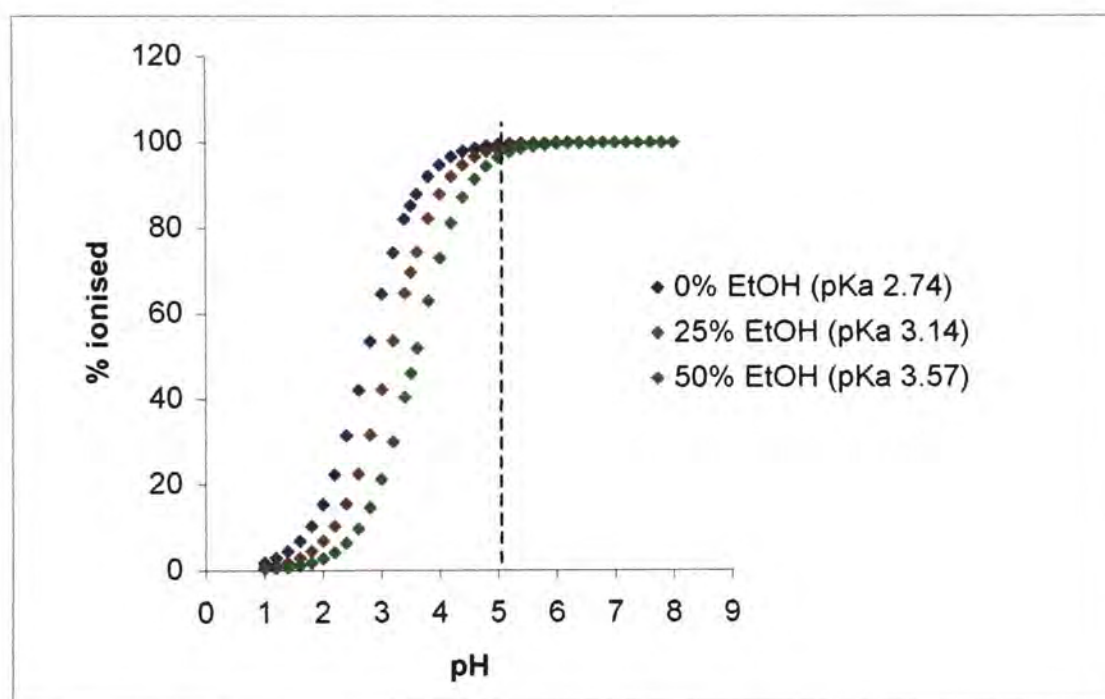


Figure 2.20. Change of pK_a with increasing % of co-solvent – SA / EtOH

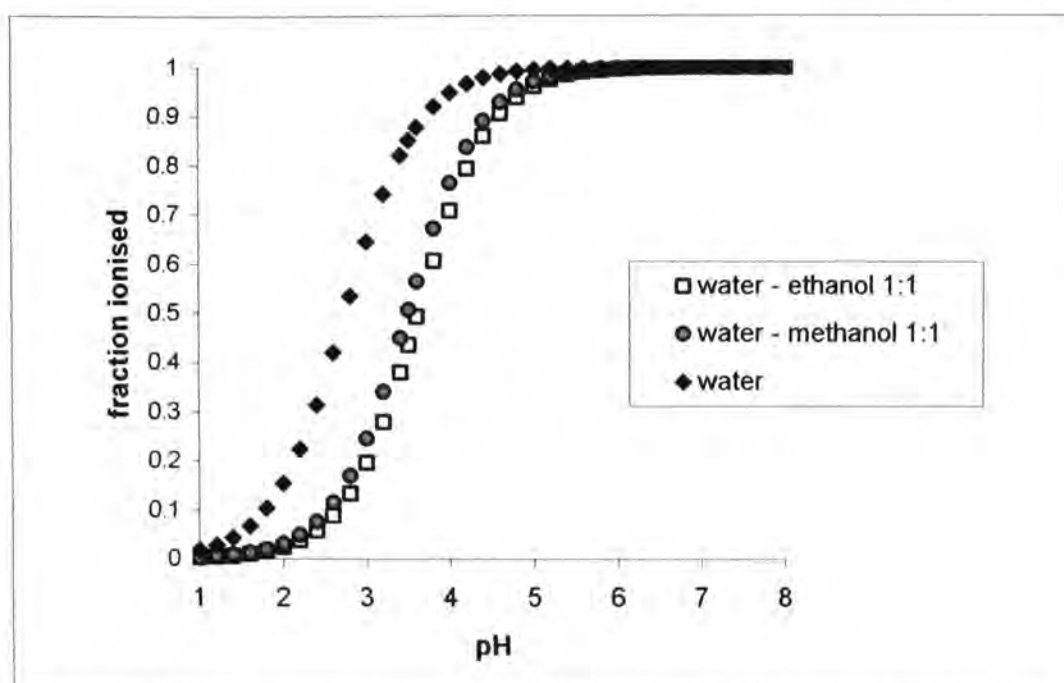


Figure 2.21. Ionised fraction of salicylic acid as a function of pH.

Ibuprofen

Yasuda-Shedlovsky plots were constructed from the raw data generated by the Sirius. These are presented in figures 2.22 and 2.23.

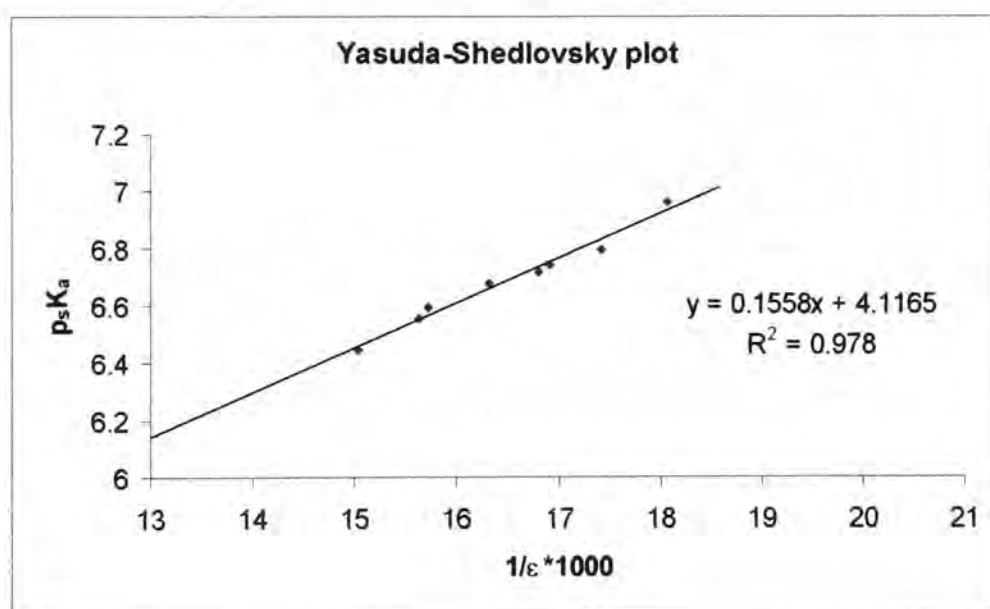


Figure 2.22. Yasuda-Shedlovsky plot of ibuprofen with methanol as a co-solvent

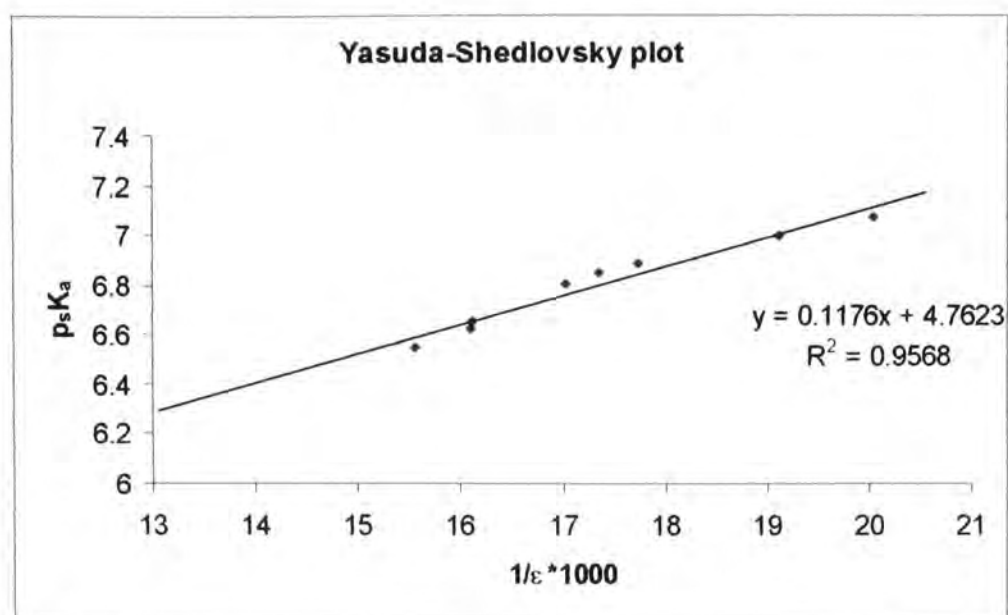


Figure 2.23. Yasuda-Shedlovsky plot of ibuprofen with ethanol as a co-solvent

As for salicylic acid, a plot of fraction of ibuprofen ionised as a function of pH (figures 2.24-2.26) shows that ethanol again has a greater effect on the pK_a , for the same reasons as previously described.

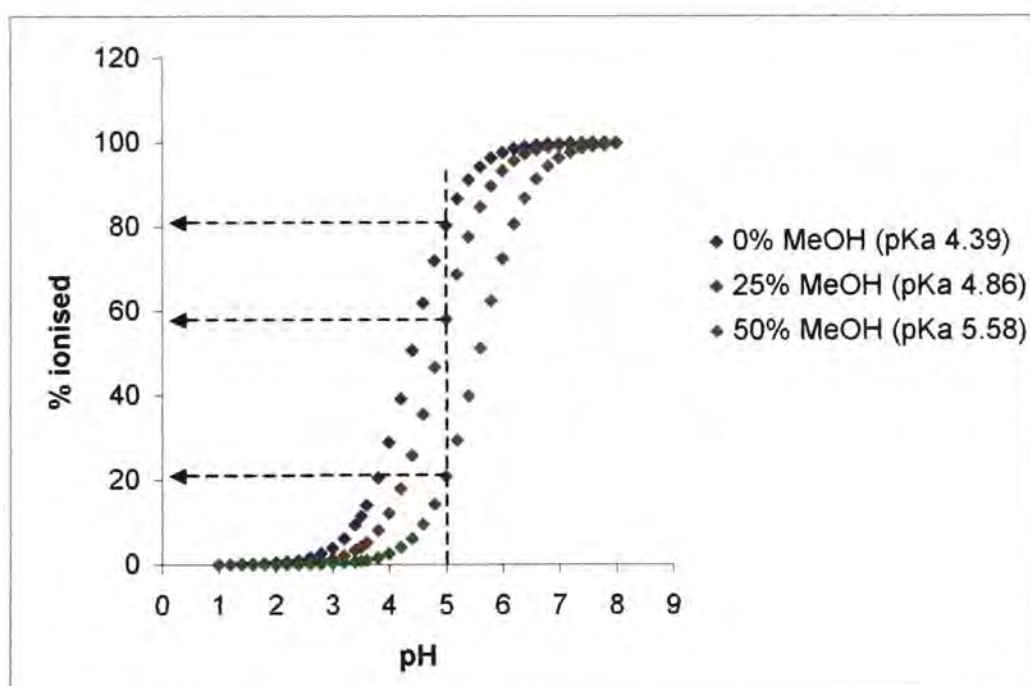


Figure 2.24. Change of pK_a with increasing % of co-solvent

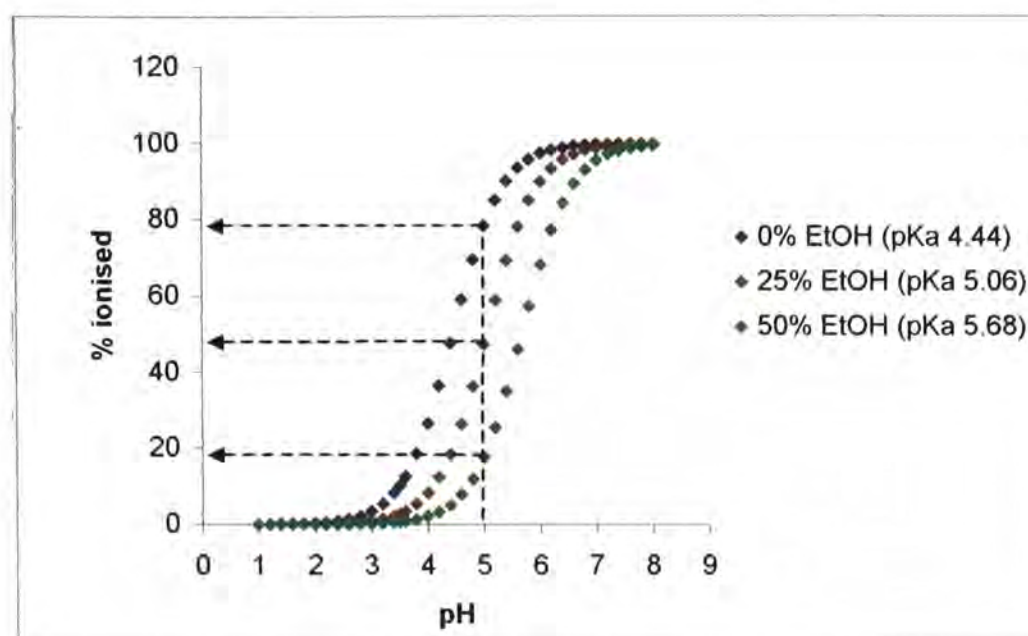


Figure 2.25. Change of pK_a with increasing % of co-solvent

Figure 2.24 shows that for a fixed ibuprofen concentration the percentage of ionised form decreases from 80% in water to 20% for a 50:50 methanol water formulation. Between methanol and ethanol as cosolvents there is not a considerable difference. In a 50:50 ethanol water formulation the percentage of ionised form decreases to $\sim 15\%$. This does demonstrate that the addition of a cosolvent has a significant effect upon the physicochemical properties of a drug in formulation. A typical cream formulation may contain up to 10% of a cosolvent such as propylene glycol, which could shift the pK_a of a weak acid or a weak base and alter its solubility and partitioning behaviour, therefore affecting permeation.

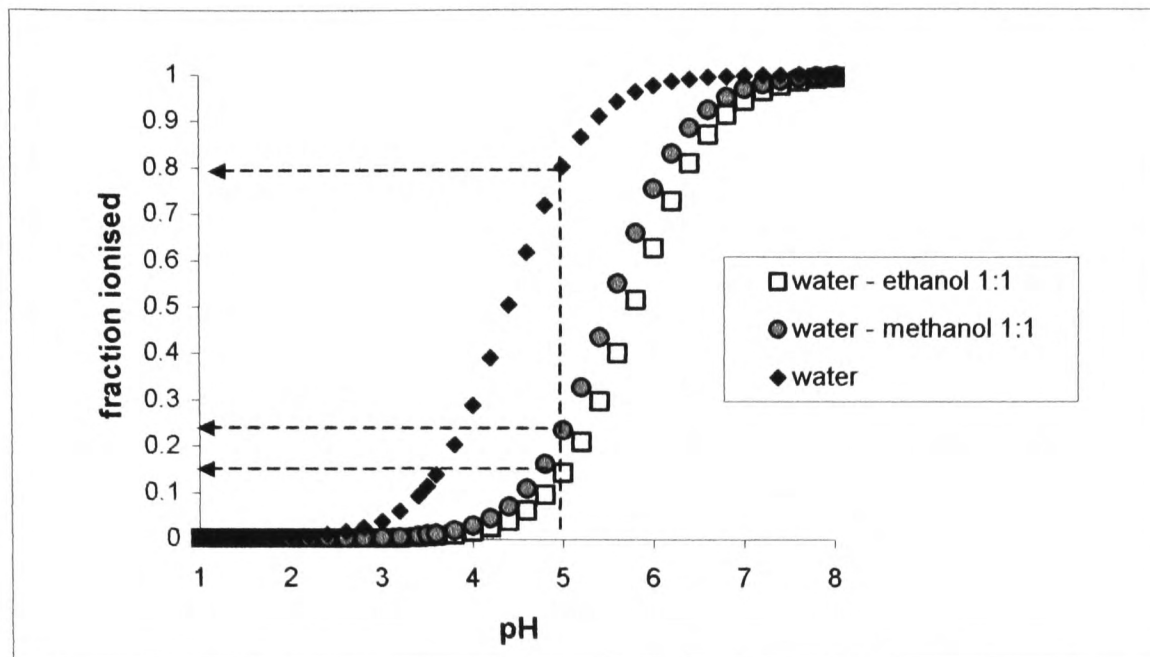


Figure 2.26. Ionised fraction of ibuprofen as a function of pH

Effect of ionisation on steady state flux

The steady-state flux of a drug through the stratum corneum is described by Fick's first law of diffusion (Eqns. 2.8 and 2.9). The degree of saturation (DS) of the drug in the vehicle and the partition coefficient (K) are two parameters, which dictate the overall flux:

$$J = \frac{K \cdot D}{h} \cdot C_{vehicle} = \frac{C_{sat, SC} \cdot D}{C_{vehicle, sat} \cdot h} \cdot C_{vehicle}$$

(Eqn. 2.8)

$$J = \frac{D \cdot C_{SC, sat}}{h} \cdot DS$$

(Eqn. 2.9)

The inclusion of cosolvent (e.g., EtOH) in a formulation, therefore, has several consequences.

At a given drug concentration and pH, the addition of an alcoholic co-solvent:

- Increases the unionized fraction (HX) of the drug. Since the latter has a higher lipophilicity relative to X^- , the overall skin flux, which is proportional to the skin-formulation partition coefficient, K (Eq.2.8) is enhanced.
- Generally increases drug solubility in the formulation. If the drug concentration is kept constant, this effectively decreases the degree of saturation (DS) and hence leads to a lower flux (Eq.2.9).

Thus, two opposing physicochemical phenomena are involved. The effect of the cosolvent on the skin membrane must also be taken into account when considering topical bioavailability. Additionally, the use of volatile cosolvents further complicates the situation by creating a dynamic formulation system, where the composition, and hence delivery kinetics, fluctuate during the topical application.

The skin partitioning of the ionized and neutral form of a weak acid can differ by several orders of magnitude and the addition of a cosolvent can significantly modify the dissociation constant of the weak acid at a given pH. The precise outcome will depend on the nature of the cosolvent, the pH of the formulation and the pK_a of the drug. This is explored in detail in Chapter Five.

2.7.3. Partitioning experiments

Experiments were conducted firstly with octanol, and then propylene glycol dipelargonate. This is because although octanol is the standard common partition solvent used in logP determinations it does not necessarily provide a good representation of partitioning into the skin. Leahy, Taylor and Wait (1989) proposed the "critical quartet" system of limiting solvents for the general modelling of biological membranes; chloroform, alkane, propylene glycol dipelargonate (PGDP) and octanol. Of these, PGDP is most relevant to this project. It is a proton acceptor and mimics the hydrogen bond acceptor groups in the skin such as esters and phosphates. It could be said that PGDP provides better modelling of the partitioning into the stratum corneum than octanol because it bears some resemblance to a typical phospholipid, but unfortunately, although it provides a more "skin-like" solvent, it does not always produce reproducible results. For this reason it is not possible to present data for the partition behaviour of salicylic acid into PGDP/water.

Many studies have been conducted with these four solvents, and there have been interesting applications of logP determined in more than one partition solvent, which have been said to shed light on the process of partitioning. For example, Testa and co-workers (1991) have suggested that $\Delta\log P = \log P_{\text{octanol/water}} - \log P_{\text{alkane/water}}$ contain information on the capacity of solutes to donate hydrogen bonds. Compounds with low H-bonding donor acidity (low $\Delta\log P$) and high lipophilicity (high logP) can readily penetrate across human skin. Hydrogen bond acceptor groups in the skin (e.g. esters, phosphates) in skin form stable H-bonds with hydrogen bond donating solutes and therefore hinder passive diffusion.

Recently, many researchers have been conducting partitioning experiments using liposomes. Liposomes are self-assembling model membranes composed of phospholipid groups such as phosphatidylcholine. LogP values for unionised molecules obtained using liposomes tend to be very similar to those measured in octanol but the ion-pair logP values differ. The "surface ion pair" logP is found to be much higher in bases, zwitterions and amphophiles. The values for acids tend to be similar to octanol values. This reflects the increased potential for partitioning of molecules with basic groups into membranes. Like PGDP, liposomes offer a more realistic model of partitioning behaviour, although clearly the experiments will have an added degree of complexity.

Determination of the distribution coefficient

The dedicated software (pK_alogP version 5.1) is able to generate "what if" data based upon experimental values obtained from pK_a determination and partitioning experiments. These theoretical curves are shown below. LogD is the distribution coefficient (logP) at a particular pH. This is not a constant and varies according to the protogenic nature of the molecule.

$$D = \frac{[unionised_{(oct)}]}{[unionised_{(aq)}] + [ionised_{(aq)}]} \quad (\text{Eqn. 2.5})$$

$$\log D = \log_{10}(\text{distribution coefficient}) \quad (\text{Eqn. 2.6})$$

For an acid logD is related to logP and the pK_a by the following equation:

$$\log D_{(pH)} = \log P - \log[1 + 10^{pH - pKa}] \quad (\text{Eqn. 2.7})$$

Salicylic acid

The results (shown in figure 2.27) show a marked difference in $\log P$ between the ionised and unionised forms of salicylic acid. At low pH the $\log P$ is 2.32, at high pH it is -0.84 . This would have a significant impact upon permeation behaviour. According to the pH partition hypothesis it is generally the unionised form of a molecule which will cross a biological membrane. If we consider the pH of the skin (~ 5) it is clear from figure 2.19 that salicylic acid will be almost entirely in its ionised form. As a result of this the solubility of salicylic acid will be increased, but the $\log P$ will be lowered (~ 0.25). Because of the complex nature of biological membranes such as the skin it is difficult to predict what how these phenomenon would affect permeation in vivo.

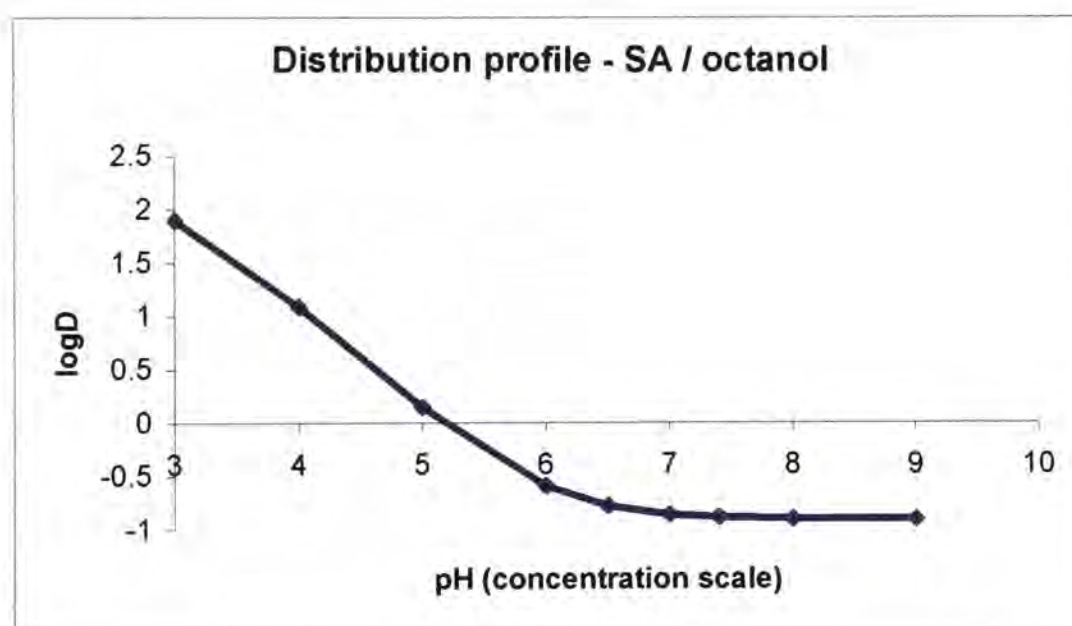


Figure 2.27. Distribution profile - based on $\log P_{\text{oct}}$

Ibuprofen

Distribution coefficient based upon $\log P_{\text{oct}}$

The results presented in figure 2.28 show that the partitioning behaviour of the ionised and unionised form of ibuprofen is very different. The $\log P$ for unionised ibuprofen is 4.01 whereas for the ionised form it is 0.07. As

for salicylic acid, in the pH range for the skin (~5) ibuprofen will be ionised, though not to such an extent. Ibuprofen would be approximately 80% ionised at pH 5. From the profile in figure 2.28, it can be seen that this corresponds to a logP of ~3.5. Along with this lowering of the logP there will also be an increase in solubility. The combination of these two effects could enhance the flux of this drug, and could be used to a formulators advantage for topical products.

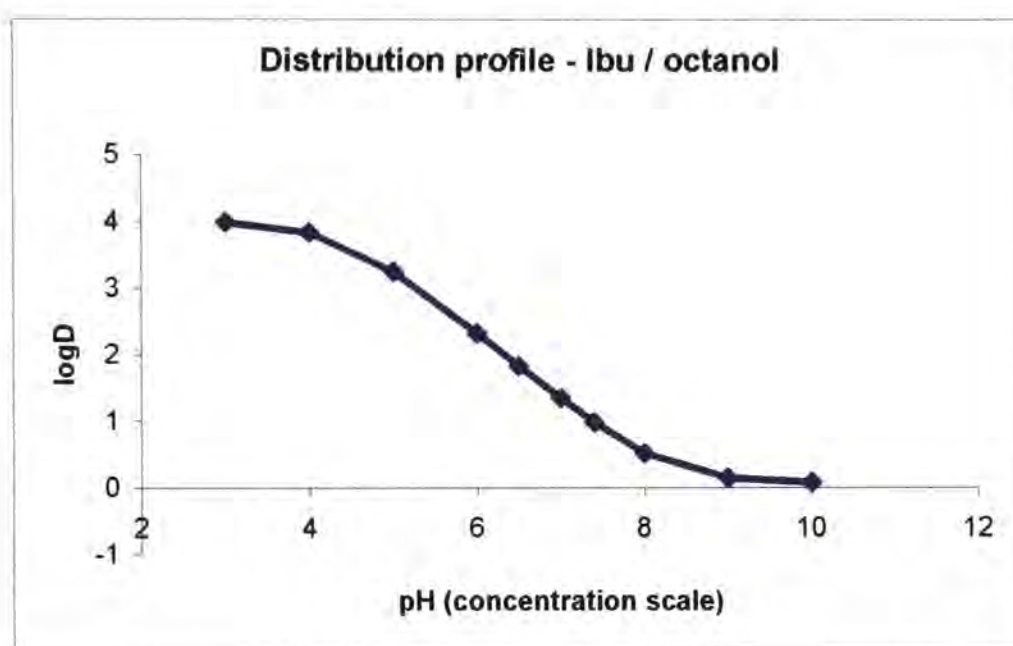


Figure 2.28. Distribution profile - based on $\log P_{\text{oct}}$

Distribution coefficient based upon $\log P_{\text{PGDP}}$

PGDP was used as a partitioning solvent because it provides a more "skin-like" structure than octanol. The distribution profile is shown in figure 2.29. Octanol provides a useful guide to partitioning behaviour, but when the complexity of skin as a membrane is considered, it seems a somewhat simple approximation of the real situation. The results show that, as for octanol/water partitioning, logP is highest at low pH (3.51) whilst at high pH it is extremely low (-1.15). In terms of formulation design, it would be vital to assess whether the solubility effect of increasing pH would also

increase flux. If not significant then using a buffer to keep vehicle pH at an optimum for permeation would be necessary.

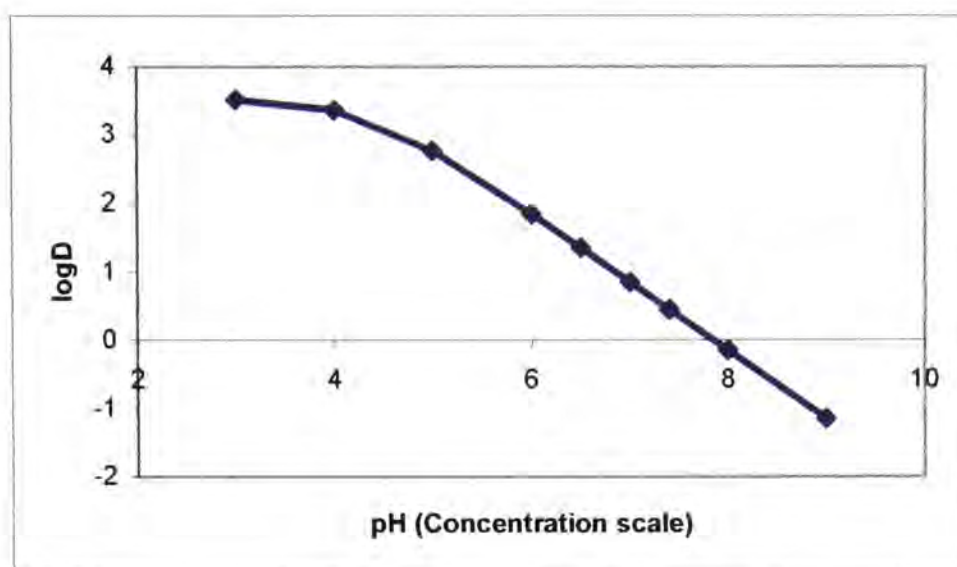


Figure 2.29. Distribution profile – based on $\log P_{PGDP}$

2.8. Prediction of physicochemical properties

pK_a prediction

Before these experiments were conducted, theoretical data were generated using ACD software. pK_a values and distribution profiles were determined. It is encouraging to see that the experimental data agree well with the theoretical data, giving a degree of confidence in this type of predictive software. If only used as a guide for the initial design of model components, it is still a valuable tool.

Table 2.11. Predicted and experimental pK_a values.

	Predicted pK_a	Experimental pK_a (extrapolated)
Ibuprofen	4.41	4.39
Salicylic acid	3.01	2.78

LogP prediction

In the same way that pK_a can be predicted, ACD is also able to generate theoretical distribution profiles. The predicted data, presented in figures 2.30 and 2.31, agree well with the experimental results obtained using the Sirius.

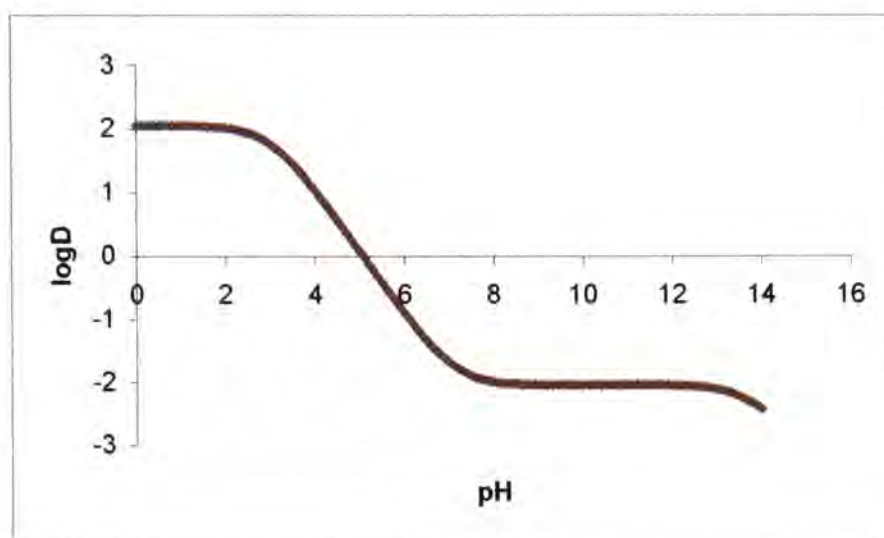


Figure 2.30. Calculated distribution profile for salicylic acid based on $\log P_{oct}$

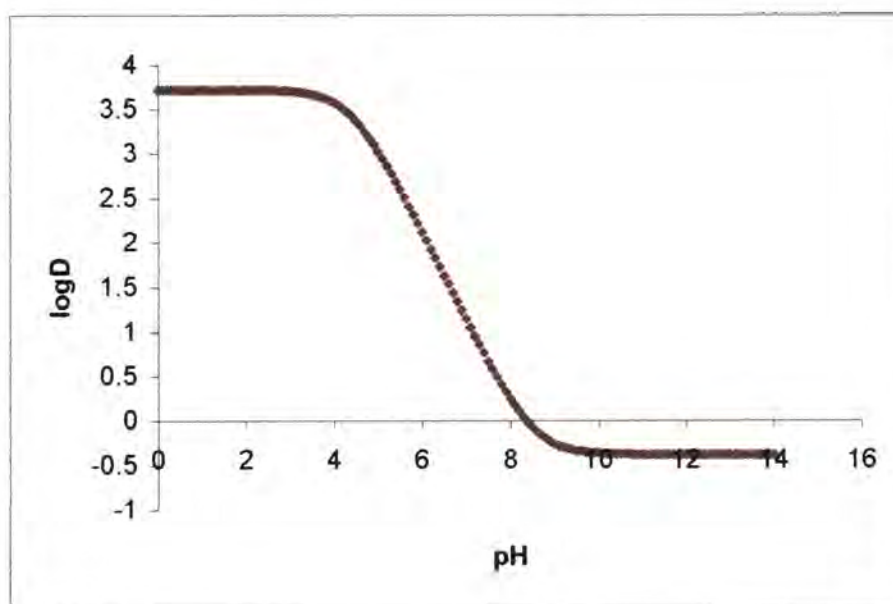


Figure 2.31. Calculated distribution profile for ibuprofen based on $\log P_{oct}$

Table 2.12. Comparison of calculated and experimental logP values.

Calculated values are in brackets

Drug	LogP	
	HX	X ⁻
Ibuprofen	4.01 (3.72 ± 0.23)	0.07 (-0.38 ± 1.0)
Salicylic acid	2.32 (2.06 ± 0.25)	-0.84 (-1.09 ± 1.0)

Simulated solubility data

ACD software provided a useful guide to the possible effect that ionisation would have upon the solubility behaviour of the three permeants. It was clear that with a high pK_a, acetaminophen would not present any significant formulation challenges in terms of ionisation effects. However, being weak acids IBU and SA are dramatically affected by any change in pH. This is clearly seen in the simulated data shown in figure 2.32. The simulated data agree well with the experimental solubility data (section 2.9.1).

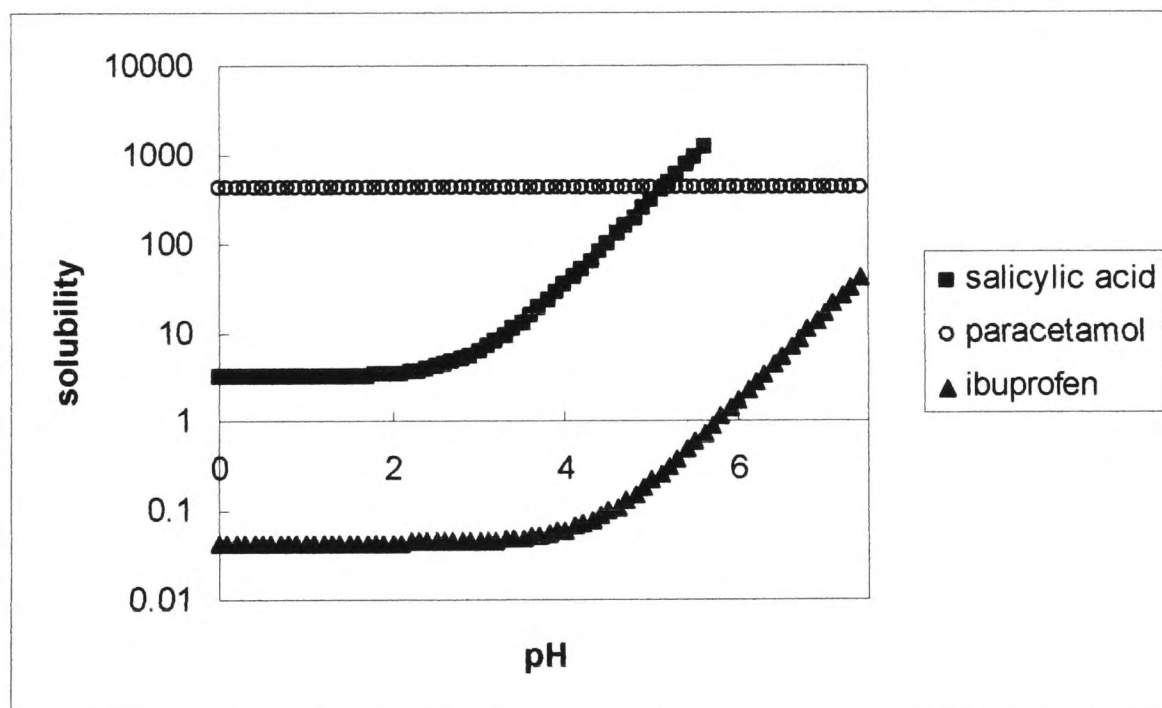


Figure 2.32. Simulated (ACD software) solubility data demonstrating the effect of pH

2.9. Summary

This Chapter has introduced many key themes that will emerge during this thesis, the most important of which is the need for a thorough understanding of the systems being investigated, both drug and vehicle.

Solubility characteristics of the three selected permeants in a number of different solvent/cosolvent combinations have been determined. Knowledge of the saturated solubility of the permeants in the vehicles will allow for further mathematical analysis, which is presented in Chapter Four.

The ionisation behaviour of IBU and SA has been investigated in methanol and ethanol/water systems. These studies have demonstrated that the presence of a cosolvent can greatly modify the dissociation of a weak acid at a given pH, and therefore this needs to be considered further in the design of dermatological vehicles. It is difficult to elucidate all the physicochemical processes occurring in mixed solvents, and the next step is to investigate the effect this change in ionisation will have upon permeation in vitro.

2.10. References

A. Albert and E. P. Seargent. *The determination of ionisation constants – A laboratory manual*. 3rd edition, Chapman and Hall. (1984)

A. Avdeef. pH-metric logP. 1. Difference plots for determining ion-pair octanol-water partition coefficients of multiprotic substances. *Quant. Struct.-Act. Relat.* **11**, 510-517 (1992).

A. Avdeef. Assessment of distribution profiles. In: *Lipophilicity in Drug Action and Toxicology*. Eds: V. Plicka, B. Testa and H. van de Waterbeemd. VCH, Weinheim. pp109-139 (1996).

A. Avdeef, J. E. A. Comer and S. J. Thomson. pH-metric logP. 3. Glass electrode calibration in methanol-water applied to pK_a determination of water-insoluble substances. *Anal. Chem.* **65**, 42-49 (1993).

B. W. Barry. Topical Preparations. In: *Pharmaceutics*. M. E. Aulton (Ed). First Edition. Churchill Livingstone. pp 381-411 (1988).

N. G. Basan and R. J. Flower. Lipid signals in pain control. *Nature.* **420**, 135-138 (2002).

C. Hansch, A. Leo and D. Elkins. Partition coefficients and their uses. *Chem. Rev.* **71**, No. 6, (1971).

J. E. Harrison, A. C. Watkinson, D. M. Green, J. Hadgraft and K. R. Brain. The relative effect of Azone and Transcutol on permeant diffusivity and solubility in human stratum corneum.

C. J. Hawkey. COX-2 Inhibitors. *Lancet*. **353**, 307-314 (1999).

M. Katz and B. J. Poulsen. Absorption of drugs through the skin. In: *Handbook of Experimental Pharmacology, Vol. XXXVIII/1*. Edited by B. B. Brodie and J. Gillette. Springer-Verlag, Berlin. pp103-174 (1971).

D. E. Leahy, P. J. Taylor and A. R. Wait. *Quant. Struct.-Act. Relat.* **8**, 17-31 (1989).

H. P. Rang, M. M. Dale, J. M. Ritter and P. K. Moore. *Pharmacology*. Fifth Edition, Churchill Livingstone. pp 244-261 (2003).

J. N. Sherwood, K. V. R. Prasad, R. T. Ristic and D. B. Sheen. Crystallization of paracetamol from solution in the presence and absence of impurity. *Int. J. Pharm.* **215**, 29-44 (2001)

Sirius Analytical Instruments Ltd. STAN (Sirius Technical Application Notes) Volume 1. (1994).

Sirius Analytical Instruments Ltd. Applications and theory guide to pH-metric pK_a and logP determination. (1993)

K. Takács-Novák, K. J. Box and A. Avdeef. pK_a determination of water insoluble compounds: validation study in methanol/water mixtures. *Int. J. Pharm.* **151**, 235-248 (1997).

N. El Tayer, R. S. Tsai, B. Testa, P. A. Carrupt, C. Hansch and A. Leo.
Partition of solutes in different solvent systems: the contribution of
hydrogen-bonding capacity and polarity. *J. Pharm Sci*, **80**, 590-598 and
744-749 (1991).

- Chapter Three -
Materials and Methods

3.1. Introduction

In this chapter all methods and materials are listed. There are many factors that can affect the outcome of a diffusion experiment, such as the selected receptor phase, temperature, occlusion etc. The exact protocol for the experiments described in this thesis is included so that all the finer points are clarified. This chapter also contains details of HPLC and UV calibrations, as well as a protocol for ATR-FTIR diffusion experiments.

3.2. Materials used

3.2.1. Chemicals used

Chemical	Source
Acetaminophen (AM) - 99%+	Aldrich Chemical Co Ltd
Acetaminophen (AM) - 98%	Sigma
Acetonitrile (ACN) - HPLC grade 99%+	VWR
Di-sodium hydrogen phosphate dihydrate (Na₂HPO₄) - GPR	Fisher chemicals
Ethanol (EtOH) - 99%+	VWR
Ethyl acetate (EtAc) - Anal R	VWR
Hexane - GPR	VWR
Ibuprofen (IBU)	A gift from Wyeth pharmaceuticals
Isopropanol - HPLC grade 99%+	Fisher chemicals
Isopropyl myristate (IPM) - 98%	Aldrich Chemical Co Ltd
Methanol (MeOH) - HPLC grade 99%+	VWR
Mineral oil (MO) - light white	Aldrich Chemical Co Ltd
Octanol (Oct) - GPR	Fisher Scientific Chemicals
Orthophosphoric acid - HPLC grade	Fisher Scientific Chemicals
Potassium dihydrogen phosphate - GPR	VWR
Propylene glycol (PG) - GPR	Aldrich Chemical Co Ltd
Propylene glycol dipelargonate (PGDP) - GPR	Fisher Scientific Chemicals
Salicylic acid (SA) - GPR 98%	Aldrich Chemical Co Ltd
Sodium chloride (NaCl) - GPR	Aldrich Chemical Co Ltd
Sodium dihydrogen phosphate dihydrate (NaH₂PO₄) - GPR	Fisher Scientific Chemicals
Transcutol (TC)	Supplied by Leo pharma (Denmark)
Vacuum grease	Dow corning
Viscoleo (MG) - Equivalent to Miglyol 812	Supplied by Leo pharma (Denmark)

3.2.2. Apparatus

Apparatus

ATR accessory for Nexus FTIR	45° ZnSE ATR crystal
Beaker	Pyrex. 5mL, 100mL, 200mL, 1000mL and 3000mL
Conical flask	Wide neck, Pyrex. 250mL
Cork board	
Cork borer	Set of eight stainless steel (VWR)
Disposable syringe	Terumo, sterile. 5mL
Fourier Transform Infrared (FTIR) spectrometer	Thermo-Nicolet Nexus. Helium Neon laser; with separate computer. Mercury Cadmium telluride detector (MCT) with KBR beamsplitter. Dedicated software: Omnic v6.0a
Franz diffusion cells	Glass. Receptor volume 3.6mL, 3.9mL and 4.5mL. Diffusional area ~ 0.95cm ²
Gilson pipette	P100, P200, P1000, P5000
Gilson pipette tips	Fisher life sciences
Glass sample vessel	BDH, 25mL
HPLC system	Thermo Separation Products. SpectraSERIES 100 HPLC system. P100 pump, 100 series autosampler (100µL loop size), UV detector and integrator
Isothermal calorimeter, Thermal Activity Monitor (TAM)	2277 Bio Activity Monitor, LKB Bromma, Thermometric, standard microwatt version.
Magnetic flea	
Magnetic stirrer/hotplate	
pH meter	

Plastic bowl	Fisher Life Sciences. Small, medium and large
Plastic weighing boat	VWR. Disposable polystyrene, 5mL and 10mL
Quartz cuvette	Fisher Life Sciences. 4mL, 10mm pathlength
Scalpel	With blades (non-sterile)
Sealing film	Whatman laboratory
Silicone membrane	Samco. 400µm thickness
Silicone tubing	Fisher Scientific
Sonicator	Clifton Ultrasonic bath. Serial number 34972, 1000W, 220-240V, 50-60Hz
Spatula	
Sterile needle	Terumo. 21G x 1 ½" (0.8 x 40)
Submersible stirrer bed	
Thermometer	
UV/Visible spectrometer	Hewlett Packard Diode-Array UV-spectrometer, HP8453; connected to a computer with HP845x UV/visible system software; HP89090A Peltier (stirrer and temperature control device). Temperature stability 10.0°K – 60.0°K ± 0.1K
Volumetric flask	5mL, 10mL, 25mL, 1000mL and 2000mL
Water bath	Grant Instruments
Weighing balances	Sartorius research Analytical balance, serial number 02455
Whirlimixer	Fisons, 220-240V, 500Hz

3.3. Methods

3.3.1. Diffusion cell studies

Diffusion studies of the selected permeants across silicone membrane were performed using Franz-type diffusion cells that have a receptor phase of ~ 2.5 ml, and a diffusional area of ~ 1 cm². Sheets of silicone membrane were cut to appropriate sizes and soaked overnight in the receptor solution. The membrane was then placed between the two compartments of the diffusion cells. Silicone grease was used to produce a leak-proof seal between the membrane and the two compartments.

The receptor compartment was filled with pH 7.4 phosphate buffered saline, and saturated solutions of the drugs were placed in the donor compartment. Excess solute was present to maintain saturation throughout the experiment. Thus, drug lost from the solution by diffusion is replenished by dissolution of the excess drug. This ensures that the depletion of the drug in the vehicle does not become the rate-limiting step in diffusion.

To remove air bubbles and prevent the build up of air pockets in the receptor phase, the phosphate buffer saline (PBS) was degassed in an ultrasonic bath. To prevent evaporation from the receptor compartment, the cell arm was covered with a glass lid.

Uniform mixing of the receptor phase was obtained with a magnetic stirrer that was placed in the receptor compartment. The diffusion cells were placed on a stirring bed immersed in a water bath at 37°C, to maintain a temperature of ~ 32 °C at the membrane surface. At 30-minute intervals, the receptor phase was completely removed and refilled with pre-

thermostatted phosphate buffer. To remove any particulates the receptor phase was filtered under vacuum using a 0.45 μ m micropore filter.

The samples were analysed using HPLC, with a dilution factor of 10. The diffusion experiments were performed under occluded conditions by covering the donor compartment with microscope cover slips. Experiments were performed in quadruplicate.

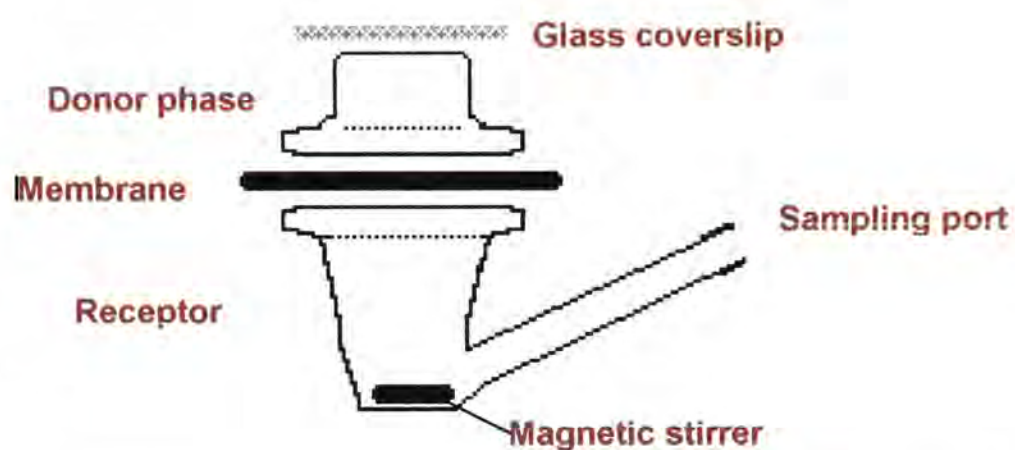


Figure 3.1. Schematic representation of a Franz diffusion cell

3.3.2. Preparation of isolated human epidermis

Human skin tissue was obtained following cosmetic surgery and stored in a freezer until required. Storage of skin tissue at temperatures below -20°C for periods of up to 466 days has been shown to have no significant effect on the permeability of water (Harrison et al, 1984).

Full thickness skin was removed from the freezer and thawed overnight. The epidermis was separated by immersing the skin in water maintained at 60°C for one minute (Kligman et al., 1963). It was then pinned to a corkboard and the epidermis was very carefully peeled away from the dermis. The epidermis was then immersed in a bowl of cold water to aid mounting onto filter paper. It was then wrapped in aluminium foil and

stored in a freezer until required. Prior to the diffusion experiment the skin was defrosted and cut to appropriate size.

3.3.3. ATR-FTIR studies

As discussed in Chapter One, ATR-FTIR has been increasingly used to study the mechanisms of permeation enhancement. Traditionally data were deconvoluted by monitoring the signal of a particular component, and although this proved successful, it relied on components of a system having discrete signals. It was not possible to deconvolute complex of overlapping spectra. For this reason a new method of analysis was sought. Chemometrics is the use of mathematical and statistical methods for handling, interpreting, and predicting chemical data. Advances in this area have opened up new possibilities for chemists and provided useful solutions for many complex problems. Factor Analysis, a regularly used technique within the pharmaceutical industry, should provide the key to understanding some of the processes occurring during permeation.

In order for chemometric analysis to be successful, it is necessary to have reference spectra for the individual components of the system being investigated. The references allow greater confidence in the obtained spectral profiles, and reduce the number of iterations required by the software to deconvolute the raw data.

Recording reference spectra for the selected permeants

The infrared spectrum of each permeant was obtained by preparing a 100 μ g/mL solution of the drug in ethanol. A small amount of the solution (~3mL) was placed on the crystal, allowing the solvent to evaporate. This left a film of drug on the crystal surface, and a spectrum was recorded. Before recording the spectrum of the drug, a background scan was taken,

in this way the drug scan was automatically corrected for atmospheric CO₂. The ZnSe crystal was wiped clean with methanol after each experiment, removing any drug residues. The resolution was set to 2cm⁻¹ and the scan rate was 32 scans per minute. A KBr beam splitter was used for all experiments.

Recording reference spectra for the vehicles

To record a single spectrum of the vehicle to be used as a reference, a few drops (~3mL) were placed onto the surface of the ZnSe crystal. The collection procedure, resolution and scan rate were the same as previously stated. The crystal was wiped clean with methanol after each experiment to remove any solvent residues.

Diffusion studies using ATR-FTIR

A zinc selenide ATR crystal was used for all the studies described. The spectrometer was linked to a PC and using Omnic software spectra were taken automatically every two minutes for a period of six hours. Ten scans were taken at each time point and an averaged spectrum was produced at each time point. Silicone grease was used to form a leak-proof seal between the donor compartment and the membrane. PDMS membranes were cut large enough to cover the entire surface of the crystal, preventing any of the sealants from coming into contact with the IR beam. The FTIR is equipped with a way to exert gentle pressure on the trough (see figure 3.3), and conveniently this had sufficient surface area to cover the donor phase and thus prevent any evaporation of the donor solution. The data collected were then analysed using principal component analysis.

Deconvoluting ATR-FTIR diffusion data using a chemometric method

The capturing of IR spectra as a function of time during the diffusion experiment generates a data matrix (D) whose rows, for this purpose represents the wavenumber points. The columns represent the spectral intensity. Because of the complex nature of the permeants (the active and solvent), membrane (or skin), the raw data generated are very difficult to interpret because of the convoluted or overlapping nature of the spectra. A method capable of deconvoluting the data significantly enhances the data interpretation and opens up the possibility of pursuing more complex studies based on spectroscopic analysis. A recent paper (Dias, 2004) describes how the application of a deconvolution technique based on target factor analysis (TFA) has enabled analysis of diffusion through a silicone membrane model. This analytical technique now opens up the possibility of studying complex diffusion systems and other permeable membranes, including skin.

TFA is used to determine whether or not a hypothetical vector, obtained from chemical principles or intuition, lies inside the factor space and contributes to the phenomenon of interest (Malinowski, 1991; Tetteh, 1997). The analytical strength of target testing lies in the fact that each hypothetical vector can be tested individually for significance in the presence of a host of other unknown factors. When a data matrix has been decomposed into abstract factors (also known as principal components) in row and column space of data, M, the number of significant factors is subjected to various forms of mathematical scrutiny to determine directly if they have real chemical or physical meaning. A data matrix D, consisting of rows R, of IR wavenumbers and C, columns of scans obtained during the diffusion process was decomposed by Principal Component Analysis (PCA) or factor analysis. In this project the mathematical technique of Singular

Value Decomposition (SVD) (Johnson, 1963) was used for the decomposition process. All the necessary algorithms and methods described in the references are embodied in software called InSight, coded in Matlab language. All the chemometric data analysis described in this thesis was performed through this software.

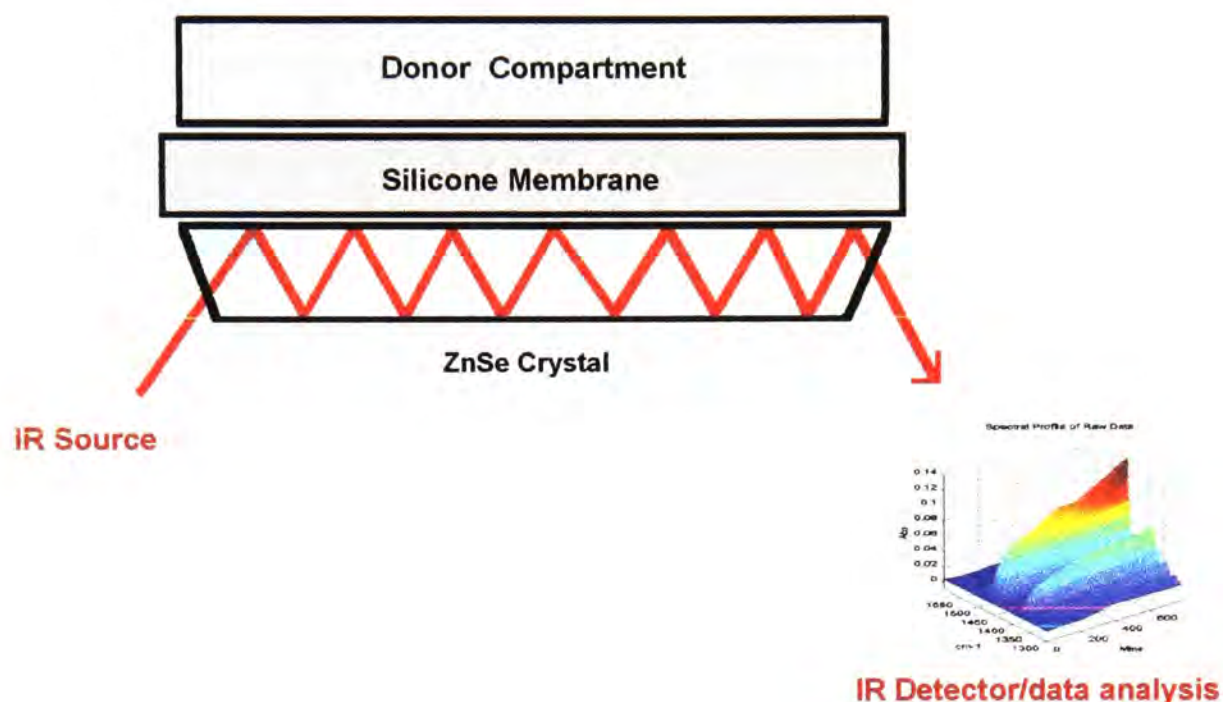


Figure.3.2. Schematic of ATR-FTIR diffusion apparatus with a typical 3D map of the raw data.

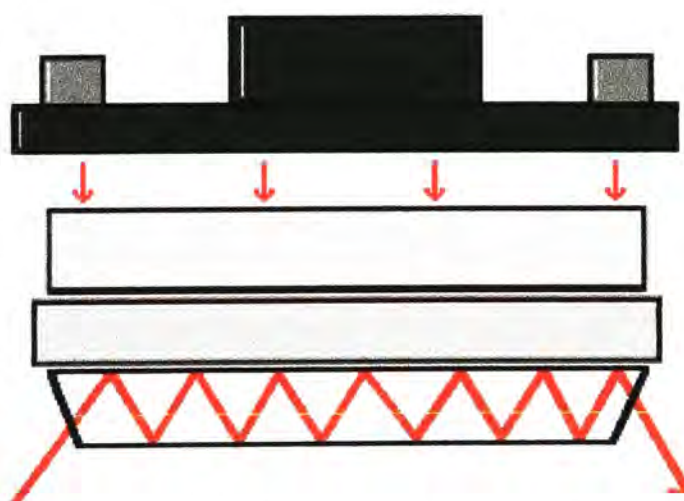


Figure.3.3. Schematic of ATR-FTIR diffusion apparatus showing the apparatus which exerts pressure upon the trough.

3.4. Analysis

3.4.1. UV Spectrophotometry

UV/visible spectrophotometry has been used throughout this research, for both calibration and other investigations. Quantitative methods based on the absorption of electromagnetic radiation such as UV/visible spectrophotometry involve measurement of the radiation or passage through an absorbing medium, i.e. the sample. The degree of absorption is determined by comparing the intensity of the transmitted beam when no absorbing species is present, i.e. a blank, with that transmitted by the sample. For monochromatic radiation passing through a homogenous liquid sample, the reduction in intensity of the incident radiation can be related to the concentration of absorbing species and to the thickness of the absorbing medium, both relations of which are described in the Beer-Lambert law.

Derivation of the Beer-Lambert law

The Lambert law is concerned with the thickness of an absorbing medium. It states that successive equal thicknesses absorb equal fractions of monochromatic incident radiation. This leads to an exponential decrease in the intensity of the radiation as it passes through the layer. This is shown in the equation below,

$$I = I_0 e^{-kl} \quad (\text{Eqn 3.1})$$

Where I and I_0 are the transmitted and incident light intensities respectively, l is the thickness of the absorbing medium, and k is a constant determined by the wavelength of the radiation and the nature of the sample. In the logarithmic form,

$$\text{Log} (I_0/I) = k'l \quad (\text{Eqn. 3.2})$$

Beer's Law deals in a similar way with the concentration c of an absorbing species and leads to the relation,

$$\text{Log } (I_0/I) = k''c \quad (\text{Eqn. 3.3})$$

Combining the two laws gives the Beer-Lambert law, which may be expressed in the form,

$$\text{Log } (I_0/I) = A = \epsilon cl \quad (\text{Eqn. 3.4})$$

Where $\log(I_0/I)$ is defined as the absorbance A and ϵ is the molar absorption coefficient (or extinction coefficient). The value of ϵ (the absorbance of a 1M solution in a 1cm cell) depends on the nature of the absorbing species and on the wavelength of the incident radiation. Absorbance is thus seen to be directly proportional both to the concentration of the absorbing species and to the thickness of the absorbing medium.

The Beer-Lambert law can be used to prepare a calibration graph, or Beer-Lambert plot, by plotting absorbance against concentration for a series of solutions of known concentration. This should give a straight line passing through the origin with a slope equal to ϵl . Measurements are generally made at less than a maximum of 1.0 AU to optimise sensitivity and to minimise errors in choosing an appropriate wavelength for the absorbing species. This also minimises apparent deviations from the Beer-Lambert law for incident radiation of wide bandwidth. The concentration of unknown samples can be read directly from the graph or calculated by dividing the absorbance value by the slope ϵl .

3.4.2. Preparation of calibration standards for UV spectrophotometry

The UV/visible spectrometer used throughout this work was a Hewlett Packard diode array (model HP8453).

10mg of drug was weighed into a plastic weighing boat on an analytical balance. It was then placed in a 100mL volumetric flask and made up to 100mL with an appropriate solvent. This is the stock solution. From this the desired standard concentrations could be prepared.

For solubility samples using PG or water, or mixtures of PG/water, methanol was used to dilute the samples because it served as a good solvent for both the drug and the vehicle. For solubility samples using MO or MG or MO/MG mixtures, hexane was used to dilute the samples. For acetaminophen samples it was not possible to find a solvent which would dissolve the mineral oil and miglyol, as well as acting as a suitable solvent for the calibration standards, because of its low logP (0.46). It was also found that many solvents that many potentially useful solvents could not be used because their UV spectrum contained overlapping signals.

Salicylic acid calibration procedure

Detection at 305nm. Calibration curves were constructed on the basis of absorbance values using standard solutions (Beer-Lambert plot).

Table 3.1. Standard solutions prepared for salicylic acid calibrations.
(Using methanol as a solvent).

Preparation	Amount ($\mu\text{g}/\text{mL}$) in solution
3mLs of stock + 7mL	30 $\mu\text{g}/\text{mL}$
2.5mLs of stock + 7.5mL solvent	25 $\mu\text{g}/\text{mL}$
2mLs of stock + 8mL solvent	20 $\mu\text{g}/\text{mL}$
1.5mLs of stock + 8.5mL solvent	15 $\mu\text{g}/\text{mL}$
1ml of stock + 9mL solvent (1:10 solution)	10 $\mu\text{g}/\text{mL}$
7.5mLs of 1:10 + 2.5mLs solvent	7.5 $\mu\text{g}/\text{mL}$
5mLs of 1:10 + 5mL solvent	5 $\mu\text{g}/\text{mL}$
2.5mLs of 1:10 + 7.5mL solvent	2.5 $\mu\text{g}/\text{mL}$
2mLs of 1:10 + 8mL solvent	2 $\mu\text{g}/\text{mL}$
1ml of 1:10 + 9mL solvent	1 $\mu\text{g}/\text{mL}$

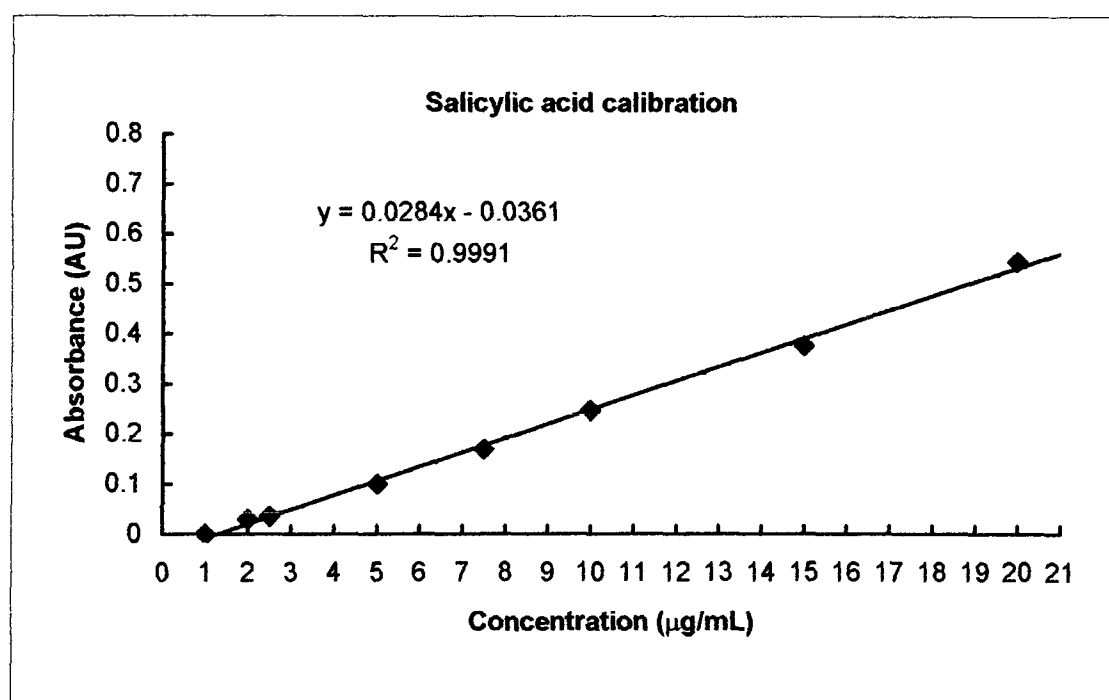


Figure 3.4. Absorbance vs. concentration plot for salicylic acid in methanol.

Table 3.2. Standard solutions prepared for salicylic acid calibrations.
(Using hexane as a solvent).

Preparation	Amount ($\mu\text{g}/\text{mL}$) in solution
0.5mL of stock + solvent	5 $\mu\text{g}/\text{mL}$
1mL of stock + solvent	10 $\mu\text{g}/\text{mL}$
1.5mL of stock + 8.5mL solvent	15 $\mu\text{g}/\text{mL}$
2mL of stock + 8mL solvent	20 $\mu\text{g}/\text{mL}$
2.5mL of stock + 7.5mL solvent	25 $\mu\text{g}/\text{mL}$
3mL of stock + 7mL solvent	30 $\mu\text{g}/\text{mL}$
3.5mL of stock + 6.5mL solvent	35 $\mu\text{g}/\text{mL}$
4.5mL of stock + 5.5mL solvent	45 $\mu\text{g}/\text{mL}$

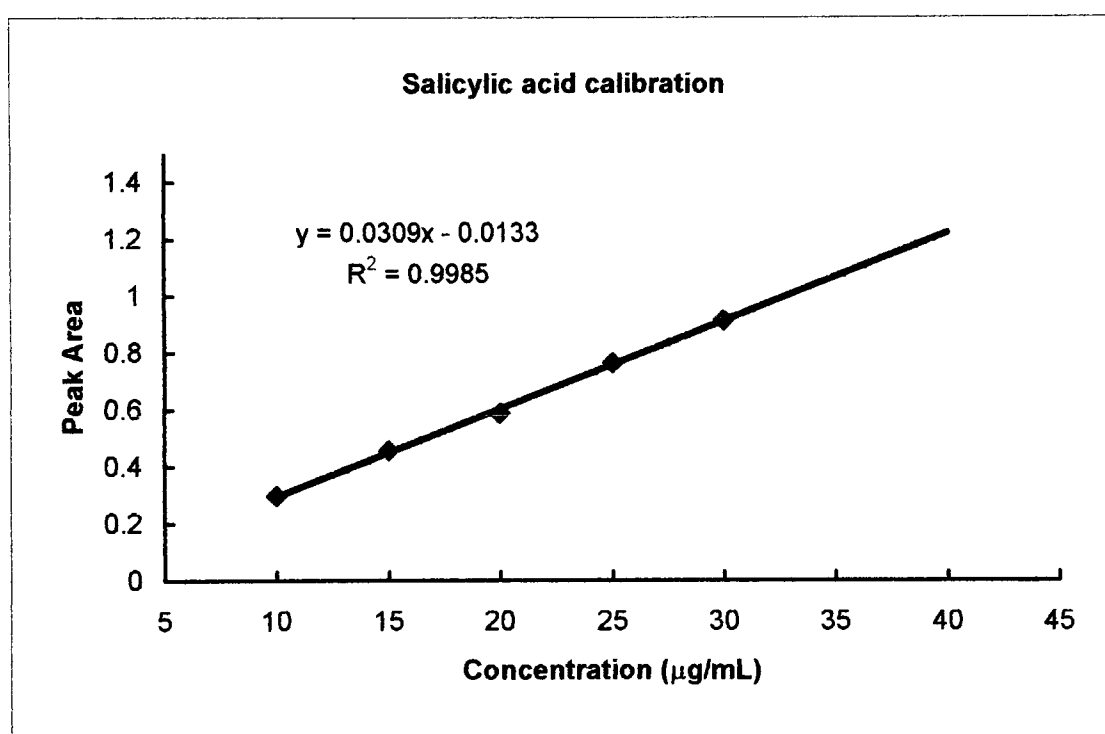


Figure. 3.5. Absorbance vs. Concentration graph for salicylic acid in hexane.

Ibuprofen calibration procedure

Detection at 225nm. Calibration curves were constructed on the basis of absorbance values using standard solutions (Beer-Lambert plot).

Table. 3.3. Standard solutions prepared for ibuprofen calibrations.
(Using methanol as a solvent).

Preparation	Amount ($\mu\text{g/mL}$) in solution
0.5mL of stock + 9.5mL solvent	5 $\mu\text{g/mL}$
1mL of stock + 9mL solvent	10 $\mu\text{g/mL}$
1.5mL of stock + 8.5mL solvent	15 $\mu\text{g/mL}$
2mL of stock + 8mL solvent	20 $\mu\text{g/mL}$
2.5mL of stock + 7.5mL solvent	25 $\mu\text{g/mL}$
3mL of stock + 7mL solvent	30 $\mu\text{g/mL}$
3.5mL of stock + 6.5mL solvent	35 $\mu\text{g/mL}$
4.5mL of stock + 5.5mL solvent	45 $\mu\text{g/mL}$

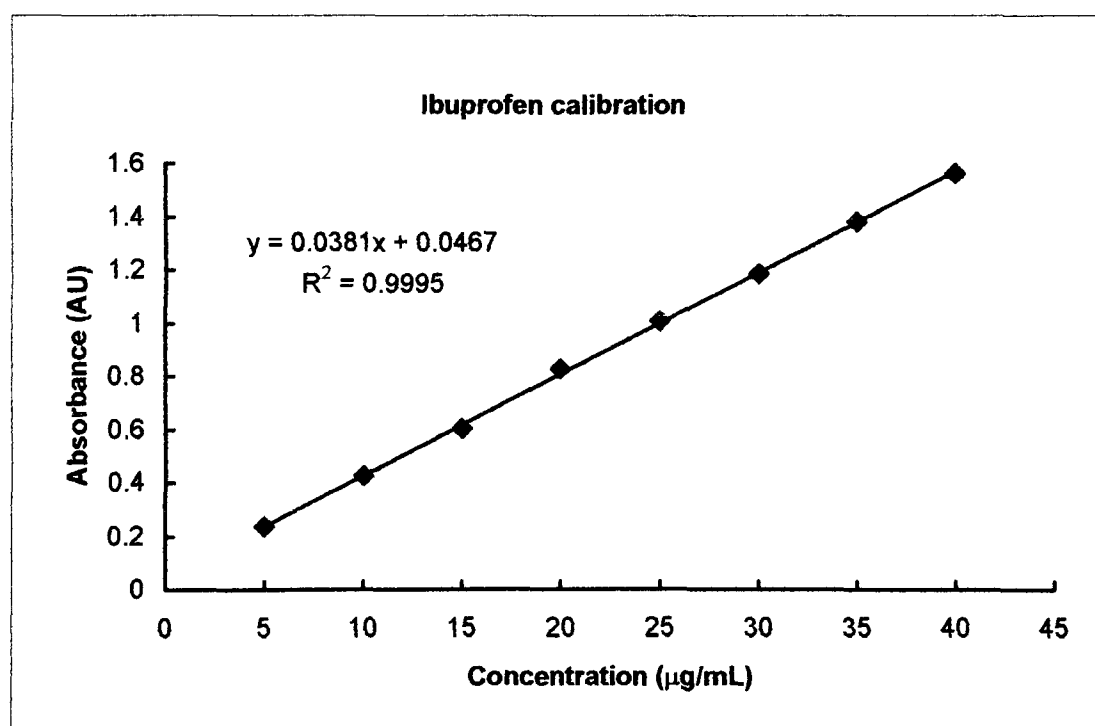


Figure 3.6. Absorbance vs. concentration plot for ibuprofen in methanol.

Table 3.4. Standard solutions prepared for ibuprofen calibrations.
(Using hexane as a solvent).

Preparation	Amount ($\mu\text{g/mL}$) in solution
1mL of 1:10 + 9mL solvent	1 $\mu\text{g/mL}$
2mL of 1:10 + 8mL solvent	2 $\mu\text{g/mL}$
5mL of 1:10 + 5mL solvent	5 $\mu\text{g/mL}$
7.5mL of 1:10 + 2.5mL solvent	7.5 $\mu\text{g/mL}$
1mL of stock + 9 mL solvent	10 $\mu\text{g/mL}$
1.5mL of stock + 8.5mL solvent	15 $\mu\text{g/mL}$
2mL of stock + 8mL solvent	20 $\mu\text{g/mL}$

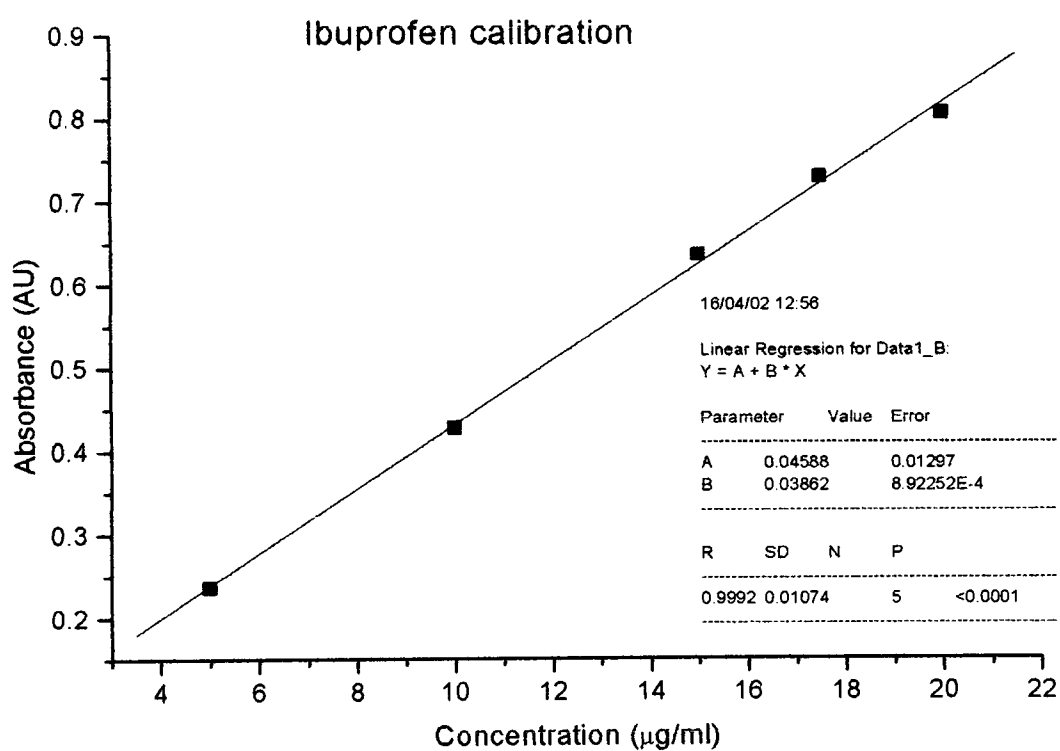


Figure 3.7. Absorbance vs. concentration plot for ibuprofen in hexane.

Acetaminophen calibration procedure

Detection at 254nm. Calibration curves were constructed on the basis of absorbance values using standard solutions (Beer-Lambert plot).

Table 3.5. Standard solutions prepared for ibuprofen calibrations.
(Using methanol as a solvent).

Preparation	Amount ($\mu\text{g/mL}$) in solution
1mL of stock + 9mL solvent (1:10 solution)	10 $\mu\text{g/mL}$
1mL of 1:10 + 9mLs solvent	1 $\mu\text{g/mL}$
200 μL of 1:10 + 800 μL solvent	2 $\mu\text{g/mL}$
200 μL of 1:10 + 600 μL solvent	2.5 $\mu\text{g/mL}$
500 μL of 1:10 + 500 μL solvent	5 $\mu\text{g/mL}$
750 μL of 1:10 + 250 μL solvent	7.5 $\mu\text{g/mL}$

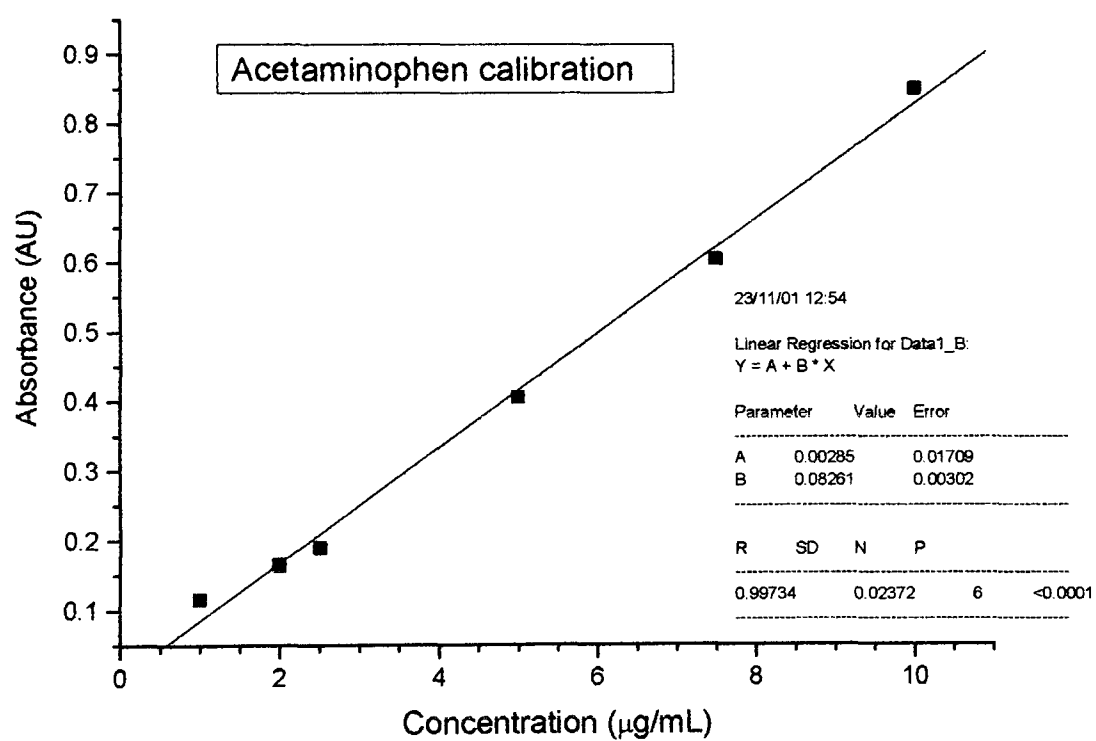


Figure 3.8. Absorbance vs. concentration plot for acetaminophen in methanol.

3.4.3. High Performance Liquid Chromatography (HPLC)

The HPLC analysis of the three selected permeants was performed using a SpectraSERIES P100 pump (Thermo separation products), a SpectraSERIES UV100 detector and a ChromJet integrator. Samples were injected using a SpectraSERIES AS100 autosampler.

HPLC Calibration procedure

10mg of drug was weighed into a plastic weighing boat on an analytical balance. It was then placed in a 100ml volumetric flask and made up to 100ml with mobile phase or an appropriate solvent. This is the stock solution. From this the following solutions were prepared:

Table 3.6. Standard solutions prepared for HPLC calibrations.

(Using the appropriate mobile phase as a solvent).

Dilution factor	Preparation	Amount ($\mu\text{g}/\text{mL}$) in solution
1:10	1mL of stock + 9mL mobile phase	10 $\mu\text{g}/\text{mL}$
1:100	1mL of 1:10 + 9mL mobile phase	1 $\mu\text{g}/\text{mL}$
1.5	200 μL of 1:10 + 800 μL mobile phase	2 $\mu\text{g}/\text{mL}$
1:4	200 μL of 1:10 + 600 μL mobile phase	2.5 $\mu\text{g}/\text{mL}$
1:2	500 μL of 1:10 + 500 μL mobile phase	5 $\mu\text{g}/\text{mL}$
1:15	750 μL of 1:10 + 250 μL mobile phase	7.5 $\mu\text{g}/\text{mL}$

System reproducibility checking procedure

A single calibration standard was injected onto the column 10 times to ensure the HPLC system was stable and producing reproducible results.

Date: 24 July 2002	
Concentration: 1µg/mL	
Sample No.	Peak Area
1	70264
2	71834
3	71481
4	70946
5	71045
6	70521
7	71523
8	71076
9	71517
10	70268
Average	71051
SD	553.53
CV	0.77

Figure 3.9. Typical result of a system reproducibility experiment.

Analytical details for the model permeants

Ibuprofen

HPLC: The stationary phase was an Apex reverse phase ODS 5µm packed column (250 mm x 4.6mm) and a mobile phase of 65% acetonitrile and 35% phosphate buffer (adjusted to pH 3.2 using orthophosphoric acid). Samples were injected through a loop of 100µL. Detection was performed by UV at 225nm and a flow rate of 1.2mL min⁻¹. The retention time was approx. 5 minutes, and calibration curves were constructed on the basis of peak area measurements using >5 standard solutions. Reproducibility was evaluated prior to injection of the samples and during analysis, and CV values were <5% in all experiments.

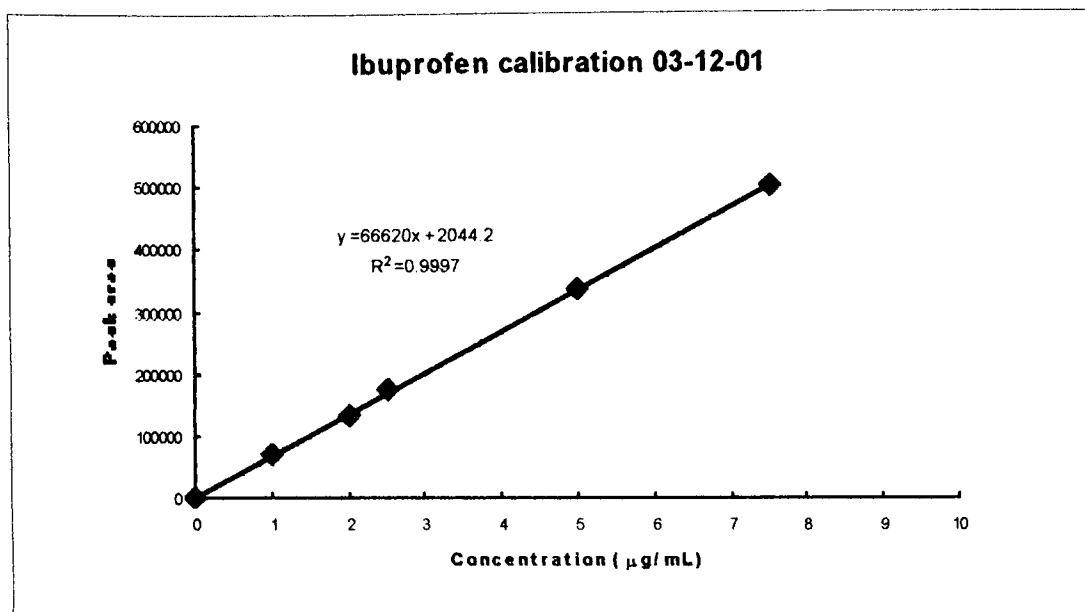


Figure 3.10. A typical example of a peak area vs. concentration plot for the calibration of ibuprofen.

Salicylic acid

HPLC: The stationary phase was as previous. The mobile phase consisted of 60% methanol and 40% phosphate buffer (adjusted to pH 3.3 using orthophosphoric acid). Detection was performed at 305nm, with a retention time of approx. 5 minutes at a flow rate of 1.0 mL min^{-1} . Calibration and reproducibility as previously described.

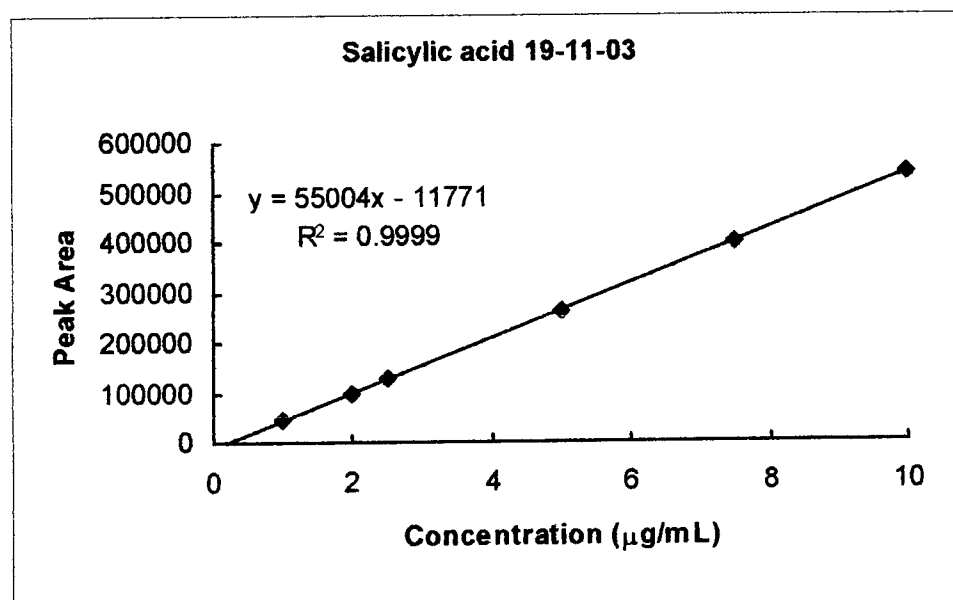


Figure 3.11. A typical example of a peak area vs. concentration plot for the calibration of salicylic acid.

Acetaminophen

HPLC: The stationary phase was as previously described. The mobile phase consisted of 10% acetonitrile and 90% de-ionised water adjusted to pH 4 using orthophosphoric acid. Detection was performed at 254nm, with a retention time of approximately 5 minutes at a flow rate of 1.1mL min⁻¹. Calibration and reproducibility are as previously described.

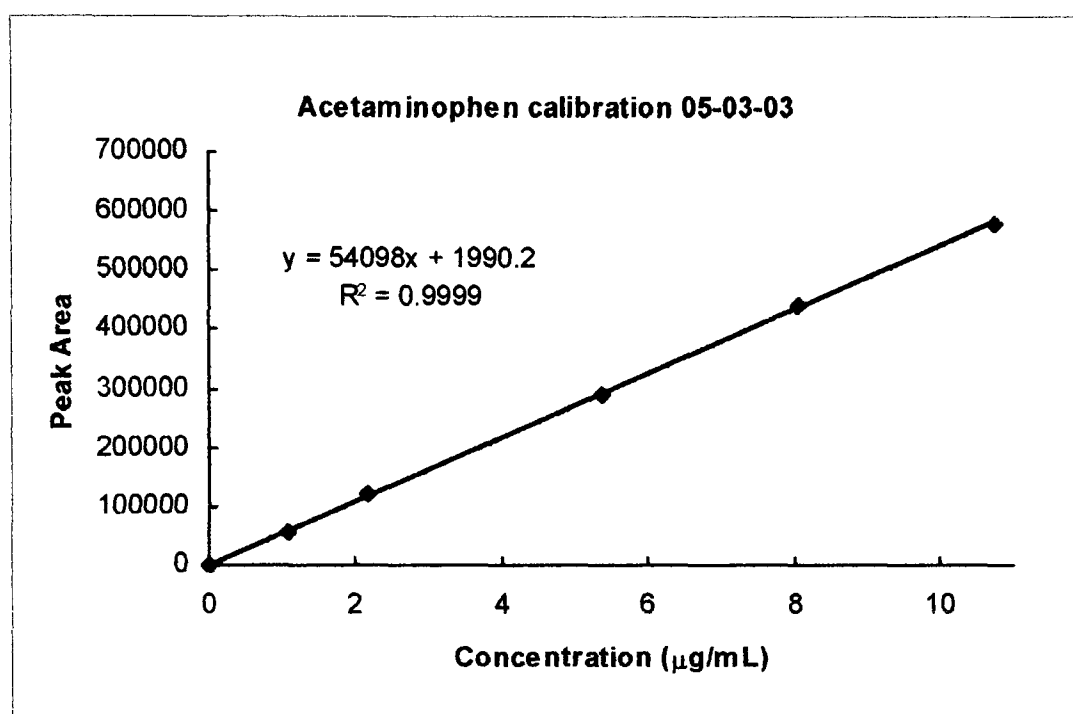


Figure 3.12. A typical example of a peak area vs. concentration plot for the calibration of acetaminophen.

3.5. Solvent uptake studies

The extent to which a vehicle can modify the membrane depends on the extent of its uptake by the membrane, and historically this has been borne out by experimental results. Factors influencing the solvent uptake include the solubility parameter and molecular weight. The uptake of the selected vehicles into silicone membrane was evaluated. Solubility parameters are used to identify plasticizers since it is thought that the effectiveness of a plasticizer is highest when its solubility parameter matches that of the membrane. Therefore it is reasonable to expect higher solvent uptake from vehicles which have similar solubility parameters to the membrane.

Another factor to consider is that if the solubility parameter of the solvent is similar to that of the membrane then the solvent will enter. If the permeant is more soluble in the solvent than in the polymeric membrane then the presence of solvent in the membrane will increase the partition coefficient, hence flux will be increased.

The uptake of vehicles into the silicone membrane was experimentally determined by a gravimetric method. Silicone membrane was cut to an appropriate size ($\sim 1\text{cm}^2$) and weighed using a balance ($10\mu\text{g}$ accuracy). They were then placed in a sample bottle containing the vehicle and soaked for 24 hours. The membranes were blotted dry with tissue paper and re-weighed. The experiments were performed in triplicate, at room temperature. The amount of solvent taken up by the membrane was expressed as a weight percent. Solubility parameters for the selected vehicles were calculated using Hansen's approach (Hansen, 2000).

Table 3.7. Solvent uptake by silicone membrane (w/w %)

Vehicle	Solvent uptake (w/w %)	Solubility parameter of vehicle (cal/cm³)^{1/2}
Mineral oil	9.5	7.1
Miglyol/mineral oil (50:50)	9.6	8.3
Miglyol	2.3	9.4
PG	-	14.0
PG/Water (50:50)	1.0	18.7
Water	1.6	23.4

Table 3.7 presents the results of solvent uptake experiments. The highest uptake was observed for a 50:50 mixture of mineral oil and Miglyol. This result confirms the idea introduced above as the lipophilic solvents have solubility parameters closest to that of the membrane. The solubility parameter of silicone membrane is reported in the literature to be 7.5 (cal/cm³)^{1/2}. Although the results of this experiment do give some idea of how well a solvent/formulation will permeate it is also necessary to consider the drug being delivered. In this case of drugs with low logP values it would be difficult to overcome poor solubility and it is unlikely that a high flux will be achieved even if the solvent flux is high. It is a case of balancing a number of factors to achieve the optimum topical vehicle.

3.6. References

M. Dias, J. Hadgraft, S. L. Raghavan and J. Tetteh. The effect of solvent on permeation through membranes studied using ATR-FTIR and chemometric data analysis. *J. Pharm. Sci.* **93**, 186-196 (2004)

C. M. Hansen. Hansen solubility parameters: a users handbook. CRC Press (2000).

S. M. Harrison, B. W. Barry and P. H. Dugard. Effects of freezing on human skin permeability. *J. Pharm. Pharmacology.* **36**, 261-262 (1984)

InSight user manual. DiKnow Ltd, London (2000)

R. M. Johnson. On a theorem stated by Eckhart and Young. *Psychometrika.* **28**, 259-263 (1963)

A. M. Kligman and E. Christophers. Preparation of isolated sheets of human stratum corneum. *Arch. Dermatol.* **88**, 70-73 (1963)

E. R. Malinowski. Factor analysis in chemistry. 2nd Edition, pp1-31 (1991)

Matlab user manual. The Mathworks Inc. USA (1999)

J. Tetteh. Enhanced target factor analysis and radial basis function neural network for analytical spectroscopy. PhD Thesis, University of Greenwich (1997)

- Chapter Four -

Diffusion Studies Through Silicone Membrane

4.1. Introduction

As described in chapter one, the driving force for a drug across a membrane is its thermodynamic activity in the formulation. Saturated solutions of a compound in any vehicle have a thermodynamic activity equal to unity and will give a constant flux provided that there are no interactions between the vehicle, solute and membrane. The diffusion across PDMS membranes of saturated solutions of the NSAIDs ibuprofen, salicylic acid and acetaminophen was investigated. Synthetic PDMS membranes were used because they offer a uniform, hydrophobic barrier to diffusion, and they have been well characterised in the literature. The steady state diffusion of a substance across a synthetic or biological membrane can be described in mathematical terms by Fick's first law of diffusion (refer to Chapter One), and this equation was used to interpret the flux values of the selected permeants in various model formulations across PDMS membranes.

4.2. Mathematical analysis using Fick's second law of diffusion

There are a limited number of methods available by which diffusion coefficients can be measured directly, and one of the most common methods involves Fick's first law of diffusion, and measurement of steady state flux across a membrane. The following description of the mathematical background to the diffusion process is adapted from Watkinson (2002). Please refer to Watkinson (2002) or Roberts (2002) for a more thorough treatment of Fick's laws and their use in the study of skin permeation.

In passive diffusion, matter moves from one region of a system to another following random molecular motions. If the cumulative mass of diffusant, μ , which passes per unit area is measured through a membrane as a function of time, a typical plot as shown below (figure 4.1) is obtained.

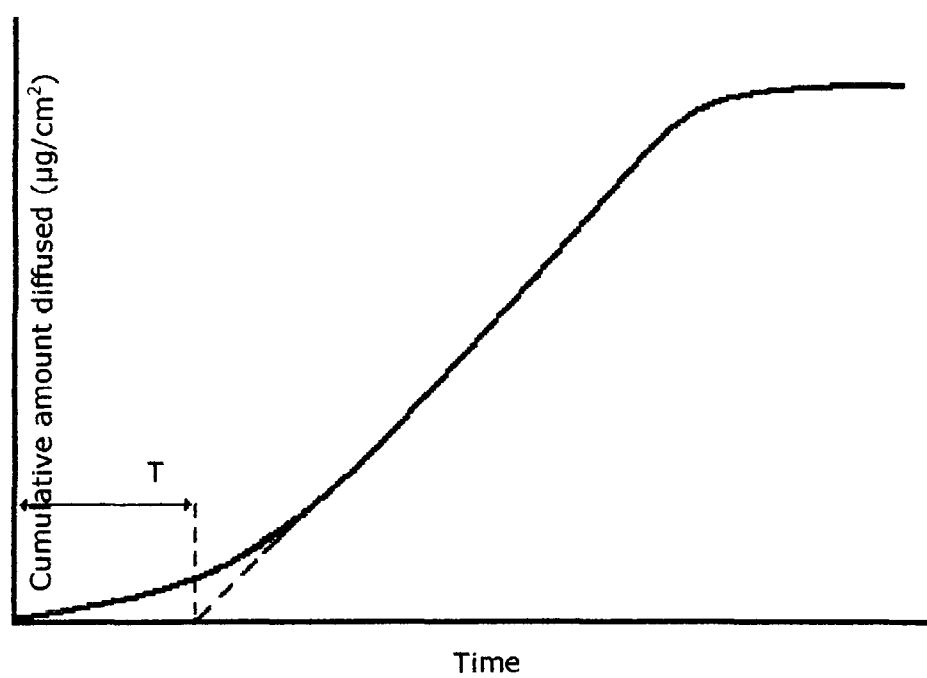


Figure 4.1. Drug-penetration time profile for an idealised drug diffusing through a membrane

The basic hypothesis underlying the mathematical theory for isotropic materials is that the rate of transfer of a diffusing substance per unit area

is proportional to the concentration gradient. This is known as Fick's first law of diffusion.

$$\frac{dQ}{dt} = J = \frac{Dc_0}{h} \quad (\text{Eqn. 4.1})$$

As stated in chapter one if a plot such as shown in figure 4.1 is extrapolated to the time axis, the intercept obtained at $m=0$ is the lag time (t_{lag}) which is related to D by:

$$t_{lag} = \frac{h^2}{6D} \quad (\text{Eqn. 4.2})$$

As a result D can be estimated provided the membrane thickness, h , is known. However there are inherent problems with this estimation. Lag time values for example, obtained from permeation experiments using the extrapolation method tend to be very variable (especially through human skin because of its biological variability, i.e. stratum corneum thickness and the number and density of appendages). It should be noted however that the skin appendages account for less than 0.1% of the total surface area and their contribution to permeation is negligible. When using stratum corneum in such studies the exact thickness is extremely difficult to measure and can vary with penetration enhancement treatment (as is dealt with in this thesis). The measured thickness of the membrane does not allow for a tortuous pathway for diffusion and therefore the value obtained for D is more often than not, an apparent one.

So there is a clear need for a better form of analysis. Consider graph 4.1, showing the lag phase followed by pseudo steady state diffusion and a plateau which indicates either depletion of the donor or, in the case of an ATR-FTIR experiment, saturation of the membrane with the diffusing

species. Fick's laws are of more applicability to this kind of data if we can specify certain parameters or boundaries within which to apply them. These boundary conditions allow us to be more exacting in defining the problem with which we are dealing. In this case we are interested in diffusion through a homogenous membrane with a constant activity difference and a constant diffusion coefficient. This is the commonest situation for diffusion studies as the constant activity allows potential enhancers to be revealed.

The mathematical boundary conditions imposed are those of a well-designed diffusion experiment when a permeant is at high, fixed activity on one side of the membrane through which it diffuses into a sink on the other side. Before the start of the experiment the membrane is entirely devoid of permeant. Diffusive flow begins at the high concentration side (donor side) of the membrane where $c = c_0$ and $x = h$ at all time t . There is no diffusant material within the membrane before ingress of the permeant being modelled, implying that at $t = 0$ we have $c = 0$ for all x . Diffusion occurs in the direction of decreasing x towards the opposite side of the membrane where $x = 0$ and $c = 0$ (sink receptor phase) at all time t . In this model the diffusion coefficient of the permeant is set as a constant D , and the concentration c , of material at any point x , within the membrane can be calculated as a function of time using equation 4.3.

$$c = \frac{c_0 x}{h} + \frac{2}{\pi} \sum_{n=1}^{\infty} \frac{c_0}{n} \cos(n\pi) \sin\left(\frac{n\pi x}{h}\right) \exp\left(\frac{-Dn^2\pi^2 t}{h^2}\right) \quad (\text{Eqn. 4.3})$$

Diffusion equations such as this are often simplified by normalizing the concentration and distance variables to their maxima. In the equation above this involves normalizing x (the distance) relative to h (membrane thickness) where $\chi = x/h$ and c (concentration in the membrane at any

point x) relative to c_0 (concentration in the outer layer of the membrane at $x = h$) where $\mu = c/c_0$. It is also convenient to introduce the term $\tau = Dt/h^2$. These simplifications yield equation 4.4, in which we can see that, for any value of τ , if $x = 0$ (i.e. at the distal side of the membrane), we obtain $\mu = 0$.

$$\mu = \chi + \frac{2}{\pi} \sum_{n=1}^{\infty} \frac{1}{n} \cos(n\pi) \sin(n\pi\chi) \exp(-n^2\pi^2\tau) \quad (\text{Eqn. 4.4})$$

Under these conditions a plot (of simulated data) is obtained that is very similar to that shown in figure 4.1. These equations have been used to analyse data acquired from skin stripping experiments, and have been taken a step further by separately modelling concentration gradients across the *stratum corneum* and viable epidermis. Although these equations have some use in the analysis of diffusion data, they are of limited practical use for interpreting permeation data, as they describe the concentration within a membrane at any time point t , and at any position x , within that membrane. A more useful solution that yields the cumulative mass of permeant, Q that passes through a unit area of a membrane in a time t is provided by equation 4.5.

$$Q = C_0 h \left[\frac{Dt}{h^2} - \frac{1}{6} - \frac{2}{\pi^2} \sum_{n=1}^{\infty} \frac{(-1)^n}{n^2} \exp\left(-\frac{Dn^2\pi^2 t}{h^2}\right) \right] \quad (\text{Eqn. 4.5})$$

As $t \rightarrow \infty$, the exponential term in equation 4.5 tends to zero; therefore equation 4.5 approximates to the line described by equation 4.6, which, on rearrangement, becomes equation 4.7.

$$Q = c_0 h \left[\frac{Dt}{h^2} - \frac{1}{6} \right] \quad (\text{Eqn. 4.6})$$

$$Q = \frac{Dc_0}{h} \left[t - \frac{h^2}{6D} \right] \quad (\text{Eqn. 4.7})$$

If we put $Q = 0$ into equation 4.7 we can solve for t and this yields the value of the time axis (the lag time, t_{lag}) as described by equation 4.2, which relates it inversely to the diffusion and directly to the diffusional pathlength. The use of this extrapolation for the calculation of diffusion coefficients is commonplace although, as mentioned before, it is inherently unreliable where skin is concerned.

If we differentiate Equation 4.7 relative to time we obtain equation 4.9, probably the most well known form of Fick's first law of diffusion, which describes the flux, J at steady state.

$$\frac{dQ}{dt} = J = \frac{Dc_0}{h} \quad (\text{Eqn. 4.8})$$

But, as before, it is often impractical to use the forms of equations 4.6, 4.7 and 4.8 as shown because they include a term, c_0 (the concentration of permeant in the outer layer of the membrane), which is very difficult to measure. We can replace the value c_0 with a term that links it to the concentration in the vehicle, c_v through the partition coefficient, K as described by equation 4.9, which rearranges to give equation 4.10

$$K = \frac{c_0}{c_v} \quad (\text{Eqn. 4.9})$$

$$c_0 = Kc_v \quad (\text{Eqn. 4.10})$$

The partition coefficient is simply a measure of the relative affinity that a diffusant has for the two media involved (i. e. the membrane and then vehicle above it). Substitution of equation 4.10 into equation 4.8 produces equation 4.11 which is of more practical use as it links flux to the concentration of the permeant in the vehicle.

$$\frac{dQ}{dt} = J = \frac{DKC_v}{h} \quad (\text{Eqn. 4.11})$$

If the membrane thickness, h , and the concentration c_v , is known then D can be measured from the determination of the flux J . For the most common conditions used for diffusion experiments (the use of sink conditions in the receptor solution below the membrane) the assumption is that the concentration at the inner surface of the membrane is zero.

An added difficulty with biological membranes is the practical difficulty in measuring the diffusional pathlength. Because of this a composite parameter is often used. The permeability coefficient, k_p , is defined as $k_p = KD/h$, and this simplifies further to give equation 4.12.

$$J = k_p c_v \quad (\text{Eqn. 4.12})$$

Equation 4.12 is possibly the most basic yet frequently used expression in the routine assessment of membrane permeability. However, the principles upon which it is based stipulate that the donor concentration is constant and that diffusion has reached steady state. For most experiments, as in those carried out in this report, this means using a saturated donor solution in the presence of excess permeant. However, as with other aspects of permeation, there are problems with the assumption of steady state and the assessment of when it has been attained. In light of this, the use of a steady state method for the assessment of permeability coefficients, lag times and other parameters has been questioned. It is difficult to assess when this period has been reached, and by using only the (assumed) steady state data, much information is potentially being lost. Information that could possibly aid

our understanding of permeation. One way to overcome this problem is to utilize equation

$$Q = KC_v h \left[\frac{Dt}{h^2} - \frac{1}{6} - \frac{2}{\pi^2} \sum_{n=1}^{\infty} \frac{(-1)^n}{n^2} \exp\left(-\frac{Dn^2 \pi^2 t}{h^2}\right) \right] \quad (\text{Eqn. 4.13})$$

The equation, in the form shown above is of quite limited use as there are three unknown parameters. But, if Kh and D/h^2 are replaced with α and β respectively, we have equation 4.14, which has two variables. By fitting α and β we can obtain a value of the permeability coefficient as $\alpha\beta = Kh/Dh^2 = KD/h$, which is equal to the permeability coefficient.

$$Q = c_v \alpha \left[\beta t - \frac{1}{6} - \frac{2}{\pi^2} \sum_{n=1}^{\infty} \frac{(-1)^n}{n^2} \exp(n^2 \pi^2 \beta t) \right] \quad (\text{Eqn. 4.14})$$

It is this equation that will be used to investigate steady state diffusional parameters for the systems used in this thesis. This equation allows the calculation of Diffusion coefficient, partition coefficient. And, through knowledge of the diffusion coefficient and diffusional pathlength, reveals the lag time.

4.3. Methods

The methods and analysis used in this chapter are detailed in Chapter Three.

4.4. Experimental

The following experiments were conducted:

Single-phase studies

Permeation of ibuprofen from saturated solutions

- Propylene glycol
- Water
- Mineral oil
- Miglyol
- Transcutol
- Ethanol

Permeation of salicylic acid from saturated solutions

- Propylene glycol
- Water
- Mineral oil
- Miglyol
- Transcutol
- Ethanol

Permeation of acetaminophen from saturated solutions

- Mineral oil
- Miglyol

Binary solvent formulations

Permeation of ibuprofen from saturated formulations containing:

- Propylene glycol and water
- Mineral oil and miglyol
- Ethanol and water (including studies to investigate membrane pre-treatment)
- Ethanol and propylene glycol
- Transcutol and water
- Transcutol and propylene glycol

Permeation of salicylic acid from saturated formulations containing:

- Propylene glycol and water
- Mineral oil and miglyol
- Ethanol and water
- Transcutol and water

Ternary solvent formulations

Permeation of ibuprofen from saturated formulations containing:

- Ethanol, propylene glycol and water (including experiments to investigate the effect of occlusion)
- Transcutol, propylene glycol and water (including studies to investigate the effect of occlusion and membrane pre-treatment)

4.5. Results and discussion

4.5.1. Single-phase studies

4.5.1.1. Ibuprofen

Permeation of ibuprofen through silicone membrane was evaluated. Six solvents were selected. Fluxes were calculated by monitoring the cumulative amount of drug diffused and measuring the slope of the graph once steady state diffusion was reached.

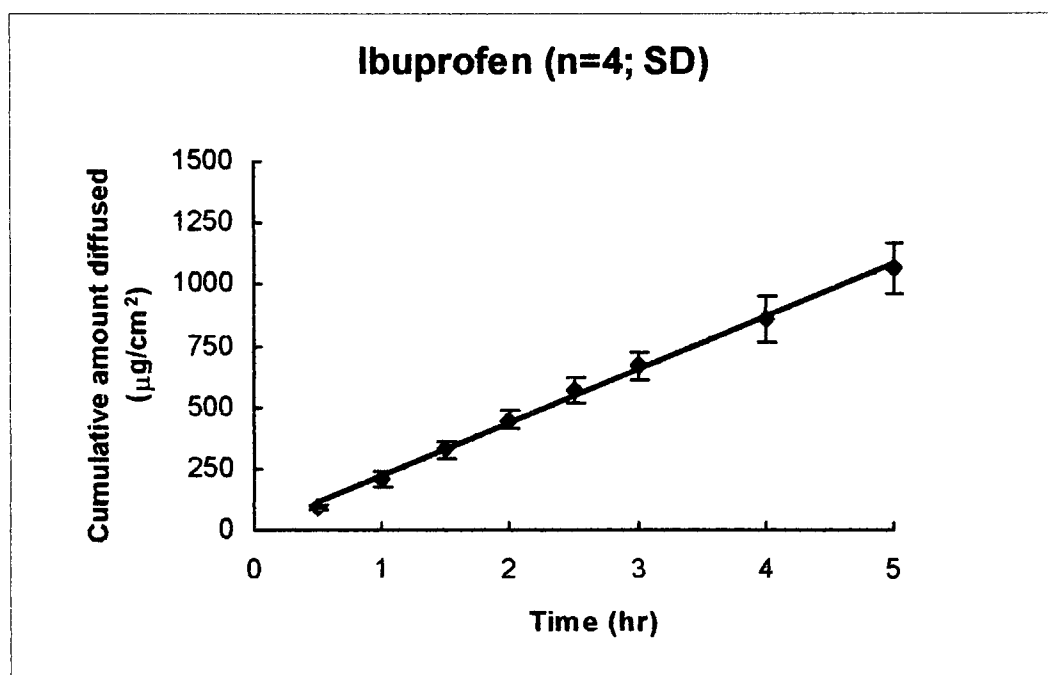


Figure 4.2. Representative diffusion profile.

All time points were used to measure the slope of the graph. Values for α , β and k_p were determined using the curve fitting procedure described in section 4.2. Table 4.1 lists the mean steady state fluxes obtained, the corresponding standard deviations and coefficient of variation. Figure 4.2 shows a representative diffusion profile.

Table 4.1. Steady state fluxes of ibuprofen in the vehicles studied and their associated thermodynamic and kinetic parameters.

Vehicle	Flux ($\mu\text{g}/\text{cm}^2/\text{hr}$) \pm SD	CV	α (cm) \pm SD	β (s^{-1}) \pm SD	k_p (cm/s) \pm SD
PG	297.1 \pm 29.43	9.90	2.14 $\times 10^{-3}$ \pm 1.1 $\times 10^{-3}$	2.84 $\times 10^{-4}$ \pm 1.01 $\times 10^{-4}$	65.25 $\times 10^{-7}$ \pm 5.03 $\times 10^{-8}$
Water	185.5 \pm 10.94	5.90	0.18 $\times 10^{-3}$ \pm 0.35	0.32 \pm 0.14	5.75 $\times 10^{-4}$ \pm 3.75 $\times 10^{-6}$
MO	579.5 \pm 35.31	6.09	2.68 $\times 10^{-3}$ \pm 5.90 $\times 10^{-3}$	1.94 $\times 10^{-4}$ \pm 3.89 $\times 10^{-5}$	5.03 $\times 10^{-6}$ \pm 4.12 $\times 10^{-7}$
MG	623.8 \pm 67.69	10.85	4.28 $\times 10^{-3}$ \pm 9.30 $\times 10^{-7}$	2.70 $\times 10^{-4}$ \pm 2.72 $\times 10^{-5}$	1.14 $\times 10^{-6}$ \pm 1.51 $\times 10^{-7}$
TC	341.9 \pm 31.83	2.28	1.35 $\times 10^{-6}$ \pm 3.07 $\times 10^{-7}$	0.20 \pm 0.06	2.18 $\times 10^{-7}$ \pm 6.18 $\times 10^{-8}$
EtOH	1446.2 \pm 75.3	5.21	5.54 $\times 10^{-6}$ \pm 2.04 $\times 10^{-6}$	0.16 \pm 0.07	8.25 $\times 10^{-7}$ \pm 3.44 $\times 10^{-8}$

Examination of the flux values presented in table 4.1 shows that the flux varies with the different solvents used. This variation implies that there is some interaction between the vehicle and the membrane that has altered the flux, and therefore the conditions have deviated from ideality (i.e. all the fluxes would have been the same).

Considering the low water solubility of ibuprofen ($\sim 0.09\text{mg/mL}$), if water did permeate into the membrane, it would not present a more favourable environment for the solute and therefore would not enhance the permeation of the drug. What this value also allows us is a 'benchmark' flux value with which to compare the performance of the other vehicles. It is highly unlikely that water interacts with the silicone and therefore it can quite reasonably be suggested that in this experiment ibuprofen is behaving ideally. Flux values from propylene glycol (PG) and Transcutol(TC) are statistically the same, 297.1 and 341.9 $\mu\text{g}/\text{cm}^2/\text{hr}$ respectively. Both of these solvents enhance permeation by increasing the

solubility of the drug in the membrane, and it is interesting that the flux is the same. The solubility parameters of PG and TC are 15.4 and 10 $(\text{cal}/\text{cm}^3)^{1/2}$ respectively, with TC being slightly closer to ibuprofen (10.2 $(\text{cal}/\text{cm}^3)^{1/2}$), this could partly explain the flux values.

The next highest fluxes are seen for mineral oil and miglyol. Like PG and TC, the flux values are statistically the same. To bring about a 3-fold increase in the permeation of ibuprofen these two solvents must have some effect upon the membrane, or increase the solubility of the drug in the membrane. The latter is unlikely, as the solubility studies (see Chapter 2) do not show the solubility of ibuprofen to be higher in these solvents than in PG or TC. Indeed, it is PG and TC that have the more favourable solubility characteristics. This leaves the former option of a vehicle-membrane interaction.

It is extremely difficult to elucidate possible interactions based upon simple diffusion experiments, and it would be foolish to try and do so. However, using ATR-FTIR spectroscopy it is possible to examine the spectra obtained during the course of a diffusion experiment and identify shifts that would indicate a clear interaction. This type of experiment was conducted and is described and discussed in Chapter Five.

Ethanol shows the greatest enhancing effect, with the flux being increased almost 8-fold. It is possible that ethanol is acting in two ways, both improving solubility in the membrane, and also having some effect upon the membrane.

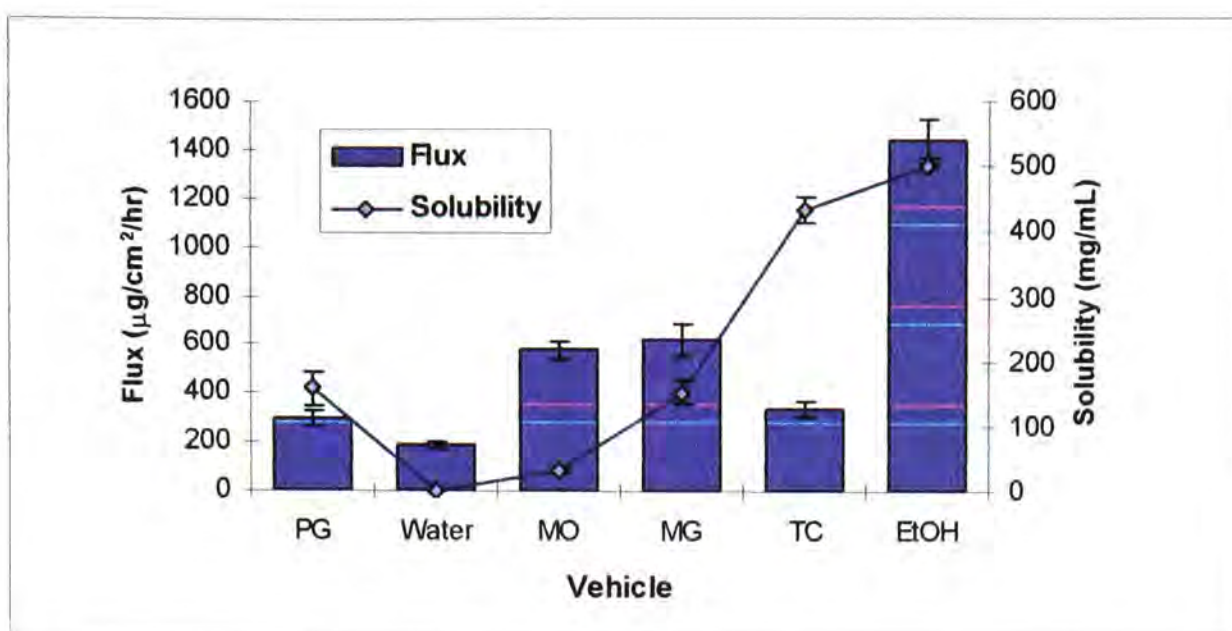


Figure 4.3. Flux values and solubilities of ibuprofen in the selected vehicles.

Figure 4.3 presents the flux values and solubilities of ibuprofen in the selected vehicles. From this it can be seen that the solubility of ibuprofen is similar in both Transcutol and ethanol. One would expect that if a permeant were to exhibit similar solubility properties in two solvents, then the flux values would be similar, because the degree of improvement of the solubility in the membrane would be of the same order of magnitude in both cases. Yet, this is not what is actually observed. The difference between the flux values is not simply attributable to the very slight variation in solubility. Ethanol has been shown to improve skin permeation by extracting skin lipids (Bommanna et al, 1990), but it is not clear by what mechanism silicone may be affected by this solvent.

4.5.1.2. Salicylic acid

The permeation of salicylic acid through silicone membrane was evaluated. The vehicles selected were the same as those used for the study of the permeation of ibuprofen. Table 4.2 lists the mean steady state fluxes obtained, the corresponding standard deviations and coefficient of variation.

Table 4.2. Steady state fluxes of salicylic acid in the vehicles studied and their solubility parameters.

Vehicle	Flux	CV	α (cm)	β (s ⁻¹)	k_p (cm/s)
	($\mu\text{g}/\text{cm}^2/\text{hr}$) \pm SD				
PG	87.1 \pm 8.12	9.32	2.23×10^{-4}	6.45×10^{-4}	1.44×10^{-7}
Water	74.9 \pm 5.55	7.42	1.15×10^{-4}	0.41	4.73×10^{-5}
MO	283.7 \pm 19.27	6.80	1.17×10^{-2}	2.14×10^{-4}	2.50×10^{-4}
MG	374.5 \pm 40.27	10.75	0.41	8.9×10^{-4}	3.32×10^{-4}
TC	308.3 \pm 66.56	21.59	-	-	-
EtOH	2018.1 \pm 374.70	18.57	-	-	-

The flux profiles for salicylic acid are similar to those of ibuprofen. As with ibuprofen, the lowest flux is from water. Although PG showed an enhancing effect for ibuprofen, for salicylic acid the flux values for water and PG are the same, suggesting no enhancement despite salicylic acid having greater solubility in PG than water.

The permeation of salicylic acid from TC, MO and MG is approximately the same, although there is a statistical difference between MO and MG, with flux being slightly higher from the latter. These solvents all improve flux 4-fold, despite the solubility of salicylic acid in MO and MG being different (41.5 and 0.2 mg/mL respectively). This would seem to indicate that these

solvents do interact with the membrane to some extent, as a similar improvement is seen for ibuprofen, again with a vast difference in solubility.

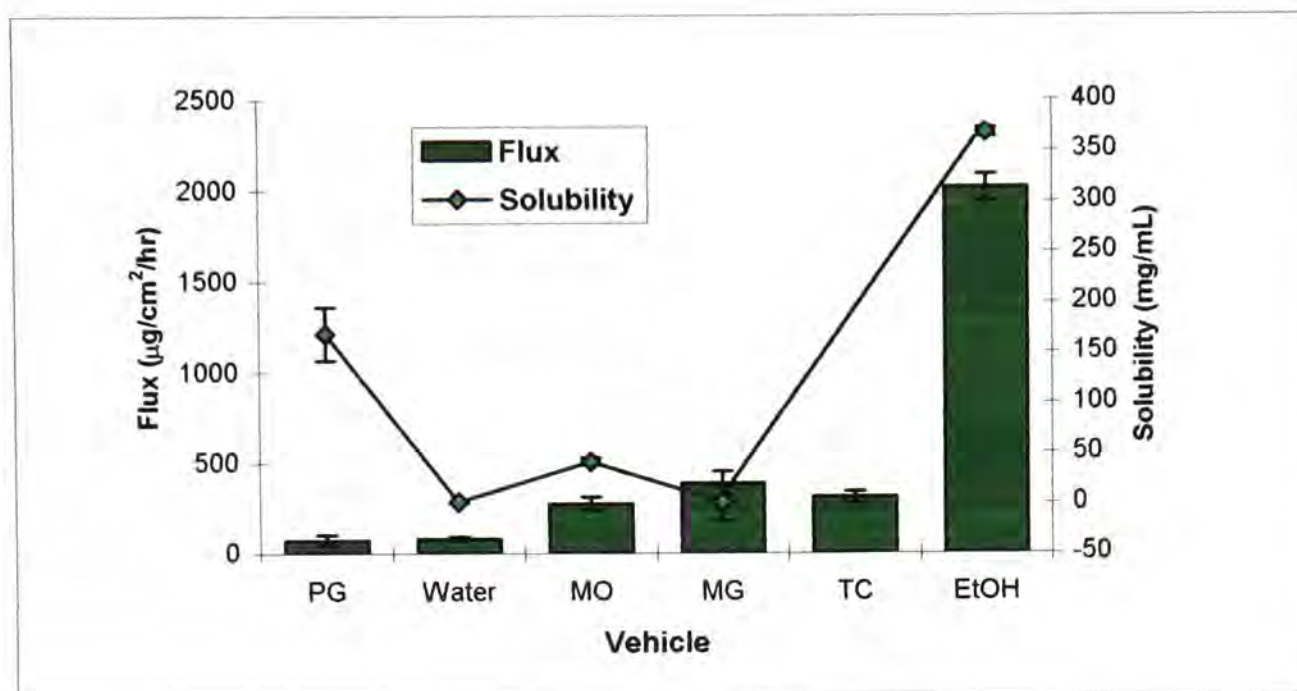


Figure 4.4. Flux values and solubilities of salicylic acid in the selected vehicles.

Salicylic acid flux from ethanol is extremely high, with a five-fold difference between ethanol and the next highest flux value for miglyol. This shows a remarkable enhancing effect on salicylic acid. This could be caused by ethanol operating in a solvent capacity, improving the solubility of salicylic acid in the membrane, or it could be attributed to an interaction between ethanol and the silicone membrane. Without further analysis and experimentation, it is impossible to unequivocally state which of these effects is dominant.

4.5.1.3. Acetaminophen

Permeation of acetaminophen through silicone membrane was evaluated. Table 4.3 lists the mean steady state fluxes obtained, the corresponding standard deviations and coefficient of variation.

Table 4.3. Steady state fluxes of acetaminophen in the vehicles studied and their solubility parameters (ND denotes that these values were not determined).

Vehicle	Flux ($\mu\text{g}/\text{cm}^2/\text{hr}$) \pm SD	CV	$\delta_{\text{vehicle}}(\text{cal}/\text{cm}^3)^{1/2}$
PG	-	-	15.4
Water	-	-	23.4
MO	1.49 \pm 0.09	6.18	7.1
MG	1.84 \pm 0.1	5.67	7.9
TC	-	-	10.0
EtOH	-	-	12.6

Because of the inherent instability of acetaminophen (see Chapter Two) it was impossible to conduct permeation experiments for the majority of the solvents selected. Only two systems were investigated, mineral oil and miglyol. However, the flux from both these solvents is extremely low (too low to be of any therapeutic use). The flux was slightly higher from miglyol than mineral oil, this can be attributed to the slight difference in polarity of the two solvents. Miglyol does contain fatty acids, which may interact with acetaminophen, whereas mineral oil would not present a favourable environment because it is made up entirely of lipophilic hydrocarbons. For this reason, work with acetaminophen was discontinued. To overcome the stability issues, and conduct experiments that would yield results of any use to formulation design would require time that is far beyond the constraints placed upon this research project.

4.5.1.4. Summary of single-phase diffusion data

Figure 4.5 shows the flux values for all drugs in the selected solvents, although the flux values for acetaminophen are far too low to be seen on the graph.

Ibuprofen had a higher permeation rate than salicylic acid from PG, water, MO and MG, which can be attributed to the relative lipophilicity of the two drugs (3.51 and 2.26 respectively). The only flux value that was the same for ibuprofen and salicylic acid was with Transcutol, and this could be the result of a solvent-membrane interaction, and warrants further investigation. Ethanol appears to be the most effective permeation enhancer for ibuprofen and salicylic acid, with an 8 and 25-fold improvement in flux for the respective permeants. It is not clear why salicylic acid permeates better than ibuprofen.

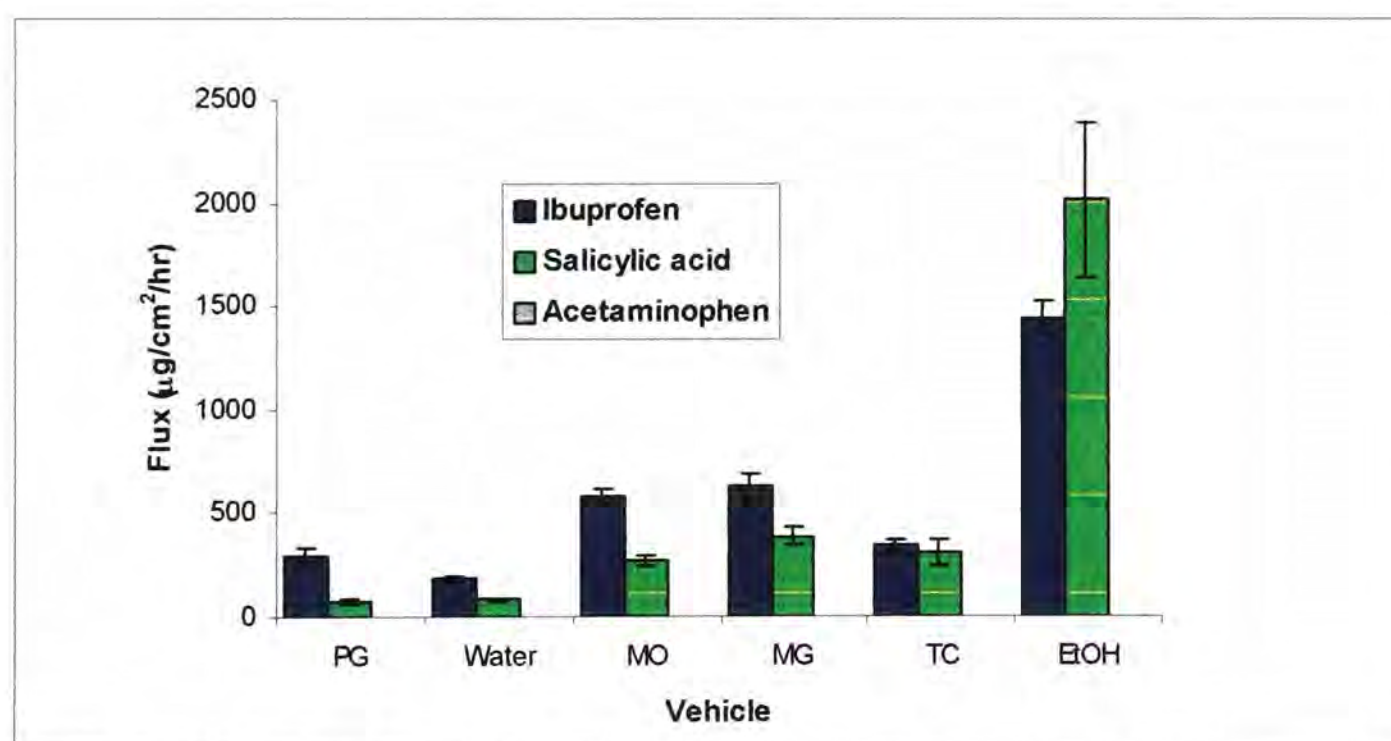


Figure 4.5. Steady state flux values for the three permeants in the selected vehicles.

4.5.2. Binary solvent vehicles

4.5.2.1. Ibuprofen

Propylene glycol/water vehicles

The permeation of ibuprofen through silicone membrane, using PG/water vehicles of varying composition was evaluated. Table 4.4 lists the flux values with associated standard deviations, the kinetic parameter β (D/h^2), the thermodynamic parameter α ($K \cdot h$) and the permeability coefficient, k_p .

Figure 4.6 shows the steady state fluxes of ibuprofen from PG/water vehicles of varying composition. The steady state fluxes across silicone membrane were expected to be constant since the drug was applied at the same thermodynamic activity in all vehicles. However, the flux values vary from $\sim 300 \mu\text{g}/\text{cm}^2/\text{hr}$ in PG to $185 \mu\text{g}/\text{cm}^2/\text{hr}$ in water. Between 60-70% PG (v/v) the flux is highest, with most flux values at approximately $200 \mu\text{g}/\text{cm}^2/\text{hr}$. The permeation profiles were analysed using a curve fitting procedure to obtain values for α ($K \cdot h$) and β (D/h^2). These values should give some insight into the processes taking place during diffusion, as $K \cdot h$ is related to the partition coefficient, whilst D/h^2 relates to the diffusion coefficient.

The obtained α values show some variation, though not as great as that seen for the β values. This is somewhat surprising, as it is generally thought that PG enhances permeation by altering the solubility of the permeant in the membrane, therefore altering the partition coefficient.

Table 4.4. Steady state fluxes, thermodynamic and kinetic parameters, permeability coefficients for the permeation of ibuprofen from saturated formulations containing propylene glycol and water through silicone membrane (mean \pm SD, n=4).

Vehicle (v/v)	J ($\mu\text{g}/\text{cm}^2/\text{hr}$) \pm SD	α (cm) \pm SD	β (s^{-1}) \pm SD	k_p (cm/s) \pm SD
0/100	185.5 \pm 10.94	0.18 \pm 0.35	0.32 \pm 0.24	5.75 $\times 10^{-4}$ \pm 3.75 $\times 10^{-5}$
10/90	225.4 \pm 31.47	2.16 $\times 10^{-3}$ \pm 1.39 $\times 10^{-3}$	0.57 \pm 0.23	8.38 $\times 10^{-4}$ \pm 2.39 $\times 10^{-4}$
20/80	229.5 \pm 14.20	2.71 \pm 2.36	8.57 $\times 10^{-2}$ \pm 0.14	1.80 $\times 10^{-3}$ \pm 2.13 $\times 10^{-4}$
30/70	216 \pm 22.47	5.24 $\times 10^{-2}$ \pm 8.30 $\times 10^{-2}$	8.43 $\times 10^{-2}$ \pm 0.15	3.78 $\times 10^{-4}$ \pm 3.68 $\times 10^{-5}$
40/60	277.1 \pm 31.22	0.18 \pm 0.20	0.41 $\times 10^{-3}$ \pm 0.17	1.62 $\times 10^{-4}$ \pm 1.31 $\times 10^{-5}$
50/50	-	-	-	-
60/40	355.4 \pm 36.34	3.01 $\times 10^{-2}$ \pm 3.80 $\times 10^{-2}$	0.25 \pm 0.29	2.90 $\times 10^{-5}$ \pm 2.48 $\times 10^{-7}$
70/30	443.3 \pm 19.86	1.50 $\times 10^{-2}$ \pm 1.90 $\times 10^{-2}$	1.04 $\times 10^{-2}$ \pm	1.12 $\times 10^{-5}$ \pm 4.37 $\times 10^{-7}$
80/20	245.2 \pm 28.55	1.38 $\times 10^{-5}$ \pm 7.21 $\times 10^{-6}$	0.17 \pm 0.08	1.92 $\times 10^{-6}$ \pm 2.03 $\times 10^{-7}$
90/10	219.6 \pm 22.32	5.77 $\times 10^{-4}$ \pm 5.01 $\times 10^{-4}$	1.75 $\times 10^{-3}$ \pm 1.20 $\times 10^{-3}$	6.42 $\times 10^{-7}$ \pm 6.54 $\times 10^{-8}$
100/0	297.1 \pm 29.43	2.14 $\times 10^{-3}$ \pm 1.1 $\times 10^{-3}$	2.84 $\times 10^{-4}$ \pm 1.01 $\times 10^{-4}$	5.25 $\times 10^{-7}$ \pm 5.03 $\times 10^{-8}$

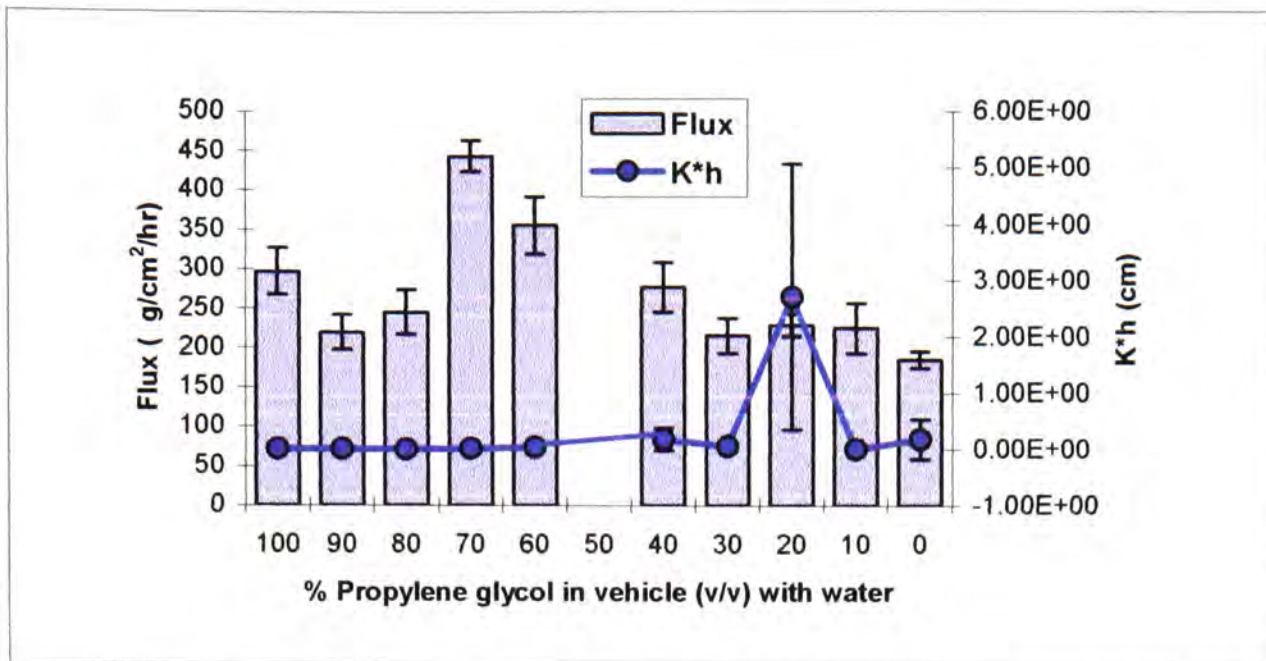


Figure 4.6. Steady state flux values and $K \cdot h$ values for the permeation of ibuprofen from saturated formulations containing PG/water.

Figure 4.7 shows the steady state fluxes and D/h^2 values for ibuprofen in saturated formulations containing PG and water. The systems with the highest diffusion coefficients are not necessarily those which exhibit high permeation rate.

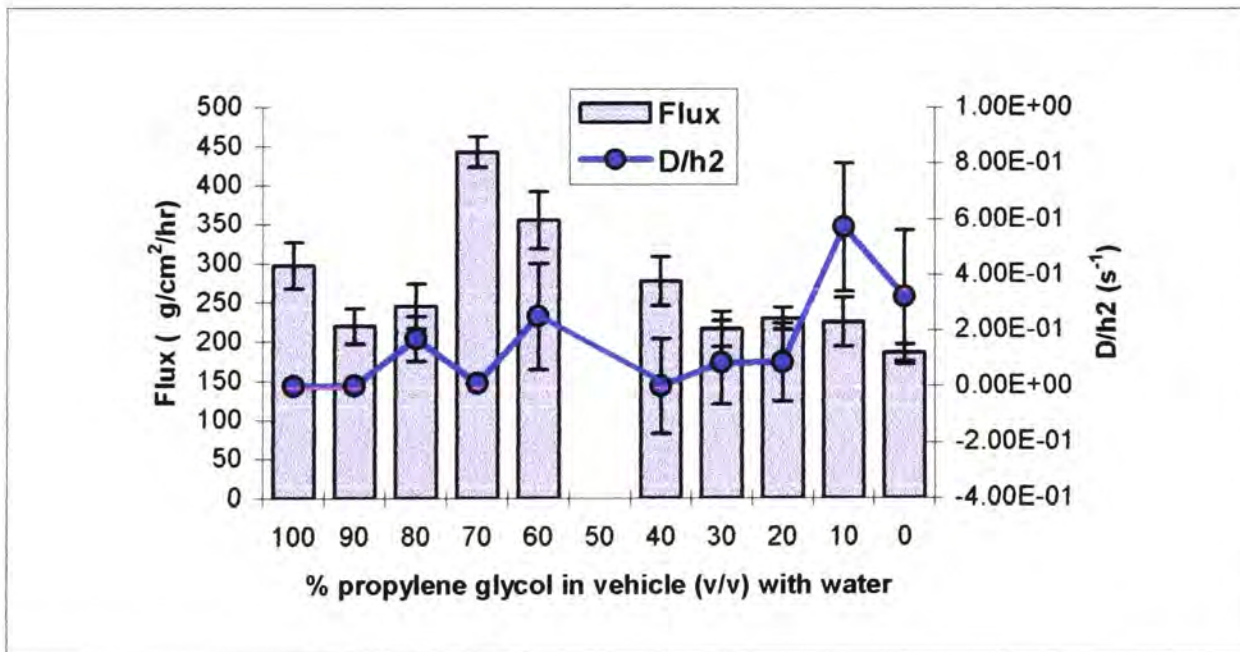


Figure 4.7. Steady state flux values and D/h^2 values for the permeation of ibuprofen from saturated formulations containing propylene glycol and water.

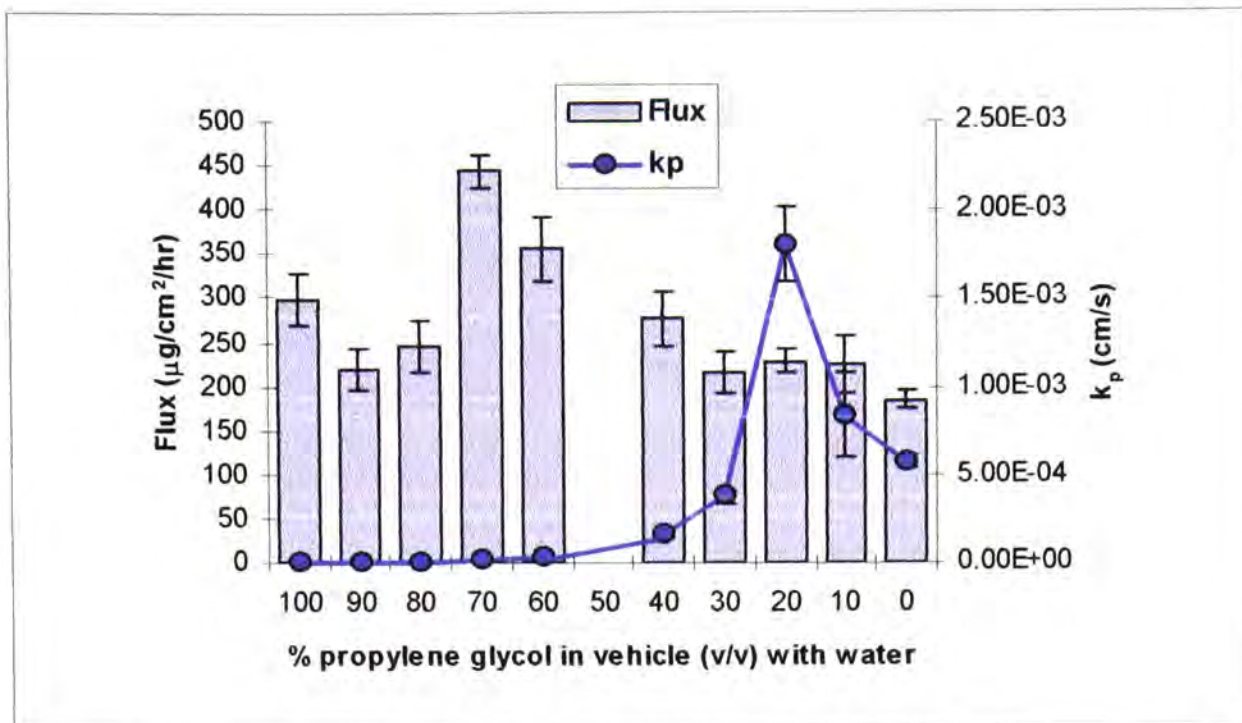


Figure 4.8. Steady state fluxes and k_p for the permeation of ibuprofen from saturated formulations containing PG/water.

It is not entirely clear from the thermodynamic and kinetic data which effect has lead to the higher permeation rates for some of the combinations. The permeability coefficients (shown in figure 4.8) increase as the proportion of propylene glycol in the formulation decreases, but then shown a decline at 0-10% PG. The permeability coefficients do not have the large error associated with K^*h and D/h^2 values because k_p is a composite of the two. The permeability coefficients for these formulations have a similar pattern to the K^*h data, in that the value at 20% PG is higher than for any other systems. To summarise, there is no predictable trend in the α or β values obtained from curve fitting. Permeability coefficients show an increase with decreasing proportion of propylene glycol in the formulation.

Mineral oil/miglyol vehicles

The permeation of ibuprofen through silicone membrane, using mineral oil/miglyol vehicles of varying composition was evaluated. Table 4.5 lists the flux values with associated standard deviations, the kinetic parameter D/h^2 , the thermodynamic parameter $K \cdot h$ and the permeability coefficient, k_p .

Table 4.5. Steady state fluxes, thermodynamic and kinetic parameters, permeability coefficients for the permeation of ibuprofen from saturated formulations containing mineral oil and miglyol through silicone membrane (mean \pm SD, n=4).

Vehicle (v/v)	J ($\mu\text{g}/\text{cm}^2/\text{hr}$) \pm SD	α (cm) \pm SD	β (s^{-1}) \pm SD	k_p (cm/s) \pm SD
0/100	623.8 \pm 67.69	4.28 $\times 10^{-3}$ \pm 9.30 $\times 10^{-4}$	2.70 $\times 10^{-4}$ \pm 2.72 $\times 10^{-5}$	1.14 $\times 10^{-6}$ \pm 1.51 $\times 10^{-7}$
10/90	439.9 \pm 23.87	1.24 $\times 10^{-2}$ \pm 1.60 $\times 10^{-2}$	1.87 $\times 10^{-4}$ \pm 4.05 $\times 10^{-5}$	2.35 $\times 10^{-7}$ \pm 1.51 $\times 10^{-7}$
20/80	569.6 \pm 63.53	4.99 $\times 10^{-3}$ \pm 7.57 $\times 10^{-4}$	1.91 $\times 10^{-4}$ \pm 2.95 $\times 10^{-5}$	6.99 $\times 10^{-6}$ \pm 3.99 $\times 10^{-6}$
30/70	573.5 \pm 54.97	2.37 $\times 10^{-3}$ \pm 2.70 $\times 10^{-3}$	3.07 $\times 10^{-2}$ \pm 6.10 $\times 10^{-2}$	1.29 $\times 10^{-6}$ \pm 1.30 $\times 10^{-7}$
40/60	409.4 \pm 13.60	6.31 $\times 10^{-3}$ \pm 1.84 $\times 10^{-3}$	1.40 $\times 10^{-4}$ \pm 4.62 $\times 10^{-5}$	8.20 $\times 10^{-7}$ \pm 3.80 $\times 10^{-8}$
50/50	311.9 \pm 33.84	-	-	-
60/40	675.1 \pm 66.81	8.77 $\times 10^{-3}$ \pm 3.81 $\times 10^{-3}$	2.19 $\times 10^{-4}$ \pm 1.08 $\times 10^{-4}$	1.62 $\times 10^{-6}$ \pm 1.64 $\times 10^{-7}$
70/30	646.9 \pm 9.91	1.29 $\times 10^{-3}$ \pm 6.31 $\times 10^{-3}$	2.32 $\times 10^{-4}$ \pm 1.32 $\times 10^{-4}$	3.37 $\times 10^{-6}$ \pm 1.91 $\times 10^{-6}$
80/20	519.1 \pm 20.16	6.16 $\times 10^{-3}$ \pm 4.62 $\times 10^{-3}$	1.77 $\times 10^{-2}$ \pm 3.48 $\times 10^{-2}$	2.99 $\times 10^{-6}$ \pm 5.94 $\times 10^{-7}$
90/10	457 \pm 53.47	2.05 $\times 10^{-2}$ \pm 1.07 $\times 10^{-2}$	2.88 $\times 10^{-4}$ \pm 2.49 $\times 10^{-4}$	6.76 $\times 10^{-6}$ \pm 8.51 $\times 10^{-6}$
100/0	579 \pm 35.31	2.68 $\times 10^{-2}$ \pm 5.90 $\times 10^{-3}$	1.94 $\times 10^{-4}$ \pm 3.89 $\times 10^{-5}$	5.03 $\times 10^{-6}$ \pm 4.12 $\times 10^{-7}$

As with the PG/water vehicles, permeation from saturated solutions of mineral oil and miglyol (MO/MG) vary. The highest permeation rate is in the range 60-75%mineral oil, with another peak at 25%. The data imply that there is an interaction between the solvents and the membrane, which is enhancing the flux. Generally the flux values for the oil-based formulations are much higher than for the corresponding PG/water systems ($300\text{-}700\mu\text{g}/\text{cm}^2/\text{hr}$ and $\sim 200\mu\text{g}/\text{cm}^2/\text{hr}$ respectively). This could be a result of the lipophilicity of ibuprofen ($\log P = 3.51$). The high flux values could also be attributed to dimerisation of ibuprofen, although without further investigation it is not possible to be certain.

Figure 4.9 shows the K^*h values obtained from curve fitting. There is no significant difference between any of the formulations, suggesting that over a range of mineral oil and miglyol combinations, the partitioning of ibuprofen is being unaltered.

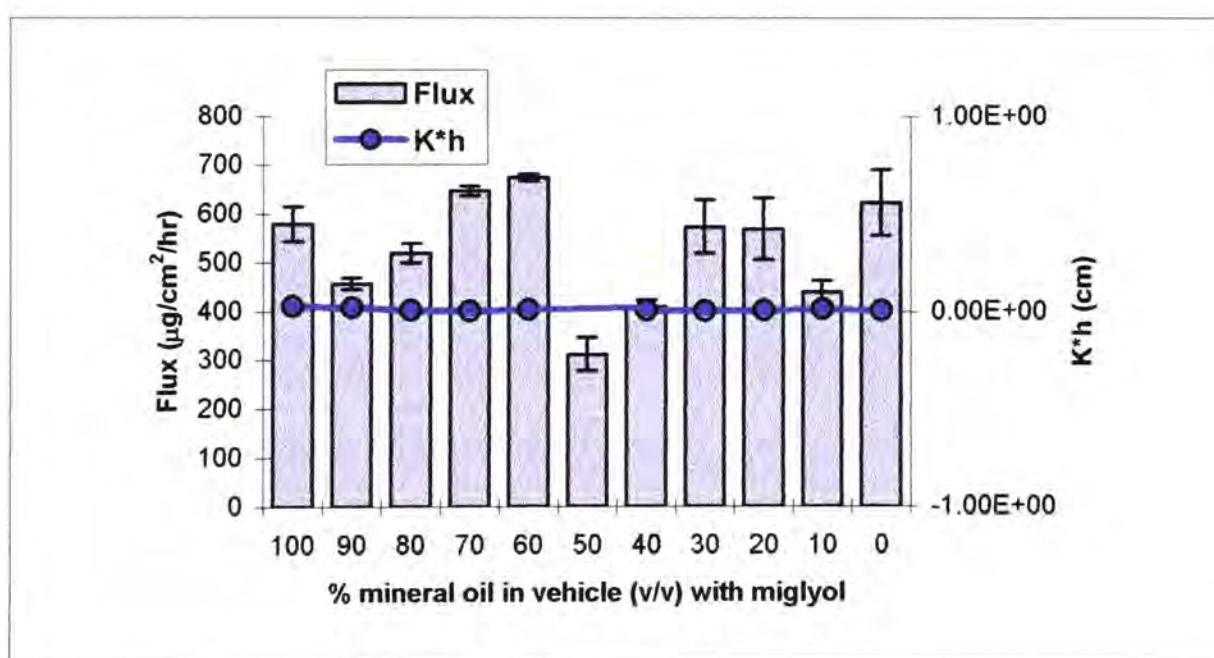


Figure 4.9. Steady state flux and K^*h values for the permeation of ibuprofen from saturated formulations containing mineral oil and miglyol.

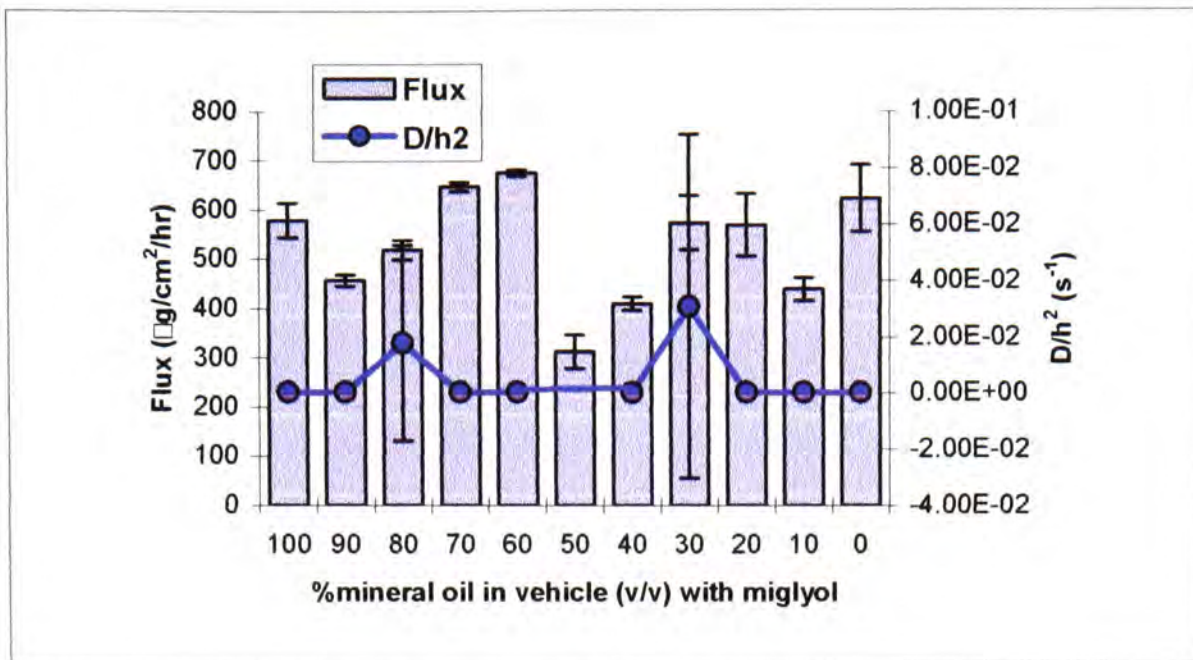


Figure 4.10. Steady state flux and D/h^2 values for the permeation of ibuprofen from saturated formulations containing mineral oil and miglyol.

Figure 4.10 shows the D/h^2 values obtained from curve fitting. The values are similar across the range. There is clearly a contribution from both the diffusion coefficient and the partition coefficient although this does not lead to a high permeation rate.

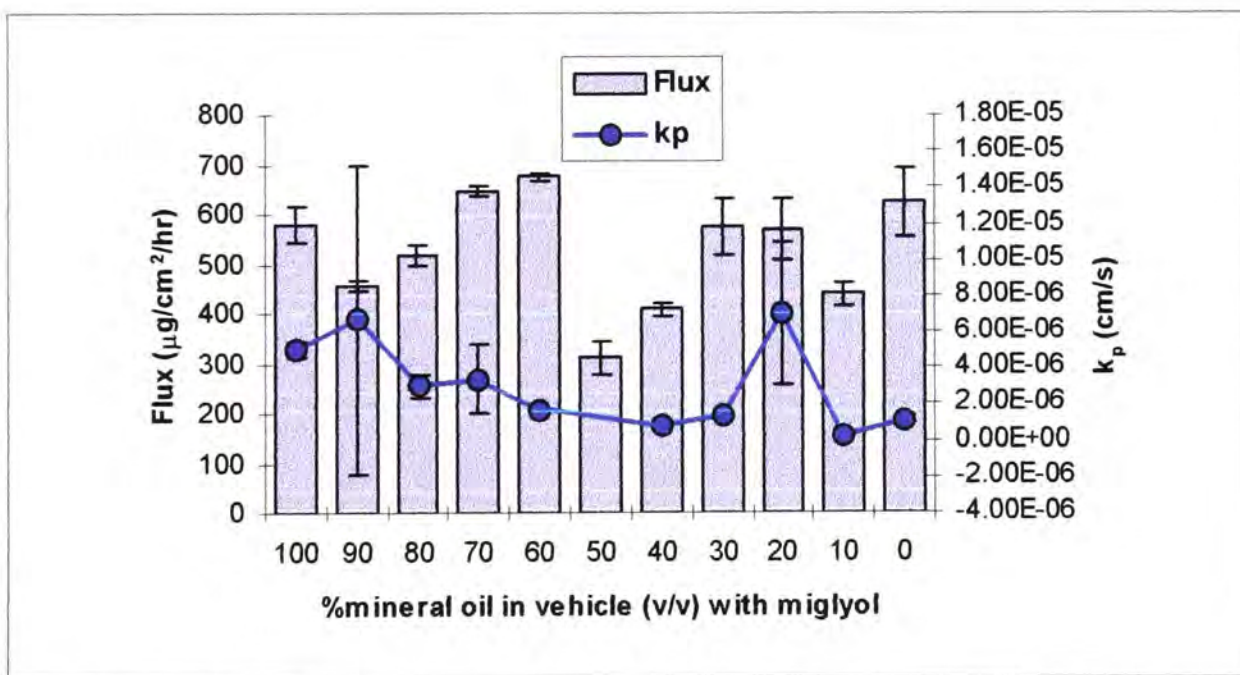


Figure 4.11. Steady state flux values and permeability coefficients for the permeation of ibuprofen from saturated formulations containing mineral oil and miglyol.

From figure 4.11 it can be seen that there are only very slight changes in the permeability coefficient across the range of formulations. The curve fitting procedure has provided data which demonstrate that there can be many factors which govern flux, in this case it would seem that there is not a straightforward explanation for the high flux seen in some of the formulations. One possible concern with testing oil-based formulations is the nature of the receptor phase. In all the studies discussed in this thesis, the donor phase was phosphate buffered saline (pH 7.4). If the formulation components pass through the silicone membrane, there may be the possibility of a small reservoir forming at the underside of the membrane. This may alter slightly the permeation rates obtained as there would be a tendency for a lipophilic drug, such as ibuprofen to stay within the layer of formulation rather than partition into the receptor phase where it can be quantified. This could lead to the spread of flux values seen in the results. Diffusion studies using ATR-FTIR would confirm whether the vehicles pass through the membrane, as their IR signal will be detected as it arrives at the membrane-crystal interface. The results of ATR-FTIR diffusion experiments are presented in Chapter Five.

Ethanol/water vehicles

The permeation of ibuprofen through silicone membrane, using ethanol and water vehicles of varying composition was evaluated. Table 4.6 lists the flux values with associated standard deviations, the kinetic parameter D/h^2 , the thermodynamic parameter $K \cdot h$ and the permeability coefficient, k_p .

Table 4.6. Steady state fluxes, thermodynamic and kinetic parameters, permeability coefficients for the permeation of ibuprofen from saturated formulations containing ethanol and water through silicone membrane (mean \pm SD, n=4).

Vehicle (v/v)	J ($\mu\text{g}/\text{cm}^2/\text{hr}$) \pm SD	CV	$K \cdot h$ (cm) \pm SD	D/h^2 (s^{-1}) \pm SD	k_p (cm/s) \pm SD
0/100	185.5 \pm 10.94	7.74	0.18 \pm 0.35	0.32 \pm 0.24	5.75 $\times 10^{-4}$ \pm 3.75 $\times 10^{-5}$
25/75	419.9 \pm 2.5	5.60	1.29 $\times 10^{-3}$ \pm 4.85 $\times 10^{-3}$	3.06 $\times 10^{-4}$ \pm 1.44 $\times 10^{-4}$	3.42 $\times 10^{-7}$ \pm 1.89 $\times 10^{-8}$
50/50	916.2 \pm 79.23	12.11	6.01 $\times 10^{-4}$ \pm 4.38 $\times 10^{-4}$	3.05 $\times 10^{-2}$ \pm 5.83 $\times 10^{-2}$	5.63 $\times 10^{-7}$ \pm 6.79 $\times 10^{-8}$
75/25	944.8 \pm 60.91	6.45	2.38 $\times 10^{-4}$ \pm 3.04 $\times 10^{-4}$	7.23 $\times 10^{-2}$ \pm 8.32 $\times 10^{-2}$	1.24 $\times 10^{-7}$ \pm 2.37 $\times 10^{-5}$
100/0	1495.3 \pm 115.8	7.74	5.54 $\times 10^{-6}$ \pm 2.04 $\times 10^{-6}$	0.17 \pm 0.07	8.25 $\times 10^{-7}$ \pm 3.44 $\times 10^{-8}$

The flux from saturated formulations containing ethanol and water was much higher than that from either propylene/glycol water formulations or mineral oil/miglyol formulations.

There is a large increase in the permeation rate (approximately doubling the flux) when 25% ethanol is added to the formulation, which indicates that ethanol is an interacting solvent. Addition of a further 25% of ethanol

again doubles the flux. Above 50% ethanol this effect is not so significant, with there being no difference in flux between the 50/50 formulation and the 75/25 formulation. In 100% ethanol, the flux is highest ($1495\mu\text{g}/\text{cm}^2/\text{hr}$), which is 1.5 times higher than for 75/25 ethanol/water.

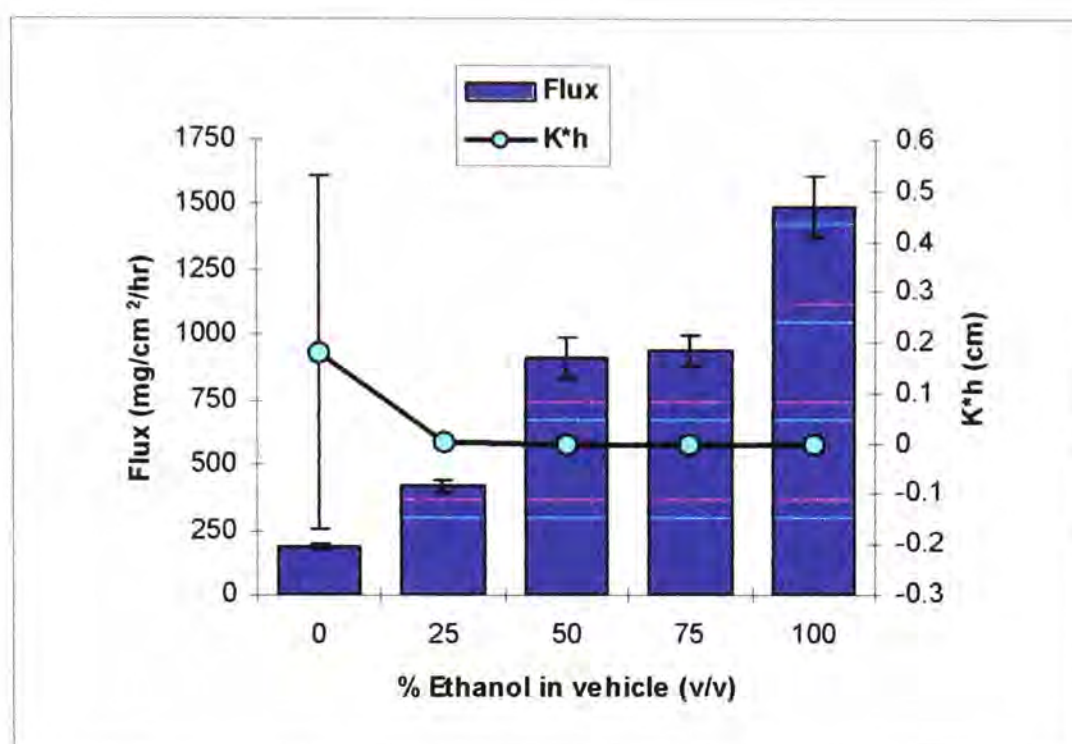


Figure 4.12. Steady state fluxes and K^*h values for the permeation of ibuprofen from saturated formulations containing ethanol and water.

It is known that the slope of a Yasuda-Shedlovsky plot (as presented in chapter two) is inversely proportional to the average ionic diameter of the solvated molecule (Shedlovsky, 1962). According to data obtained from experiments using the Sirius GlpK_a, there is change in the solvation structure at around 30% v/v ethanol and water, as there is a change in slope at this point. The reason that this would increase the flux is because ethanol permeates at a much faster rate than water, and so the ibuprofen, within an ethanol cage is taken across the membrane. Figure 4.12 shows the K^*h values obtained from curve fitting using Easyplot software. The values show that there is no change in the partitioning behaviour of ibuprofen across the different formulations. With respect to the D/h^2

values, there is only a significant difference between 0-25% ethanol, which may be anticipated as even addition of a small amount of ethanol could permeate the membrane, altering diffusion in some way. Further experiments with ATR-FTIR will give a more comprehensive picture of what processes are occurring during permeation.

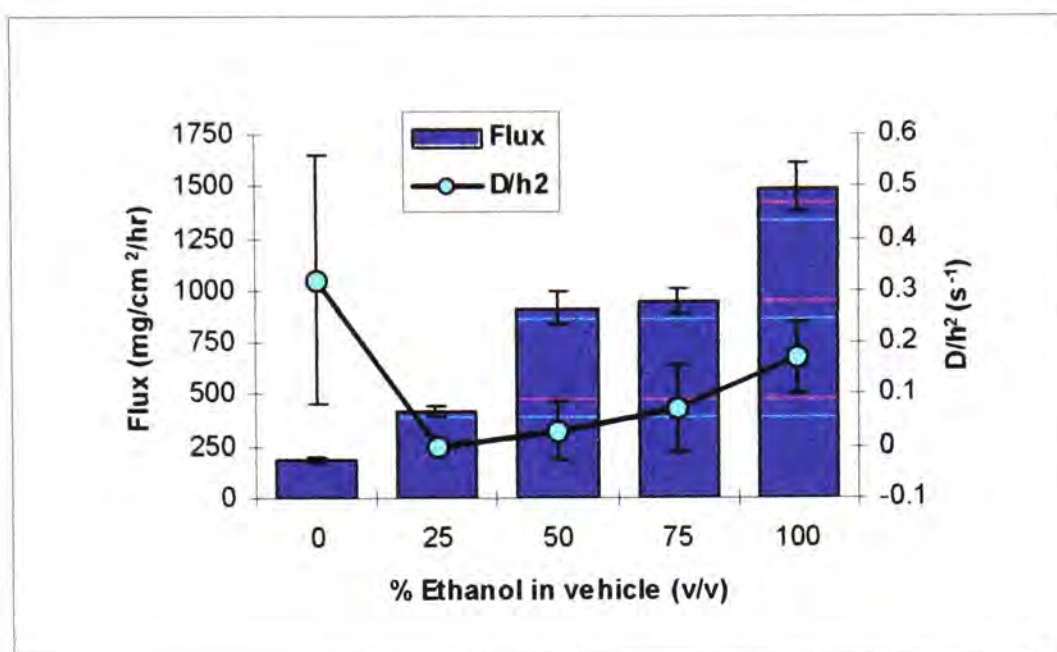


Figure 4.13. Steady state flux and D/h^2 values for the permeation of ibuprofen from saturated formulations containing ethanol and water.

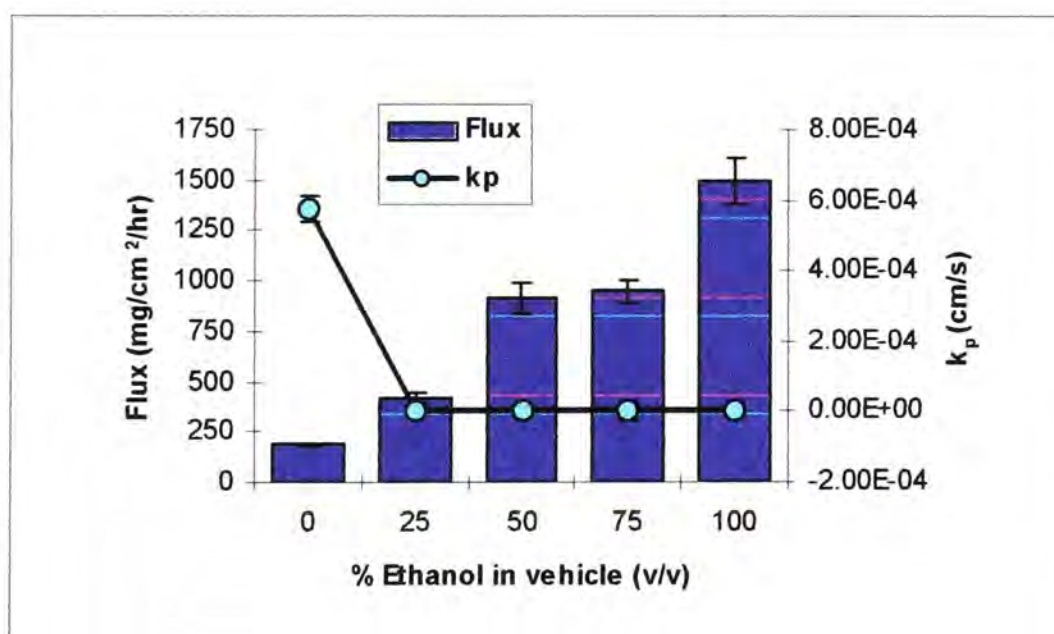


Figure 4.14. Steady state fluxes and permeability coefficients for the permeation of ibuprofen from saturated formulations containing ethanol and water.

The permeability coefficients for the permeation of ibuprofen from formulations containing ethanol and water show that there is a dramatic increase in permeability upon addition of ethanol to the formulation. What is interesting is that above 25%, further addition of ethanol has no effect upon the permeability coefficient. However, perhaps at this stage a possible issue with the use of this type of curve-fitting procedure should be addressed. The use of solutions to Fick's laws of diffusion to identify the mechanism of action of enhancers is widely used. However, their use relies upon certain assumptions, or boundary conditions. The boundary conditions for the equation utilised in this thesis were outlined in section 4.2, and are those of a well-designed diffusion experiment when a permeant is at high, fixed activity on one side of the membrane through which it diffuses into a sink on the other side.

If, as the data suggest, ethanol is interacting with the membrane, either by improving solubility of the drug or by chemical alteration, then the model used is no longer applicable because the membrane is not inert. One way to overcome this is to pre-treat the membrane with solvent (in this case ethanol) so that any effect on the membrane is eliminated, so allowing the model to once again be valid. For this reason, a series of experiments were conducted using ethanol and water formulations to investigate the effect of pre-treatment, and to obtain more reliable values for $K \cdot h$ and D/h^2 .

Ethanol/water vehicles - membrane pre-treatment studies

The permeation of ibuprofen through pre-treated silicone membrane, using ethanol and water vehicles of varying composition was evaluated. The results of the pre-treatment studies showed that for the 25/75 and 75/25 vehicles, the $K \cdot h$ values were lower than for the permeation of ibuprofen

through untreated membrane. This demonstrates that the ethanol does improve the flux by altering the partition behaviour of the permeant.

Table 4.7 lists the flux values with associated standard deviations, the kinetic parameter D/h^2 , the thermodynamic parameter $K \cdot h$ and the permeability coefficient, k_p .

Table 4.7. Steady state fluxes, thermodynamic and kinetic parameters, permeability coefficients for the permeation of ibuprofen from saturated formulations containing ethanol and water through silicone membrane pre-treated with ethanol (mean \pm SD, n=4).

Vehicle (v/v)	J ($\mu\text{g}/\text{cm}^2/\text{hr}$) \pm SD	CV	$K \cdot h$ (cm) \pm SD	D/h^2 (s) $\times 10^{-3}$ \pm SD	k_p (cm/s) \pm SD
0/100	-	-	-	-	-
25/75	449.2 \pm 31.30	6.96	2.59 $\times 10^{-5}$ \pm 4.19 $\times 10^{-6}$	0.19 \pm 0.17	2.62 $\times 10^{-7}$ \pm 2.35 $\times 10^{-8}$
50/50	-	-	-	-	-
75/25	712.2 \pm 29.04	4.08	8.46 $\times 10^{-7}$ \pm 1.39 $\times 10^{-7}$	0.46 \pm 0.09	3.81 $\times 10^{-7}$ \pm 1.17 $\times 10^{-8}$
100/0	1681.3 \pm 79.95	4.34	7.89 $\times 10^{-4}$ \pm 3.30 $\times 10^{-4}$	1.38 $\times 10^{-3}$ \pm 5.65 $\times 10^{-4}$	9.50 $\times 10^{-7}$ \pm 4.45 $\times 10^{-8}$

The D/h^2 are very similar for the 25/75 and 75/25 formulations, which illustrates well the point of these experiments. If the membrane is pre-treated the conditions of the system will remain the same throughout the course of an experiment, giving much more reliable information about the diffusion process.

The flux values for the permeation of ibuprofen through silicone membrane pre-treated with ethanol are only slightly higher than for the corresponding systems through membrane that has not been pre-treated. The exception

is the 75/25 ethanol/water formulation which has a slightly lower flux ($\sim 700\mu\text{g}/\text{cm}^2/\text{hr}$ vs. $\sim 900\mu\text{g}/\text{cm}^2/\text{hr}$). The higher flux values are a result of reduced lag time as the formulation will not have to partition into the membrane as there will already be solvent present at the start of the experiment. As a result of this ibuprofen will partition much more readily into the membrane and diffuse through it more rapidly.

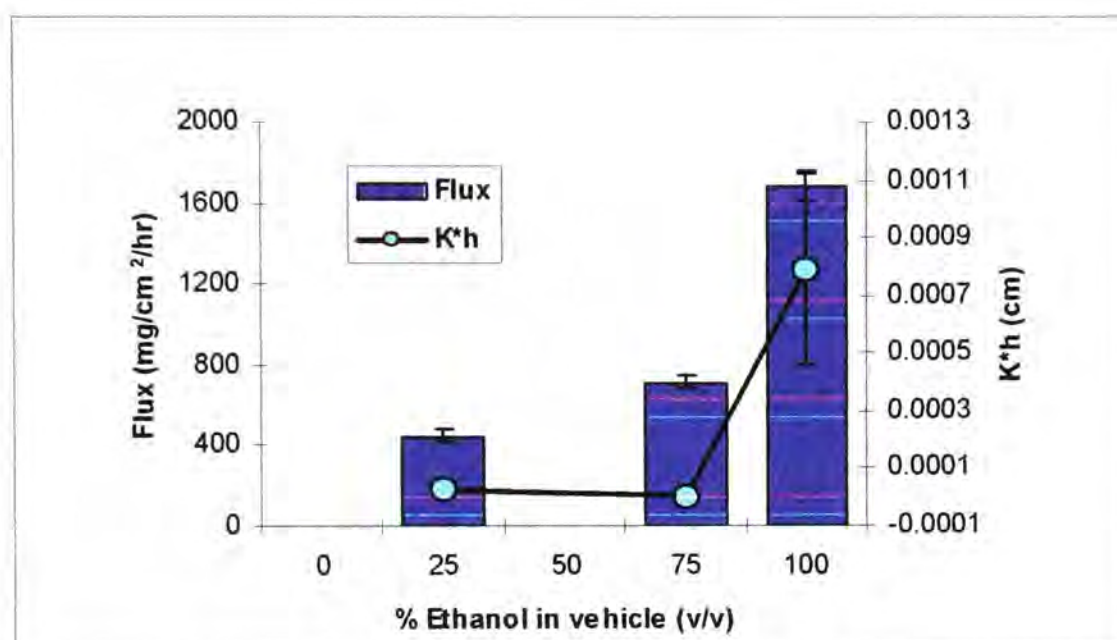
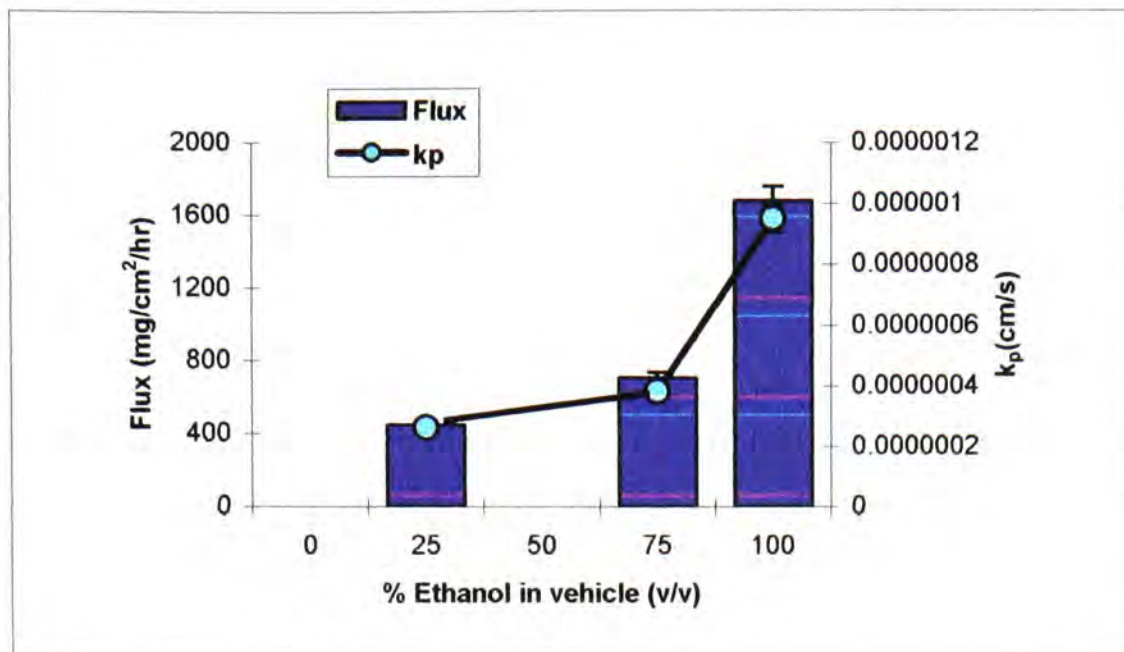


Figure 4.15. Steady state flux and $\log(K \cdot h)$ values for ibuprofen in vehicles containing ethanol and water using silicone membrane pre-treated with ethanol.

The $K \cdot h$ and D/h^2 parameters for 100% ethanol are different from those of 25/75 and 75/25, suggesting that it is ethanol alone is enhancing the flux through both the partitioning and diffusion parameters. The important region in terms of designing an optimum vehicle appears to be around 75%, however these experiments serve only as a guide and it seems that addition of even a small amount of ethanol to a formulation would improve flux.



4.16. Steady state fluxes and permeability coefficients for the permeation of ibuprofen from saturated formulations containing ethanol and water using silicone membrane pre-treated with ethanol.

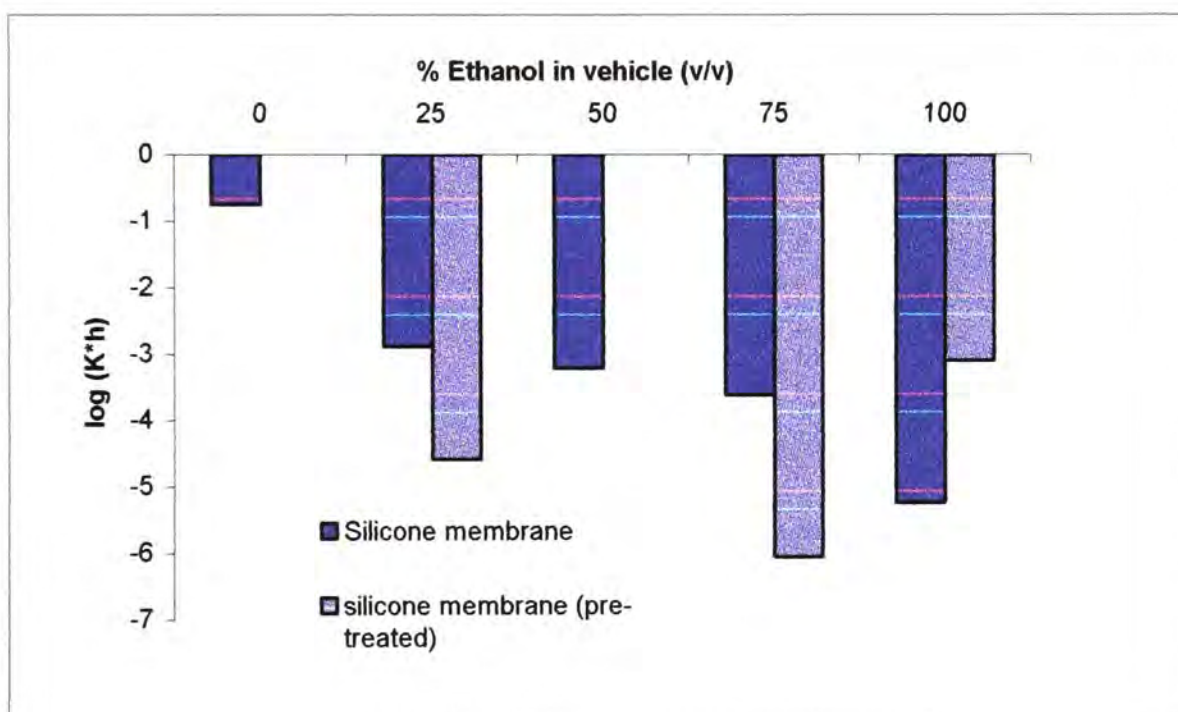


Figure 4.17. Log(K*h) values for the permeation of ibuprofen from saturated formulations containing ethanol and water.

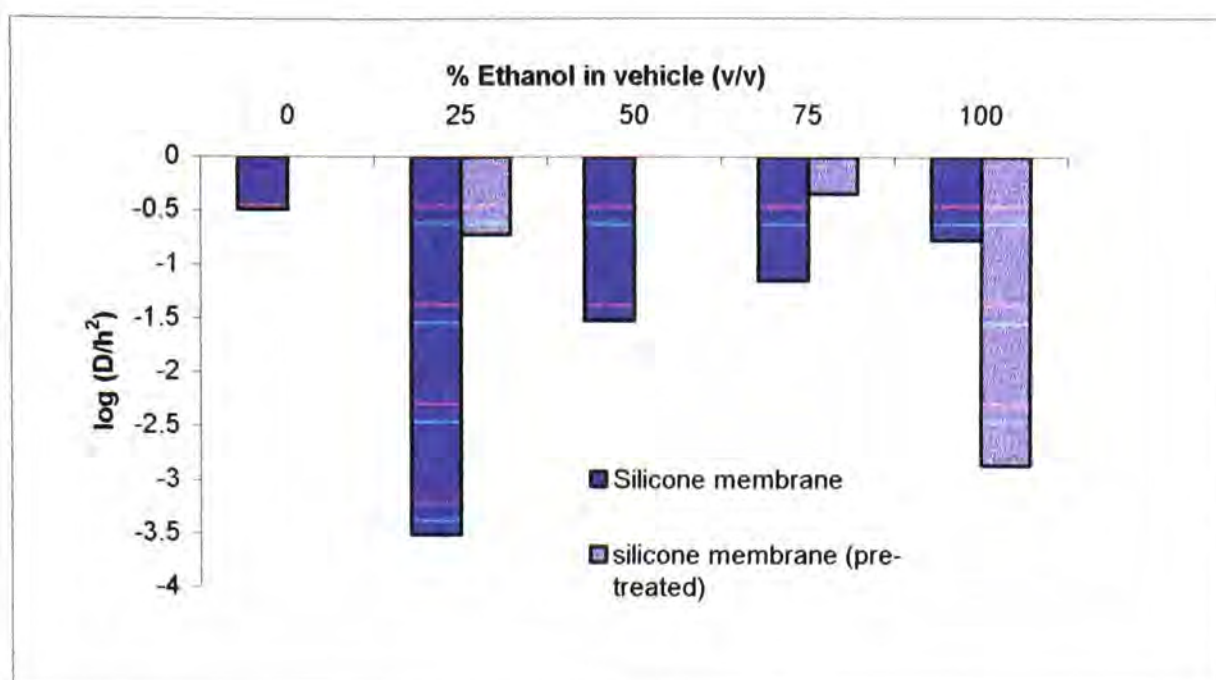


Figure 4.18. Log(D/h²) values for the permeation of ibuprofen from saturated formulations containing ethanol and water.

Figures 4.17 and 4.18 compare the log(K*h) and log(D/h²) values obtained from each permeation study, and shows how the values change when the membrane is pre-treated with ethanol. The logD/h² values vary the most, giving a strong indication that it is this aspect of permeation which ethanol influences to the greatest extent.

Ethanol/Propylene glycol vehicles

The permeation of ibuprofen through silicone membrane, using ethanol and propylene glycol vehicles of varying composition was evaluated. Steady state fluxes were calculated by monitoring the cumulative amount of drug diffused and measuring the slope of the graph once steady state diffusion was reached. All time points were used to measure the slope of the graph.

As for the previous systems investigated, the permeation rate of ibuprofen from formulations containing ethanol and propylene glycol varies across the range of solvent combinations studied. From the results of the

experiments using ethanol/water formulations, it is clear that ethanol dramatically enhances the flux of ibuprofen across silicone membrane.

Table 4.8. Steady state fluxes values for the permeation of ibuprofen from saturated formulations containing ethanol and propylene glycol through silicone membrane (mean \pm SD, n=4).

Vehicle (v/v)	J ($\mu\text{g}/\text{cm}^2/\text{hr}$) \pm SD	CV
0/100	297.1 \pm 29.43	9.90
25/75	380.3 \pm 42.74	11.24
50/50	605.6 \pm 93.71	15.47
75/25	955.2 \pm 79.03	8.27
100/0	1495.3 \pm 115.80	7.74

Propylene glycol has also been shown to increase the permeation rate. The aim of this set of experiments is to determine whether these two solvents act in a synergistic manner when combined in a formulation. Chapter One introduced the concept of using two known enhancers to improve flux further, but most synergistic combinations are enhancers which act in different ways (i.e. Oleic acid enhancing diffusion, Transcutol enhancing partition). In this case, enhancers which act in a similar manner have been combined in an attempt to increase the flux of ibuprofen.

Figure 4.19 shows the flux values for the permeation of ibuprofen from formulations containing ethanol, and propylene glycol. It has already been proposed that for ethanol/water the nature of the solvation shell alters when the formulation comprises more than 30% ethanol. The situation in ethanol/PG formulations may not be the same, as for ethanol/water formulations. Unfortunately it was not possible to use propylene glycol as a solvent for experiments using the GLpk_a and therefore no Yasuda-

Shedlovsky plot can be constructed which would reveal how the solvation shell changes with the addition of ethanol.

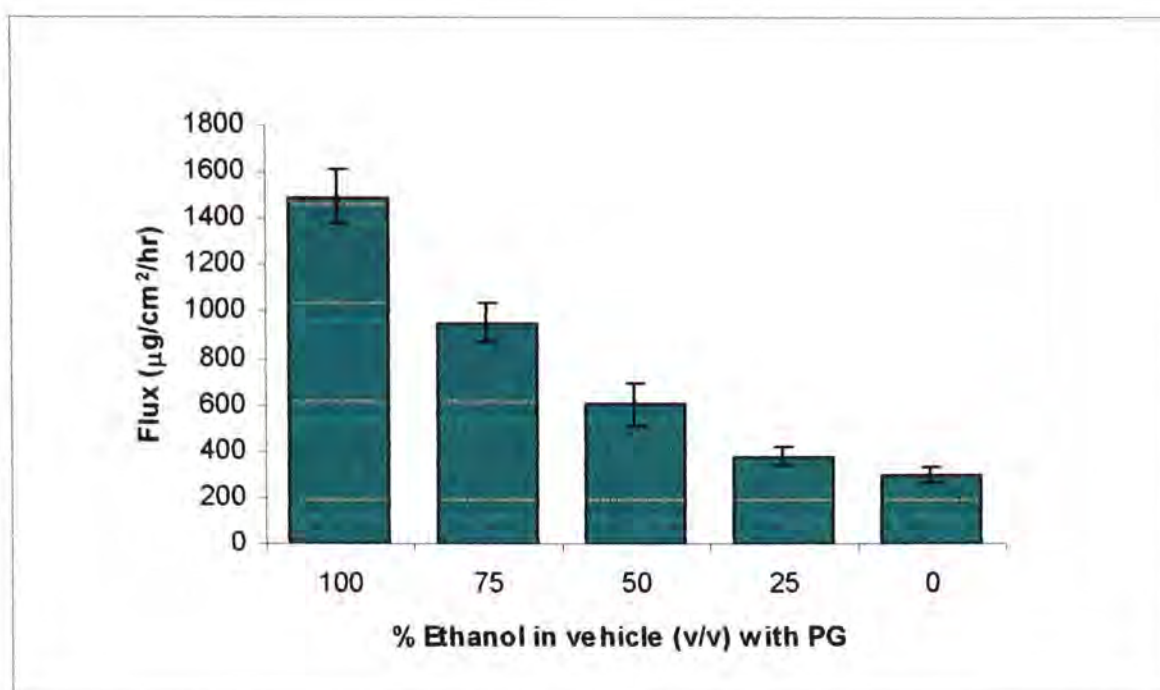


Figure 4.19. Steady state flux values for the permeation of ibuprofen from saturated formulations containing ethanol and propylene glycol.

The flux increases at 75% ethanol, where it is possible that the entire inner solvation shell is composed of ethanol molecules. Because of technical difficulties there is no solubility data for the ethanol/propylene glycol formulations it was not possible to determine thermodynamic and kinetic parameters through curve fitting.

Transcutol/water vehicles

The permeation of ibuprofen through silicone membrane, using Transcutol and water vehicles of varying composition was evaluated. Steady state fluxes were calculated by monitoring the cumulative amount of drug diffused and measuring the slope of the graph once steady state diffusion was reached. All time points were used to measure the slope of the graph.

Table 4.9. Steady state fluxes for the permeation of ibuprofen from saturated formulations containing Transcutol and water through silicone membrane (mean \pm SD, n=4).

Vehicle (v/v)	J ($\mu\text{g}/\text{cm}^2/\text{hr}$) \pm SD	CV
0/100	185.6 \pm 10.94	5.90
25/75	215.8 \pm 17.37	8.05
50/50	327.2 \pm 50.88	15.55
75/25	314.4 \pm 42.53	13.53
100/0	373.9 \pm 8.52	2.28

The permeation rate of ibuprofen from formulations containing Transcutol with water was generally lower than the other systems investigated, with PG/water vehicles being the exception. Transcutol acts as a solubilising agent for many drugs and it was for this reason that it was chosen as one of the solvents to be studied further.

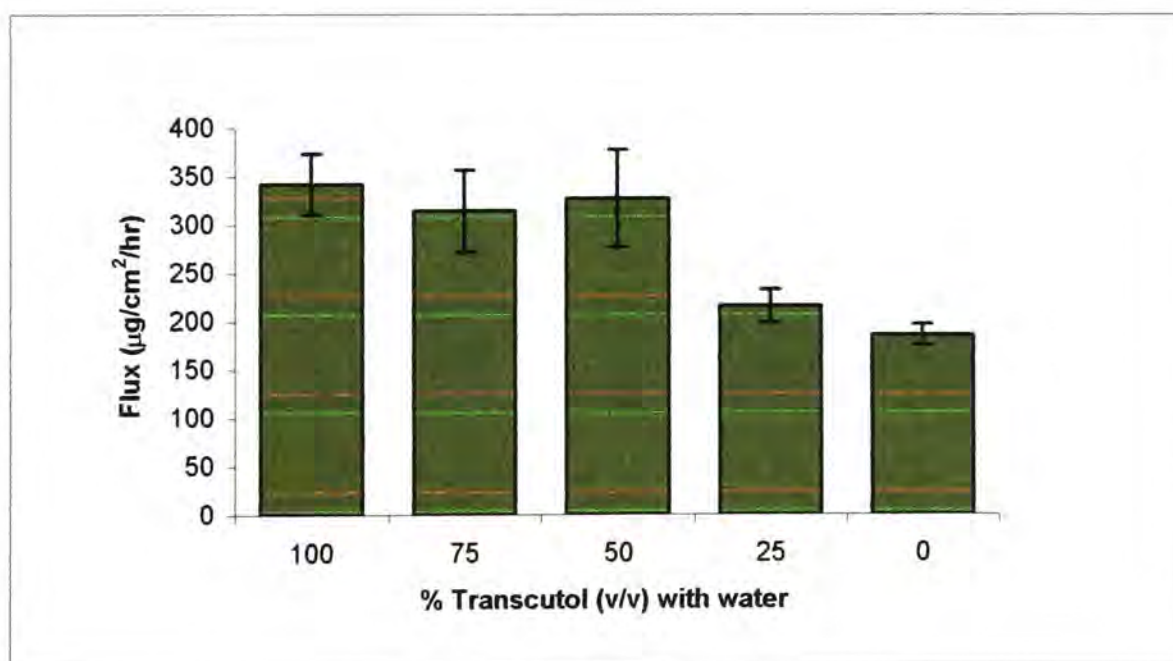


Figure 4.20. Steady state flux values for the permeation of ibuprofen from saturated formulations containing Transcutol and water

There is not a great deal of variation in the flux values between 50-100% Transcutol, but there is a marked decrease between 25% and 50%. As for ethanol and propylene glycol formulations, it was not possible to determine thermodynamic and kinetic parameters because of a lack of solubility data.

Figure 4.20 shows how the flux increases slightly as the proportion of Transcutol in the formulation increases.

Transcutol/propylene glycol vehicles

The permeation of ibuprofen through silicone membrane, using Transcutol and propylene glycol vehicles of varying composition was evaluated. Table 4.10 lists the flux values with associated standard deviations, the kinetic parameter D/h^2 , the thermodynamic parameter $K \cdot h$ and the permeability coefficient, k_p .

Table 4.10. Steady state fluxes, thermodynamic and kinetic parameters, permeability coefficients for the permeation of ibuprofen from saturated formulations containing Transcutol and propylene glycol through silicone membrane (mean \pm SD, n=4).

Vehicle (v/v)	J ($\mu\text{g}/\text{cm}^2/\text{hr}$) \pm SD	CV	K*h (cm) \pm SD	D/h² (s⁻¹) \pm SD	k_p (cm/s) \pm SD
0/100	297.1 \pm 29.43	9.90	2.14 $\times 10^{-4}$ \pm 1.10 $\times 10^{-3}$	2.84 $\times 10^{-4}$ \pm 1.01 $\times 10^{-4}$	5.25 $\times 10^{-7}$ \pm 5.03 $\times 10^{-8}$
25/75	265.9 \pm 7.1	2.67	1.35 $\times 10^{-4}$ \pm 1.93 $\times 10^{-4}$	1.31 $\times 10^{-2}$ \pm 6.18 $\times 10^{-8}$	2.18 $\times 10^{-7}$ \pm 6.18 $\times 10^{-8}$
50/50	319.1 \pm 17.38	5.45	3.19 $\times 10^{-4}$ \pm 2.65 $\times 10^{-4}$	3.70 $\times 10^{-2}$ \pm 7.46 $\times 10^{-2}$	1.17 $\times 10^{-7}$ \pm 1.34 $\times 10^{-5}$
75/25	376.4 \pm 8.5	2.26	2.68 $\times 10^{-4}$ \pm 2.27 $\times 10^{-4}$	8.09 $\times 10^{-3}$ \pm 1.29 $\times 10^{-2}$	2.27 $\times 10^{-7}$ \pm 5.29 $\times 10^{-9}$
100/0	373.9 \pm 8.52	2.28	1.35 $\times 10^{-4}$ \pm 2.06 $\times 10^{-6}$	0.20 \pm 0.06	2.59 $\times 10^{-7}$ \pm 1.89 $\times 10^{-8}$

The flux values for ibuprofen from formulations containing Transcutol and propylene glycol were similar to those from formulations containing Transcutol and water. Flux values were in the range of 300-400 $\mu\text{g}/\text{cm}^2/\text{hr}$. $\text{Log}(K^*h)$ values obtained from fitting the data to equation 4.21 are shown in figure 4.22.

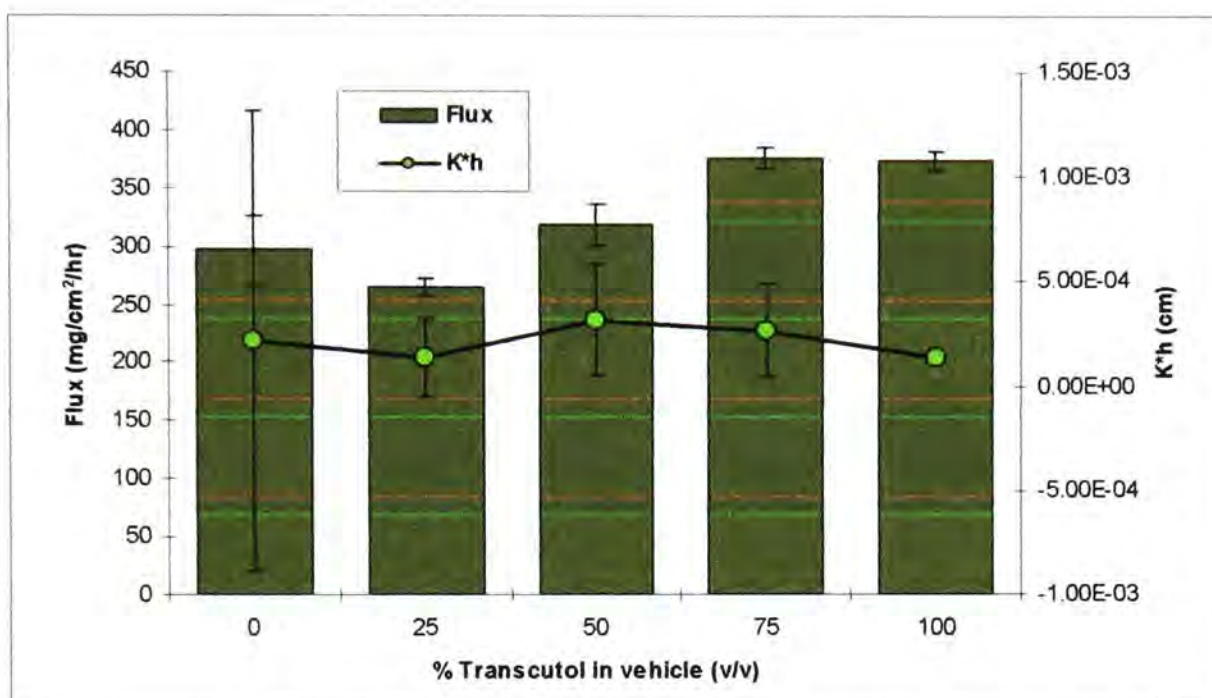


Figure 4.21. Steady state flux and $\text{log}(k^*h)$ values for the permeation of ibuprofen from saturated formulations containing Transcutol and propylene glycol.

The K^*h values show no trend over the range of formulations investigated. Figure 4.22 shows the D/h^2 values for the same formulations, and it is clear that there is an alteration in the diffusion of ibuprofen in pure Transcutol. This goes against the generally accepted view that Transcutol works as an enhancer by increasing the solubility of a drug within a vehicle. In pure Transcutol the solvation shell of ibuprofen would be entirely composed of Transcutol molecules which could increase permeation by reducing the resistance of the membrane.

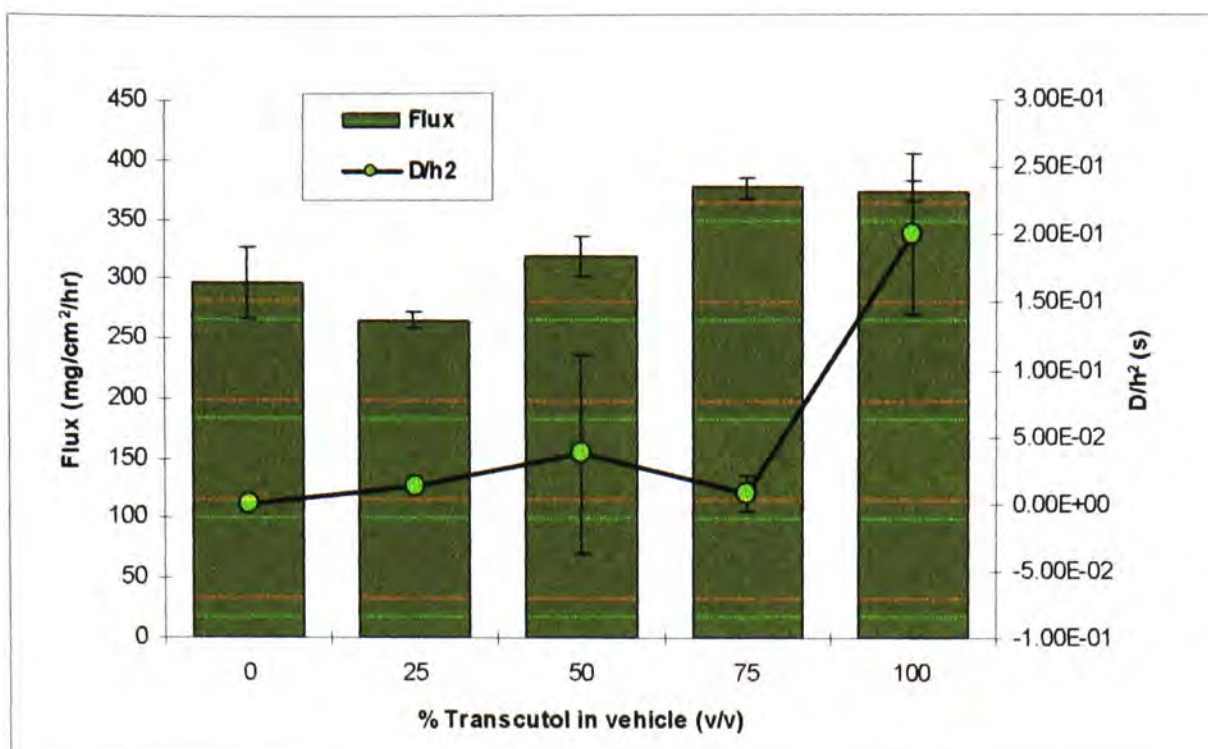


Figure 4.22. Steady state fluxes and $\log(D/h^2)$ values for ibuprofen in vehicles containing Transcutol and propylene glycol.

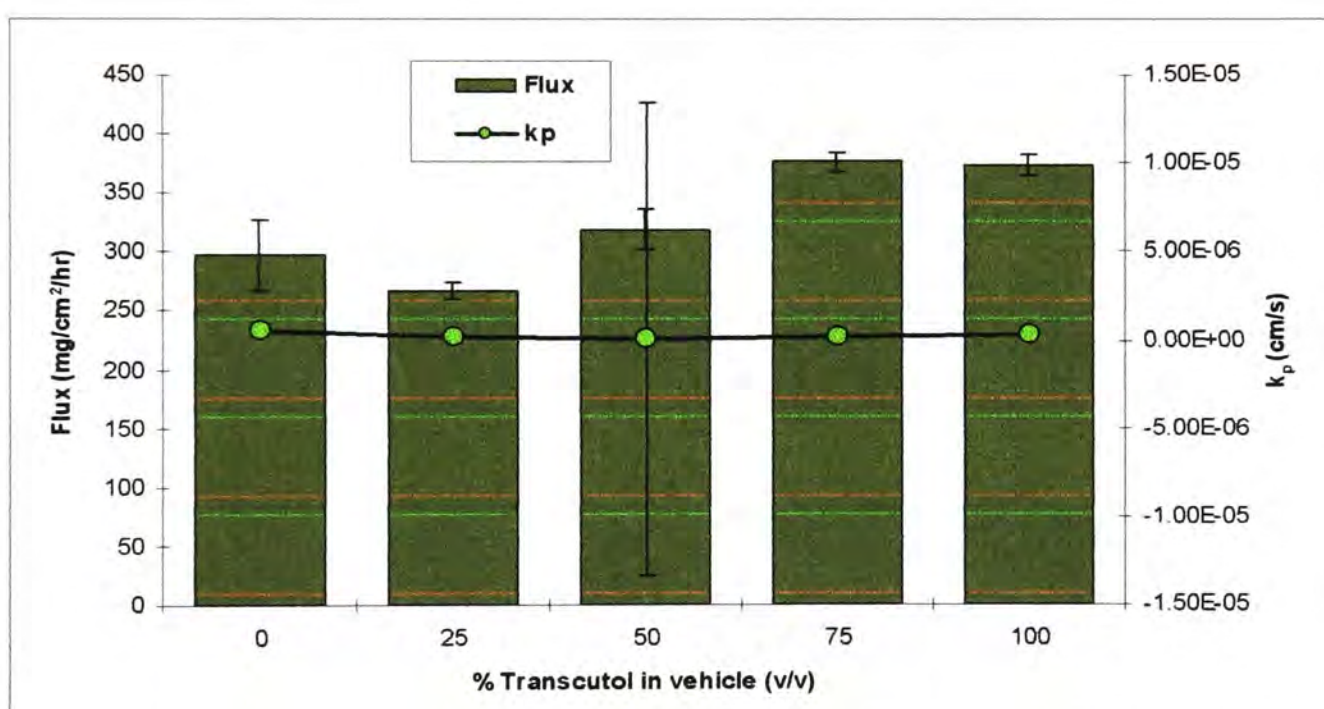


Figure 4.23. Steady state flux values and permeability coefficients for the permeation of ibuprofen from saturated formulations containing Transcutol and propylene glycol.

The permeability coefficients for ibuprofen in Transcutol/propylene glycol vehicles show no variation across the range of formulations, suggesting

that altering the relative amounts of propylene glycol and Transcutol would not affect permeation. This is borne out by the flux values which show only slight variation with increasing Transcutol.

Summary of the results of binary formulation permeation studies - ibuprofen

Diffusion studies using the model drug ibuprofen have shown that permeation can be enhanced using binary combinations of solvents. The vehicles used in this study appear to affect both the diffusion and partitioning behaviour of the drug, though for most solvents it is the change in partition coefficient that dominates.

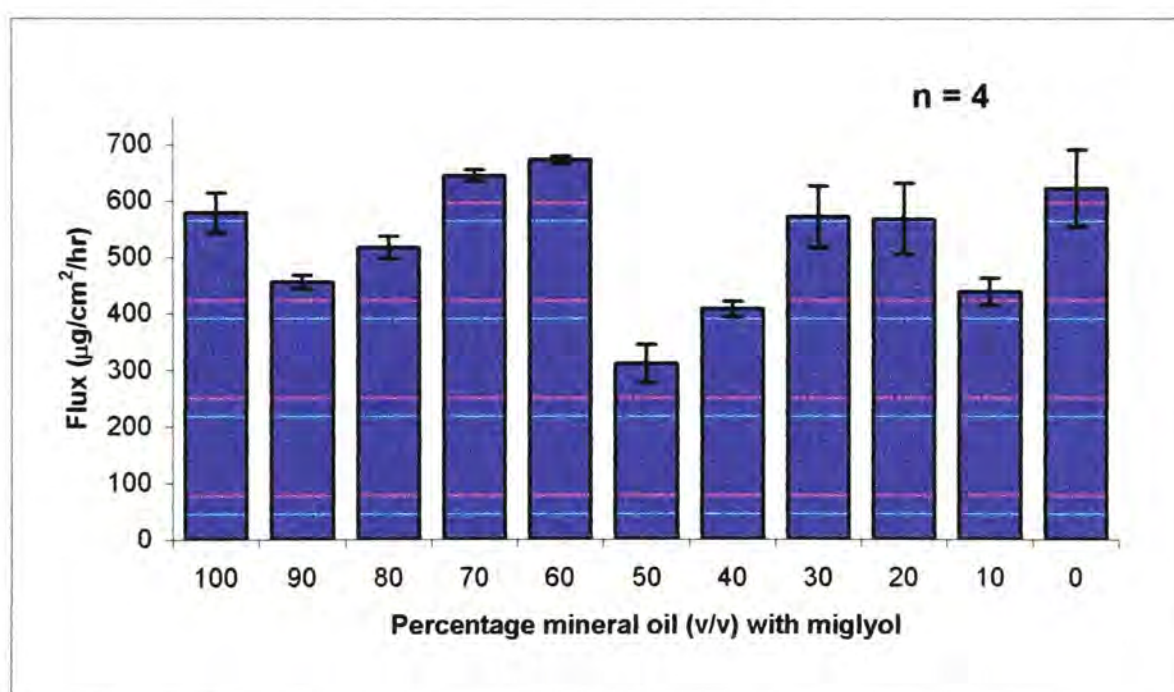


Figure 4.24. Flux values for the permeation of ibuprofen from saturated formulations containing mineral oil and miglyol.

The flux from the lipophilic formulations was greater than for the corresponding hydrophilic formulations. This difference in flux could mainly be attributed to the lipophilicity of ibuprofen ($\log P = 3.51$). If mineral oil is, as the data suggest, permeating into the membrane it could aid the

passage of ibuprofen along the lipid based intercellular pathways in the skin, influencing the permeation of the drug. Propylene glycol and water formulations showed good permeation rates, and although lower than for the lipophilic vehicles, still demonstrated that the flux of ibuprofen could be enhanced using certain binary combinations of solvents.

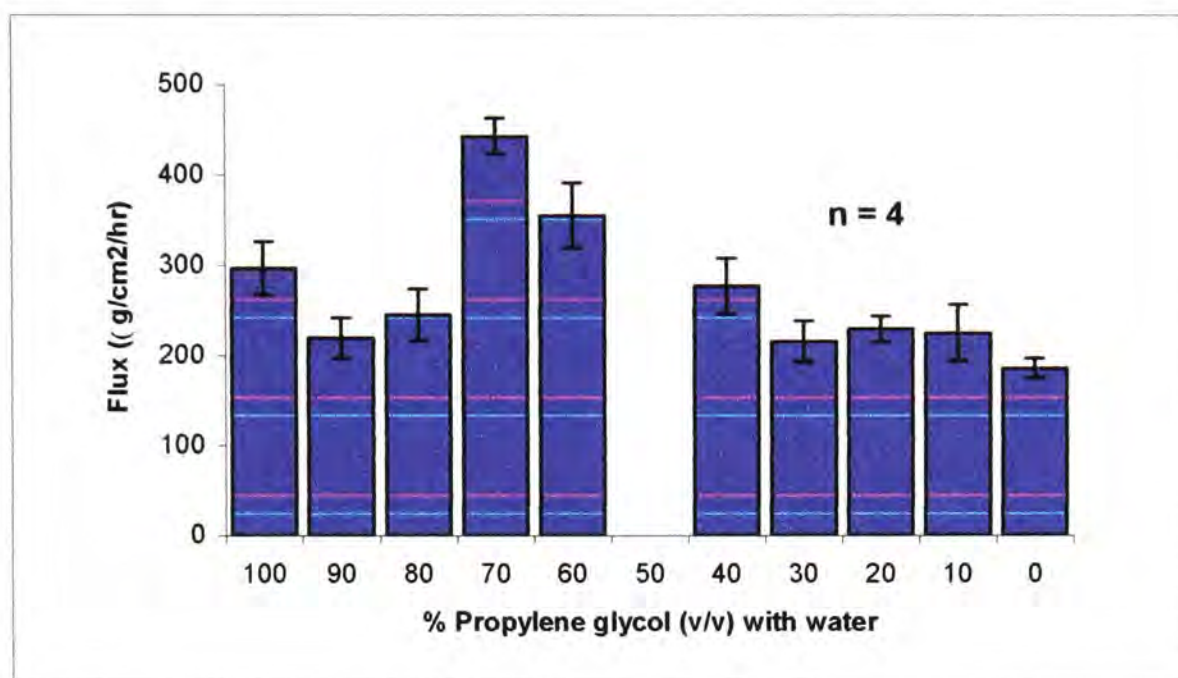


Figure 4.25. Flux values for the permeation of ibuprofen from saturated formulations containing propylene glycol and water.

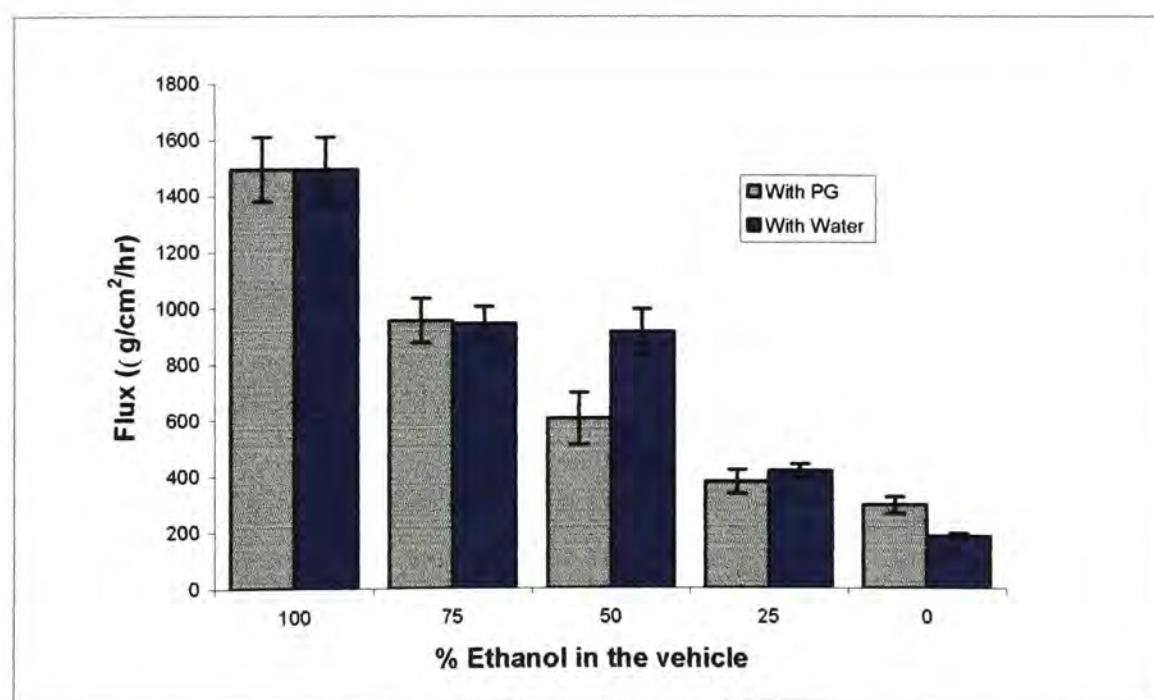


Figure 4.26. Flux values for the permeation of ibuprofen from saturated formulations containing ethanol/water and ethanol/propylene glycol.

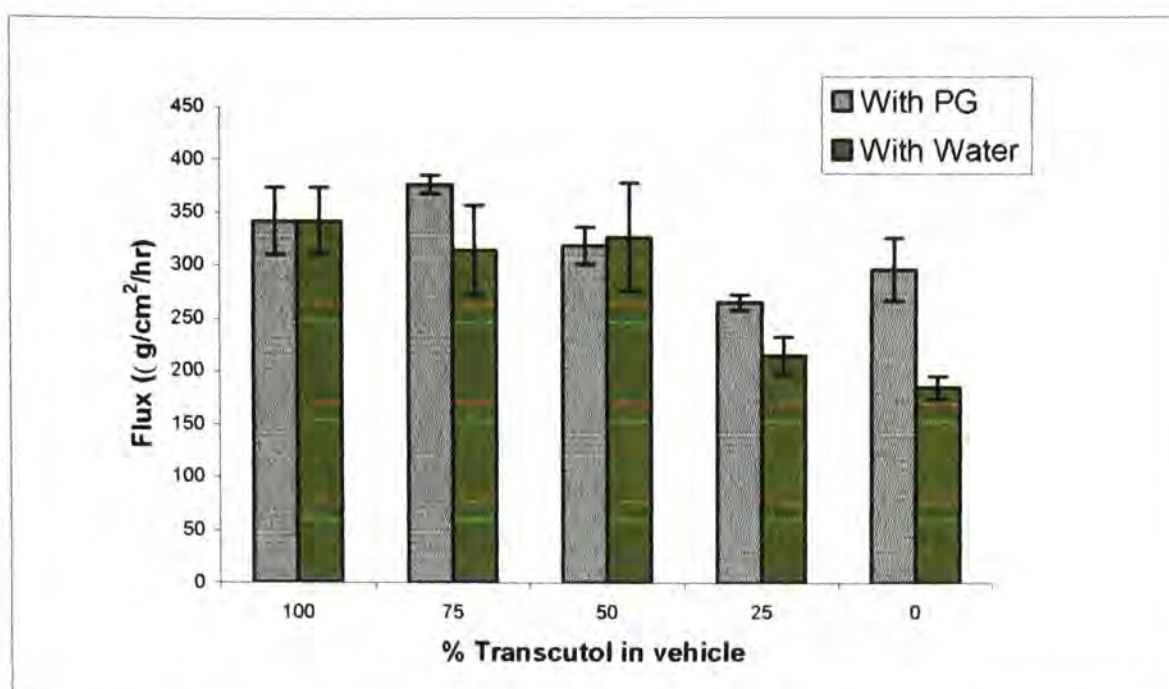


Figure 4.27. Flux values for the permeation of ibuprofen from saturated formulations containing Transcutol/water and Transcutol/PG.

The ethanol and water formulations showed very high flux values even using relatively low amounts of ethanol. Ethanol is safe to use on the skin to enhance permeation and therefore this is a strong candidate for further testing using both ATR-FTIR (to elucidate mechanism of action) and diffusion experiments using human skin. Combined with propylene glycol rather than water, the flux values were not greatly affected. The one difference being the higher flux for a 50% ethanol/propylene glycol formulation than for the corresponding ethanol/water formulation. It is not clear why there is a difference, and because of a lack of solubility data it was not possible to obtain diffusion and partition information for the ethanol and propylene glycol formulations. Again, ATR-FTIR could go some way to providing an answer to this question.

4.5.2.2. Salicylic acid

Propylene glycol/water vehicles

The permeation of salicylic acid through silicone membrane, using propylene glycol/water vehicles of varying composition was evaluated. Table 4.11 lists the flux values with associated standard deviations, the kinetic parameter D/h^2 , the thermodynamic parameter $K \cdot h$ and the permeability coefficient, k_p .

Table 4.11. Steady state fluxes, thermodynamic and kinetic parameters, permeability coefficients for the permeation of salicylic acid from saturated formulations containing propylene glycol and water through silicone membrane (mean \pm SD, n=4).

Vehicle (v/v)	J ($\mu\text{g}/\text{cm}^2/\text{hr}$) \pm SD	$K \cdot h$ (cm) \pm SD	D/h^2 (s) $\times 10^{-3}$ \pm SD	k_p (cm/s) \pm SD
0/100	74.9 \pm 5.55	0.18 \pm 0.35	0.32 \pm 0.24	5.75 $\times 10^{-4}$ \pm 3.75 $\times 10^{-5}$
10/90	148.7 \pm 11.71	0.15 \pm 0.19	0.20 \pm 0.14	1.75 $\times 10^{-5}$ \pm 1.05 $\times 10^{-5}$
20/80	-	-	-	-
30/70	155.5 \pm 15.27	0.04 \pm 0.01	0.14 \pm 0.16	1.42 $\times 10^{-5}$ \pm 1.37 $\times 10^{-6}$
40/60	-	-	-	-
50/50	190.7 \pm 11.61	5.04 $\times 10^{-3}$ \pm 5.92 $\times 10^{-3}$	0.08 \pm 0.11	3.42 $\times 10^{-6}$ \pm 1.92 $\times 10^{-7}$
60/40	135.1 \pm 7.52	0.01 \pm 6.3 $\times 10^{-3}$	2.73 $\times 10^{-4}$ \pm 2.19 $\times 10^{-3}$	2.37 $\times 10^{-6}$ \pm 1.92 $\times 10^{-7}$
70/30	126.5 \pm 9.38	3.20 $\times 10^{-6}$ \pm 1.37 $\times 10^{-6}$	0.35 \pm 0.18	9.41 $\times 10^{-7}$ \pm 1.10 $\times 10^{-7}$
80/20	129.5 \pm 24.35	8.24 $\times 10^{-4}$ \pm 9.54 $\times 10^{-4}$	0.11 \pm 0.14	4.57 $\times 10^{-7}$ \pm 6.69 $\times 10^{-8}$
90/10	187.3 \pm 11.49	7.38 $\times 10^{-4}$ \pm 8.29 $\times 10^{-4}$	0.04 \pm 0.07	4.25 $\times 10^{-7}$ \pm 2.33 $\times 10^{-8}$
100/0	87.1 \pm 8.12	4.39 $\times 10^{-4}$ \pm 6.73 $\times 10^{-4}$	0.13 \pm 0.18	1.47 $\times 10^{-7}$ \pm 8.30 $\times 10^{-9}$

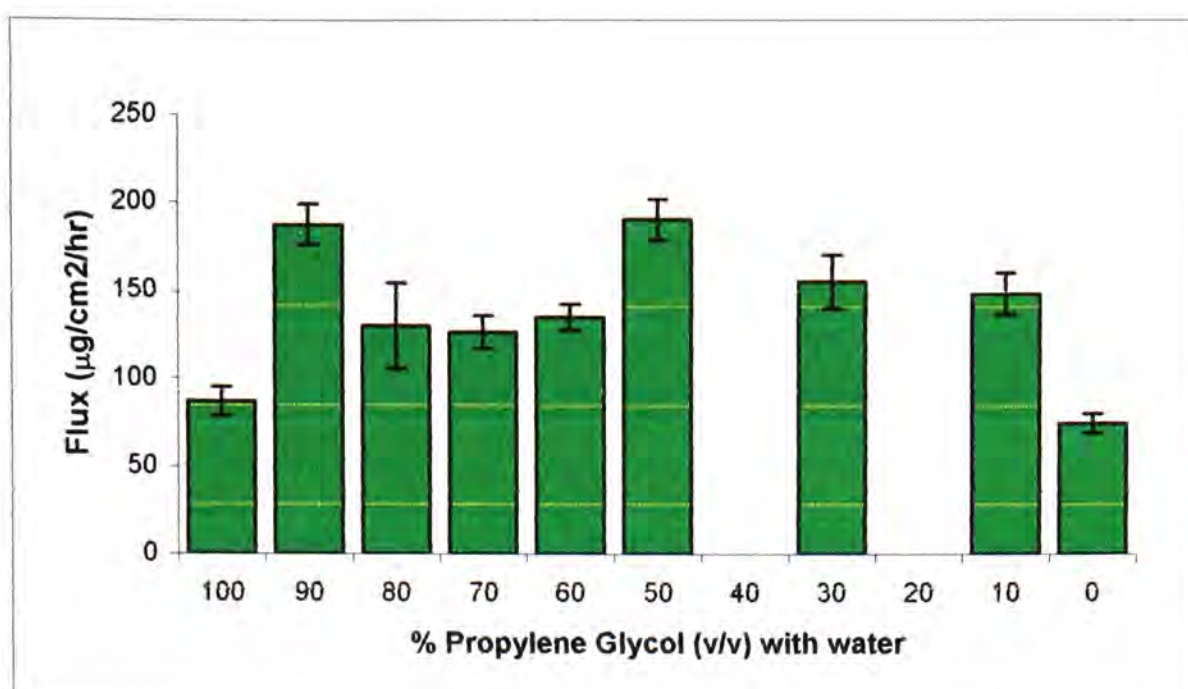


Figure 4.28. Steady state flux values for the permeation of salicylic acid from saturated formulations containing propylene glycol and water.

Figure 4.28 shows how the flux values for salicylic acid from propylene glycol and water formulations varies across the solvent combinations from pure water through to pure propylene glycol. The data suggest that, as in the previous experiments using ibuprofen, there is an interaction between the propylene glycol and the silicone membrane. Water is a non-interacting solvent and therefore it is highly unlikely that any change in flux is brought about by that component of the formulation.

The greatest permeation rates are for the 90/10 and 50/50 propylene glycol and water formulations (148.69 and $155.47\mu\text{g}/\text{cm}^2/\text{hr}$ respectively). This is similar to the behaviour of ibuprofen in these solvent combinations implying that these mixtures could be important to the enhancement of permeation.

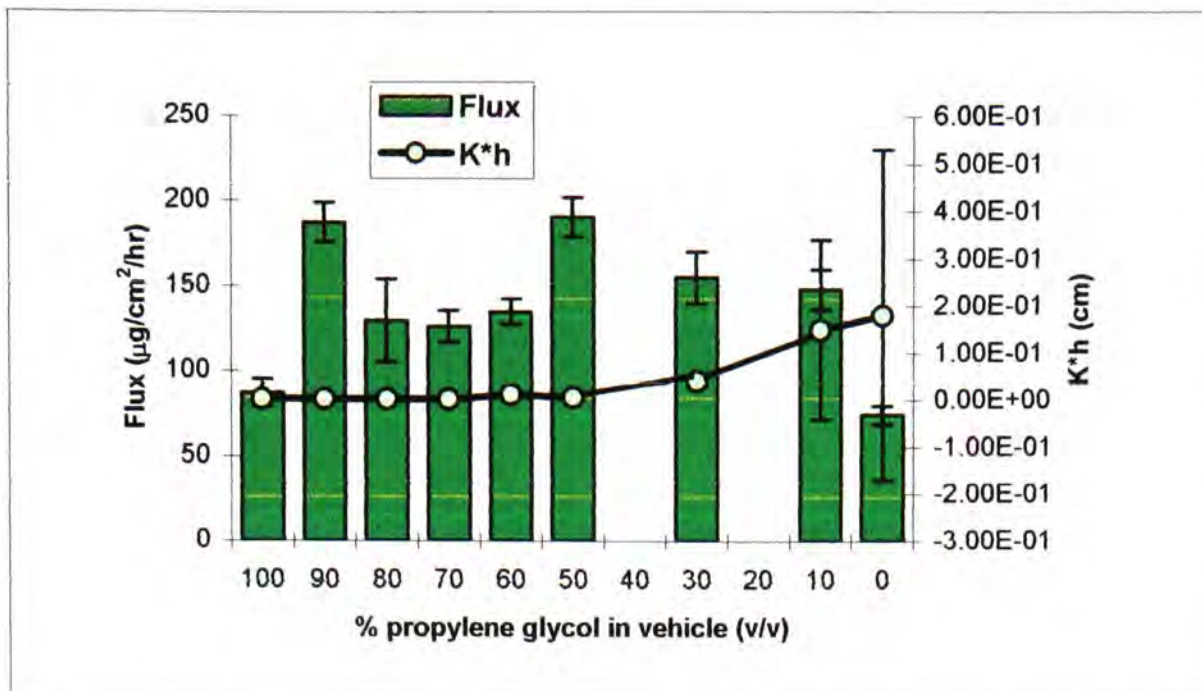


Figure 4.29. Steady state fluxes and $K \cdot h$ values for the permeation of salicylic acid from saturated formulations containing propylene glycol and water.

The partition coefficients (figure 4.29 shows the $K \cdot h$ values) for salicylic on these formulations do not show a predictable trend. They are all similar, with few exceptions being 10, 50 and 60% propylene glycol.

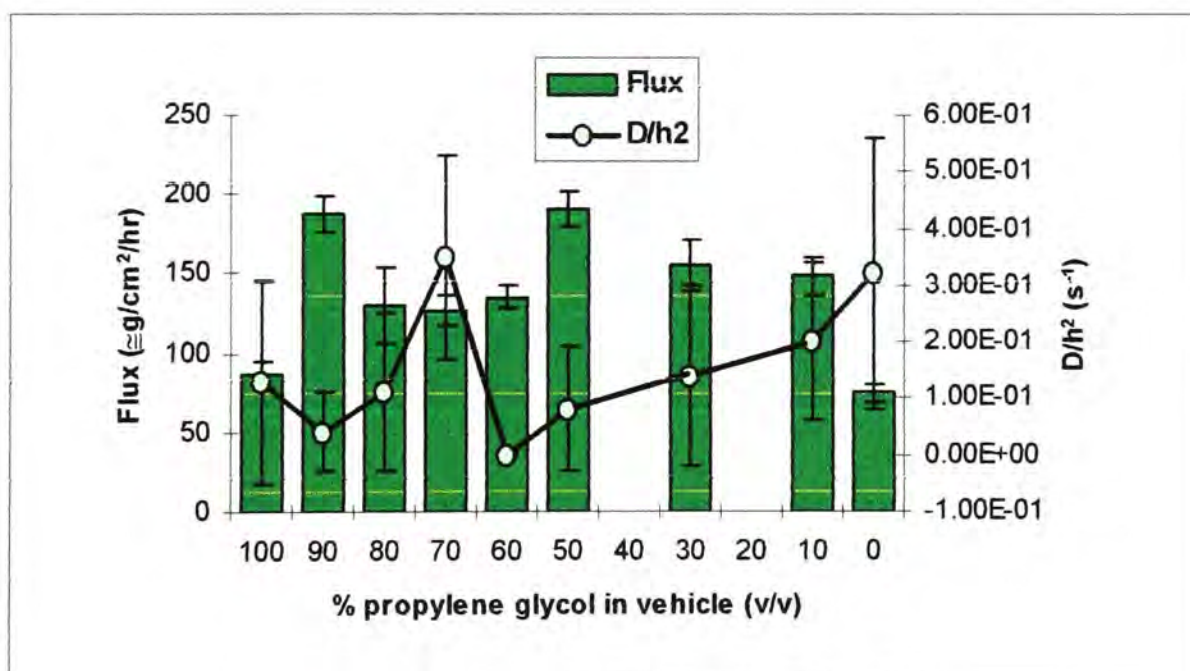


Figure 4.30. Steady state fluxes and D/h^2 values for the permeation of salicylic acid from saturated formulations containing propylene glycol and water.

The diffusion parameter shows quite significant changes for some of the formulations (0/100, 30/70 and 70/30 PG/water). This indicates changes in the diffusion coefficient for these mixtures. It is not clear why these are the only formulations affected, and it does not seem to impart any improvement in the flux values. It would appear that in the case of salicylic acid, a change in the partition coefficient has a greater effect than a change in the diffusion coefficient.

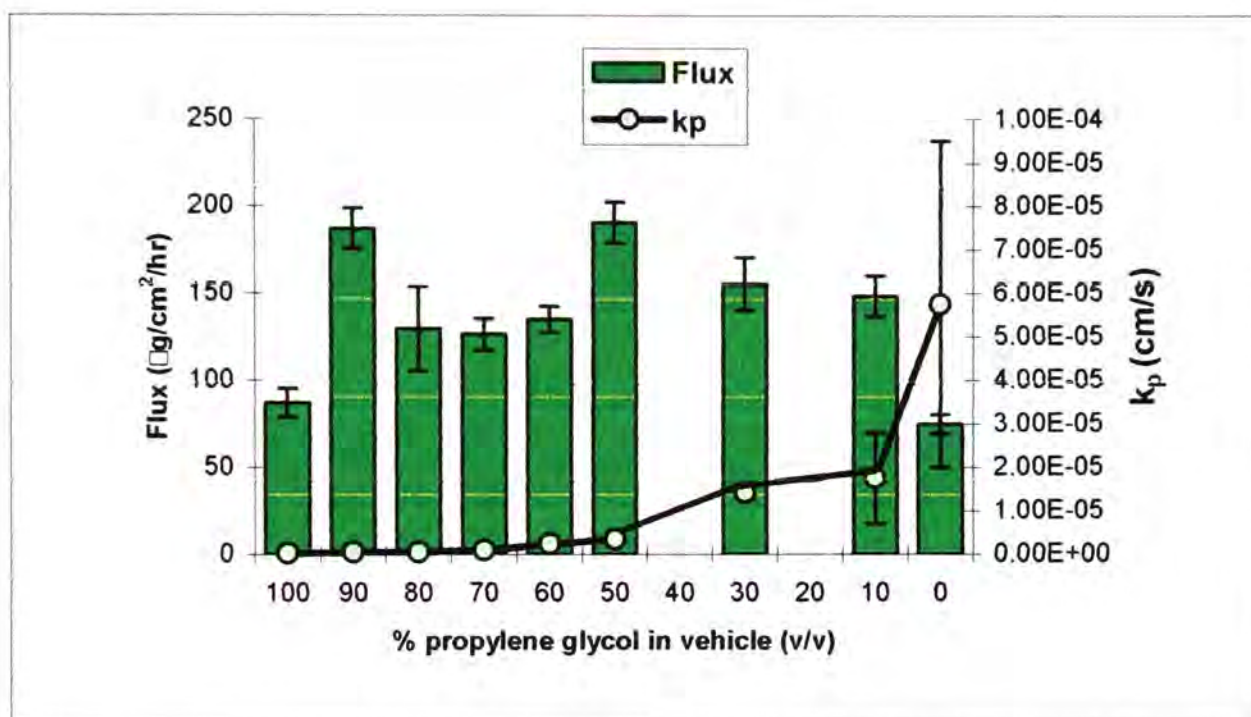


Figure 4.31. Steady state flux values and permeability coefficients for the permeation of salicylic acid from saturated formulations containing propylene glycol and water.

The permeability coefficients do not show a trend across the range of propylene glycol and water formulations, and all are of a similar order of magnitude.

Mineral oil/miglyol vehicle

The permeation of salicylic acid through silicone membrane, using mineral oil/miglyol vehicles of varying composition was evaluated.

Table 4.12. Steady state fluxes, thermodynamic and kinetic parameters, permeability coefficients for the permeation of ibuprofen from saturated formulations containing mineral oil and miglyol through silicone membrane (mean \pm SD, n=4).

Vehicle (v/v)	J ($\mu\text{g}/\text{cm}^2/\text{hr}$) \pm SD	K*h (cm)	D/h ² (s ⁻¹)	k _p
0/100	374.5 \pm 40.27	1.46 $\times 10^{-2}$ \pm 1.47 $\times 10^{-2}$	1.37 $\times 10^{-2}$ \pm 2.69 $\times 10^{-2}$	2.54 $\times 10^{-6}$ \pm 3.81 $\times 10^{-7}$
10/90	214.9 \pm 11.22	3.37 $\times 10^{-6}$ \pm 2.32 $\times 10^{-7}$	0.55 \pm 5.17 $\times 10^{-2}$	1.89 $\times 10^{-6}$ \pm 8.91 $\times 10^{-8}$
20/80	225.8 \pm 10.06	3.79 $\times 10^{-6}$ \pm 6.29 $\times 10^{-7}$	0.55 \pm 8.74 $\times 10^{-2}$	2.10 $\times 10^{-6}$ \pm 1.11 $\times 10^{-7}$
30/70	-	-	-	-
40/60	374.5 \pm 22.93	7.64 $\times 10^{-3}$ \pm 8.70 $\times 10^{-3}$	2.97 $\times 10^{-2}$ \pm 3.54 $\times 10^{-2}$	4.71 $\times 10^{-6}$ \pm 3.85 $\times 10^{-7}$
50/50	153.1 \pm 3.36	4.10 $\times 10^{-2}$ \pm 1.59 $\times 10^{-2}$	6.60 $\times 10^{-5}$ \pm 2.79 $\times 10^{-5}$	2.35 $\times 10^{-6}$ \pm 1.91 $\times 10^{-7}$
60/40	198.2 \pm 20.26	7.10 $\times 10^{-2}$ \pm 6.52 $\times 10^{-2}$	5.26 $\times 10^{-5}$ \pm 3.39 $\times 10^{-5}$	4.15 $\times 10^{-6}$ \pm 6.78 $\times 10^{-7}$
70/30	243.1 \pm 41.67	2.28 $\times 10^{-2}$ \pm 6.29 $\times 10^{-7}$	3.45 $\times 10^{-4}$ \pm 1.71 $\times 10^{-4}$	6.57 $\times 10^{-6}$ \pm 1.39 $\times 10^{-6}$
80/20	313.1 \pm 36.30	5.97 $\times 10^{-2}$ \pm 1.59 $\times 10^{-2}$	3.04 $\times 10^{-4}$ \pm 4.75 $\times 10^{-5}$	1.76 $\times 10^{-5}$ \pm 2.18 $\times 10^{-6}$
90/10	305.5 \pm 40.02	6.86 $\times 10^{-2}$ \pm 6.71 $\times 10^{-2}$	2.63 $\times 10^{-3}$ \pm 4.0 $\times 10^{-2}$	1.17 $\times 10^{-4}$ \pm 1.56 $\times 10^{-4}$
100/0	283.7 \pm 19.29	0.44 \pm 0.35	6.23 $\times 10^{-4}$ \pm 0.14	3.27 $\times 10^{-4}$ \pm 2.43 $\times 10^{-5}$

Flux values for salicylic acid are higher for the mineral oil and miglyol formulations than propylene glycol and water formulations. The flux values vary from $\sim 150\mu\text{g}/\text{cm}^2/\text{hr}$ to $\sim 370\mu\text{g}/\text{cm}^2/\text{hr}$. Most of the values are

around $200\text{mg}/\text{cm}^2/\text{hr}$, which is considerably lower than for the corresponding formulations containing ibuprofen. The change can be attributed to the relative lipophilicities of salicylic acid and ibuprofen ($\log P = 2.26$ and 3.51 respectively). It follows that a lipophilic vehicle such as mineral oil would present a more favourable environment to ibuprofen than salicylic acid. As with the experiments using ibuprofen, there is high flux at around 80% mineral oil formulations. The similarity of both drugs in the formulations implies that the permeation is mainly affected by the interaction between the vehicles and the membrane.

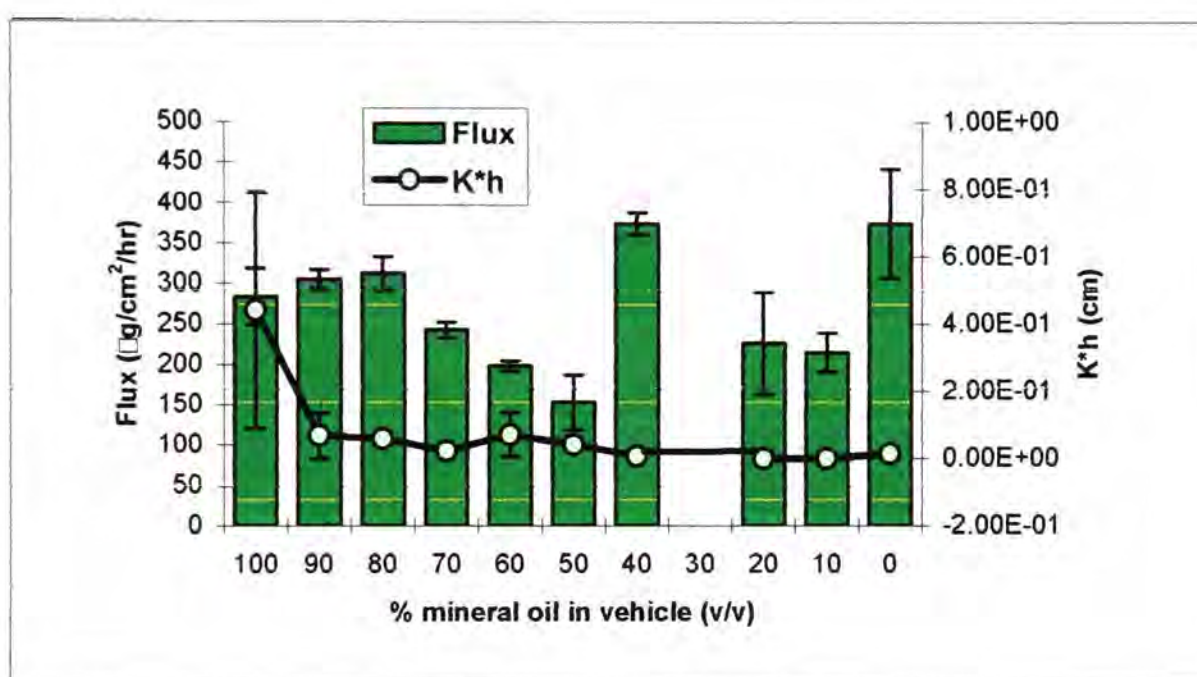


Figure 4.32. Steady state flux and K^*h values for the permeation of salicylic acid from saturated formulations containing mineral oil and miglyol.

The partitioning behaviour of salicylic acid in mineral oil and miglyol formulations show a change at 40% mineral oil, with the skin-vehicle partition coefficient dropping to from -0.73 to -4 . Generally the partition coefficients are similar in magnitude, with most values between -0.5 and 1 . The data indicate that when the amount of mineral oil in the formulation is higher, there is a greater tendency for the drug to move into the silicone

than remain in the formulation. The diffusion parameters mostly correspond in magnitude to the diffusion of water ($D = 1.5 \times 10^{-7} \text{ cm}^2\text{s}^{-1}$) quoted by Potts et al (1991). The exceptions to this are those formulations which also showed a change in the partition coefficient (10/90 and 20/80 mineral oil and miglyol). However, there is not an increase in flux associated with these changes, suggesting that altering the diffusion coefficient and partition coefficient by the magnitude that is seen, does not constitute a large enough effect to enhance permeation.

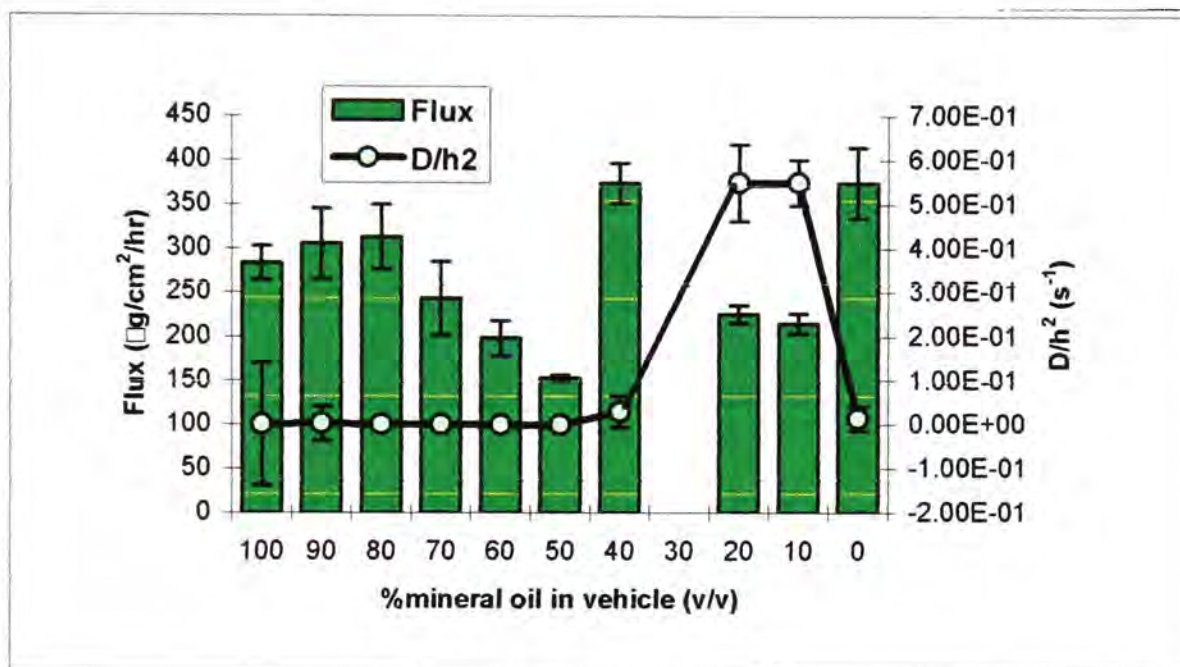


Figure 4.33. Steady state fluxes and D/h^2 values for the permeation of salicylic acid from saturated formulations containing mineral oil and miglyol.

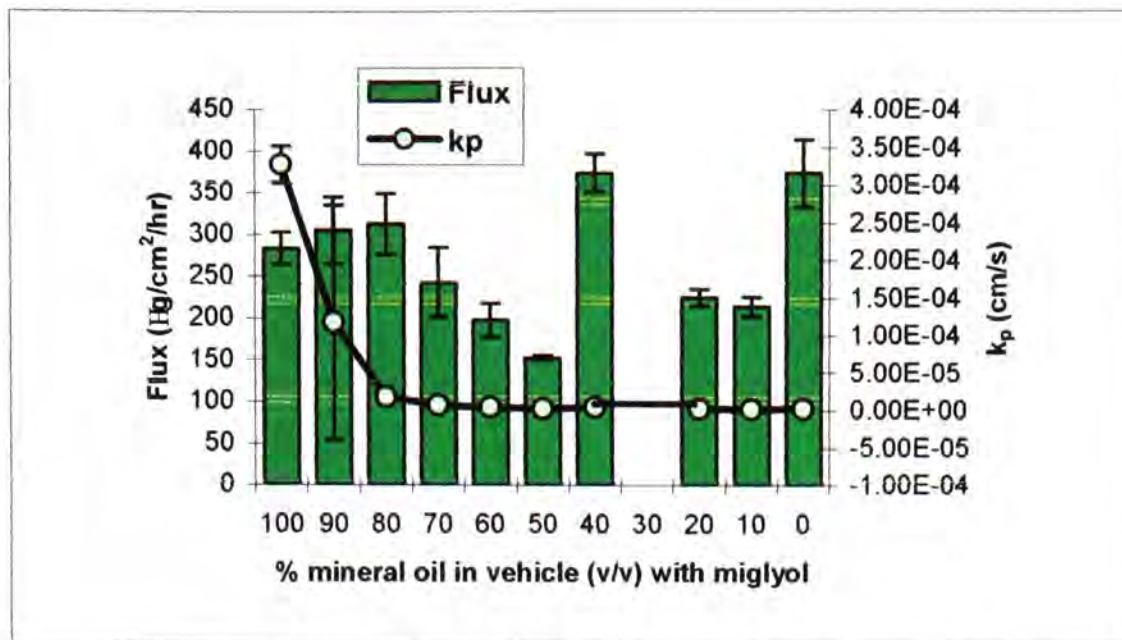


Figure 4.34. Steady state flux values and permeability coefficients for the permeation of salicylic acid from formulations containing mineral and miglyol.

The permeability coefficients for the lipophilic vehicles do not show any trend between 0-90% mineral oil and miglyol. However, the permeability coefficient is larger for 100% mineral than for 100% miglyol, which according to the data is a result of a change in the partition parameter.

Ethanol/water vehicles

The permeation of salicylic acid through silicone membrane, using ethanol/water vehicles of varying composition was evaluated. Table 4.13 lists the flux values with associated standard deviations.

Permeation of salicylic acid through silicone membrane from formulations containing ethanol and water was much higher than for any other vehicles investigated. Standard deviations were fairly high for some of the formulations, and this could have been a result of unavoidable evaporation of the ethanol in the formulation in some of the diffusion cells.

Table 4.13. Steady state fluxes for the permeation of salicylic acid from saturated formulations containing ethanol and water through silicone membrane (mean \pm SD, n=4).

Vehicle (v/v)	J ($\mu\text{g}/\text{cm}^2/\text{hr}$) \pm SD	CV
0/100	81.2 \pm 8.39	7.42
25/75	454.9 \pm 71.61	15.74
50/50	1024.8 \pm 41.87	4.09
75/25	1241 \pm 184.16	14.84
100/0	2018.1 \pm 374.70	18.57

Because of a lack of solubility data for salicylic acid in these vehicles it was not possible to use a curve fitting procedure to obtain kinetic and thermodynamic parameters for ethanol and water formulations.

The increase in flux shows a similar pattern to that for the same vehicles, containing ibuprofen. More importantly, this increase is the same for both ibuprofen and salicylic acid, being 1.5x and 1.6x respectively.

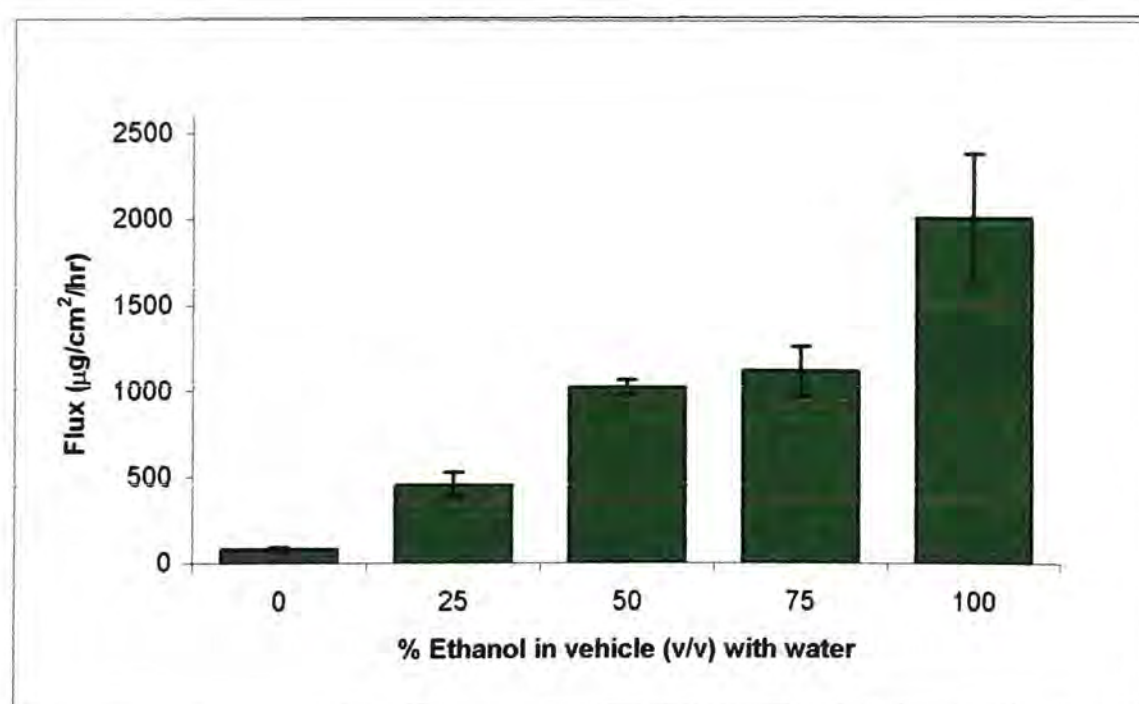


Figure 4.35. Steady state flux values for the permeation of salicylic acid from saturated formulations containing ethanol and water.

As with other formulations studied, this strongly implies that it is the interaction between the vehicle and the membrane which is the dominating factor in enhancing permeation. Of course, the structure and physicochemical properties of the permeants will affect the flux, but the evidence from this investigation has demonstrated how powerful the effect of the formulation is, and just how important it is to utilise these effects to our advantage.

Transcutol/water vehicles

The permeation of salicylic acid through silicone membrane, using Transcutol/water vehicles of varying composition was evaluated. Table 4.14 lists the flux values with associated standard deviations.

Table 4.14. Steady state fluxes for the permeation of salicylic acid from saturated formulations containing Transcutol and water through silicone membrane (mean \pm SD, n=4).

Vehicle (v/v)	J ($\mu\text{g}/\text{cm}^2/\text{hr}$) \pm SD	CV
0/100	74.9 \pm 5.55	7.42
25/75	212.2 \pm 37.06	17.46
50/50	123.9 \pm 21.77	17.57
75/25	213.2 \pm 34.21	16.03
100/0	308.3 \pm 66.56	21.59

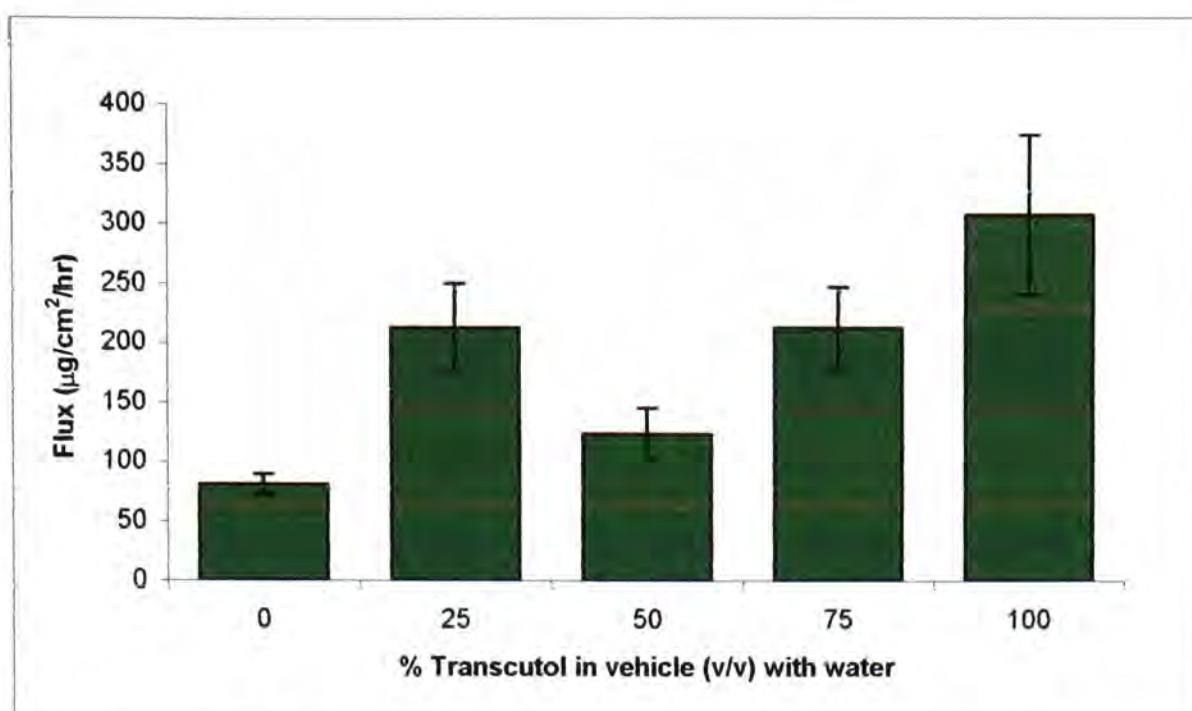


Figure 4.36. Steady state flux values for the permeation of salicylic acid from saturated formulations containing Transcutol and water.

The permeation of salicylic acid from Transcutol and water formulations was slightly lower than those for corresponding formulations containing ibuprofen. As with the ethanol and water vehicles, there is a similar pattern in the data for both permeants, suggesting that Transcutol acts in a similar manner, independent of the permeant used.

There is not a significant difference between 25, 75 and 100% Transcutol, which indicates that between 0-25% the addition has a greater effect than above 25%. This is encouraging, as with any formulation generally the enhancer (be it diffusional enhancer or solubility enhancer) is not added in quantities above 5-10%. It would be of use to have more data in this range to determine at what point permeation is enhanced.

4.5.2.3. Acetaminophen

Mineral oil/miglyol vehicles

The permeation of acetaminophen through silicone membrane, using mineral oil/miglyol vehicles of varying composition was evaluated. Steady state fluxes were calculated by monitoring the cumulative amount of drug diffused and measuring the slope of the graph once steady state diffusion was reached. All time points were used to measure the slope of the graph. Table 4.14 lists the flux values with associated standard deviations.

Table 4.15. Steady state fluxes for the permeation of acetaminophen from saturated formulations containing mineral oil and miglyol through silicone membrane (mean \pm SD, n=4).

Vehicle (v/v)	J ($\mu\text{g}/\text{cm}^2/\text{hr}$)	SD
0/100	1.84	0.10
10/90	1.37	0.3
20/80	1.36	0.2
30/70	1.54	0.02
40/60	1.40	0.20
50/50	1.34	0.59
60/40	1.35	0.12
70/30	2.02	0.3
80/20	1.72	0.03
90/10	1.85	0.08
100/0	1.49	0.09

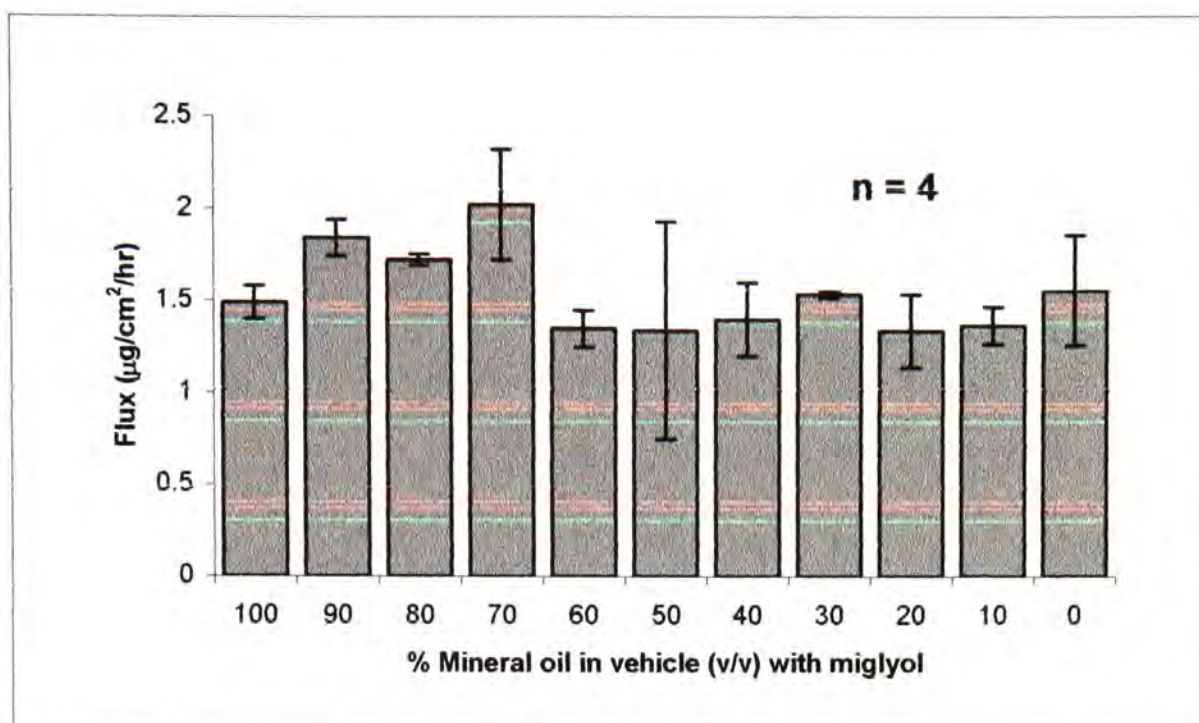


Figure 4.37. Steady state flux values for the permeation of acetaminophen from saturated formulations containing mineral oil and miglyol.

Flux values for acetaminophen for lipophilic vehicles was extremely low, with no apparent trends across the range. The low flux can be attributed to the logP of acetaminophen (0.46). Any drug with a low logP value such as this would not find a formulation as lipophilic in nature as mineral oil and miglyol a favourable environment to exist in. However, the lipophilic vehicle may act as an occlusive, slowing water loss, thus increasing the moisture content of the stratum corneum which may actually aid acetaminophen permeation. Acetaminophen is much better suited to more hydrophilic vehicles, but as described in Chapter Two, acetaminophen is relatively unstable in any solvents which are capable of hydrogen bonding.

4.5.2.4. Summary of the results of binary formulation permeation studies

Generally, the permeation of salicylic acid from the selected formulations was lower than for the same formulations containing ethanol. Many similar patterns emerged which suggest that despite differences in structure and lipophilicity, the same solvent interactions affected both permeants.

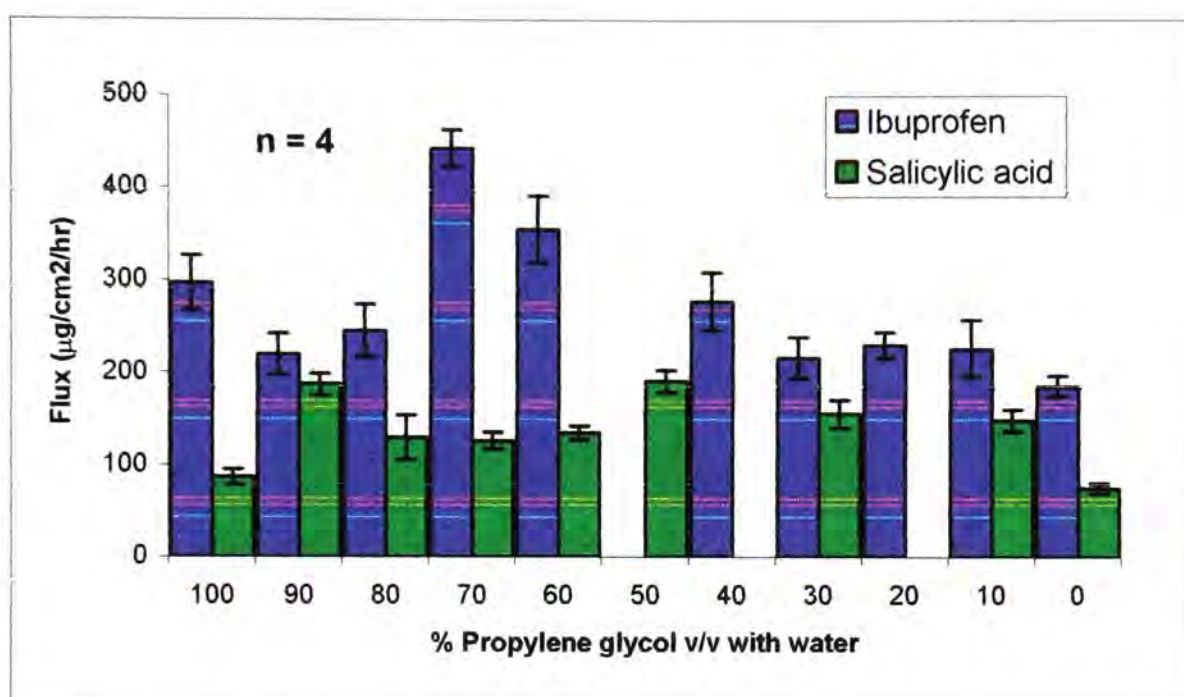


Figure 4.38. Steady-state flux values for ibuprofen and salicylic acid from saturated formulations containing propylene glycol and water.

Figure 4.38 compares the flux values for ibuprofen and salicylic acid in propylene glycol and water formulations. In some cases the flux is half of that achieved using ibuprofen, and this effect is most likely the result of the difference in lipophilicity between the two model permeants (3.51 and 2.26 for ibuprofen and salicylic acid respectively).

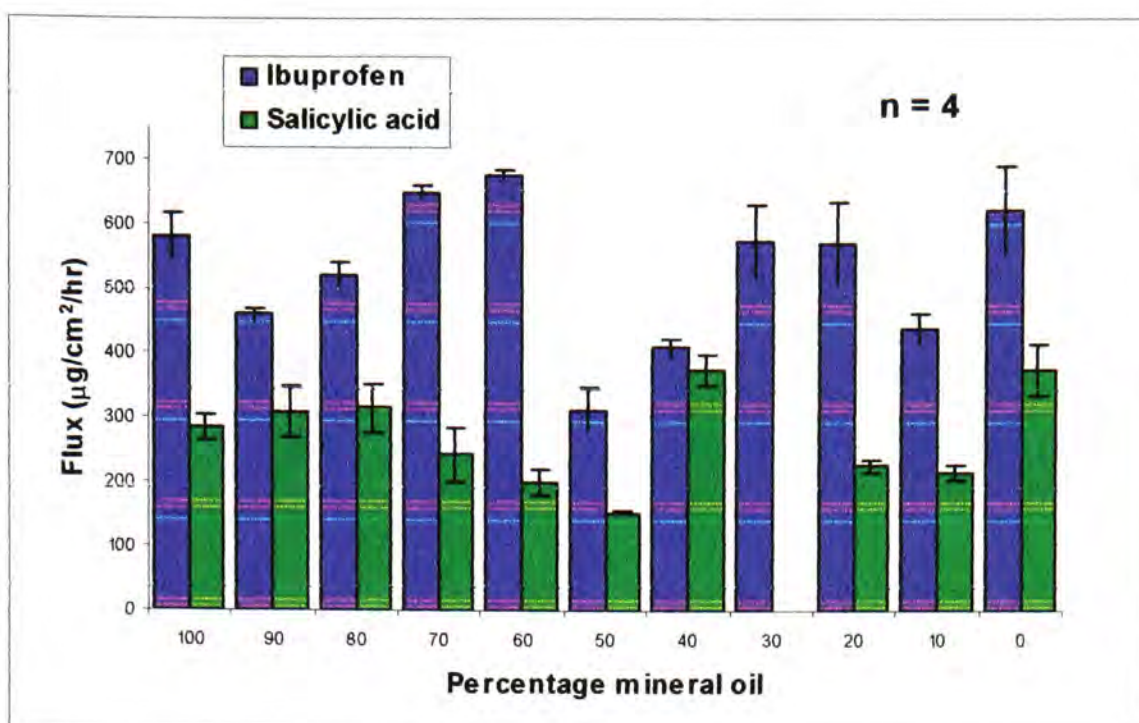


Figure 4.39. Steady-state flux values for ibuprofen and salicylic acid from saturated formulations containing mineral oil and miglyol.

As with the propylene glycol and water formulations, the flux values from mineral oil and miglyol vehicles was lower for salicylic acid. Again, this is because of the permeants relative lipophilicities.

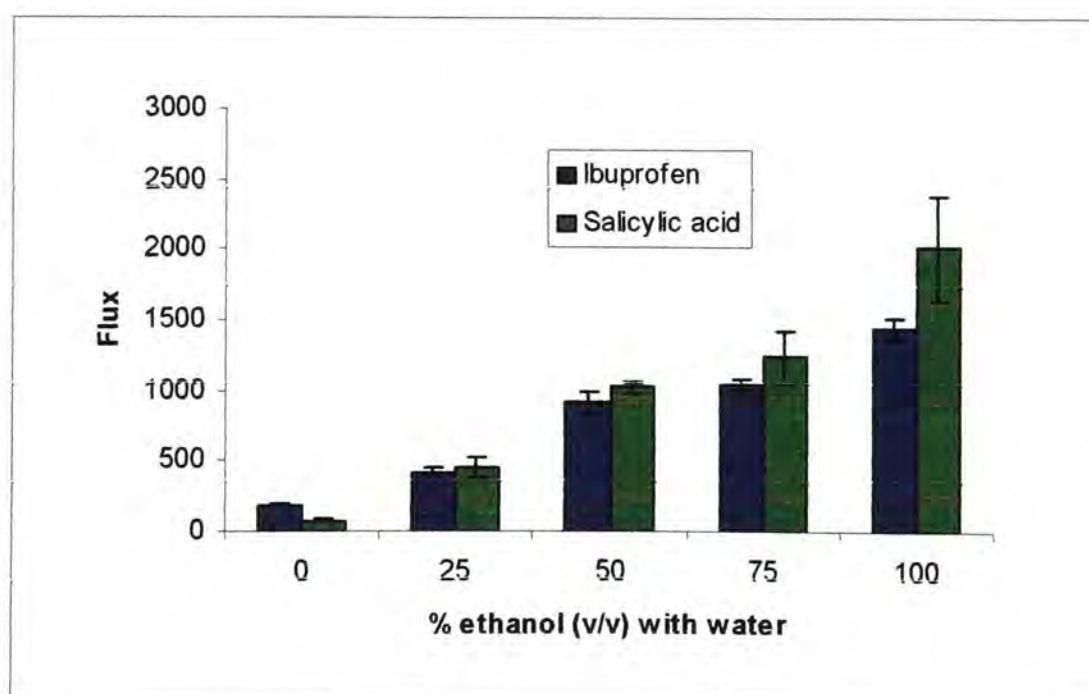


Figure 4.40. Steady state flux values for ibuprofen and salicylic acid from saturated formulations containing ethanol and water.

The similarity in the diffusion profiles for ibuprofen and salicylic acid in ethanol and water formulations is striking. Although diffusion and partition parameters were not determined for salicylic acid in these vehicles, one would expect that the effects would be the same for both permeants and therefore we can make some informed guesses as to what is happening in these systems. Data from the studies using ibuprofen suggest a strong dominating influence is the partition coefficient, and this is in line with the ideas introduced in Chapter Two.

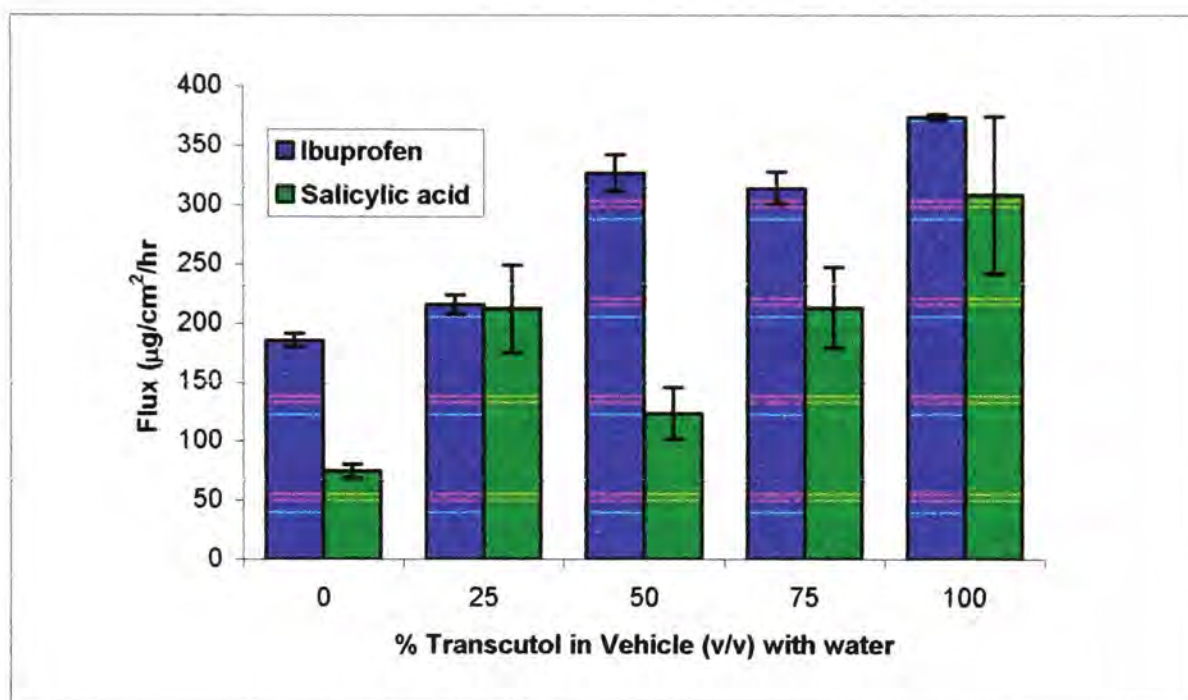


Figure 4.41. Steady-state flux values for ibuprofen and salicylic acid from saturated formulations containing Transcutol and water.

4.5.3. Ternary solvent vehicles

Ibuprofen was selected as the model permeant for studies of formulations containing three solvents. The reason for this choice is quite straightforward, and it relates to the concerns about using salicylic acid at high concentrations in topical products. Salicylic acid is a keratolytic agent, which means that at high concentrations it could cause severe damage to the barrier function of the skin. There are no such concerns with the use of ibuprofen and so it seemed logical to use this drug for studies using formulations more representative of an actual formulation.

However, the one problem with the use of a weak acid such as ibuprofen has already been highlighted in Chapter Two and in section 4.5.2 of this Chapter. The issue is of ionisation. It has already been demonstrated that the addition of ethanol to a formulation will increase the pK_a of ibuprofen, and it is highly likely (though it cannot be tested) that this effect will also occur with a diol such as propylene glycol. It is not clear what the effect of using both of these solvents in one formulation will be, and to overcome this carefully designed experiments are needed to determine whether this has any effect upon permeation.

Ethanol/propylene glycol/water vehicles

The permeation of ibuprofen through silicone membrane, using ternary vehicles composed of ethanol, propylene glycol and water with varying composition was evaluated. Table 4.16 lists the flux values with associated standard deviations, the kinetic parameter D/h^2 , the thermodynamic parameter $K \cdot h$ and the permeability coefficient, k_p .

Table 4.16. Steady state fluxes, thermodynamic and kinetic parameters, permeability coefficients for the permeation of ibuprofen from saturated formulations containing ethanol, propylene glycol and water through silicone membrane (mean \pm SD, n=4).

Vehicle (v/v)	J ($\mu\text{g}/\text{cm}^2/\text{hr}$) \pm SD	CV	K*h (cm) \pm SD	D/h ² (s) \pm SD	k _p (cm/s) \pm SD
25/25/5 0	525.8 \pm 37.32	7.10	2.90 $\times 10^{-3}$ \pm 1.8 $\times 10^{-3}$	4.65 $\times 10^{-4}$ \pm 1.89 $\times 10^{-3}$	1.08 $\times 10^{-7}$ \pm 5.78 $\times 10^{-8}$
50/25/2 5	641.1 \pm 84.08	13.22	2.11 $\times 10^{-3}$ \pm 1.5 $\times 10^{-3}$	4.34 $\times 10^{-4}$ \pm 3.3 $\times 10^{-4}$	6.09 $\times 10^{-7}$ \pm 8.01 $\times 10^{-8}$

The permeation rate of ibuprofen from ternary formulations was found to be the same for both vehicles tested. The flux values were lower than for simple formulations containing ethanol and water, and were similar to those containing ethanol and propylene glycol.

This implies that when used in combination, propylene glycol counteracts the enhancing effect of ethanol in some way. It could be the two solvents interact, which affects the way in which ethanol permeates into the membrane, thus preventing any interaction with the membrane itself.

The amount of ethanol in the formulation did not have any effect upon either the partition coefficient or the diffusion coefficient, and the permeability coefficient was also of the same order of magnitude for both formulations, though was significantly different for the formulation containing a greater amount of ethanol.

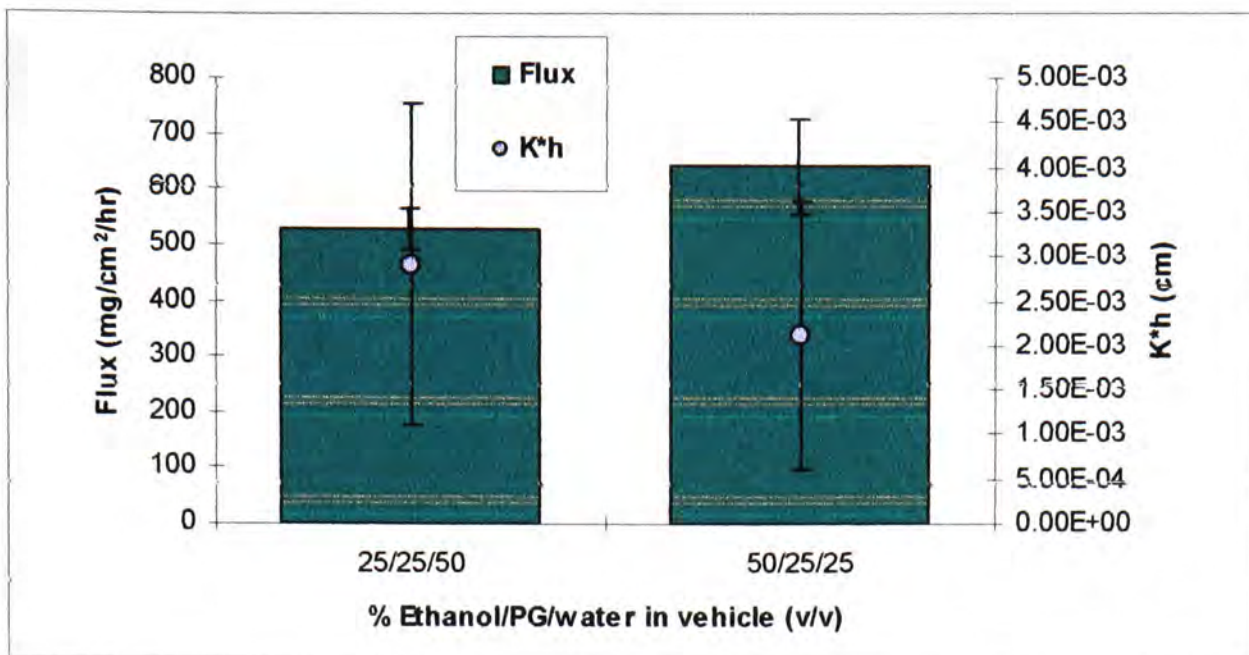


Figure 4.42. Steady state fluxes and $K \cdot h$ values for the permeation of ibuprofen in ternary vehicles containing ethanol, propylene glycol and water.

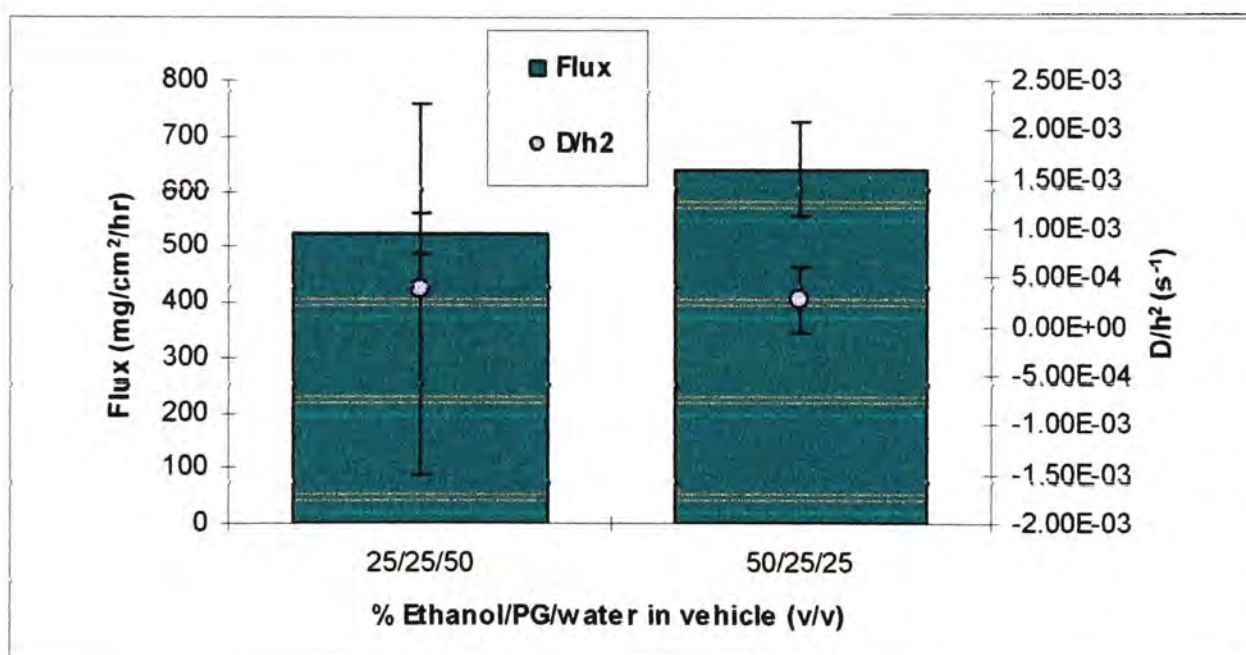


Figure 4.43. Steady state fluxes and D/h^2 values for the permeation of ibuprofen in ternary vehicles containing ethanol, propylene glycol and water.

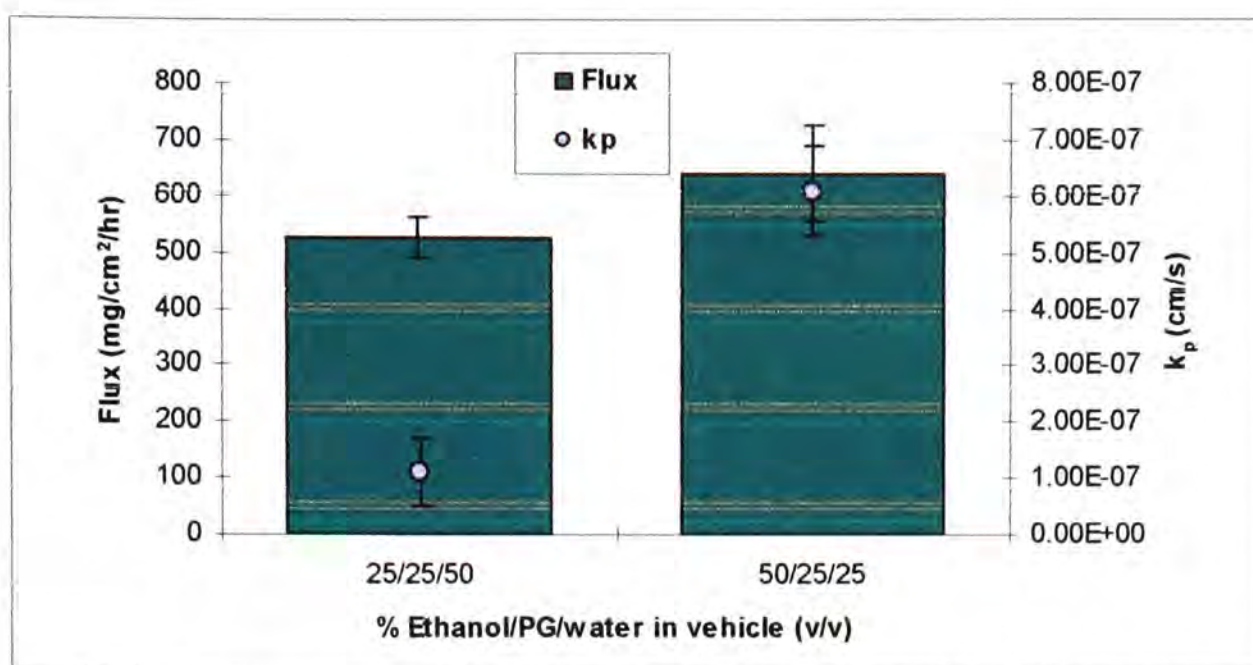


Figure 4.44. Steady state fluxes and k_p values for the permeation of ibuprofen in ternary vehicles containing ethanol, propylene glycol and water.

Diffusion studies under non-occluded conditions.

In order to model the situation of a topical product, diffusion studies were conducted under non-occluded conditions. In everyday life, a person applying a topical cream or lotion may wear clothes, but these would not occlude the application site entirely. Until now, all the studies described in this thesis have been conducted under occlusion. To mimic 'in use' formulations it is relevant to investigate the effect of occlusion upon permeation. As for the occluded studies, 1mL of a saturated solution of ibuprofen in the relevant formulation was applied.

Whereas the flux values for these formulations were the same under occluded conditions, when left open to the air, there was an increase in flux for the formulation containing more ethanol, compared with the formulation having less. This is perhaps a result of the formation of a supersaturated solution as ethanol evaporates from the vehicle. This will increase the thermodynamic activity of the drug in the vehicle, leading to

an increase in the permeation. However this seems to be contradicted by the data obtained from curve fitting.

Table 4.17. Steady state fluxes, thermodynamic and kinetic parameters, permeability coefficients for the permeation of ibuprofen from saturated formulations containing ethanol, propylene glycol and water through silicone membrane under non-occluded conditions (mean \pm SD, n=4).

Vehicle (v/v)	J ($\mu\text{g}/\text{cm}^2/\text{hr}$) \pm SD	cv	K*h (cm) \pm SD	D/h ² (s ⁻¹) \pm SD	k _p (cm/s) \pm SD
25/25/50	376.2 \pm 39.98	10.63	4.16 $\times 10^{-3}$ \pm 7.91 $\times 10^{-4}$	0.17 \pm 0.16	8.10 $\times 10^{-7}$ \pm 7.92 $\times 10^{-8}$
50/25/25	558.2 \pm 48.94	8.77	1.64 $\times 10^{-3}$ \pm 1.15 $\times 10^{-3}$	7.06 $\times 10^{-2}$ \pm 0.14	5.38 $\times 10^{-7}$ \pm 3.37 $\times 10^{-8}$

The partition coefficient and diffusion coefficient for the formulation containing 50% ethanol are similar to those obtained for the occluded study, whereas the other system shows significant changes in both the partition coefficient and the diffusion coefficient. The flux is also much lower for this formulation when it is non-occluded. The other difference is that the flux values for the formulations with the higher proportion of ethanol are statistically the same whether occluded or non-occluded, perhaps implying that at higher concentrations it does not play such a significant role, and that evaporation is not what is affecting the flux.

Figures 4.45, 4.46 and 4.47 present the results of the curve fitting along with the flux values for vehicles containing ethanol/propylene glycol and water. Presented in this way, it is clear that together the partition and diffusion parameters are increasing the flux in these systems.

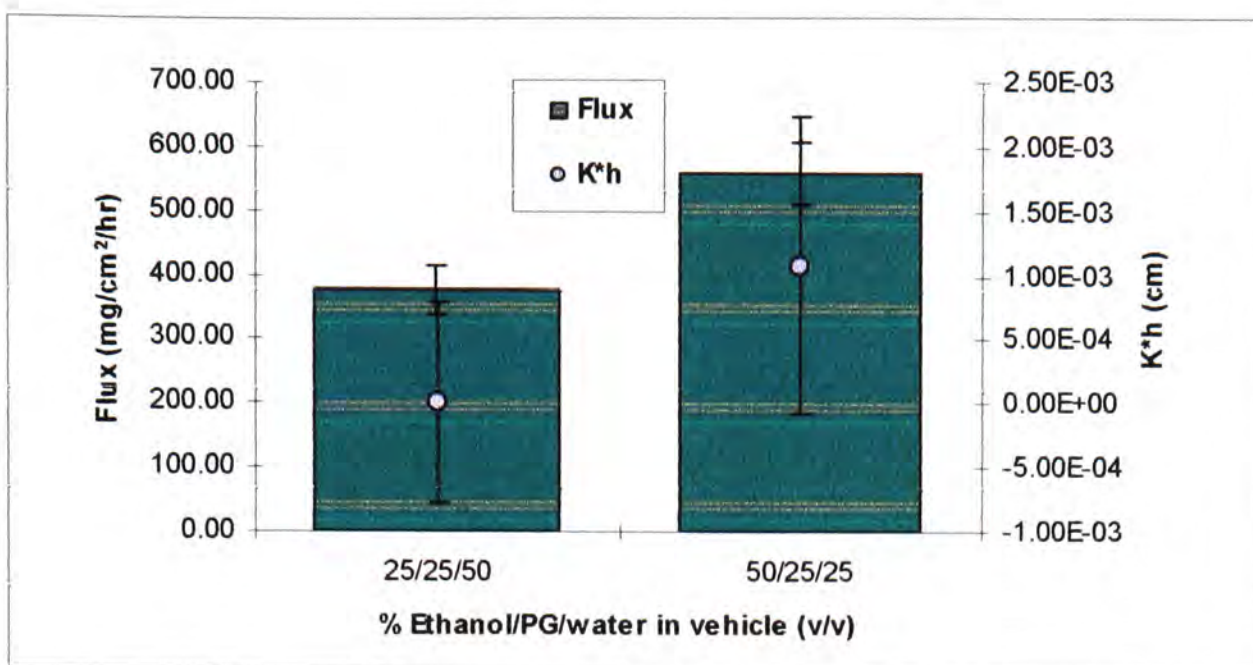


Figure 4.45. Steady state fluxes and $\log(K \cdot h)$ values for the permeation of ibuprofen in ternary vehicles containing ethanol, propylene glycol and water under non-occluded conditions.

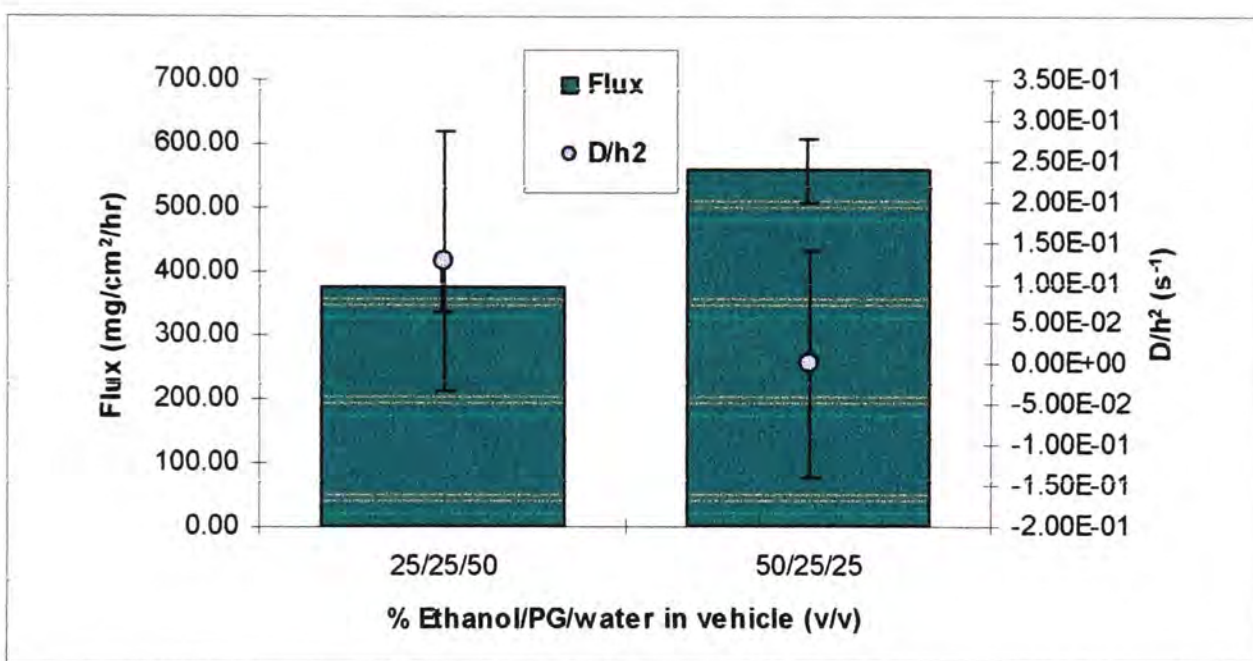


Figure 4.46. Steady state fluxes and $\log(D/h^2)$ values for the permeation of ibuprofen in ternary vehicles containing ethanol, propylene glycol and water under non-occluded conditions.

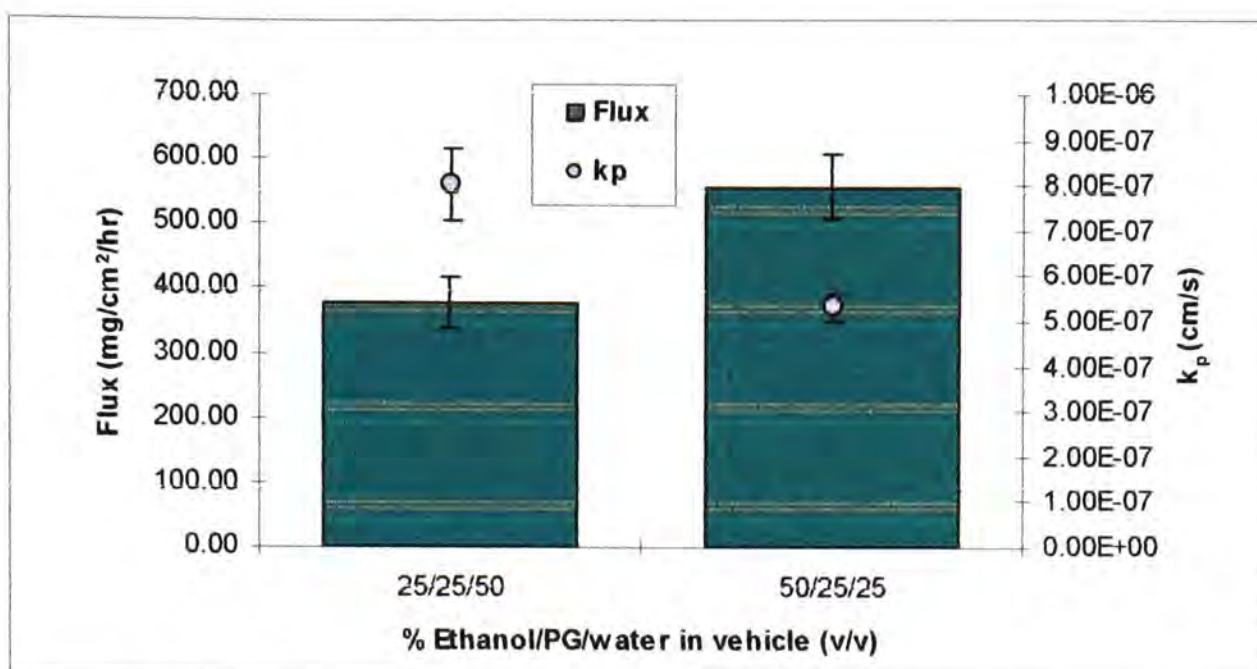


Figure 4.47. Steady state fluxes and $\log(k_p)$ values for the permeation of ibuprofen in ternary vehicles containing ethanol, propylene glycol and water under non-occluded conditions.

To understand fully what is happening in these systems it is necessary to conduct ATR-FTIR experiments in which each component can be monitored, and this is described in Chapter Five.

Transcutol/propylene glycol/water vehicles

The permeation of ibuprofen through silicone membrane, using ternary vehicles composed of Transcutol, propylene glycol and water with varying composition was evaluated. Table 4.18 lists the flux values with associated standard deviations, the kinetic parameter D/h^2 , the thermodynamic parameter $K \cdot h$ and the permeability coefficient, k_p .

The flux of ibuprofen was lower for formulations containing Transcutol, propylene glycol and water than for the corresponding systems containing ethanol as an 'enhancing' solvent.

Table 4.18. Steady state fluxes, thermodynamic and kinetic parameters, permeability coefficients for the permeation of ibuprofen from saturated formulations containing Transcutol, propylene glycol and water through silicone membrane (mean \pm SD, n=4).

Vehicle (v/v)	J ($\mu\text{g}/\text{cm}^2/\text{hr}$) \pm SD	CV	K*h (cm) \pm SD	D/h ² (s ⁻¹) \pm SD	k _p (cm/s) \pm SD
25/25/50	222.9 \pm 6.84	3.07	1.67 \times 10 ⁻³ \pm 2.20 \times 10 ⁻³	5.27 \times 10 ⁻³ \pm 9.04 \times 10 ⁻³	8.51 \times 10 ⁻⁷ \pm 1.67 \times 10 ⁻⁷
50/25/25	257.1 \pm 11.19	4.35	9.28 \times 10 ⁻⁵ \pm 1.25 \times 10 ⁻⁴	2.02 \times 10 ⁻² \pm 3.87 \times 10 ⁻⁴	2.87 \times 10 ⁻⁷ \pm 4.75 \times 10 ⁻⁹

Solubility studies showed that the ibuprofen was more soluble in the ethanol, propylene glycol and water vehicles, and this could account for the slightly lower flux values. In theory, saturated formulations should have identical flux, because the thermodynamic activity is equal to unity, but throughout this chapter there has been evidence contradicting this. The most plausible explanation is an interaction between the solvents and the membrane which alters the activity within that membrane.

There is no difference in the partition coefficients for the two formulations, suggesting that any enhancement seen is not a result of a change in partitioning behaviour. Harrison (1996) proposed that the mechanism of action of Transcutol was similar to the action of propylene glycol, both solvents permeate the membrane, increasing the solubility of the drug within in it, thereby increasing flux.

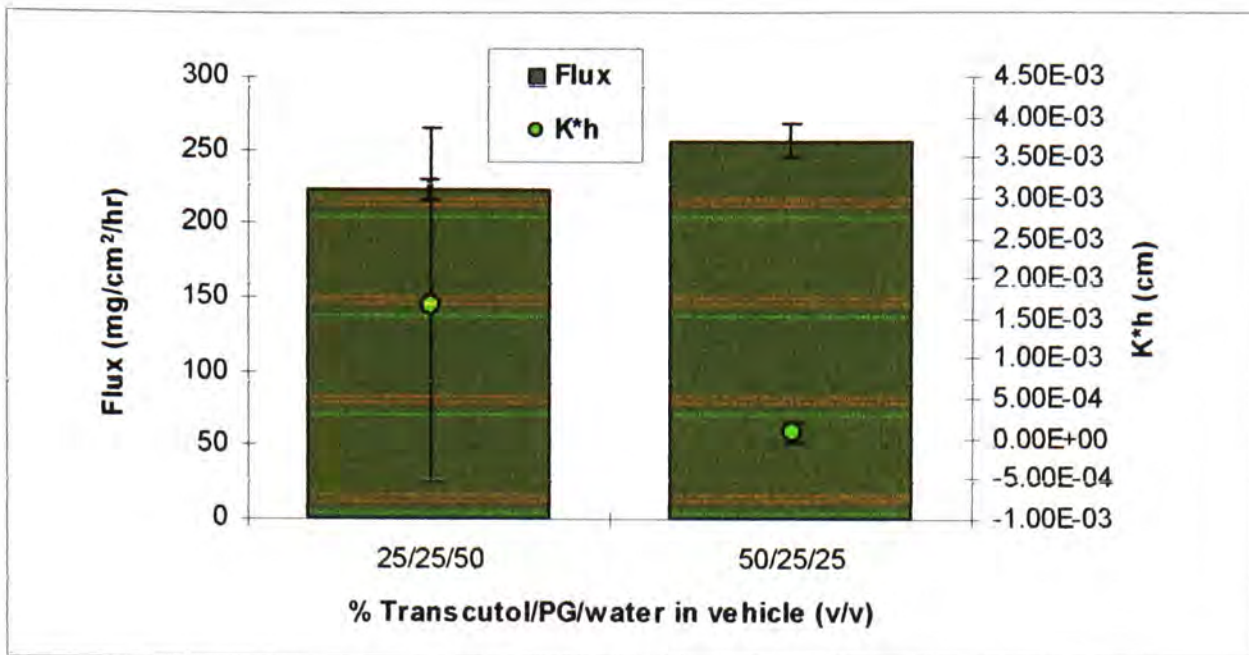


Figure 4.48. Steady state fluxes and K*h values for the permeation of ibuprofen in ternary vehicles containing Transcutol, propylene glycol and water.

The data presented here would seem to disagree with the findings of Harrison, for figure 4.49, showing the diffusion parameters for Transcutol formulations, clearly shows that the diffusion of ibuprofen is being altered by increasing the Transcutol content of the formulation.

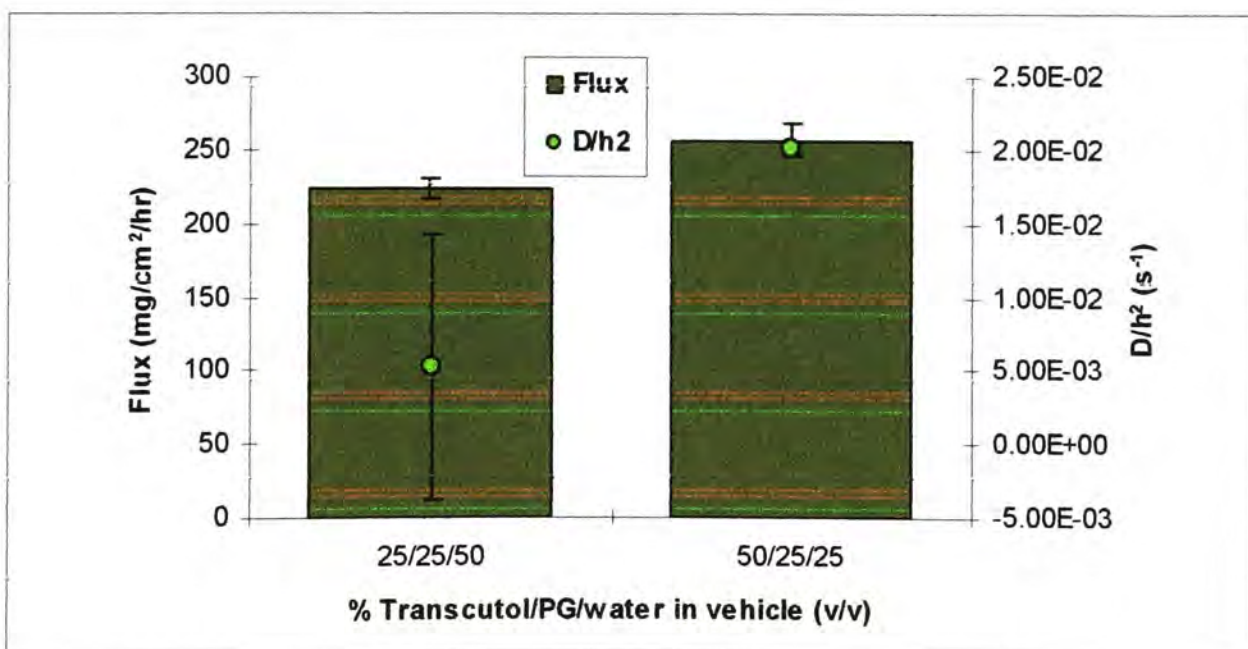


Figure 4.49. Steady state fluxes and D/h² values for the permeation of ibuprofen in ternary vehicles containing Transcutol, propylene glycol and water.

The permeability coefficients (shown in figure 4.50) are of the same order of magnitude for both formulations.

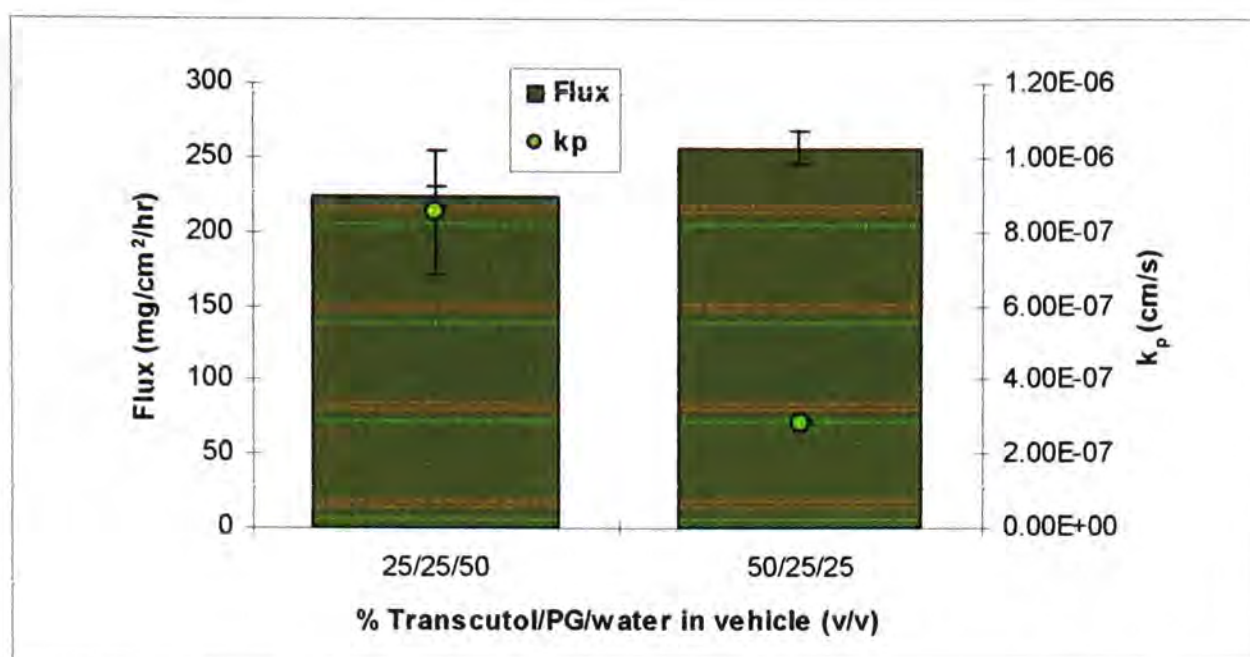


Figure 4.50. Steady state fluxes and k_p values for the permeation of ibuprofen in ternary vehicles containing Transcutol, propylene glycol and water.

Diffusion studies under non-occluded conditions.

In the same way that ethanol, propylene glycol and water formulations were tested under non-occluded conditions, Transcutol, propylene glycol and water formulations were also investigated.

This study provided some unexpected results, in that it was the formulation containing a higher proportion of Transcutol which had the lowest permeation rate. This is the reverse of the result seen for formulations containing ethanol, propylene glycol and water. It is possible that although propylene glycol is a relatively viscous liquid, it is more volatile than Transcutol and so when there is a higher proportion of Transcutol in the formulation it actually prevents the propylene glycol evaporating because of their combined viscosity.

Table 4.19. Steady state fluxes, thermodynamic and kinetic parameters, permeability coefficients for the permeation of ibuprofen from saturated formulations containing Transcutol, propylene glycol and water under non-occluded conditions through silicone membrane (mean \pm SD, n=4).

Vehicle (v/v)	J ($\mu\text{g}/\text{cm}^2/\text{hr}$) \pm SD	CV	K*h \pm SD	D/h ² \pm SD	k _p \pm SD
25/25/50	357.2 \pm 38.52	10.79	2.53 $\times 10^{-3}$ \pm 1.15 $\times 10^{-3}$	5.52 $\times 10^{-4}$ \pm 2.4 $\times 10^{-4}$	1.23 $\times 10^{-6}$ \pm 1.32 $\times 10^{-7}$
50/25/25	224.9 \pm 15.05	6.69	1.40 $\times 10^{-5}$ \pm 2.76 $\times 10^{-5}$	0.12 \pm 0.11	3.93 $\times 10^{-8}$ \pm 3.93 $\times 10^{-9}$

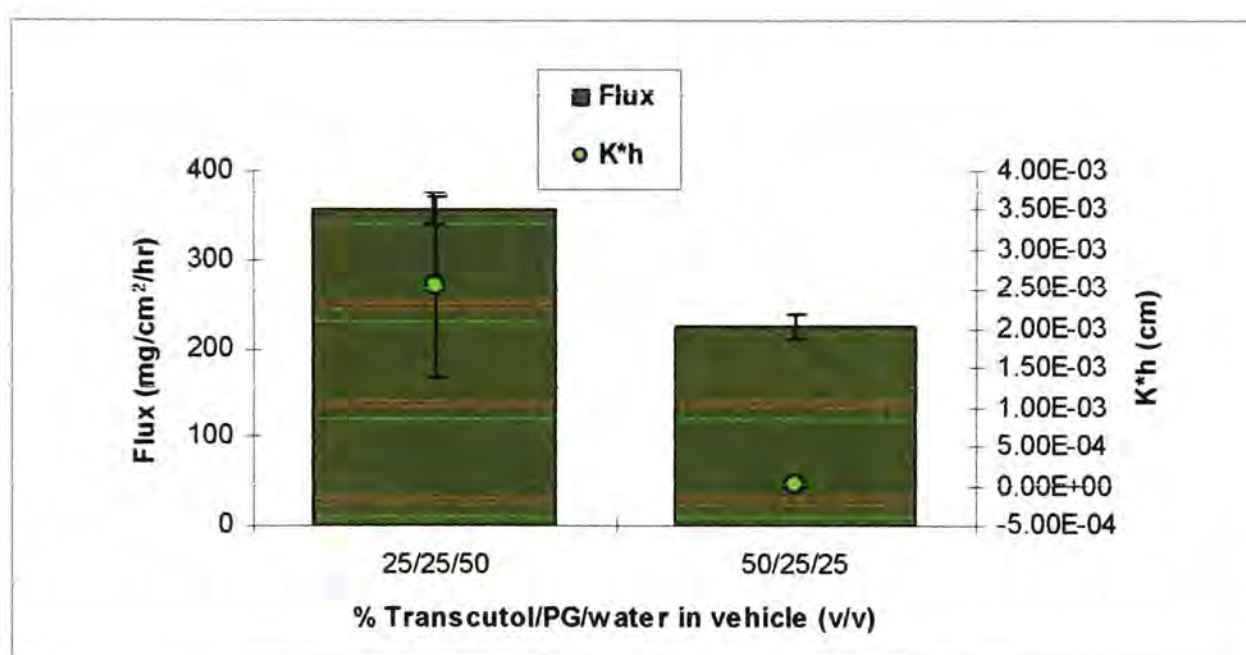


Figure 4.51. Steady state fluxes and K*h values for the permeation of ibuprofen in ternary vehicles containing Transcutol, propylene glycol and water under non-occluded conditions.

There is a significant difference in partition coefficient between the two formulations (-1.19 and -3.46 for 25/25/50 and 50/25/25 respectively, calculated from K*h values). This suggests that for these systems, under non-occluded conditions, there is a strong tendency for the drug to stay in the formulation rather than partition into the skin when there is a higher proportion of Transcutol in the vehicle. This has a profound effect on the

flux, as can be seen from figure 4.51. However, combined with this, the diffusion coefficient is much larger for this system. This, along with the partition effect leads to a reduced flux for this formulation.

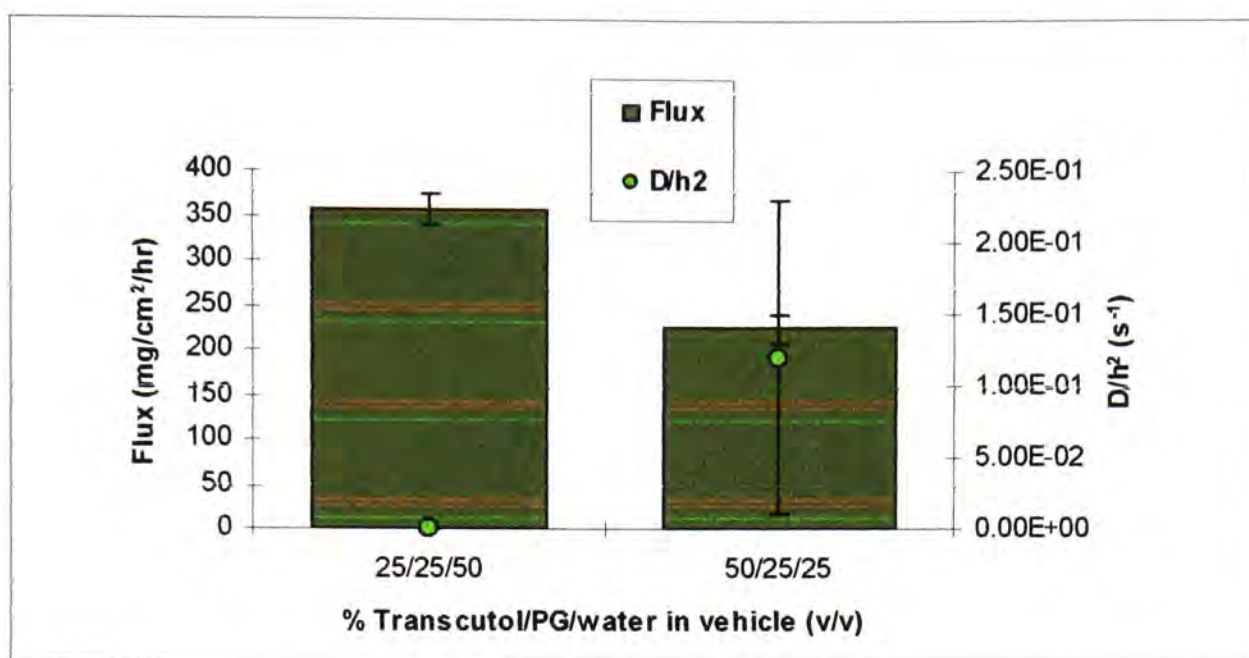


Figure 4.52. Steady state fluxes and D/h^2 values for the permeation of ibuprofen in ternary vehicles containing Transcutol, propylene glycol and water under non-occluded conditions.

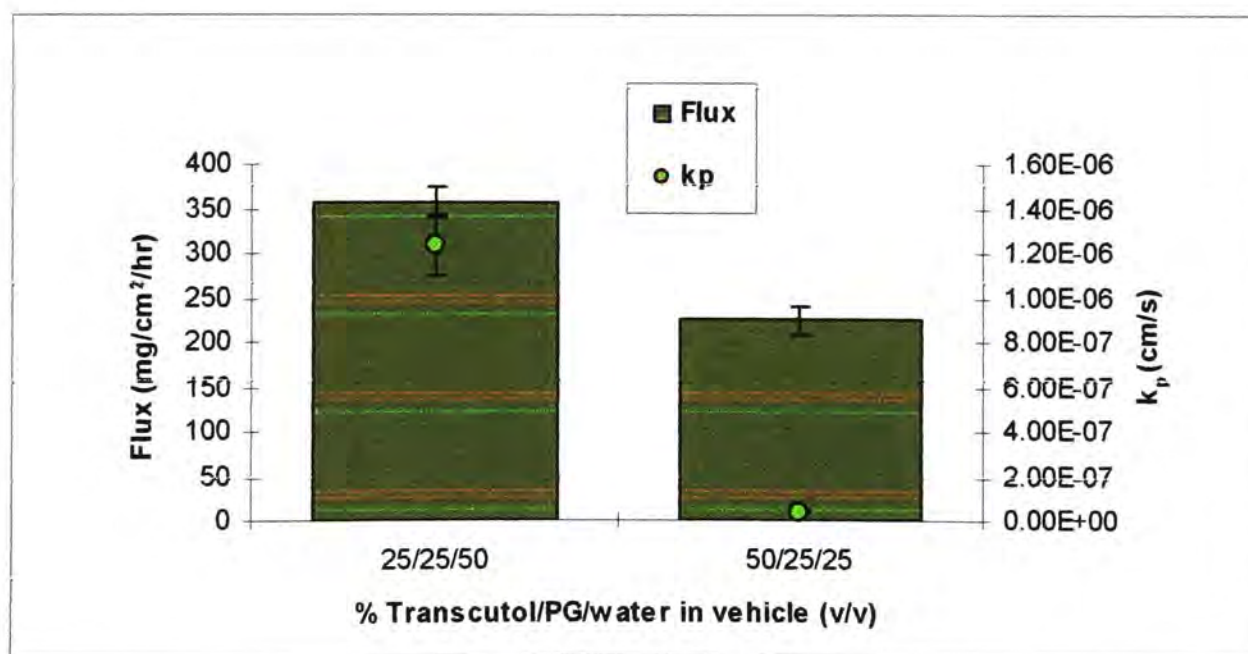


Figure 4.53. Steady state fluxes and $\log(k_p)$ values for the permeation of ibuprofen in ternary vehicles containing Transcutol, propylene glycol and water under non-occluded conditions.

These experiments have demonstrated that it is difficult to predict the outcome of formulation changes. The effects of the component solvents of a formulation are complex, and become even more so when they are combined. Each solvent used adds another degree of complexity to the situation. It is also difficult to design experiments which can take into account all these different effects, without losing sight of the reality of the situation in which a formulation will eventually be used.

Transcutol/propylene glycol/water vehicles - membrane pre-treatment studies

In order to eliminate any possible time-dependent effects that the enhancer could be having upon the membrane, experiments were conducted in which the membrane was soaked in Transcutol for 24 hours before the experiment so that the membrane was entirely saturated.

Table 4.20. Steady state fluxes, thermodynamic and kinetic parameters, permeability coefficients for the permeation of ibuprofen from saturated formulations containing Transcutol, propylene glycol and water through pre-treated silicone membrane (mean \pm SD, n=4).

Vehicle (v/v)	J ($\mu\text{g}/\text{cm}^2/\text{hr}$) \pm SD	CV	K*h \pm SD	D/h ² \pm SD	k _p \pm SD
25/25/50	294.2 \pm 20.66	7.02	2.88 \times 10 ⁻⁶ \pm 4.12 \times 10 ⁻⁷	0.35 \pm 0.04	1.01 \times 10 ⁻⁶ \pm 7.12 \times 10 ⁻⁸
50/25/25	330.7 \pm 34.09	10.31	1.21 \times 10 ⁻⁷ \pm 1.68 \times 10 ⁻⁸	0.28 \pm 0.05	3.36 \times 10 ⁻⁸ \pm 3.73 \times 10 ⁻⁹

Diffusion experiments showed that the flux improved upon using membranes pre-treated with Transcutol. The increase in flux was not significant, and it was the same for both formulations tested. Figure 4.54,

4.55 and 4.56 present K^*h , D/h^2 and k_p values respectively, along with flux values.

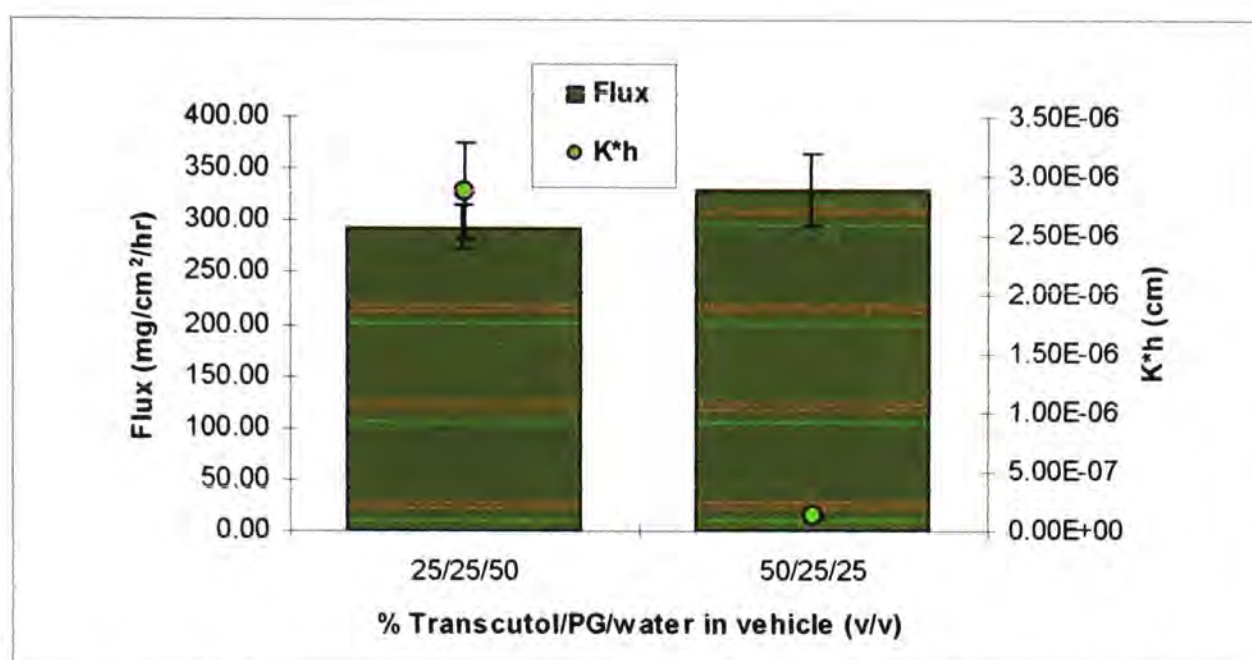


Figure 4.54. Steady state fluxes and K^*h values for the permeation of ibuprofen in ternary vehicles containing Transcutol, propylene glycol and water using silicone membranes pre-treated with Transcutol.

The partition coefficients for the formulations show a similar pattern to those for the corresponding system under non-occluded conditions. These values, calculated from K^*h values, are quite different to those obtained from corresponding formulations under different experimental conditions. It should be noted that the h value ($400\mu\text{m}$) used to calculate the partition coefficient was known as this is the thickness of the silicone membrane used throughout this study.

The diffusion coefficients are altered significantly by pre-treating the membrane with Transcutol, when compared with the values from previous experiments using the same formulations, implying that it is this component of the formulation that enhances flux to the greatest extent. It also demonstrates the idea that it is easier for a drug to move through a

membrane if the membrane is already saturated with solvent. The pre-treatment reduces the time lag that occurs while the Transcutol partitions into the membrane and diffuses through it. If the drug is dependent upon the solvent to be able to permeate, then it follows that the diffusion of solvent will be the rate-limiting step for diffusion of the drug. When this is eliminated the drug diffuses through the silicone membrane at a much faster rate.

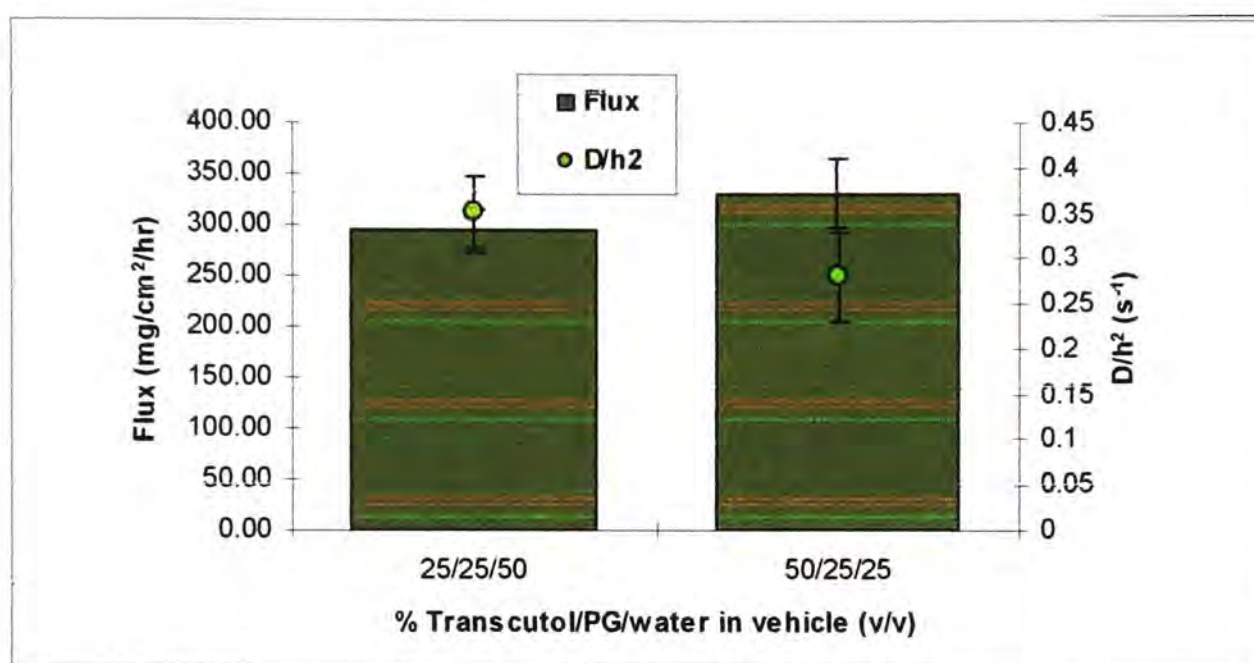


Figure 4.55. Steady state fluxes and D/h^2 values for the permeation of ibuprofen in ternary vehicles containing Transcutol, propylene glycol and water using silicone membranes pre-treated with Transcutol.

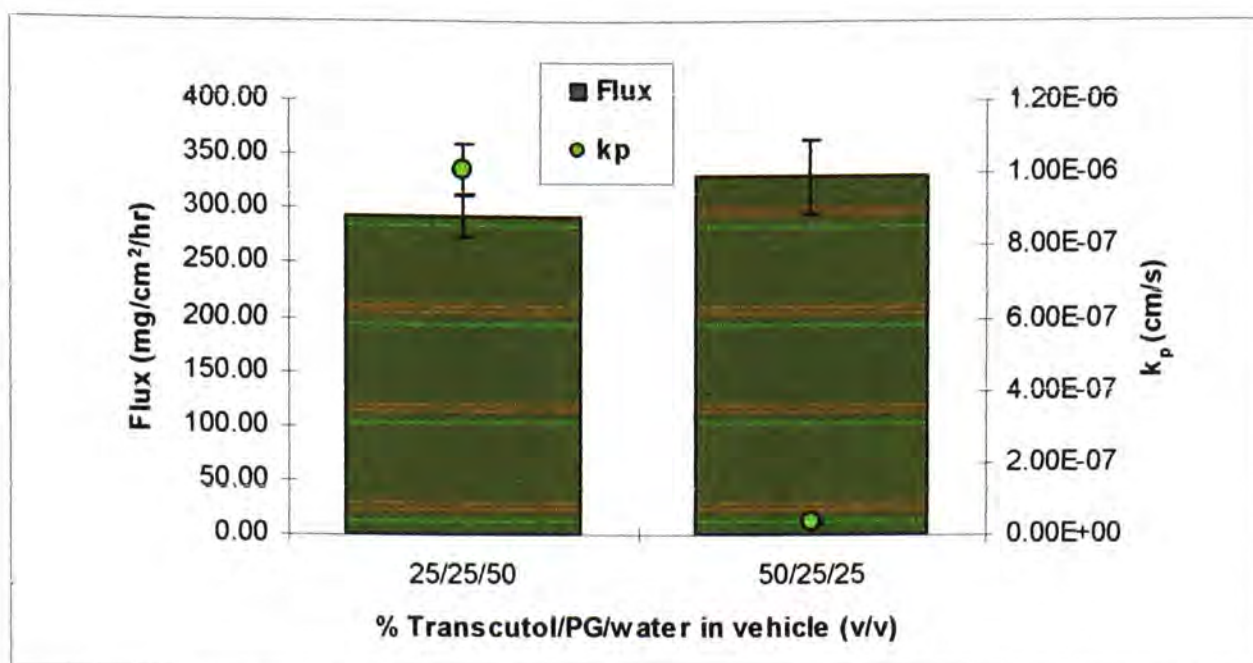


Figure 4.56. Steady state fluxes and k_p values for the permeation of ibuprofen in ternary vehicles containing Transcutol, propylene glycol and using silicone membranes pre-treated with Transcutol.

The permeability coefficients for the two systems reflect the $K \cdot h$ values, suggesting that the alteration of the partitioning process is the dominating factor in permeation. The permeability coefficients obtained from this study are also of the same order of magnitude to those for the other experiments. This implies that although in each case the diffusion and partition effects are different, this does not really have a significant effect upon the flux.

Summary of results for ternary solvent formulations

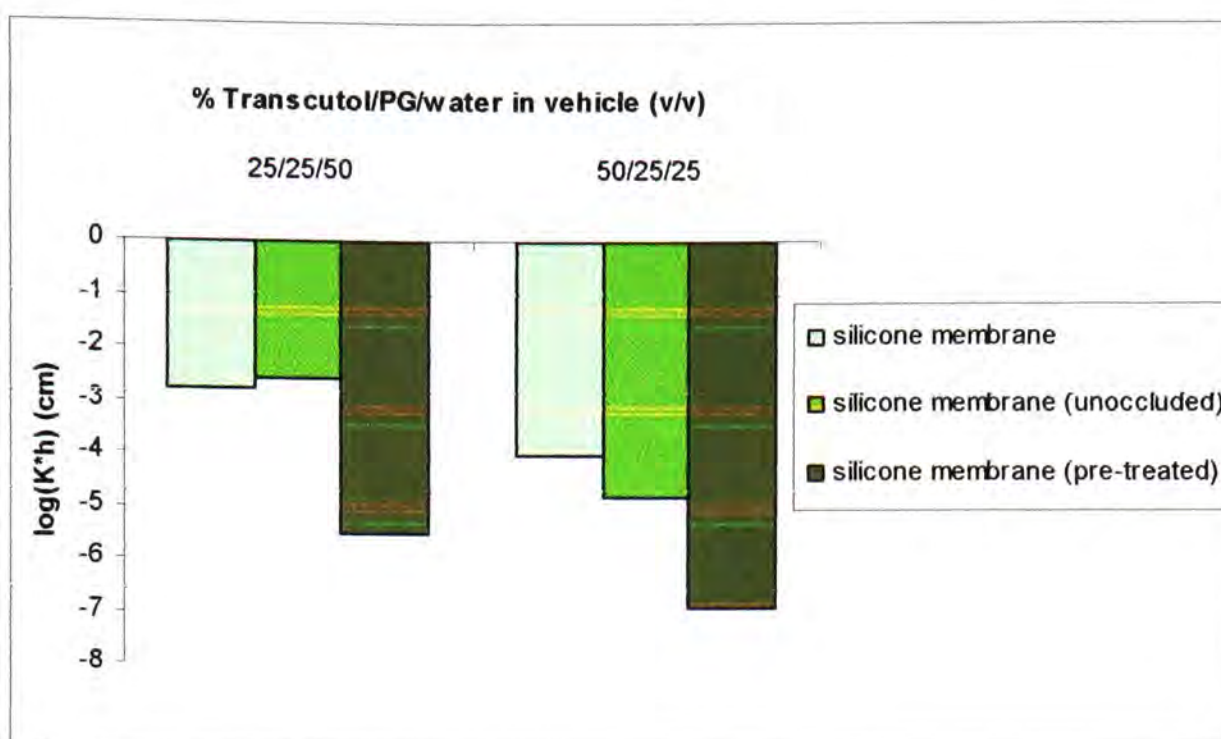


Figure 4.57. Comparison of $\log(K \cdot h)$ values obtained from the fitting of the permeation profiles from saturated ibuprofen formulations containing Transcutol, propylene glycol and water

Figures 4.57 and 4.58 show how the different experimental conditions affected the partition and diffusion parameters for ibuprofen in formulations composed of Transcutol, propylene glycol and water. It was generally found that the partition effect was more dominant in the enhancement of flux than the diffusion effect. However, pre-treatment studies demonstrated that flux could be improved further by charging a membrane with solvent.

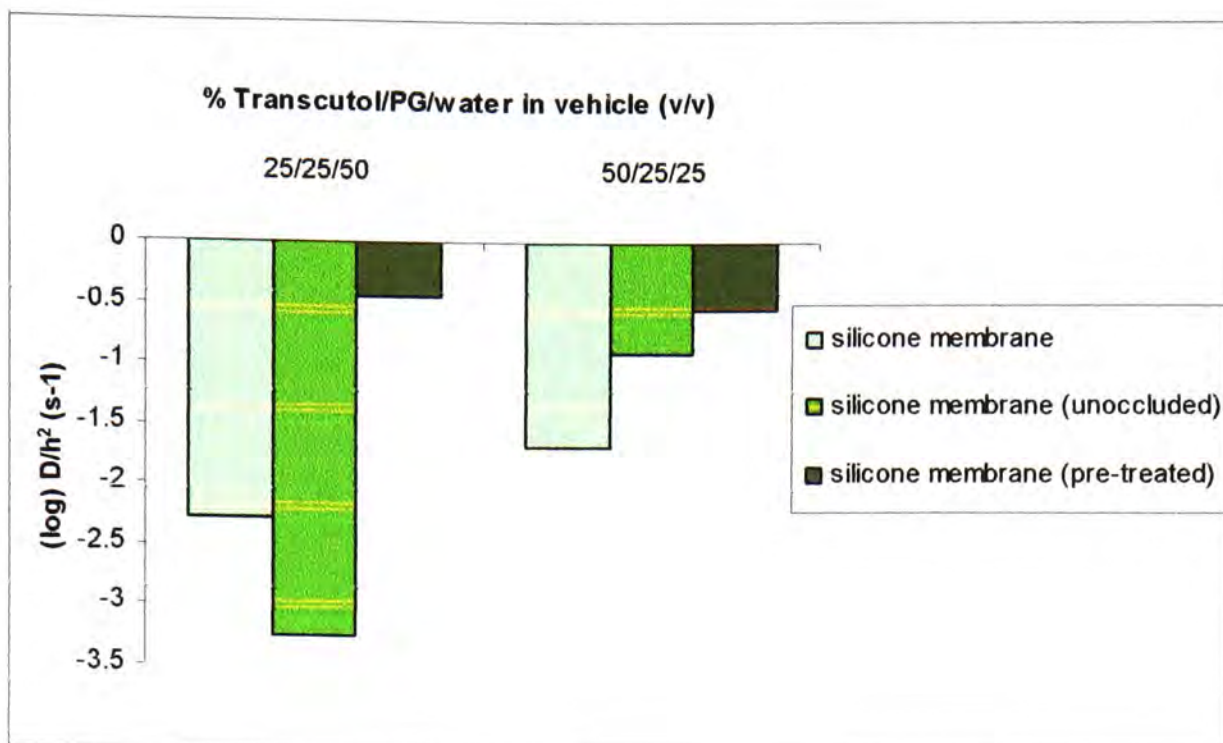


Figure 4.58. Comparison of $\log(D/h^2)$ values obtained from the fitting of the permeation profiles from saturated ibuprofen formulations containing Transcutol, propylene glycol and water

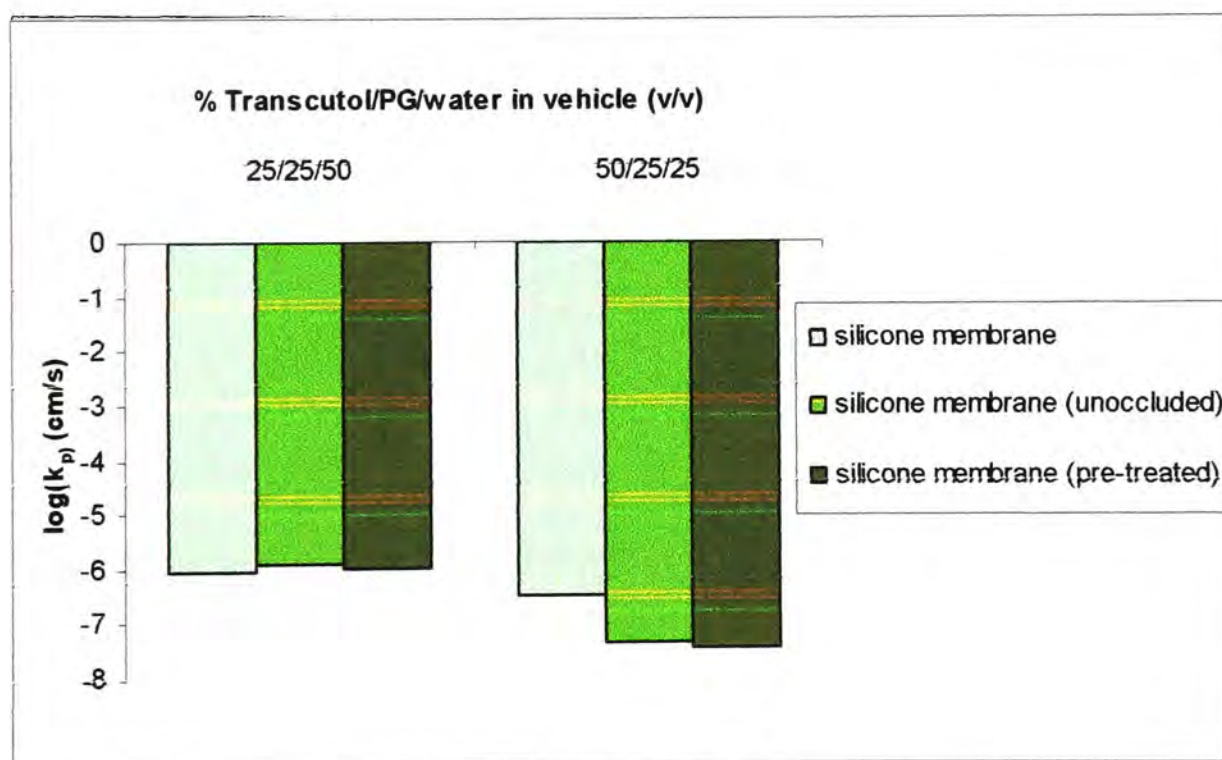


Figure 4.59. Comparison of $\log(k_p)$ values obtained from the fitting of the permeation profiles from saturated ibuprofen formulations containing Transcutol, propylene glycol and water

Figure 4.59 shows the permeability coefficients for all formulations and illustrates that despite differences in both the partition coefficient and the diffusion coefficient, the permeability coefficient does not alter significantly. This is reflected in the flux values, which are similar for most of the formulations.

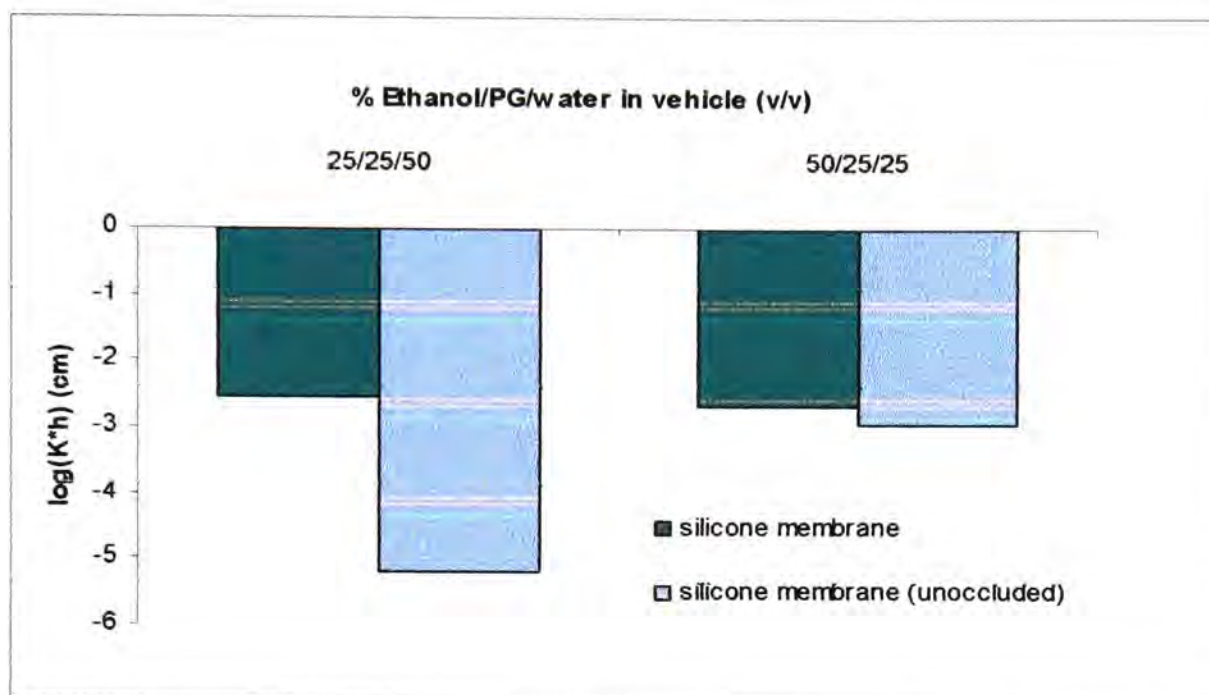


Figure 4.60. Comparison of $\log(K \cdot h)$ values obtained from the fitting of the permeation profiles from saturated ibuprofen formulations containing Transcutol, propylene glycol and water

Figure 4.60 compares the $\log(K \cdot h)$ values for ethanol/propylene glycol and water systems. The partition parameter is dramatically altered for the non-occluded formulation containing 50% ethanol. This could be caused by evaporation of the ethanol leading to the creation of a supersaturated formulation which would drive flux. The $\log(D/h^2)$ values, compared in figure 4.61 reveal why the flux is lower for a formulation containing 25% ethanol. The diffusion parameter is adversely affected under non-occluded conditions. Figure 4.62 compares the k_p values for the two experimental conditions, and it follows that the lowest permeability coefficient is for the 25/25/50 formulation of ethanol/propylene glycol and water.

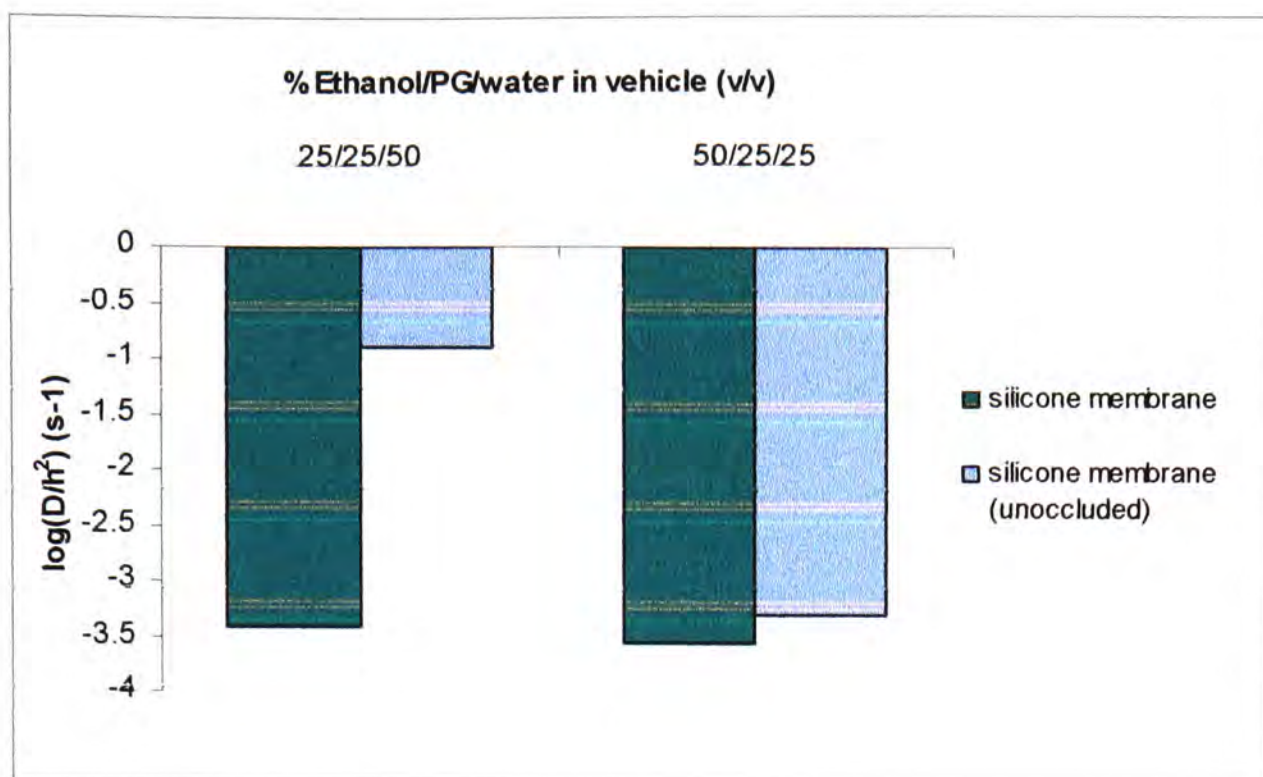


Figure 4.61. Comparison of $\log(D/h^2)$ values obtained from the fitting of the permeation profiles from saturated ibuprofen formulations containing Ethanol, propylene glycol and water

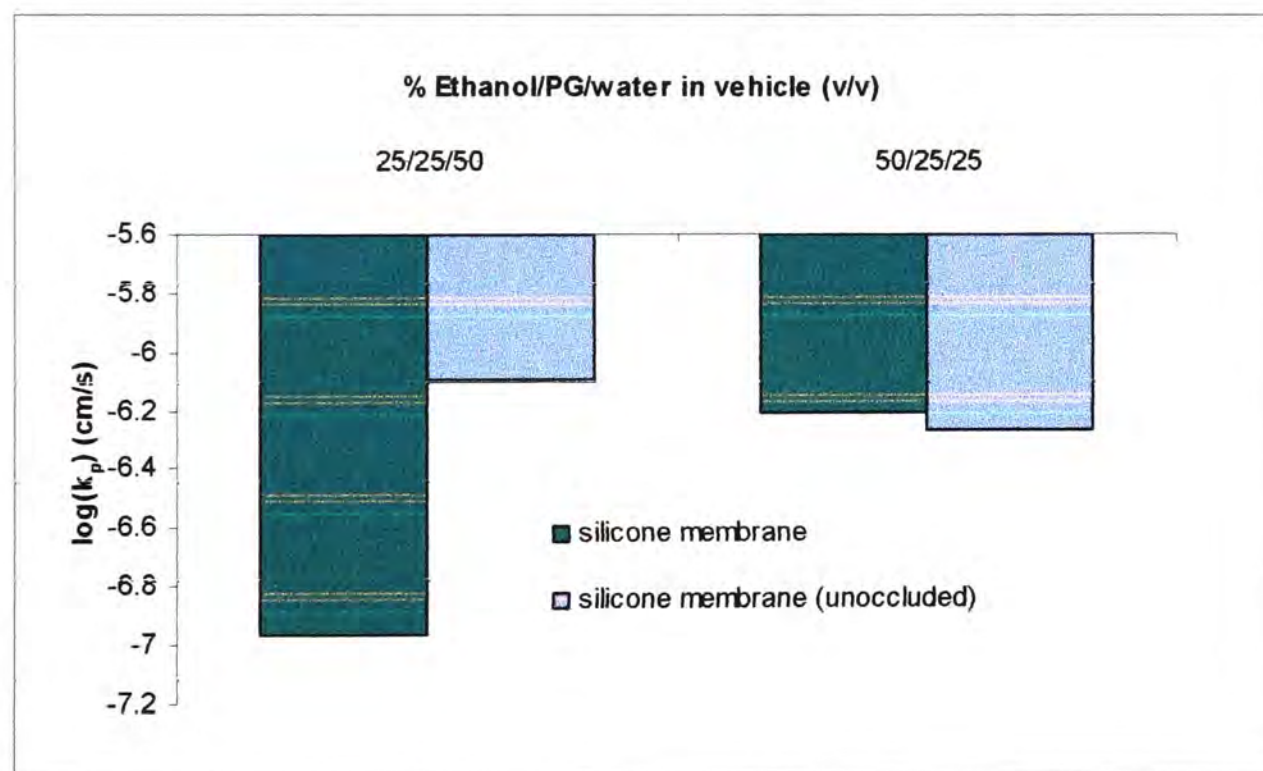


Figure 4.62. Comparison of $\log(k_p)$ values obtained from the fitting of the permeation profiles from saturated ibuprofen formulations containing Transcutol, propylene glycol and water

Comparison of ternary formulations

The results show that in all cases the flux was higher for the formulations containing ethanol compared with those containing Transcutol.

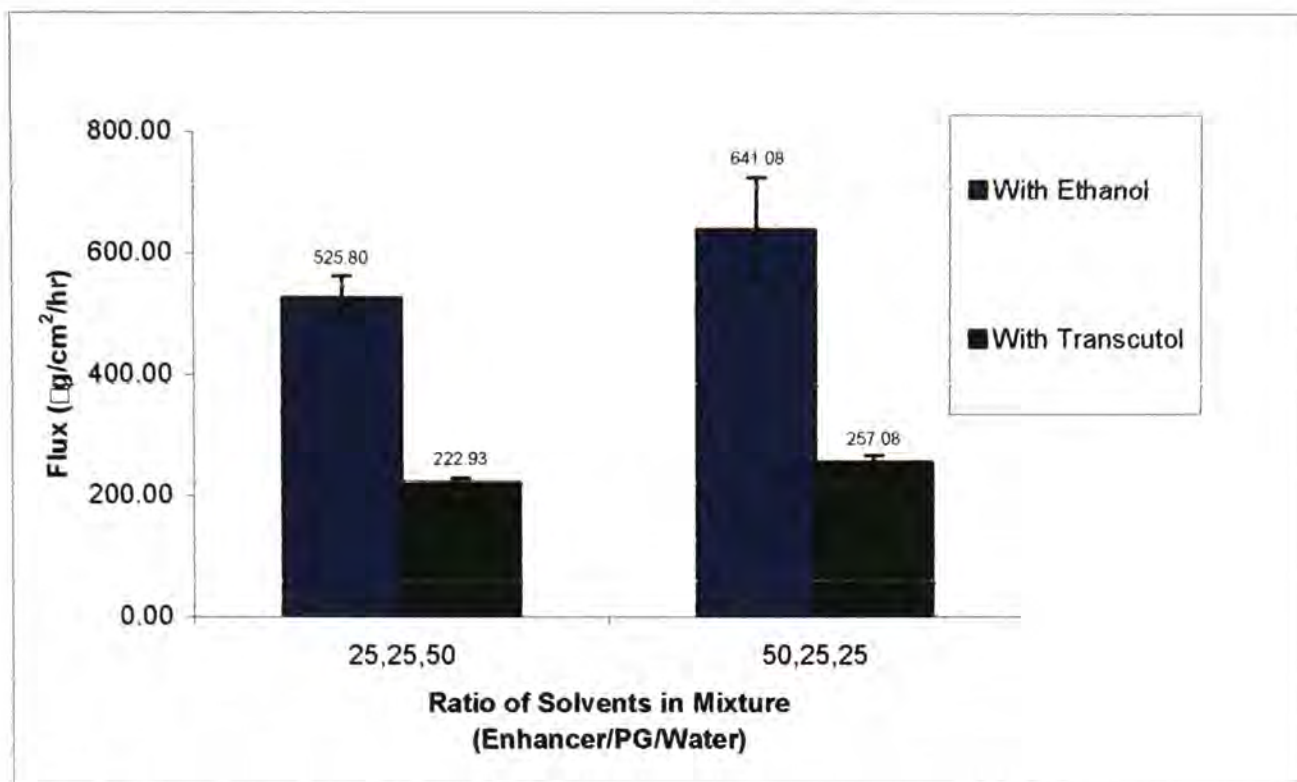


Figure 4.63. Comparison of the steady state flux values for the permeation of ibuprofen from saturated formulations containing Transcutol or ethanol, propylene glycol and water.

Figure 4.63 compares the flux data for the ternary solvent formulations. For both systems, substituting ethanol for Transcutol increases the flux 2.4x. This indicates that ethanol interacts to a greater extent than Transcutol, and in terms of designing a topical vehicle, it would be preferable to use ethanol.

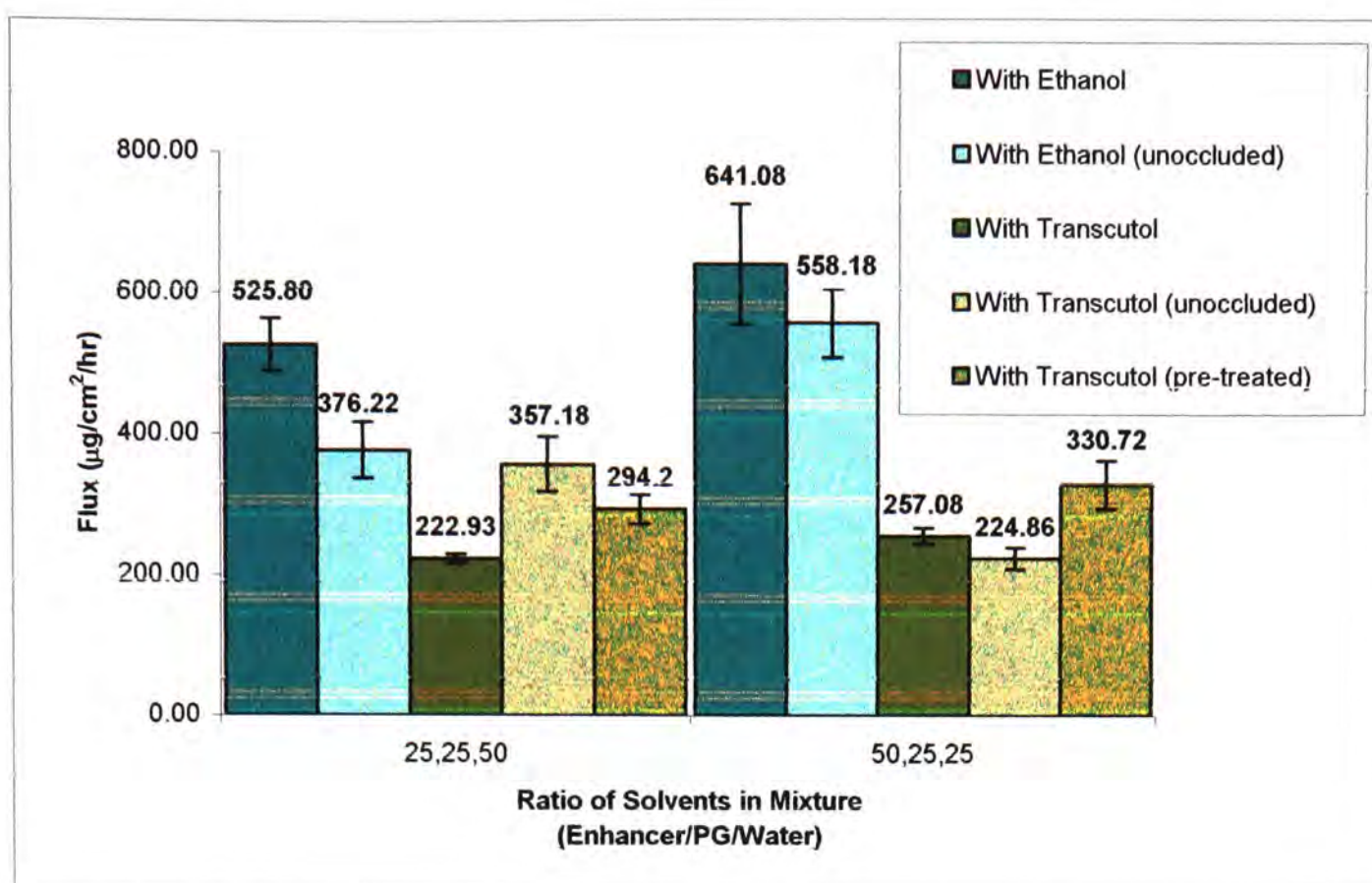


Figure 4.64. Comparison of the steady state flux values for the permeation of ibuprofen from saturated formulations containing Transcutol or ethanol, propylene glycol and water, under various conditions.

Figure 4.64 compares the flux values obtained for all experimental conditions used in this study of ternary formulations. There are no data for the pre-treatment of silicone membrane with ethanol, but based upon the general trends seen in figure 4.61 it would seem likely that pre-treatment would improve permeation to the same extent as Transcutol, perhaps more so. For all experiments the flux was consistently higher for formulations containing ethanol.

4.6. Conclusions

This chapter has demonstrated that the interactions involved in the permeation process are complex, even when simple vehicles are considered. Throughout this chapter an attempt had been made to understand the way in which solvents, drugs and membranes interact with each other to improve or retard flux. This has led us to a point where we have confirmed what was already proposed, that enhancers such as propylene glycol, ethanol and Transcutol work by improving the solubility of the drug within a membrane. Possibly more interesting is the discovery that when used in combination, these effects are not always as straightforward as they seem. Ethanol alone increases the flux of both salicylic acid and ibuprofen to a great extent, yet when used in combination with propylene glycol this effect is muted. The challenge now is to try and elucidate the nature of this interaction between the solvents. Previous studies tend to focus upon the interactions occurring which involve the drug, but what this chapter has shown is that there are many common patterns occurring amongst the formulations used.

The next stage of this thesis is to examine some of these formulations using ATR-FTIR which enables the diffusion profile of each component to be deconvoluted. Although much information can be gleaned from studies of the type described in this chapter, sometimes it is necessary to look at a problem in a different way in order to understand further the system being investigated.

4.7. References

J. E. Harrison, A. C. Watkinson, D. M. Green, J. Hadgraft and K. Brain. The relative effect of azone and transcutol on permeant diffusivity and solubility in human stratum corneum. *Pharm. Res.* **13**, 542-546 (1996).

R. O. Potts and M. L. Francoeur. The influence of stratum corneum morphology on water permeability. *J invest. Dermatol.* **96** (4), 496-499 (1991).

M. S Roberts, S. E. Cross and M. Pellett. Skin transport. In: *Dermatological and transdermal formulations*. Ed. Walters, K. A. Marcel Dekker Inc. New York. pp87-89-195 (2002).

T. Shedlovsky. The behaviour of carboxylic acids in mixed solvents. In: *Electrolytes*. Ed. B. Pesce. Pergamon, New York. pp146-151 (1962).

A. C. Watkinson and K. R. Brain. Mathematical principles in skin permeation. In: *Dermatological and transdermal formulations*. Ed. Walters, K. A. Marcel Dekker Inc. New York. pp61-86 (2002).

- Chapter Five -

Diffusion Studies Through Silicone Membrane:

ATR-FTR Spectroscopy

5.1. Introduction

As described in chapters one and two, Attenuated Total Reflectance Fourier Transform Infra-Red (ATR-FTIR) spectroscopy has found increasing use for the study of skin permeation. Partly this is because of the ease of the technique, but primarily it is because ATR-FTIR can yield considerably more information than traditional permeation experiments. The aim of any permeation experiment is to evaluate the flux of a drug across a membrane and assess whether different vehicles improve or retard permeation. There are many well-known penetration enhancers, but the mechanism by which they act is not easy to determine. Some work by intercalating with skin lipids, disordering them and allowing diffusion of the permeant. Alternatively, the enhancer can act in a solvent capacity, improving the partitioning into the skin and the solubility of the permeant in the skin. It is also possible for both mechanisms to occur simultaneously in which case separation is even more difficult but synergy in the degree of enhancement is seen. This is why ATR-FTIR is now a popular method for deconvoluting enhancement mechanisms. In this Chapter, ATR-FTIR has been used to monitor the diffusion profiles of not only the drug, the solvents into which it is incorporated and the silicone membrane.

5.2. Methods

The methods used in this chapter are described in Chapter Three of this thesis.

5.3. Experimental

Single phase and binary formulations

Salicylic acid

Salicylic acid in ethanol and water

Ibuprofen

Mineral oil

Mineral oil and miglyol formulation

Ethanol

Ternary formulations

Ibuprofen in ethanol, propylene glycol and water formulations

Ibuprofen in Transcutol, propylene glycol and water formulations

5.4. Results

5.4.1. Infrared spectra of the permeants investigated

In order to understand fully the need for reference spectra when using this technique, it is necessary to explain why every molecule has a distinctive set of infrared vibrations. The aim of this section is to present some background to the origin of infrared vibrations, and those vibrations which are seen in the drugs selected for this project.

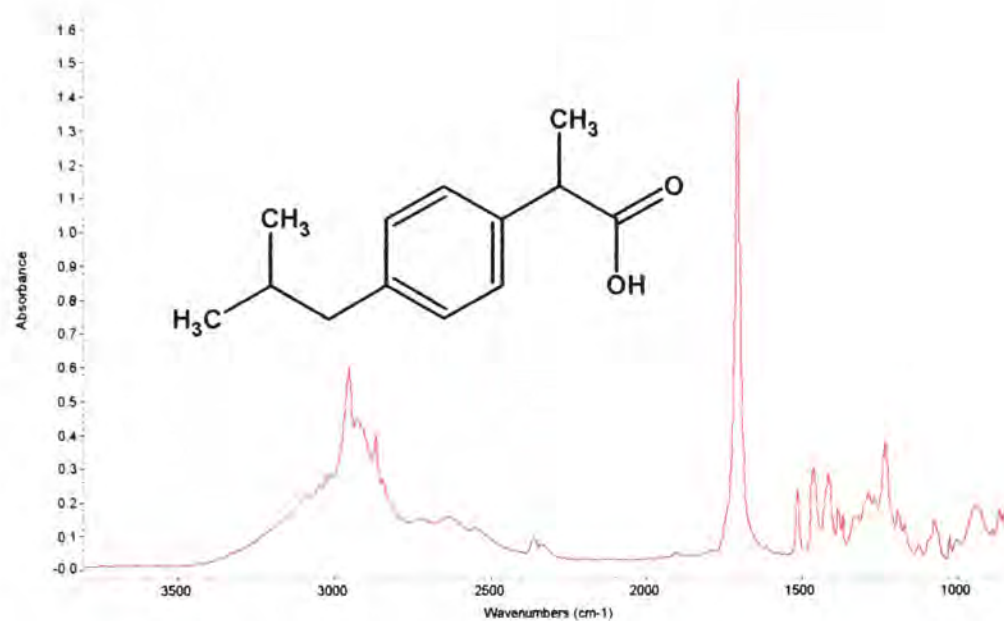


Figure 5.1. Infrared spectrum of ibuprofen.

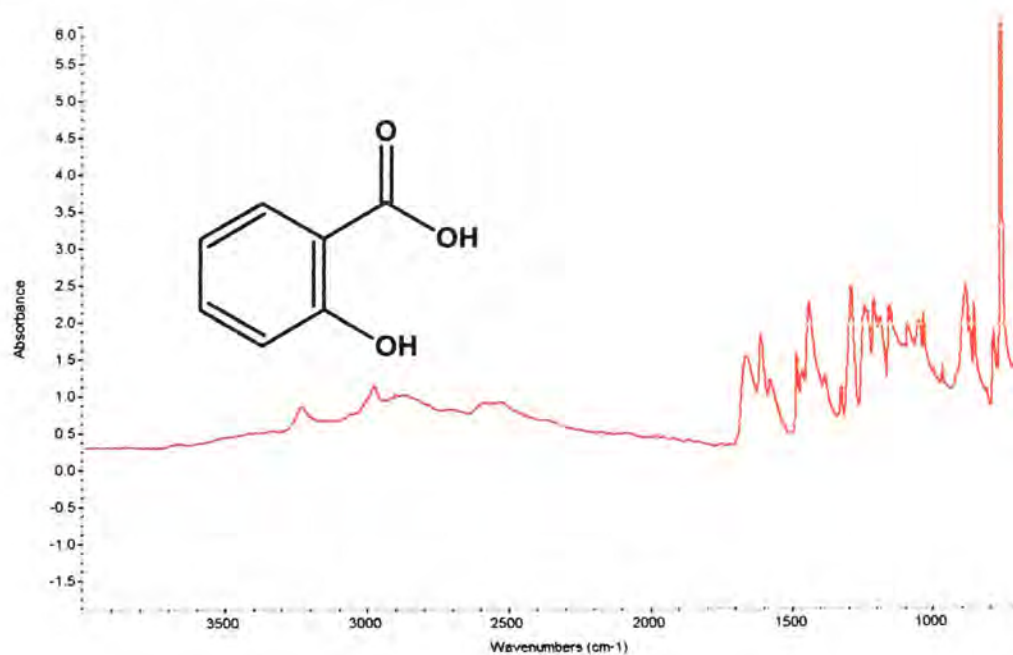


Figure 5.2. Infrared spectrum of salicylic acid.

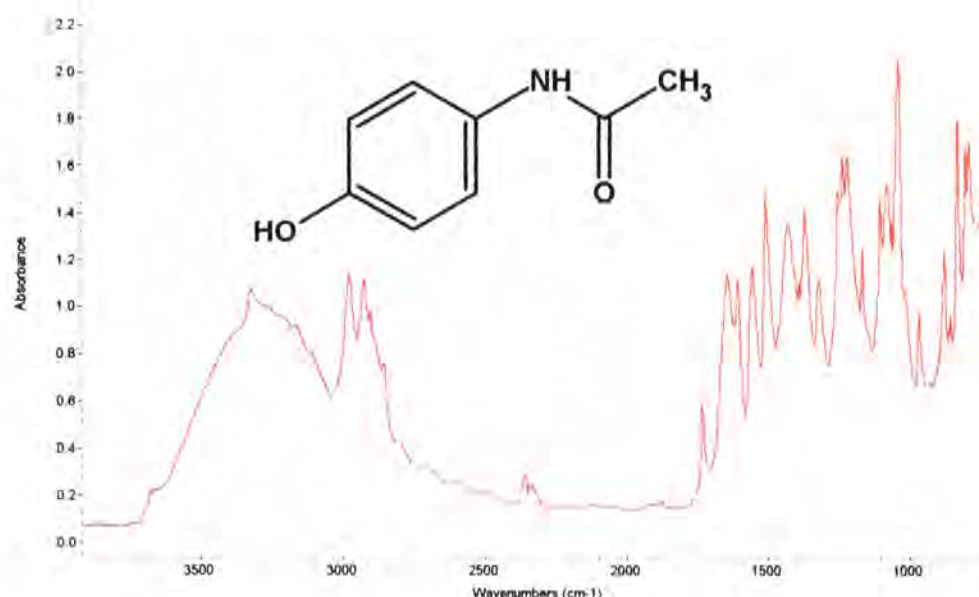


Figure 5.3. Infrared spectrum of acetaminophen.

All of the drugs in this study contain aromatic functionality, therefore a brief background to the types of vibrations that may be seen is presented. Figures 5.1 to 5.3 show the infrared spectra of the permeants along with their structures. For simplicity the vibrational modes of aromatic compounds are usually considered to consist of separate C-H and or ring C=C vibrations. While this works as a first order approximation, in reality "complex" molecular interactions occur resulting in the actual measured spectrum.

The position of aromatic hydrogen atoms on substituted aromatic rings gives rise to a characteristic pattern of out-of-plane deformation vibrations in the region between 2000 and 1700 cm⁻¹ as shown in figures 5.4 and 5.5.

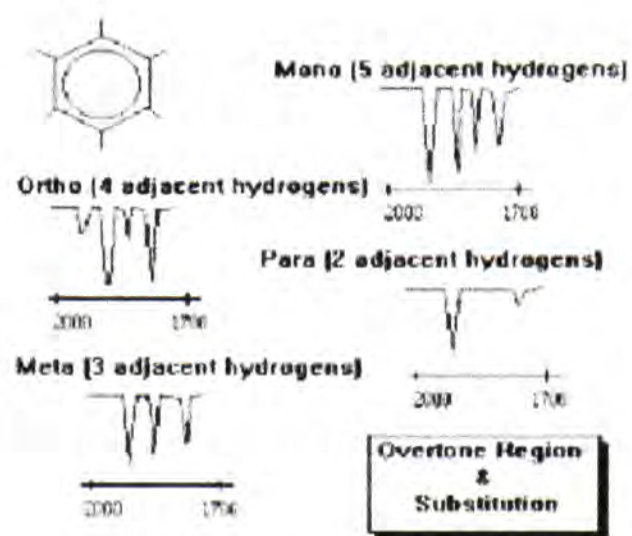


Figure 5.4. Out of plane deformations of substituted aromatic rings.

These bands are weak and may be interfered with by olefin and carbon-oxygen double bonds.

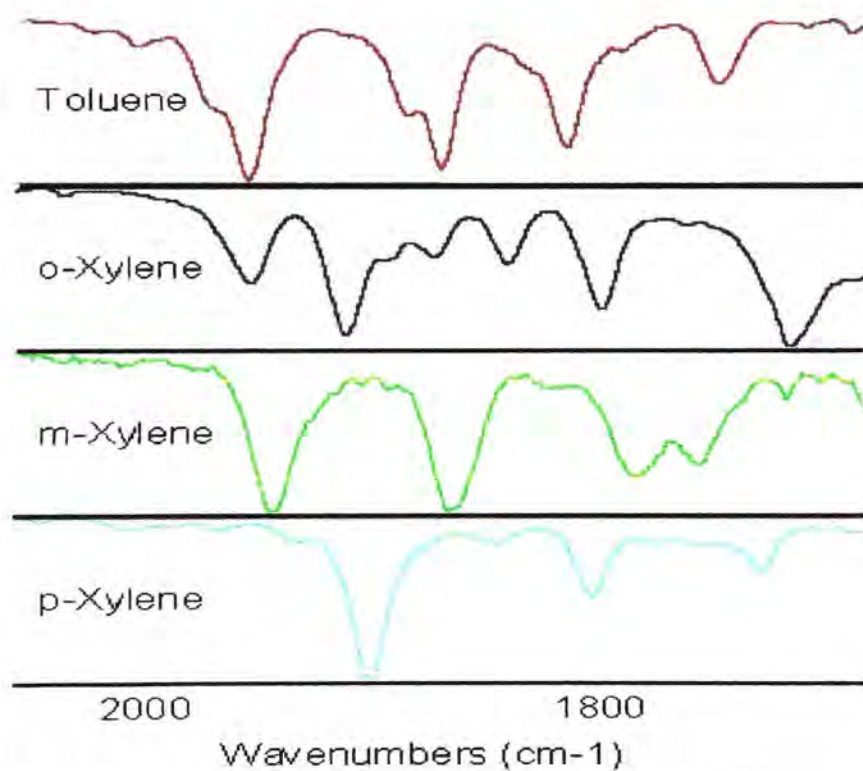


Figure 5.5. Examples of the characteristic out-of plane deformation absorption bands of substituted xylenes.

Both ibuprofen and salicylic acid contain carboxylic acid groups (see figures 5.1 and 5.2), which affect their permeation behaviour. This functionality makes them very good candidates for ATR-FTIR experiments because they have distinctive absorption bands. Carboxylic acids normally exist in a

dimeric form in non-polar environments, with very strong hydrogen bonds between the carbonyl and hydroxyl groups. This association results in the very broad, unusual -OH stretching absorption which occurs from about 3100 to 2200 cm^{-1} . A number of other absorptions are also very indicative of the acid group, particularly the C=O stretching absorption at $\sim 1700\text{cm}^{-1}$

The CH_3 asymmetric stretching vibration occurs at 2975-2950 cm^{-1} while the CH_2 absorption occurs at about 2930 cm^{-1} . The symmetric CH_3 vibration occurs at 2885-2865 cm^{-1} while the CH_2 absorption occurs at about 2870-2840 cm^{-1} . The CH_3 asymmetric deformation vibration occurs at 1470-1440 cm^{-1} . This band is overlapped with the CH_2 scissor vibration, which occurs at 1490-1440 cm^{-1} . The symmetric CH_3 vibration occurs at 1390-1370 cm^{-1} . The relative intensities of the asymmetric CH_3 and the CH_2 scissor bands can be used as an indicator of their proportions in the molecule. When there is more than one methyl group on a single carbon the symmetric CH_3 vibration which occurs at 1390-1370 cm^{-1} becomes split into two bands. When three methyl groups are on a single carbon (t-butyl) a band appears near 1365 cm^{-1} and a weaker band appears near 1390 cm^{-1} . When two methyl groups are on a single carbon (isopropyl) bands of approximately equal intensity occur at near 1390 and 1365 cm^{-1} . The presence of the t-butyl group can be confirmed by the presence of bands around 1255 and 1210 cm^{-1} while the isopropyl group shows bands near 1170 and 1145 cm^{-1} .

5.4.2. Infrared spectra of solvents

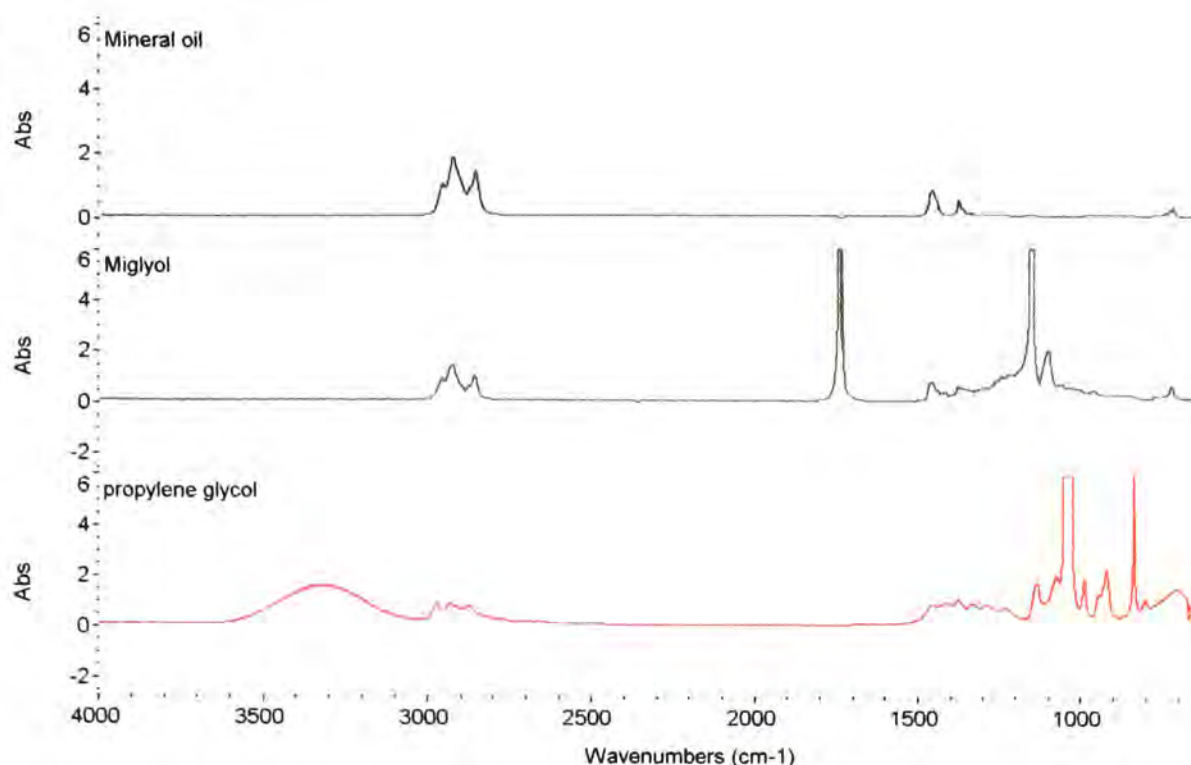


Figure 5.6. Infrared spectra of mineral oil, miglyol and propylene glycol.

From figure 5.6 it can be seen that particularly for miglyol, there is a characteristic absorbance, which can be monitored spectroscopically. These characteristic bands will also be the basis of identification using reference spectra. By comparing the extracted spectral profiles with those of all the components, it should be possible to identify each component of the system, and gain information regarding the mechanism of action.

5.4.3. Results of ATR-FTIR diffusion experiments

5.4.3.1. Salicylic acid

In the first instance experiments were conducted in which only the solvent and the drug were monitored. The results are presented in figures 5.8 to 5.10. Figure 5.8 shows how the raw data appears, along with spectral profiles extracted using the InSight. In this experiment 4 separate profiles have been identified based upon the reference spectra of the components of the system, i.e. salicylic acid, ethanol and water.

Ethanol/water

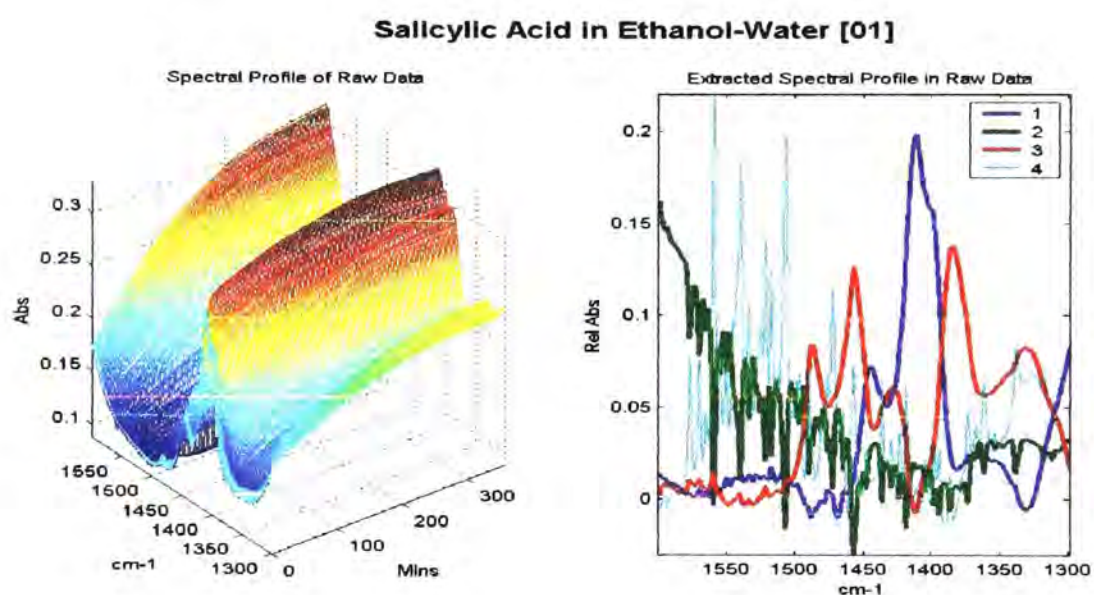


Figure 5.7. Raw data (left) and extracted spectral profiles found in raw data (right).

The complex nature of the raw data can be clearly seen in figure 5.7, and it is virtually impossible to determine how the different components contribute to the diffusion process from this type of data because many components overlap. Figure 5.8 presents the evolution profiles and cumulative evolution profiles extracted from the raw data. The legends in figure 5.9 are merely to show how many components have been identified.

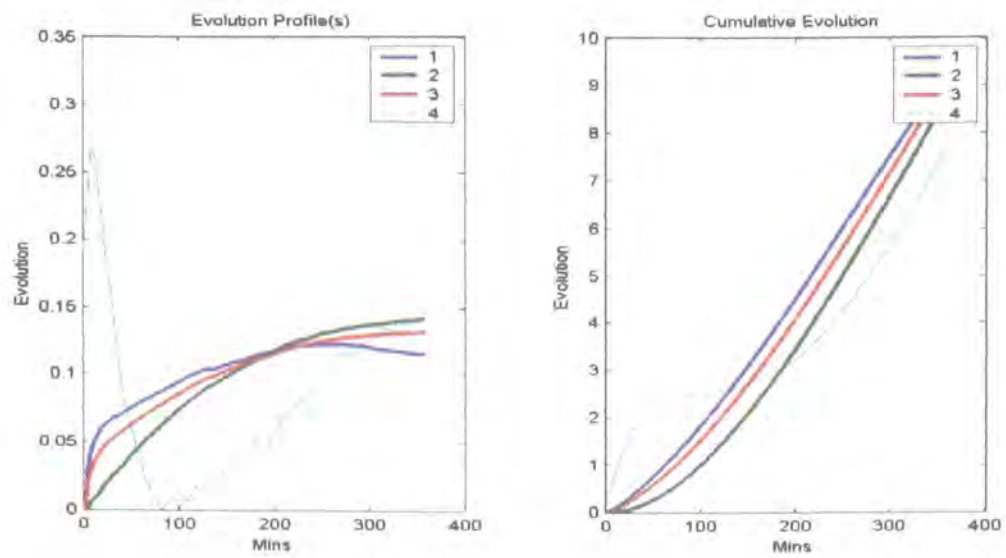
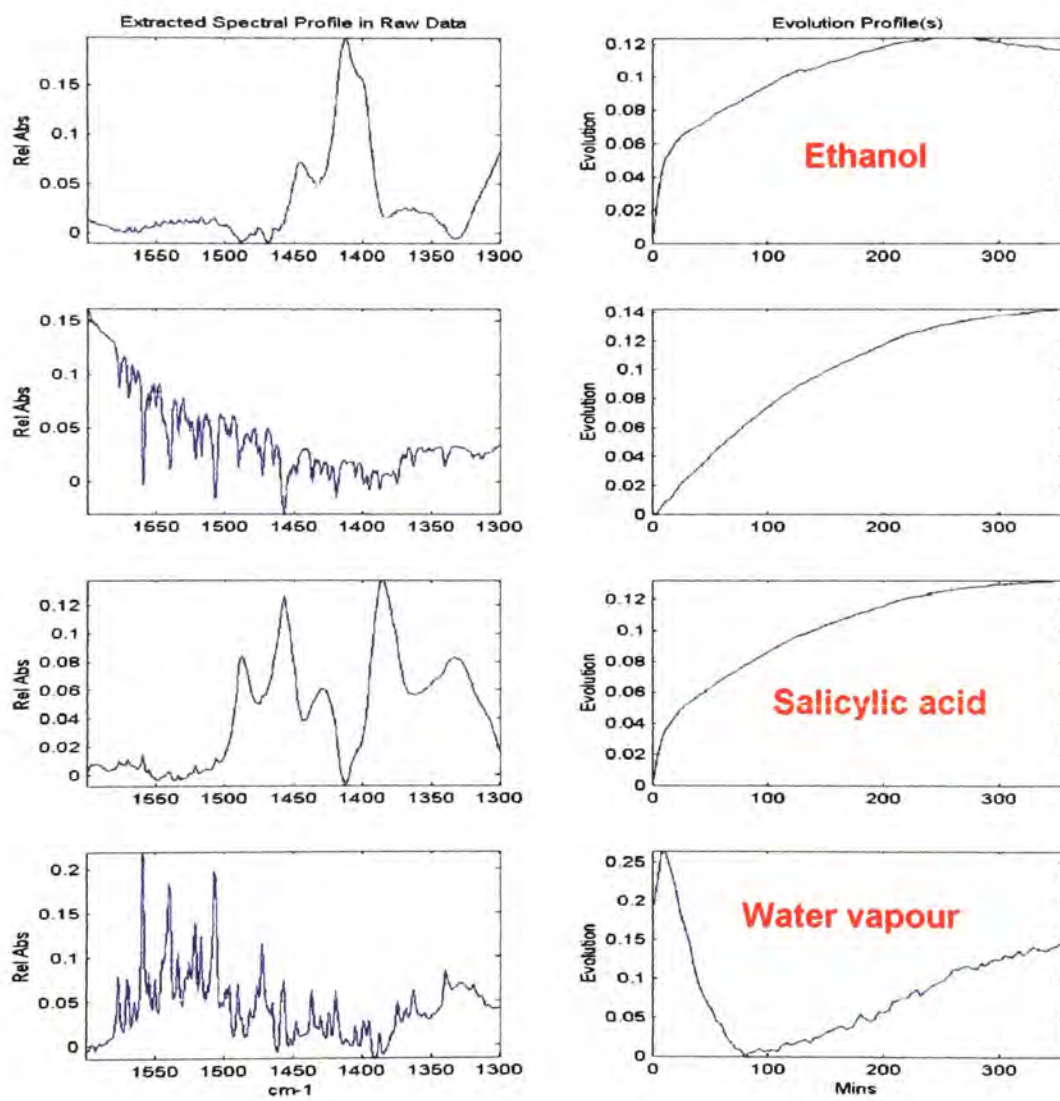


Figure 5.8. Evolution profiles for salicylic acid in an ethanol/water formulation.



5.9. Extracted spectral profiles and cumulative evolution plots for salicylic acid in an ethanol and water formulation.

The first attempt to use this technique was carried out 'blind' in that no references spectra were entered into the InSight program. The analysis was carried out in this way to prevent bias. The extracted profiles, along with the evolution profiles of the four components identified are shown in figure 5.10. Three of the four components were identified from reference spectra of the single solvents and the drug.

Ethanol water (repeat)

The same procedure was repeated to ensure reproducibility and the results are shown in figures 5.10 to 5.12. As for the result presented above, the legends in the figures indicate how many components were identified.

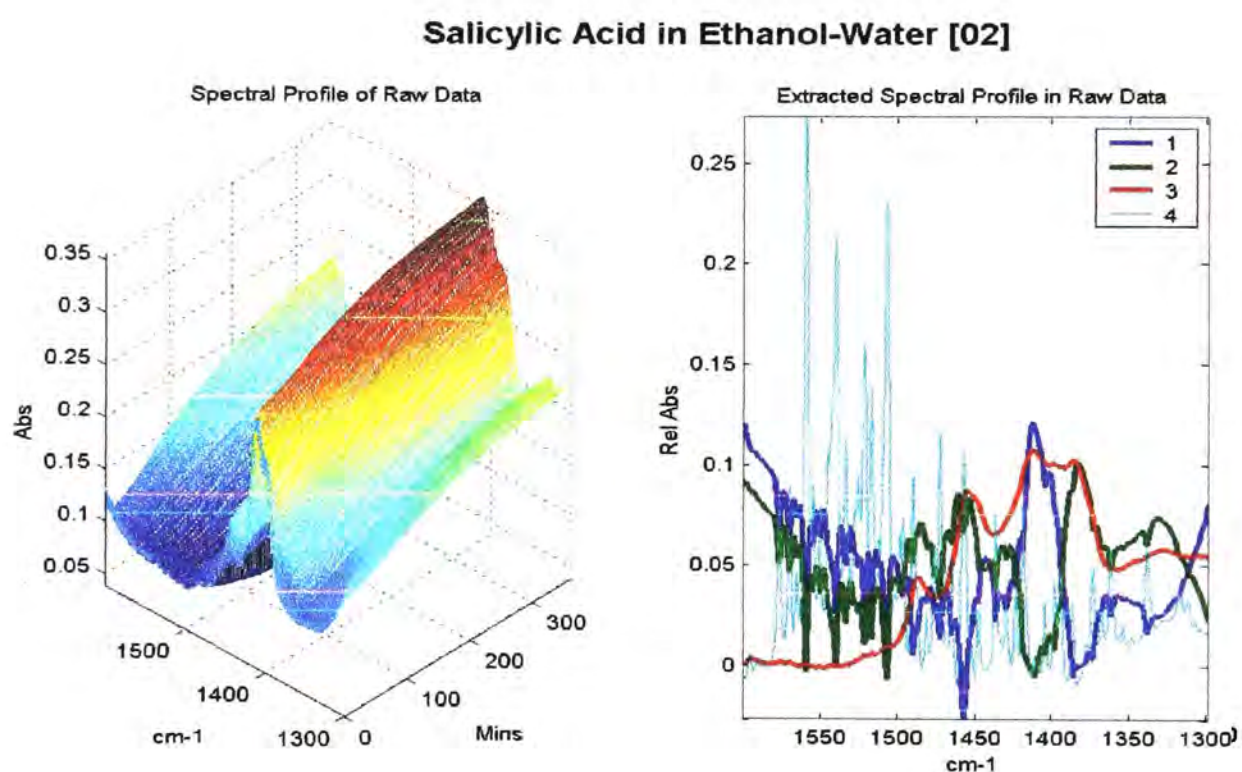


Figure 5.10. Raw data (left) and extracted spectral profiles found in raw data (right).

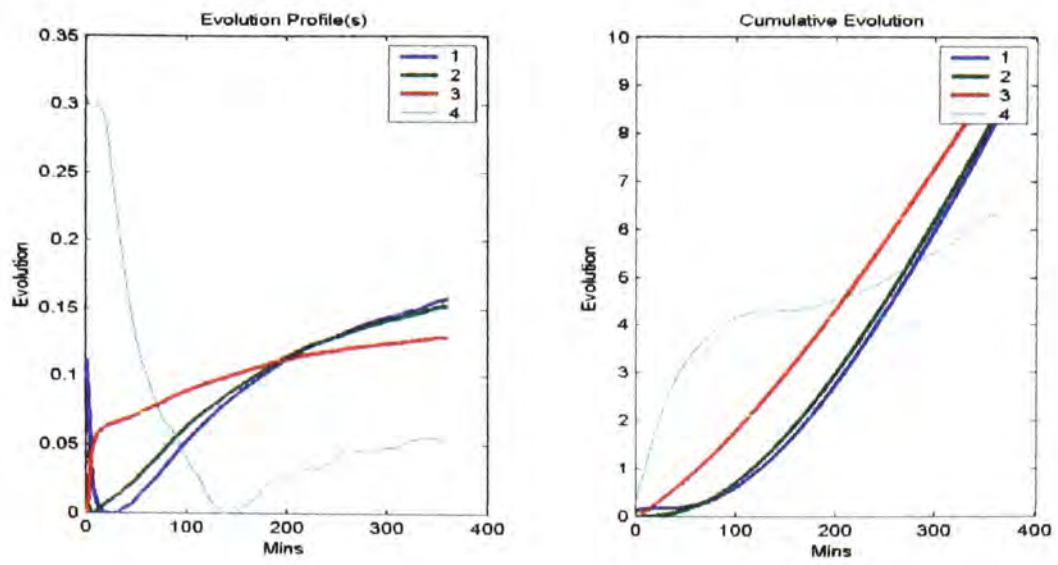


Figure 5.11. Evolution profiles and cumulative evolution of salicylic acid in an ethanol and water formulation.

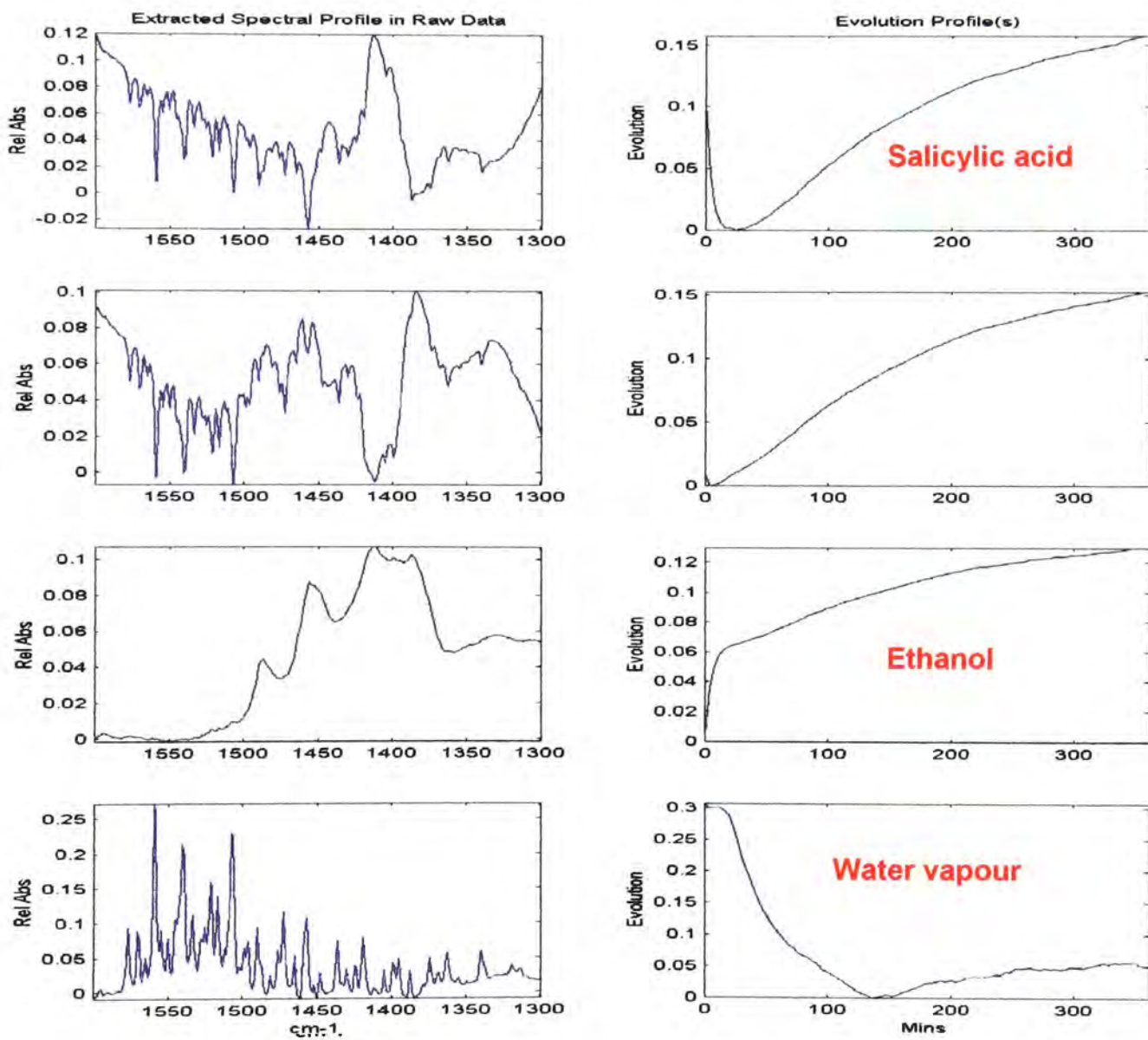


Figure 5.12. Extracted spectral profiles and cumulative evolution plots for salicylic acid in an ethanol and water formulation.

The only difference evident in the data is a change in the shape of the profile for salicylic acid, with a sharp drop in the first stages of permeation. It is not clear what has caused this, and it could be the result of poor contact between the membrane and the crystal which is resolved by the appearance of solvent at the membrane-crystal interface. The two events do correlate, and this seems the most likely explanation.

5.4.3.2. Ibuprofen

For the next series of experiments ibuprofen was used as a model drug. The predominant reason for this choice is that ibuprofen has a strong carbonyl stretching band at $\sim 1700\text{cm}^{-1}$. This distinctive band affords the easy identification of the drug.

Mineral oil

Mineral oil was selected as the solvent for this experiment to determine whether a solvent with relatively few absorbances in the infrared could be successfully identified. An added complication is the overlapping absorbances of the drug and solvent at $\sim 3000\text{cm}^{-1}$. Figures 5.13 and 5.14 present the results of this experiment. The legends denote how many profiles have been extracted.

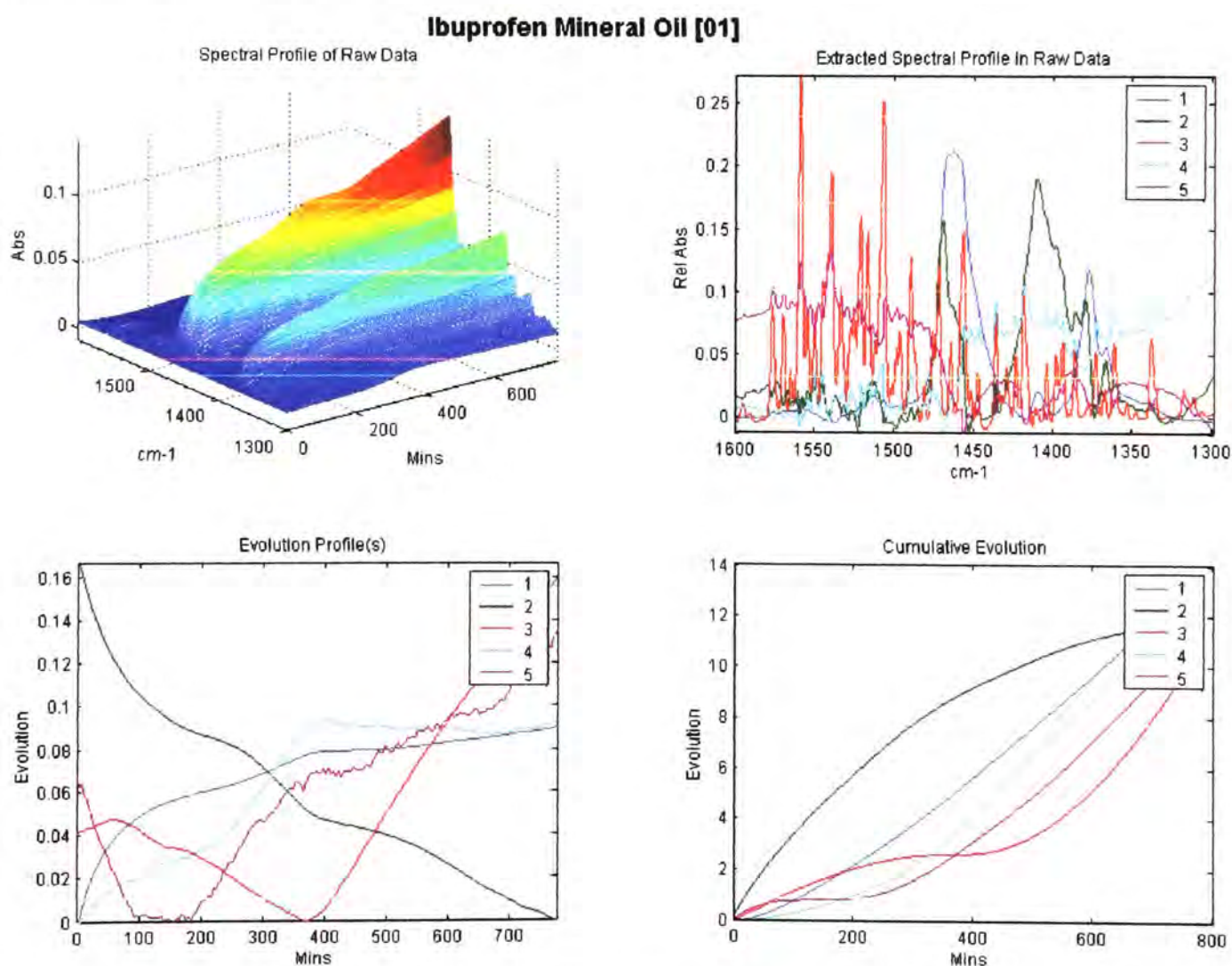


Figure 5.13. Raw data, extracted spectral profiles and cumulative evolution plots for ibuprofen in mineral oil.

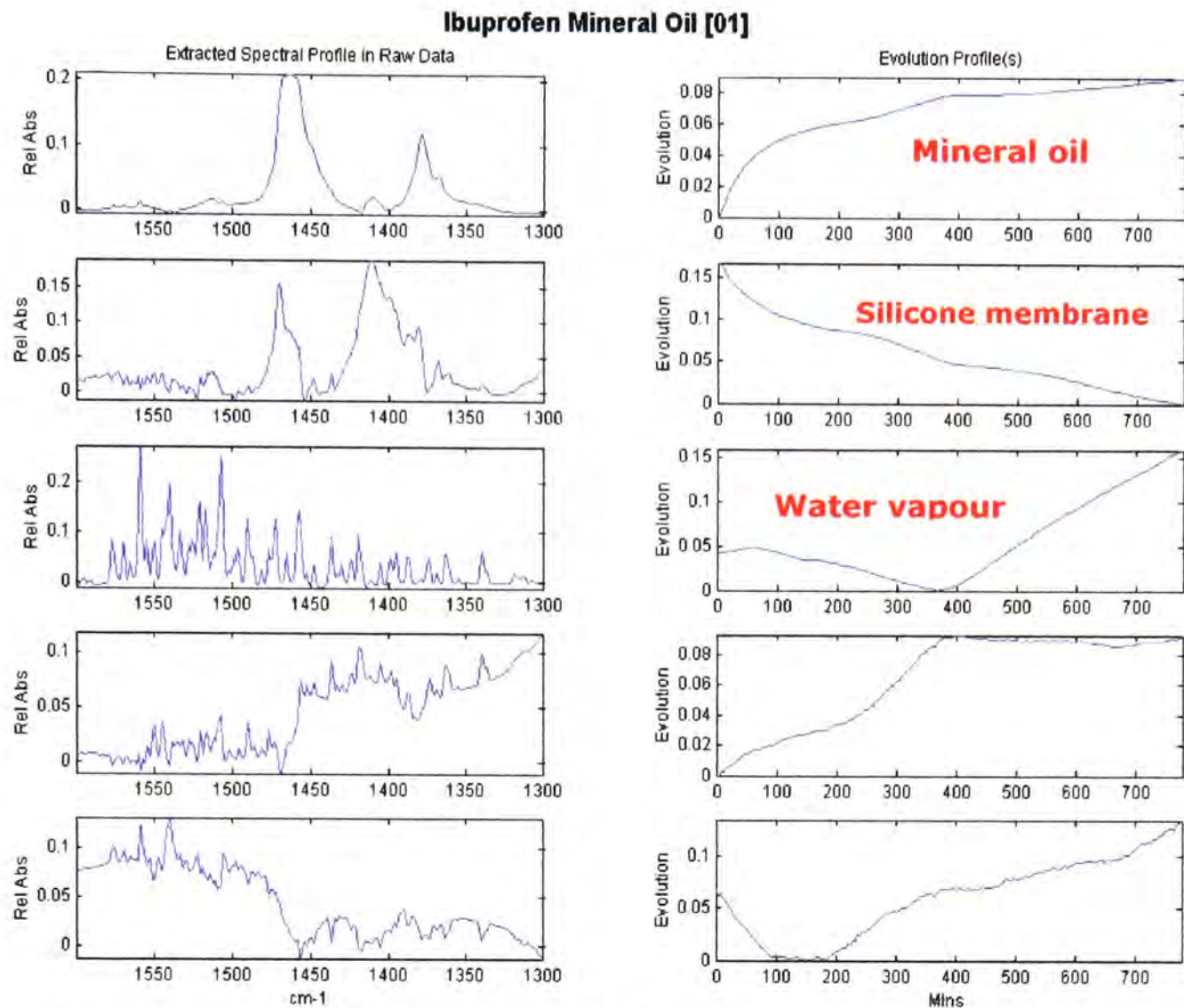


Figure 5.14. Extracted spectral profiles and cumulative evolution plots for ibuprofen in mineral oil.

Figure 5.14 shows the five profiles produced by the software from the raw data. Three of these are easy to assign to components of the system, based upon reference spectra of the single components and these have been labelled accordingly. As for the experiments using salicylic acid in an ethanol vehicle, it seems that the solvent appears at the membrane-crystal interface at a faster rate than the drug. The evolution profile of the drug suggests that the amount of drug at the interface decreases, which is something of a mystery, and at odds with the data from previous experiments.

Mineral oil and miglyol

Following deconvolution of single phase systems it seemed a natural progression to investigate binary combinations. Using a combination of solvents would test the ability of the software to deconvolve overlapping or complex spectral profiles. Miglyol, like ibuprofen shows a strong carbonyl stretching absorption at 1700cm^{-1} . In the analysis for this experiment, reference spectra were 'loaded' into the software, and profiles were extracted based upon their likeness to these references. This would rule out any human errors of judgement or bias in comparing the extracted profiles and the references. Only those profiles which were a 98% - 100% match to the references would be extracted from the raw data. The legends in figure 5.15 indicate the number of extracted profiles.

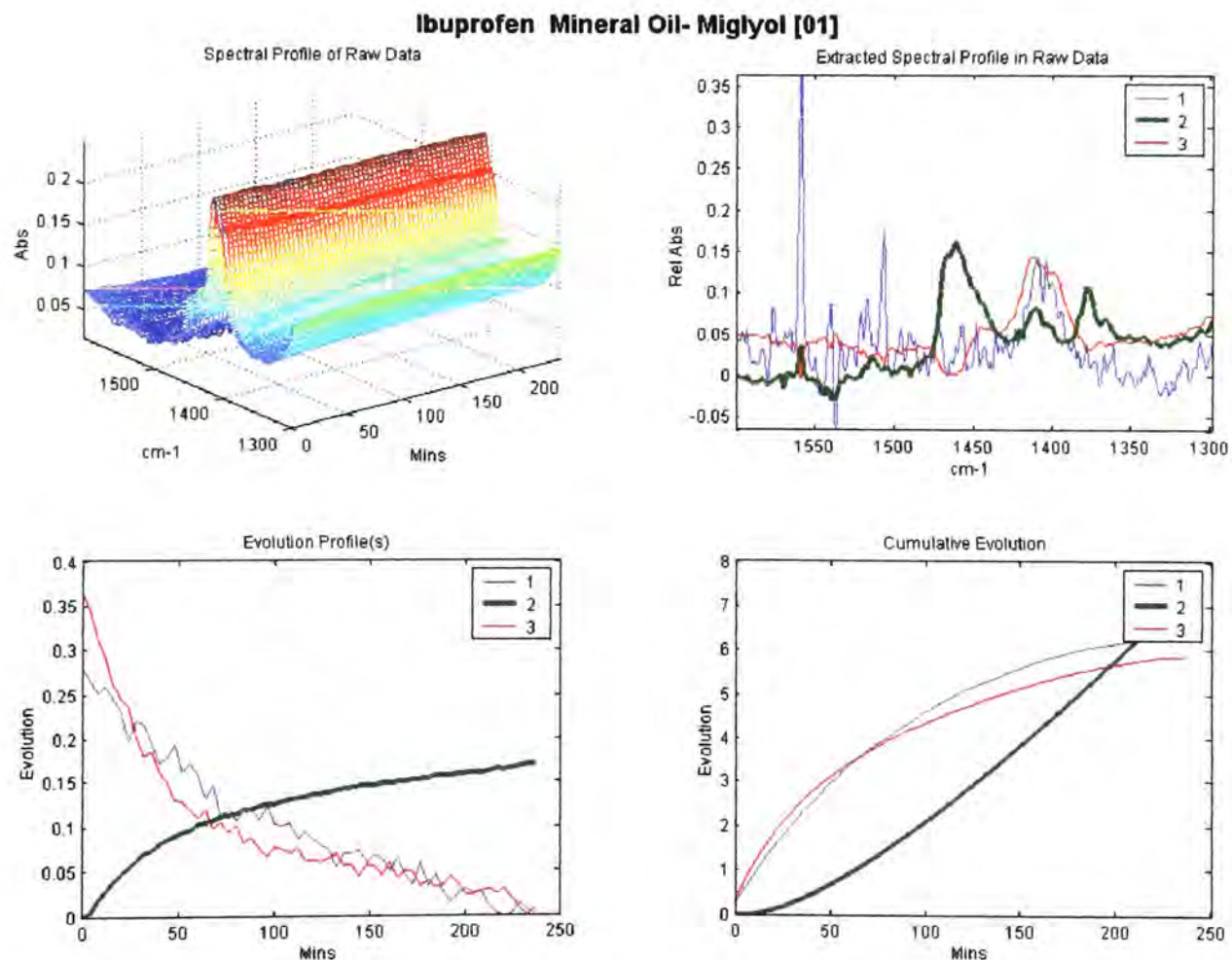


Figure 5.15. Raw data, extracted spectral profiles and cumulative evolution plots for ibuprofen in a mineral oil and miglyol formulation.

This approach to the analysis appeared to work considerably better than making a judgement 'by eye'. In the first instance, the 1300-1600 cm^{-1} region of the raw data was evaluated. This did provide useful information, but the software had difficulty in detecting the presence of the drug, so a further analysis was conducted.

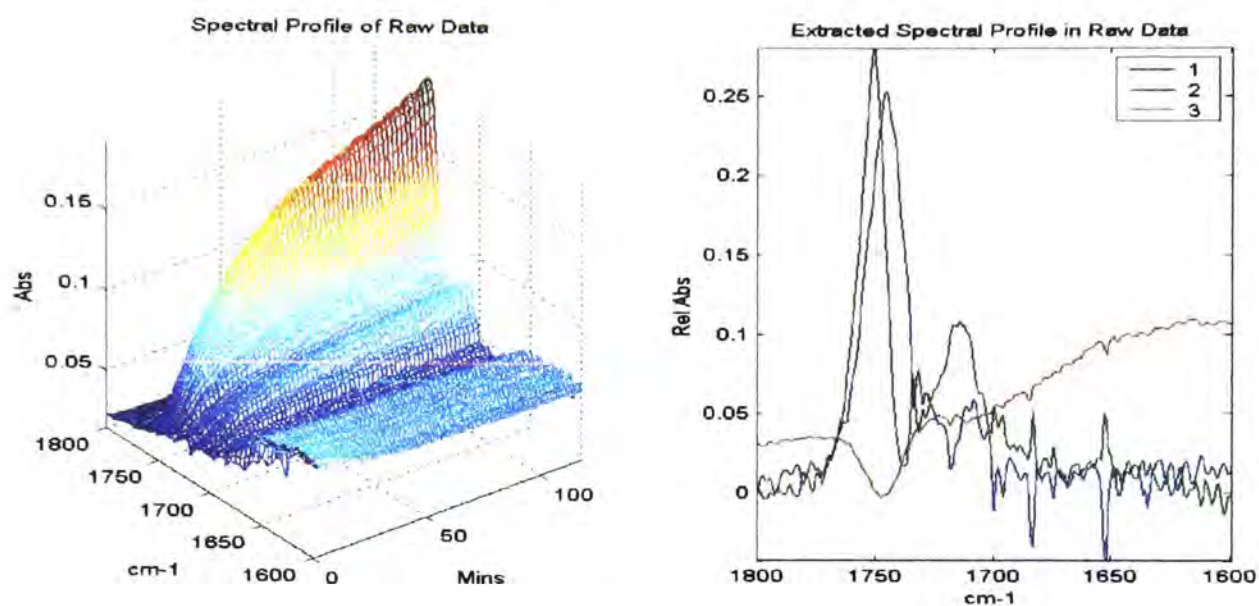


Figure 5.16. Raw data and extracted spectral profiles found in raw data, for ibuprofen in a mineral oil and miglyol formulation.

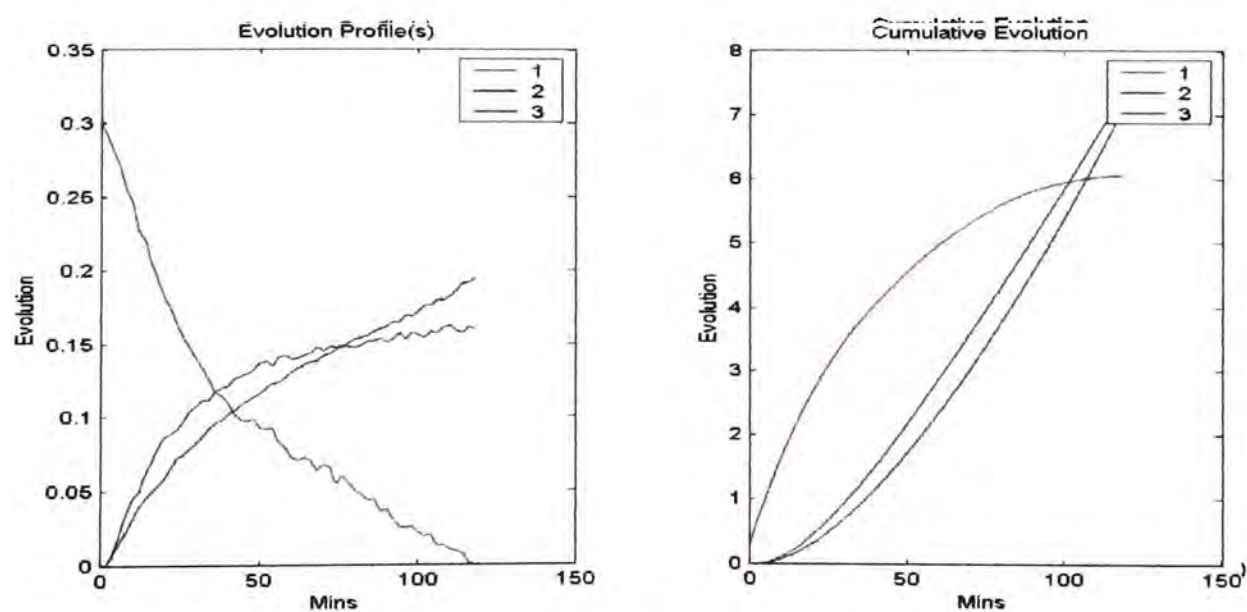


Figure 5.17. Evolution profiles and cumulative evolution profiles for ibuprofen in a mineral oil and miglyol formulation.

Figures 5.16 and 5.17 show the raw data and extracted profiles (spectral, evolution and cumulative) for ibuprofen in a mineral oil and miglyol formulation. The legends in each figure show how many components were extracted.

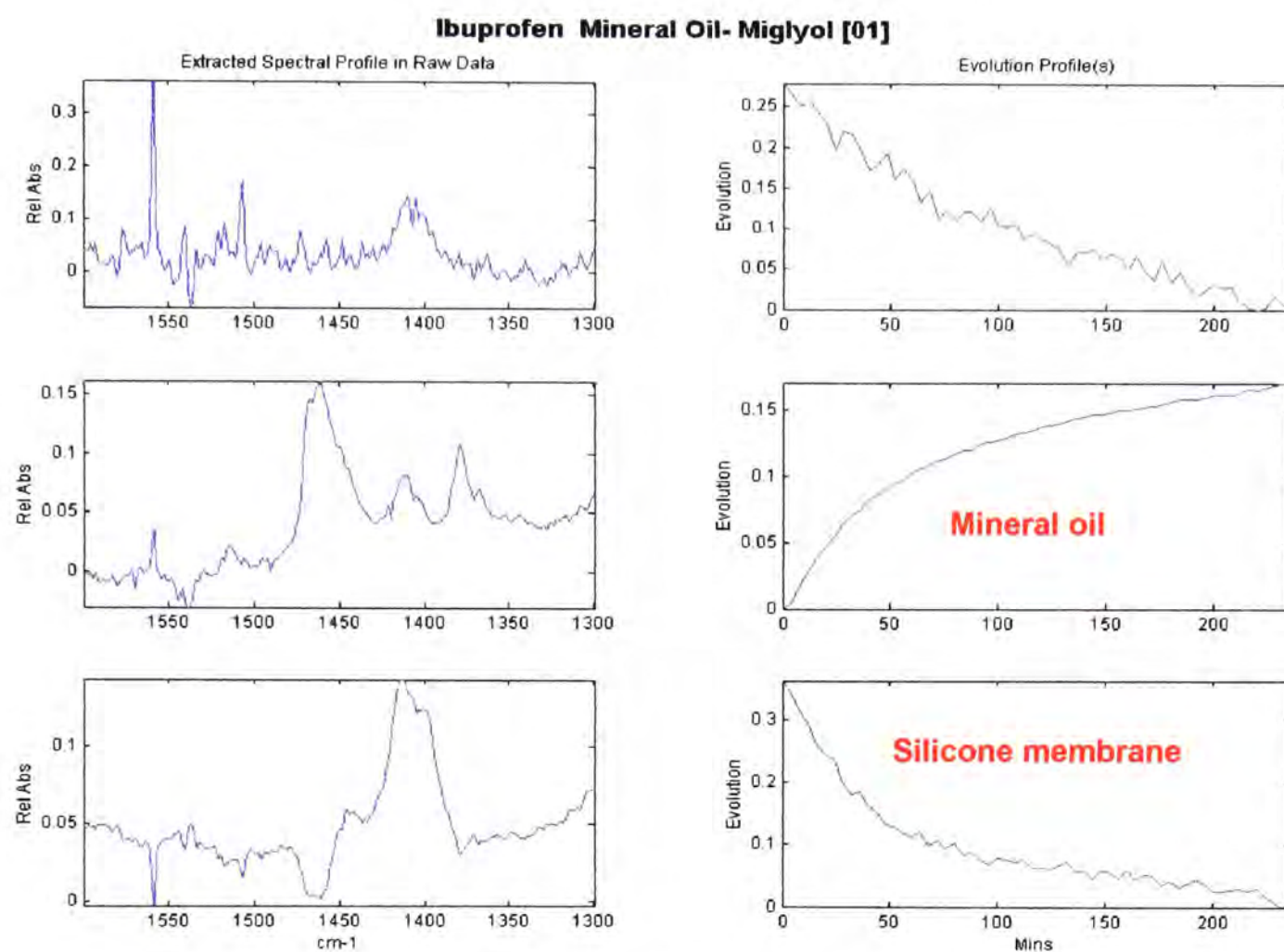


Figure 5.18. Extracted spectral profiles for ibuprofen in a mineral oil and miglyol vehicle

Figure 5.18 shows the extracted spectral profiles alongside the corresponding evolution profile for each component. Only two of the three components could be identified with confidence.

Figure 5.18 shows the extracted profiles from the second analysis of the data. In this region of the spectrum (between 1600cm^{-1} and 1800cm^{-1}) the difference between the spectral profiles is not as clear, but it is enough to identify confidently each component. In the extracted profile and the

reference had to be a 99% match to be extracted. The most interesting aspect of these profiles is the difference in the evolution profiles of the drug and solvent. The solvent appears to permeate quicker than the drug, supporting the view that it is an increase in the solubility of the drug within the membrane (and therefore improves partitioning) that facilitates permeation.

Ibuprofen in Miglyol-Mineral Oil

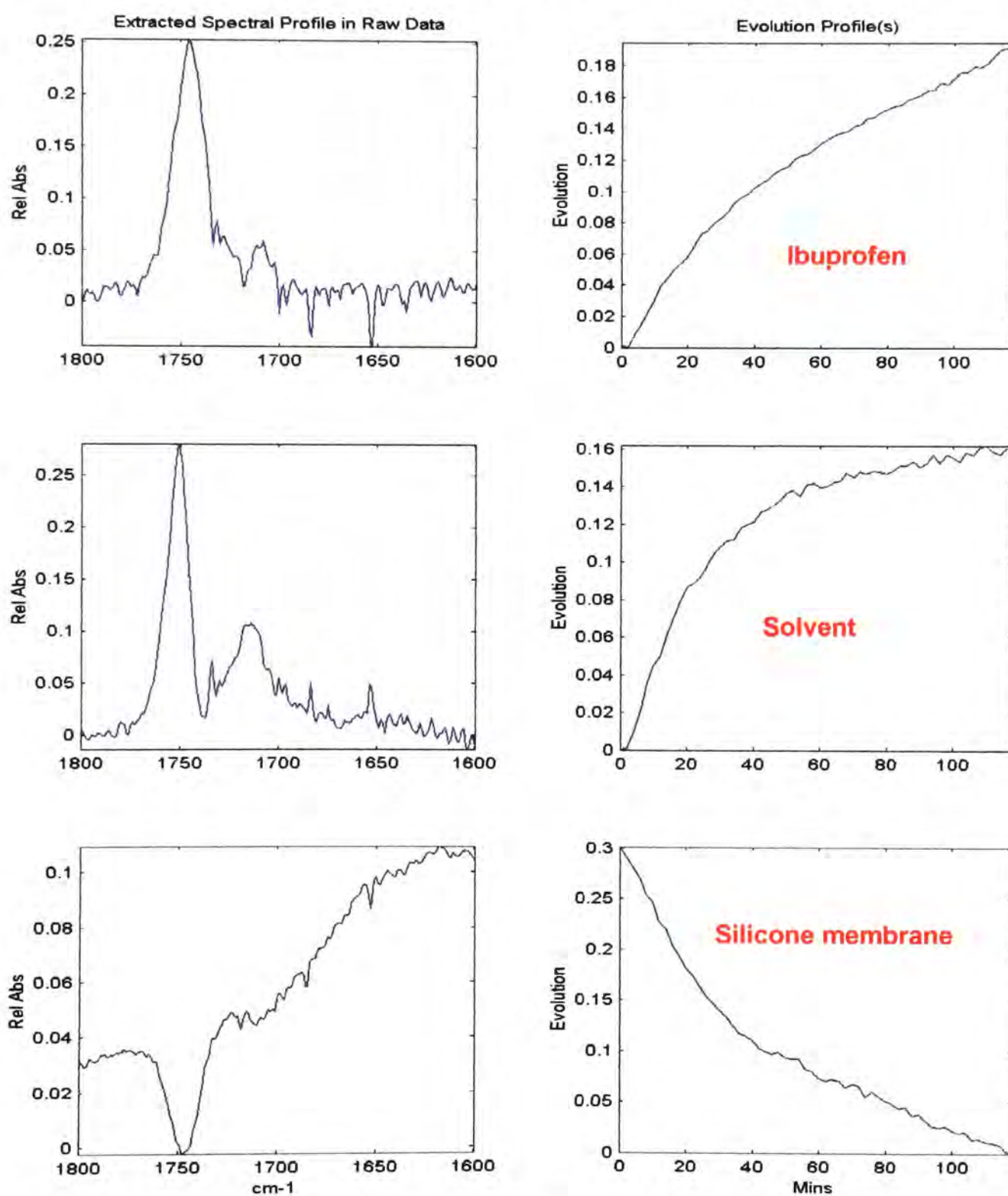


Figure 5.19. Extracted spectral profiles and evolution plots for ibuprofen in a mineral oil and miglyol formulation.

Ibuprofen in ethanol

Having demonstrated that this technique can provide useful information, it was time to use it to investigate the mechanism of action of enhancers. Franz-type diffusion experiments had shown that ethanol dramatically improved the permeation of ibuprofen across silicone membrane. It was hoped that using a chemometric approach for the analysis of data from ATR-FTIR diffusion experiments would reveal how this enhancement occurs.

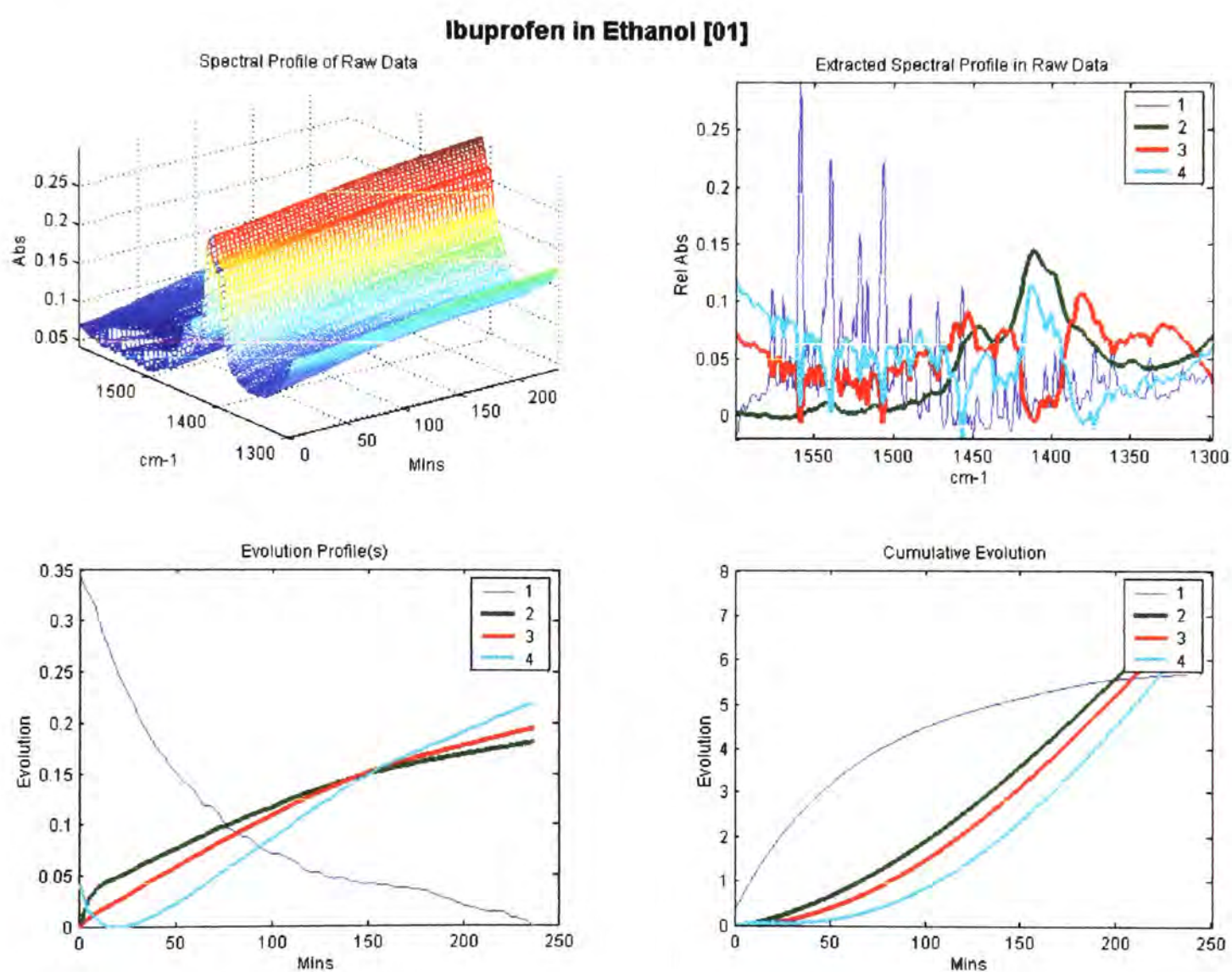


Figure 5.20. Raw data, extracted spectral profiles in raw data, evolution profiles and cumulative evolution profiles for ibuprofen in ethanol.

Figure 5.20 and 5.21 show the results of experiments using an ethanol vehicle. What became immediately apparent is the astonishingly rapid rate of appearance of ethanol at the membrane-crystal interface.

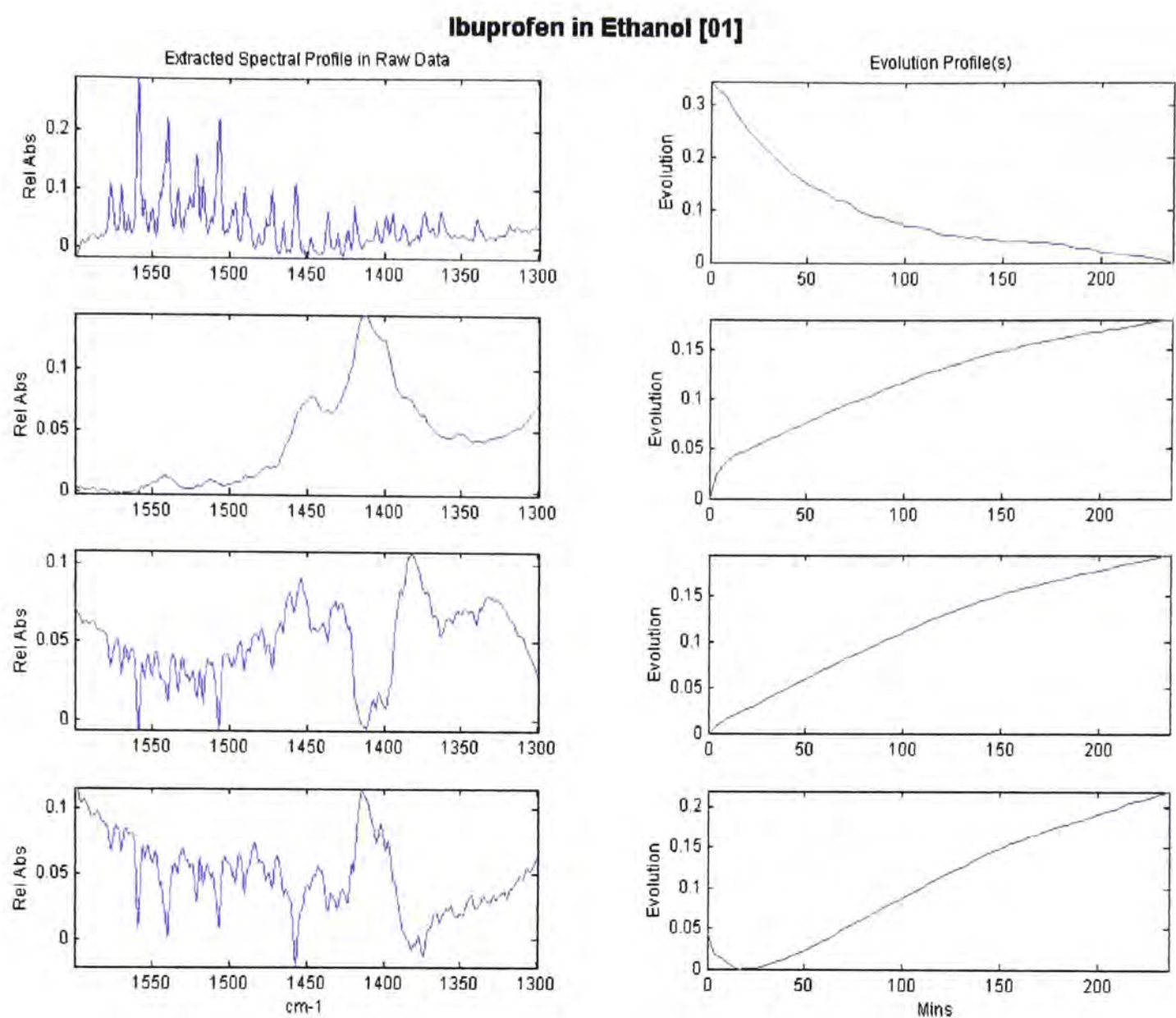


Figure 5.22. Extracted spectral profiles and evolution profiles for ibuprofen in an ethanol vehicle.

Inspection of the above profiles leads to the conclusion that, as for the lipophilic vehicles, ethanol is enhancing permeation by improving the solubility of the drug in the membrane. The ethanol rapidly moves into the membrane and by doing so makes it much easier for ibuprofen to do so as the partitioning behaviour will now be altered in favour of permeation. The solvent eventually saturates the membrane, allowing free passage of ibuprofen and all the while sink conditions are retained there will be movement of drug across the silicone until depletion occurs.

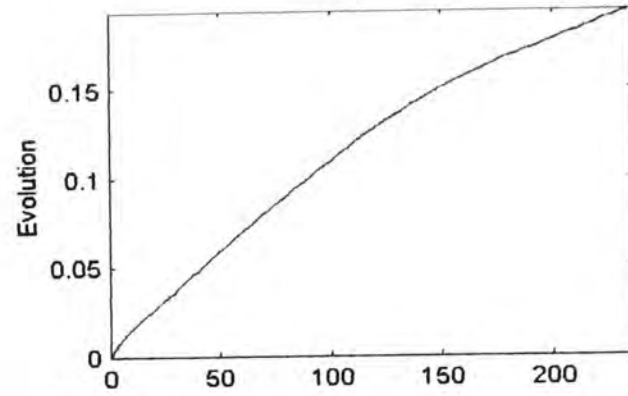
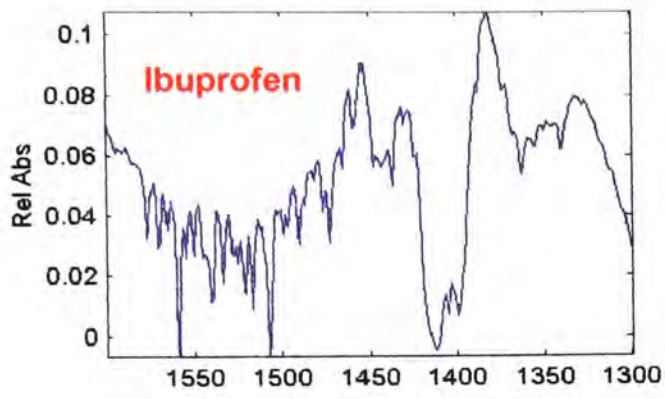
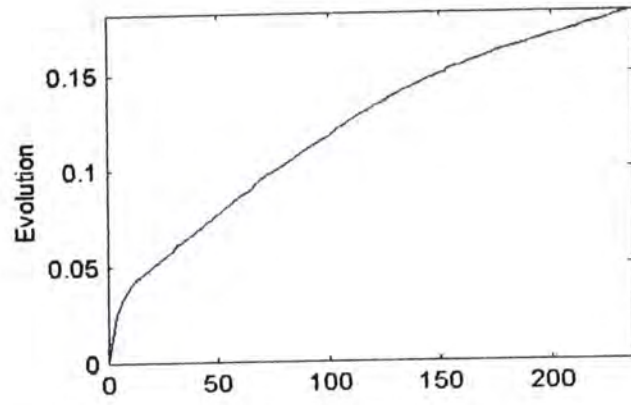
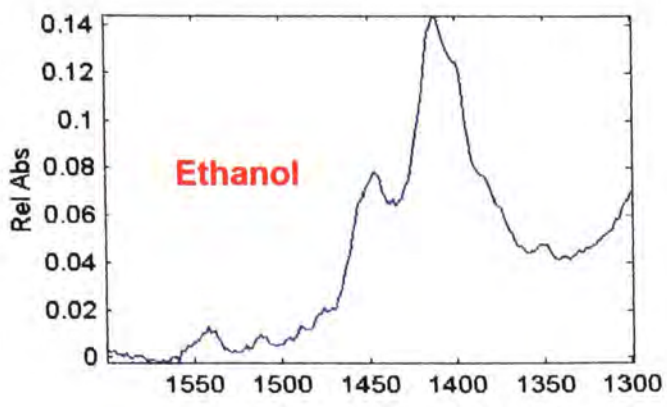


Figure 5.23. Extracted spectral profiles and evolution profiles for ibuprofen in an ethanol vehicle.

5.4.3.3. Ibuprofen in ternary solvent formulations

Ethanol, propylene glycol and water

Each component was identified using the reference spectra shown above. For each component, a different region was analysed, in order to optimise the results and to aid identification.

Ethanol

The evolution profile of ethanol is shown in figure 5.24. The profile shows that ethanol builds up fairly rapidly, and permeates the membrane with relative ease. After 2.6 hours (the end of the experiment) the profile does not reach a plateau, indicating that there is ethanol moving through the membrane for at least this length of time.

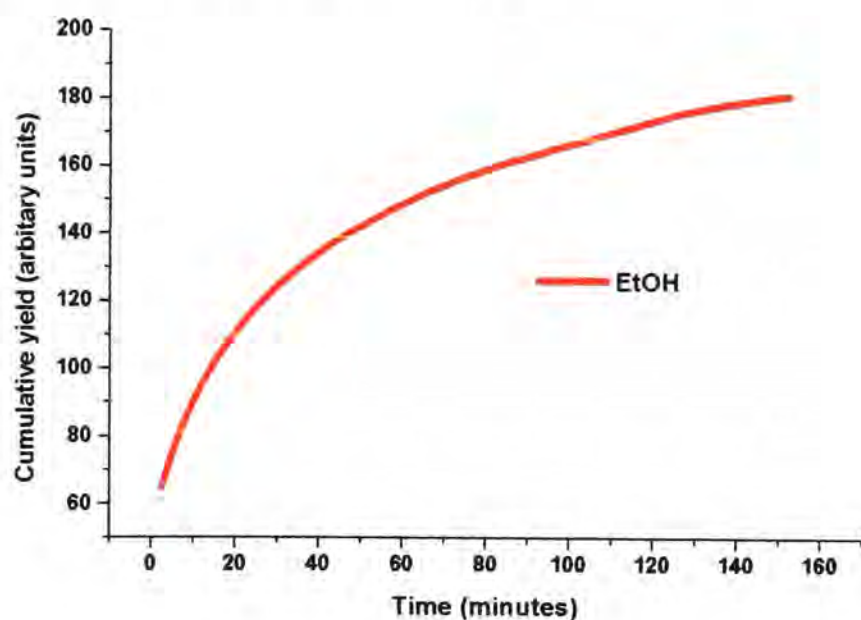


Figure 5.24. Evolution profile for ethanol extracted from the data for ibuprofen in a ternary formulation of ethanol, propylene glycol and water

The profile obtained from this experiment is markedly different to that obtained for previous experiments (see section 5.4.2 and 5.4.6). However, these experiments were conducted over a longer time period (six hours)

and so it could be that had the experiment run for a longer time, the profile would actually look similar to the previous ones.

Propylene glycol

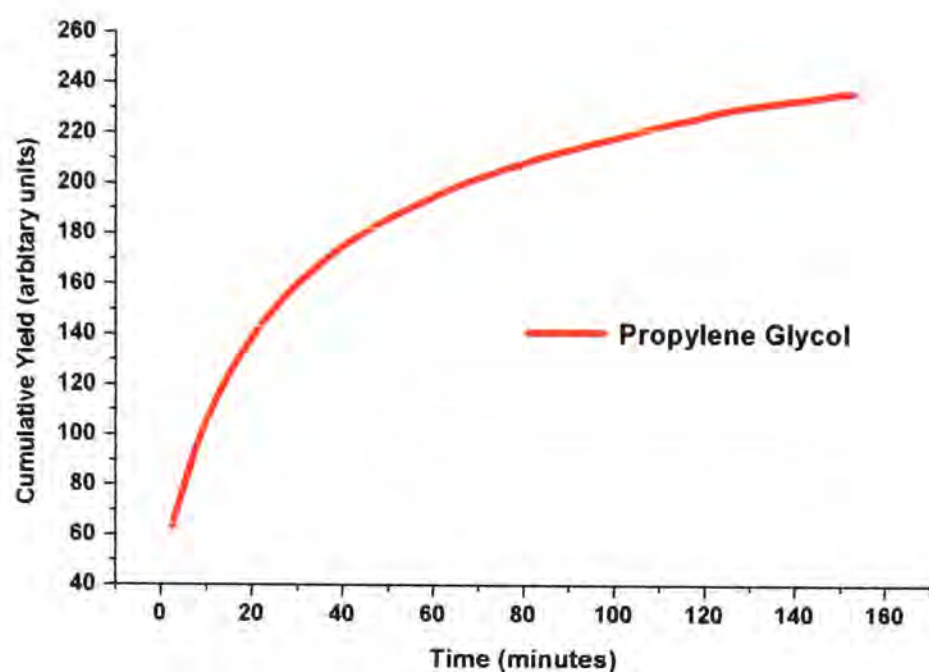


Figure 5.26. Evolution profile of propylene glycol extracted from the data for ibuprofen in a ternary formulation of ethanol, propylene glycol and water.

The profile for propylene glycol is a similar shape to that of ethanol. Comparing the profiles of the two (see figure 5.26) it is apparent that propylene glycol permeates at a slightly faster rate than ethanol as the slope of the earlier period is steeper. It also follows the profile of ethanol almost exactly, perhaps suggestive of some sort of co-operative effect between these two solvents. Bearing in mind that the plateau corresponds to the solubility of the drug or solvent within the membrane, it appears that PG is more soluble within silicone membrane than ethanol. This could help to explain the results of traditional diffusion experiments, where the effect of ethanol in a ternary vehicle was not as pronounced as one may expect.

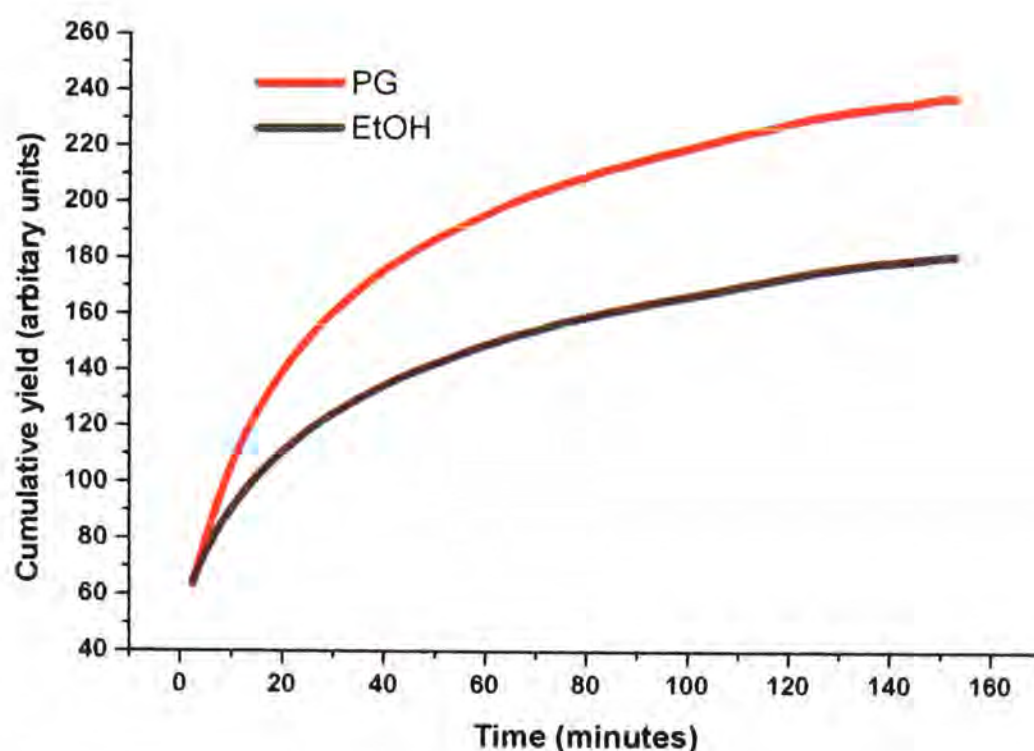


Figure 5.26. Evolution profiles of propylene glycol and ethanol extracted from the data for ibuprofen in a ternary formulation of ethanol, propylene glycol and water.

Figure 5.27 compares the profiles of propylene glycol and ethanol in the systems investigated, 50/25/25 and 25/25/50 (v/v ethanol/propylene glycol and water). Figure 5.27 also shows that the profiles of propylene glycol and ethanol are unaffected by the proportion of each in the mixture. This is easily explained for propylene glycol as the proportion of this component does not change in each system. However, a change might be expected for ethanol, as the flux values for ethanol in binary formulations water and propylene glycol shows a large increase from 25-50%, suggesting that there is some interaction with the membrane which alters flux. Surprisingly, this change is not detected using this technique.

The profiles also demonstrate the reproducibility of the technique, already demonstrated using salicylic acid in ethanol and water. Therefore, it can be concluded that this is not an experimental artefact, and is a phenomenon within the system.

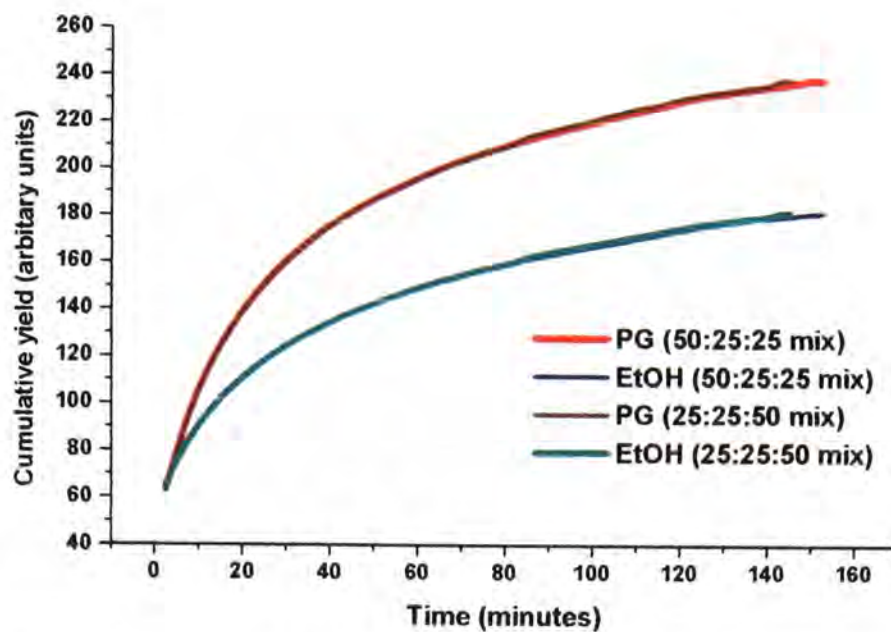


Figure 5.27. Evolution profile of propylene glycol and ethanol extracted from the data for ibuprofen in a ternary formulations of ethanol, propylene glycol and water.

Water

The profile obtained for water in a ternary formulation containing ethanol, propylene glycol and water follows that of propylene glycol and ethanol. The interesting aspect of this profile is that it is more like the profile of ethanol than propylene glycol. This suggests that both ethanol and water permeate in a similar manner.

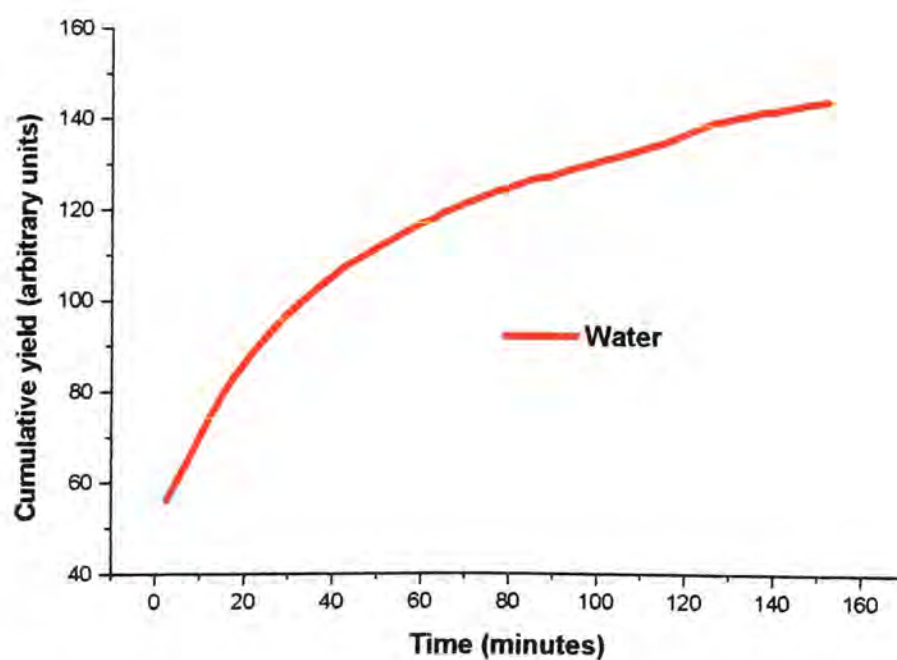


Figure 5.28. Evolution profile of water extracted from the data for ibuprofen in a ternary formulation of ethanol, propylene glycol and water.

Figure 5.29 compares the profiles of the three solvents, and from this plot it is clear that the plateau of water is lower than all the other components. Silicone membrane is a hydrophobic membrane, and so it is quite reasonable to see this sort of behaviour.

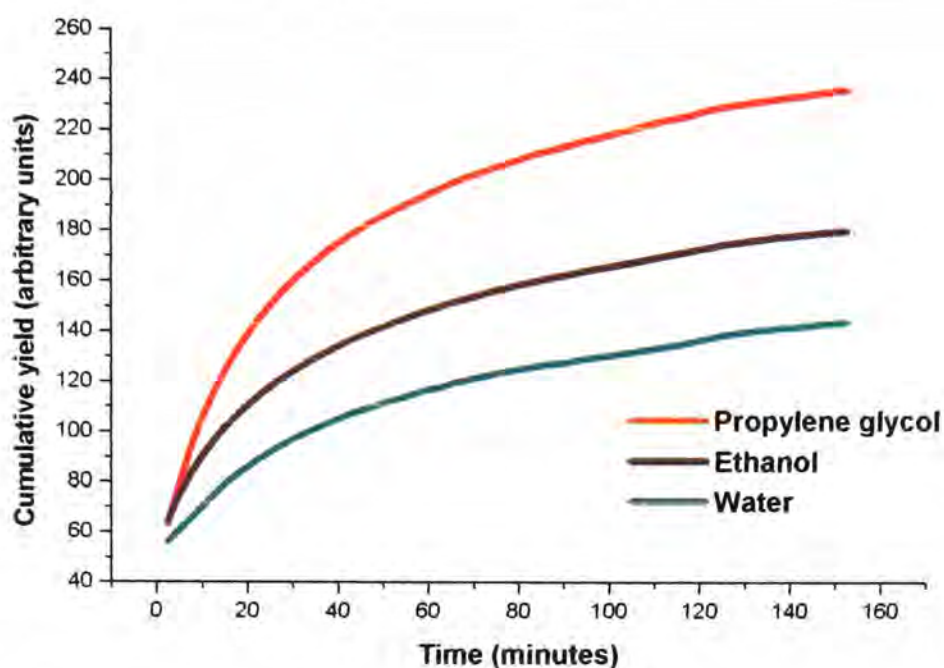


Figure 5.29. Evolution profile of propylene glycol, ethanol and water extracted from the data for ibuprofen in a ternary formulation of ethanol, propylene glycol and water.

Ibuprofen

The evolution profile for ibuprofen is most similar to that of ethanol, though the profile is the same shape as all of the components. Figure 5.30 illustrates how quickly ibuprofen is able to permeate silicone membrane in this formulation, with more permeating in the first hour of the experiment. None of the obtained profiles show a lag phase at the beginning of the experiment, suggesting that using this thickness of membrane, the drug is permeating even between the start of the experiment and the first spectrum being collected (2.5 minutes)

A key result of this investigation is that it highlights some of the issues involved with the use of traditional diffusion cell. In all the experiments described in this thesis, the first sample was taken after 30 minutes, which means that valuable information is being lost. In light of the studies detailed here, using ATR-FTIR it may be of use to take a spectrum every few seconds rather than minutes. The early time data could be most valuable in terms of investigating the way in which vehicles and drugs diffuse through membranes.

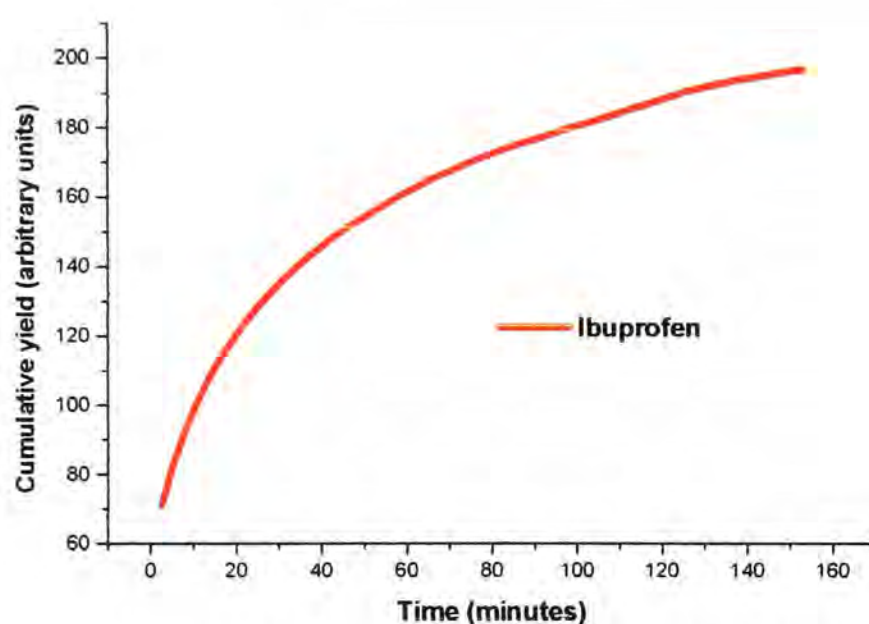


Figure 5.30. Evolution profile of ibuprofen extracted from the data for ibuprofen in a ternary formulation of ethanol, propylene glycol and water.

Figure 5.31 compares the obtained profiles of the solvents along with that of the permeant ibuprofen. From this plot it can be seen that ibuprofen permeates in a similar manner to ethanol, and this could suggest that ethanol is a key component of the vehicle for in the permeation of ibuprofen.

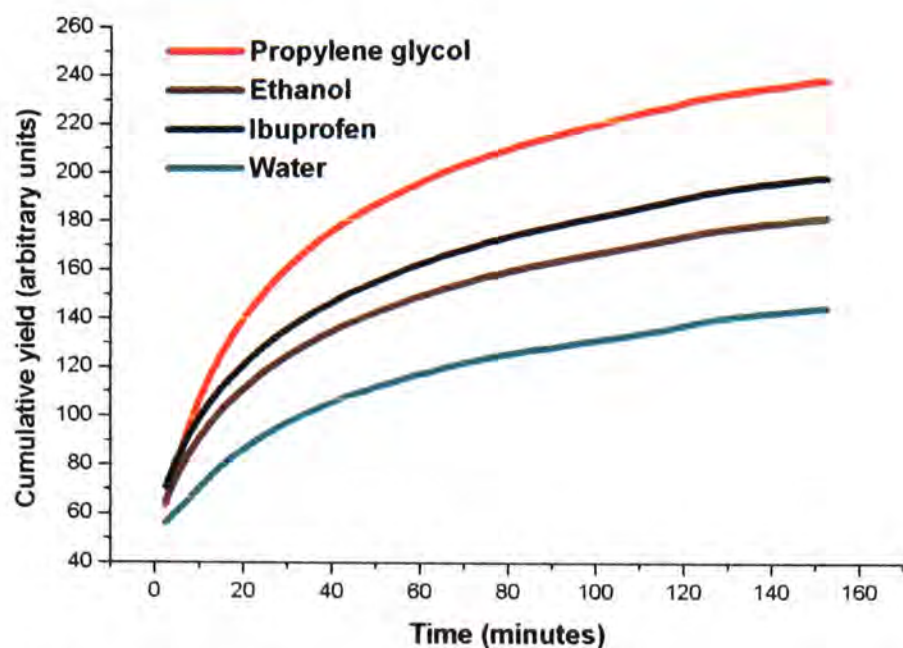


Figure 5.31. Evolution profile of drug along with vehicle components extracted from the data for ibuprofen in a ternary formulation of ethanol, propylene glycol and water.

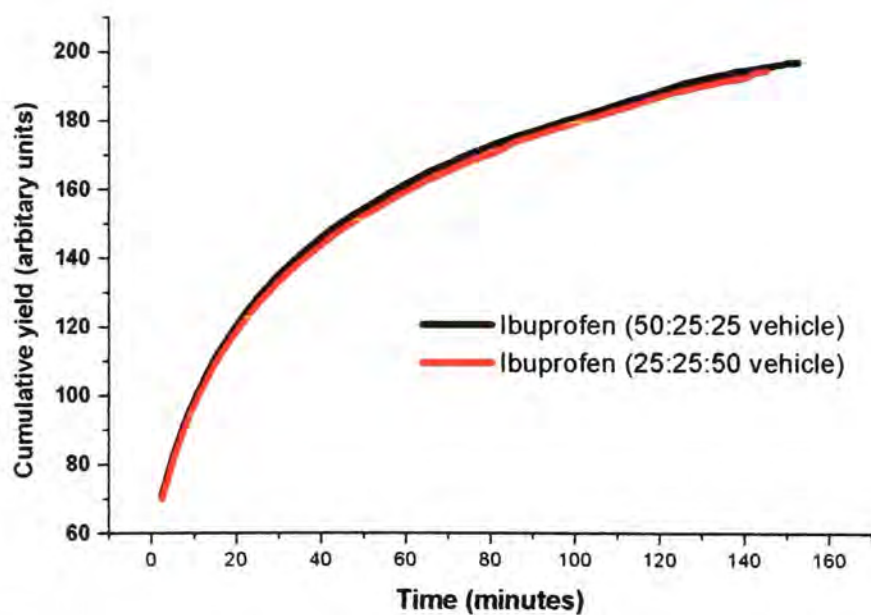


Figure 5.32. Evolution profile of ibuprofen extracted from the data for ibuprofen in ternary formulations of ethanol, propylene glycol and water.

Comparing the obtained profiles for ibuprofen (figure 5.32), there is no improvement in flux for the system containing more ethanol.

Polydimethylsiloxane (PDMS) membrane

Figure 5.33 shows the evolution profile for PDMS membrane during the course of the experiment. As in previous studies the cumulative yield for the membrane drops as a function of time, implying a change in the refractive index as the solvent permeates, or the solvent having some effect upon the membrane which decreases its signal.

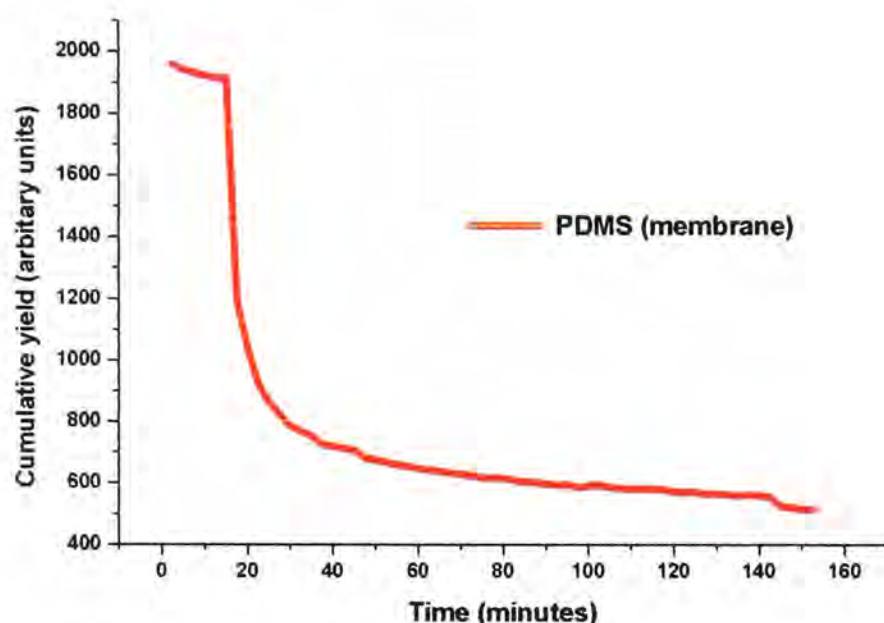


Figure 5.33. Evolution profile of PDMS membrane extracted from the data for ibuprofen in a ternary formulation of ethanol, propylene glycol and water.

When experiments of this type were first conducted it seemed that this decrease was caused by the former effect. However, it now appears that it could be the result of an interaction between the solvents and the membrane. The reason for this is that if it was caused by a change in refractive index, all of the components of the system would be affected, but this is not the case. There is no decrease in signal, or 'blip' in any of the profiles to suggest that this occurs. The new challenge is to try and understand exactly what is happening to the membrane. The way to unravel this mystery is to look at the region of the PDMS membrane spectrum used to follow this particular component. The infrared absorption

spectra of silicon organic compounds are very distinctive. The Si-H absorptions occur around 2100 cm^{-1} . This band is generally strong in intensity and somewhat broad in nature. The Si-H deformation occurs in the $900\text{-}800\text{ cm}^{-1}$ region (figure 5.34).

Silicon organic compounds with a methyl group attached to the silicon atom are very common. Methyl groups attached to a silicon atom give rise to a characteristic sharp symmetrical deformation absorption around 1260 cm^{-1} . The asymmetrical deformation is weaker and occurs around 1400 cm^{-1} .

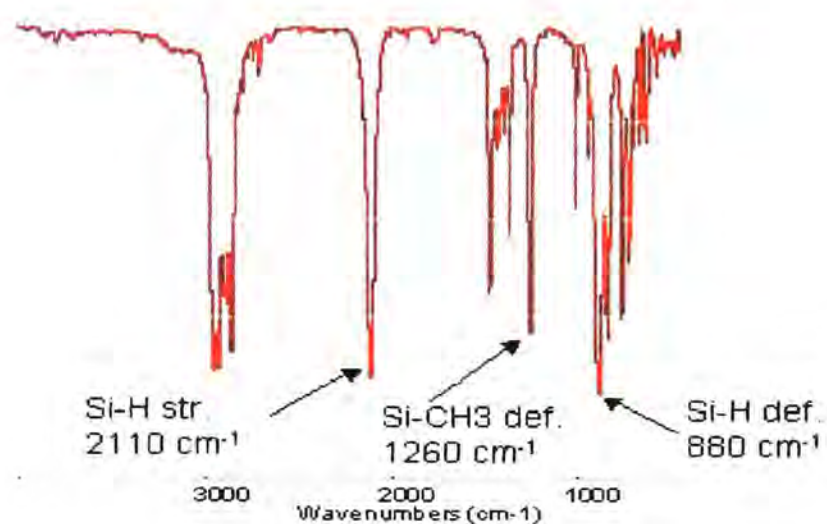


Figure 5.34. Example of an infrared spectrum for a siloxane.

For PDMS membrane, there is a strong absorption at $1260\text{-}1280\text{ cm}^{-1}$, and this is used to monitor this component. Any reduction in the signal may suggest that ethanol and propylene glycol interact with the membrane causing a shift and therefore an apparent reduction in the signal.

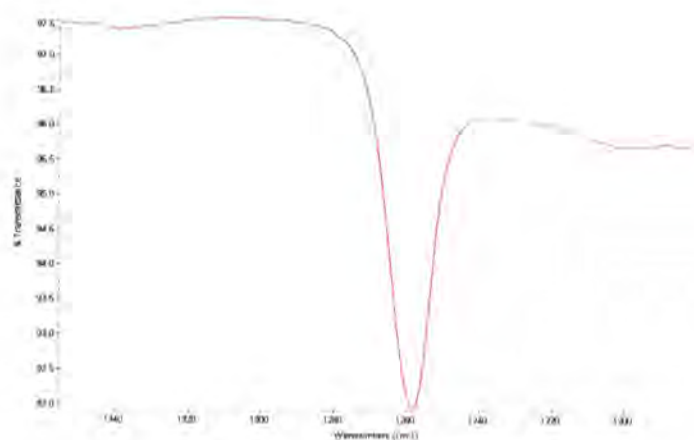


Figure 5.35. Peak in the infrared spectrum of PDMS which is attributed to Si-CH₃ deformation.

When the profiles for both systems are compared, it becomes apparent that there is a difference between the two experiments. The interesting aspect of this is that in the first part of the profile (up to 20 minutes) the profiles are identical, but from this point the 25/25/50 (ethanol/propylene glycol/water) drops to a greater extent. It is extremely difficult to determine what is happening in this system to alter the membrane in such a way, and more experiments, with a wider range of solvent combinations would be needed to investigate this further.

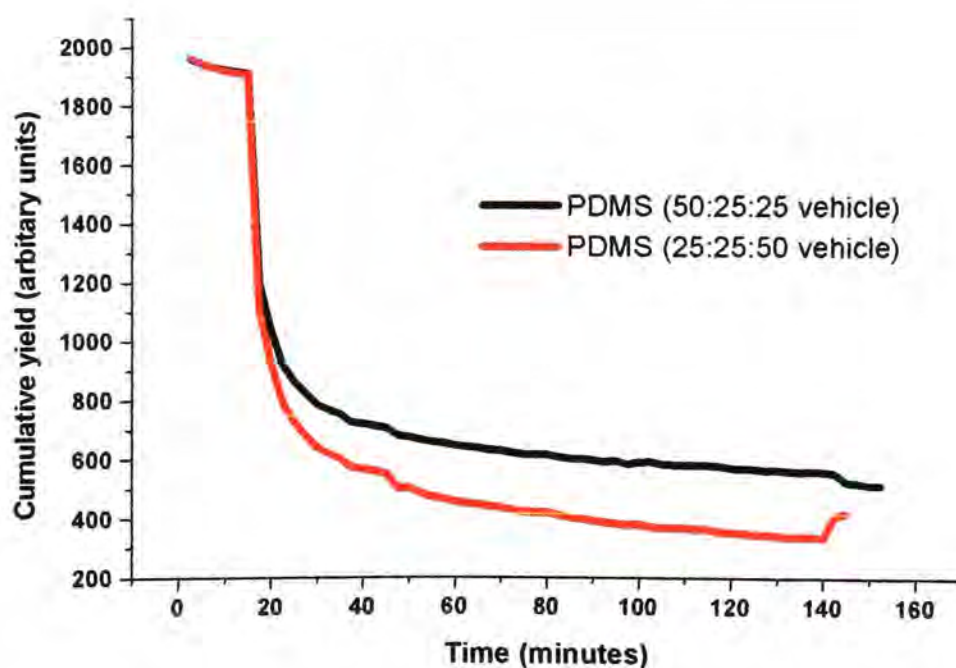


Figure 5.36. Evolution profile of PDMS membrane extracted from the data for ibuprofen in ternary formulations of ethanol, propylene glycol and water.

Transcutol, propylene glycol and water

Each component was identified using the reference spectra shown above. For each component, a different region was analysed, in order to optimise the results and to aid identification.

Transcutol

The evolution profile for Transcutol in the ternary formulation containing Transcutol with propylene glycol and water formulation shows very rapid permeation in the first 10 minutes of the experiment. After this point the diffusion of Transcutol slows, but continues to permeate to the end of the experiment.

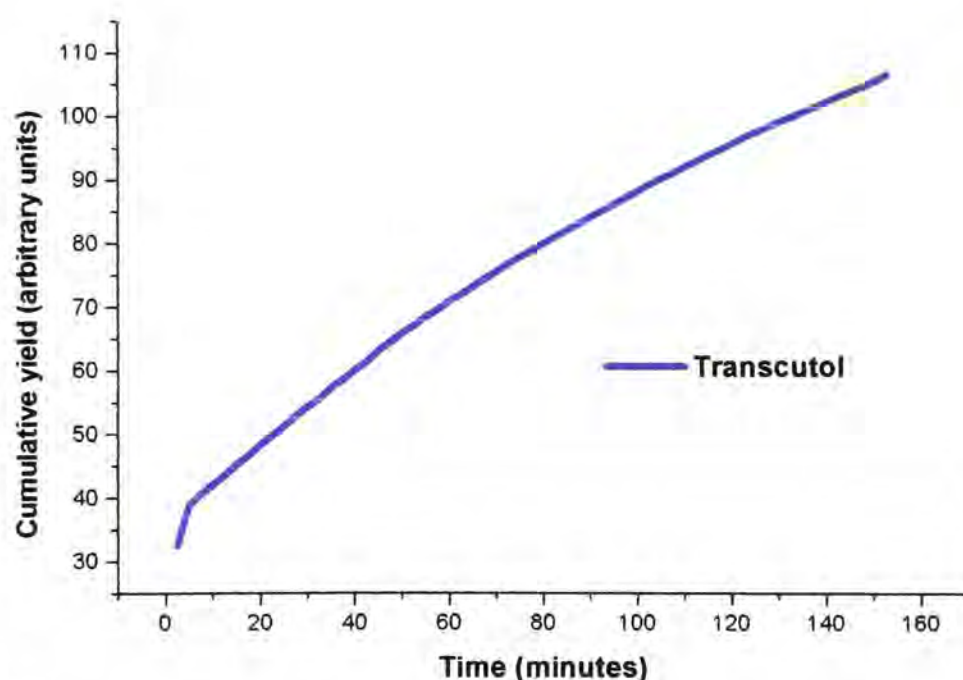


Figure 5.37. Evolution profile of Transcutol extracted from the data for ibuprofen in a ternary formulation of Transcutol, propylene glycol and water.

The profile is very different to any of the ethanol, propylene glycol and water systems, indicating that Transcutol is permeating faster than the components of the previous formulation. When the profiles of both types of enhancer formulations are plotted it becomes clear that at the end of the

diffusion experiment the Transcutol has permeated the membrane to a greater extent. In Chapter Four the results of traditional diffusion experiments were presented, which showed that the flux was 2.5x higher for formulations containing ethanol than for the formulations containing Transcutol. The one factor which would account for the results seen in this investigation using ATR-FTIR is the difference in solubility of ibuprofen in the two enhancers. Ibuprofen has much better solubility in ethanol than Transcutol, which means that even though less ethanol will be present in the membrane, it will be outweighed by the excellent solubility enhancing effect of ethanol.

Propylene glycol

In the case of propylene glycol, the profile is almost identical to that of Transcutol, which is similar to the behaviour seen in the previous formulation containing ethanol. The main difference between the two is that for this formulation the amount measured at the crystal-membrane interface is apparently less than for the corresponding formulation containing ethanol. It is not clear why this should be so, but it could reflect some degree of interaction between Transcutol and propylene glycol.

In a series of experiments investigating the permeation of the monoethyl-ether of diethylene glycol (DG), Boháček (1996) found that when in the presence of a cosolvent the permeability of DG was altered. Two types of cosolvent were used, propylene glycol and propylene glycol dipelargonate (DPPG). Both DPPG and propylene glycol increased the permeability of DG through rat skin. DPPG improved permeation to a greater extent than propylene glycol, but the most interesting aspect of this study is that in this study Boháček found that DG penetrated stratum corneum in substantially smaller amounts than other hydrophilic solvents (water,

ethanol). Bearing this in mind, it is perhaps the case that although the permeation of Transcutol (the trade name for monoethyl-ether of diethylene glycol produced by Gattefosse) in this study is increased, the permeation of propylene glycol may be adversely affected.

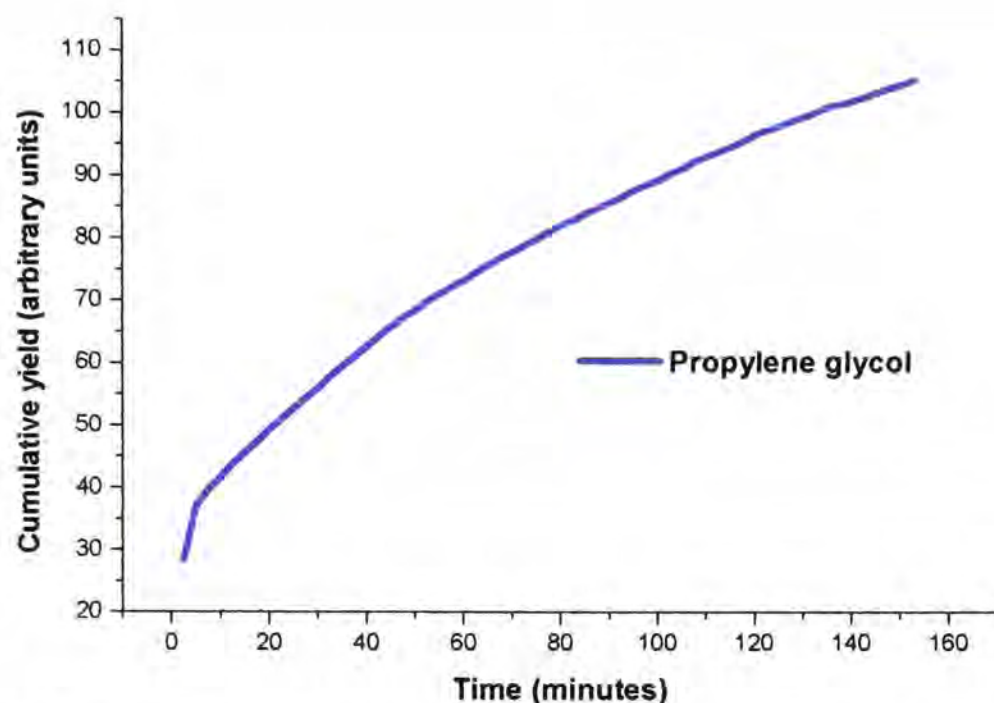


Figure 5.38. Evolution profile of propylene glycol extracted from the data for ibuprofen in a ternary formulation of Transcutol, propylene glycol and water.

There is slightly less propylene glycol permeated than Transcutol, which could indicate that Transcutol is the dominant solvent for the permeation of ibuprofen in this formulation.

Water

As with propylene glycol, the profile for water is a similar shape to that of Transcutol. There is a difference in the shape of the profiles between the two formulations tested containing Transcutol, with the profile of the 25:25:50 formulation being more regular in appearance than that shown below.

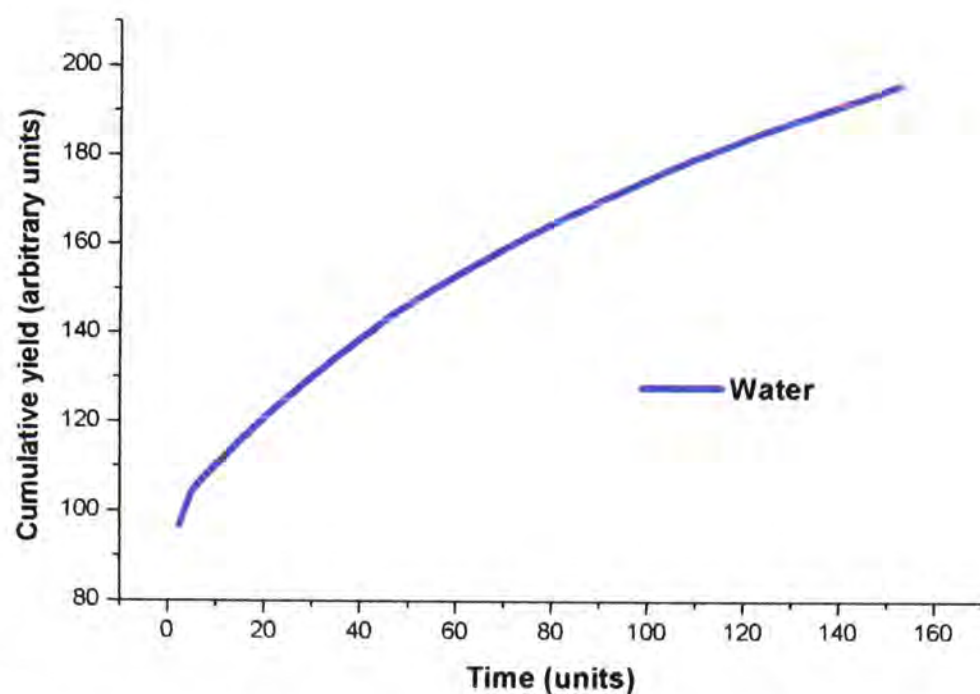


Figure 5.39. Evolution profile of water extracted from the data for ibuprofen in a ternary formulation of Transcutol, propylene glycol and water.

The shape of the profiles obtained for water (shown in figure 5.39) is similar to that obtained for Transcutol and propylene glycol, suggesting that the three solvents are diffusing through the membrane in a similar fashion.

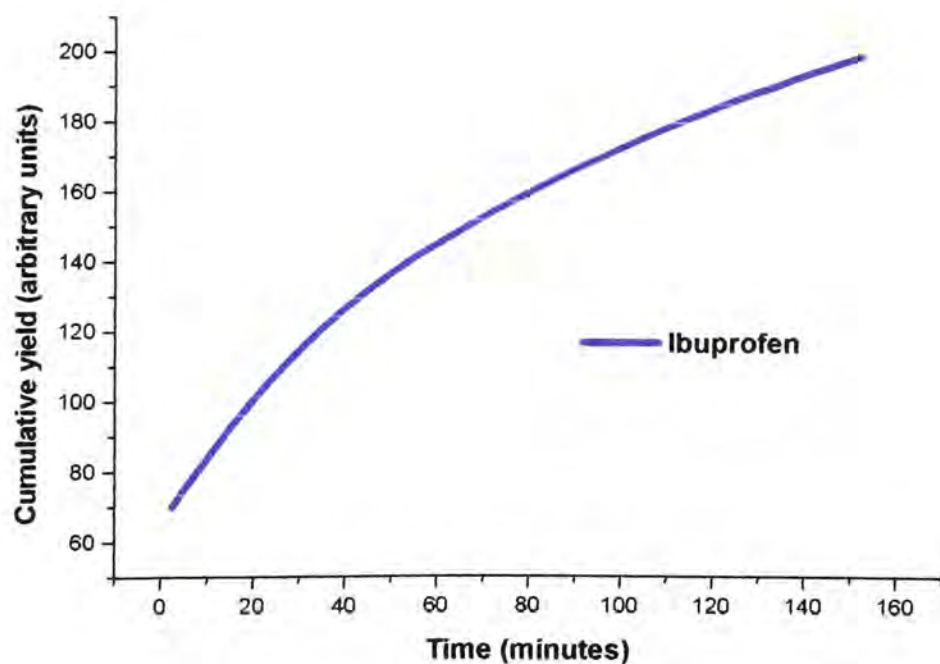


Figure 5.40. Evolution profile of ibuprofen extracted from the data for ibuprofen in a ternary formulation of Transcutol, propylene glycol and water.

Ibuprofen has a different profile to the solvents used in this experiment. A possible reason for this is that the solvents permeate first, allowing the movement of ibuprofen into, and across the membrane. This would give rise to a difference in the profiles, as is seen here.

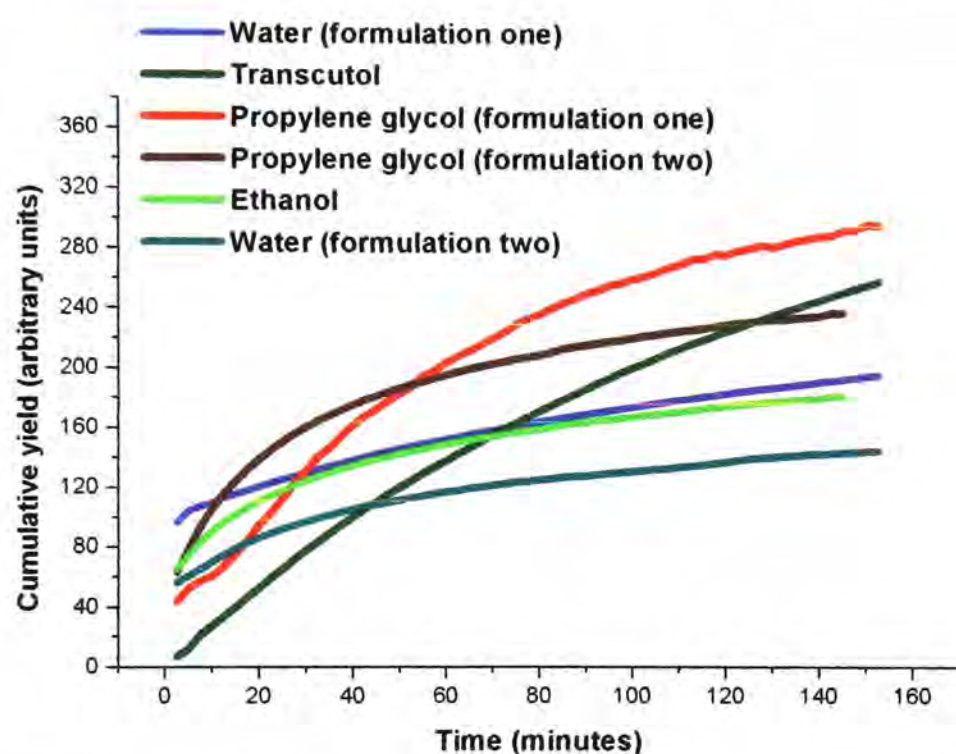


Figure 5.41. Evolution profile of drug and vehicle components extracted from the data for ibuprofen in ternary formulations of ethanol (formulation one) or Transcutol (formulation two), propylene glycol and water.

When all the profiles are placed together the effect the solvents have upon each other becomes somewhat clearer. Water and propylene glycol both permeate in greater amounts from formulation one, containing ethanol. It is not clear why this should be the case, but the most plausible explanation is an interaction between the three solvents, which serves to reduce the extent to which they are able to traverse the membrane.

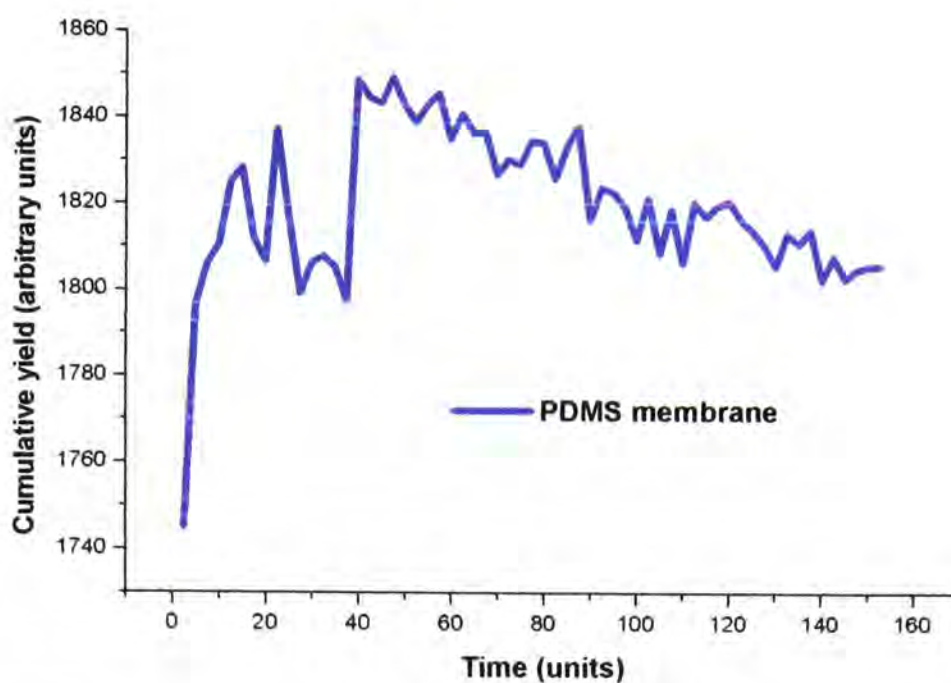


Figure 5.42. Evolution profile of PDMS membrane extracted from the data for ibuprofen in a ternary formulation of Transcutol, propylene glycol and water.

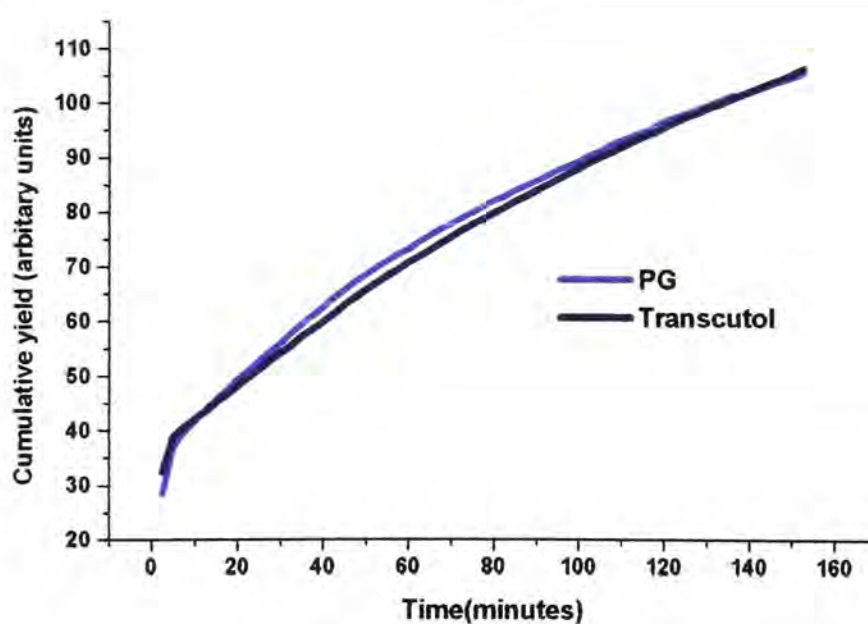


Figure 5.43. Evolution profile of Transcutol and propylene glycol extracted from the data for ibuprofen in a ternary formulation of Transcutol, propylene glycol and water.

Figure 5.43 compares the evolution profiles of the two solvents in the formulation. In this experiment they have almost identical profiles, perhaps suggestive of a co-operative process during diffusion. The two solvents are known to act in a similar manner, increasing the solubility of

the drug in the skin, therefore it follows that their profiles may be expected to contain some similarities.

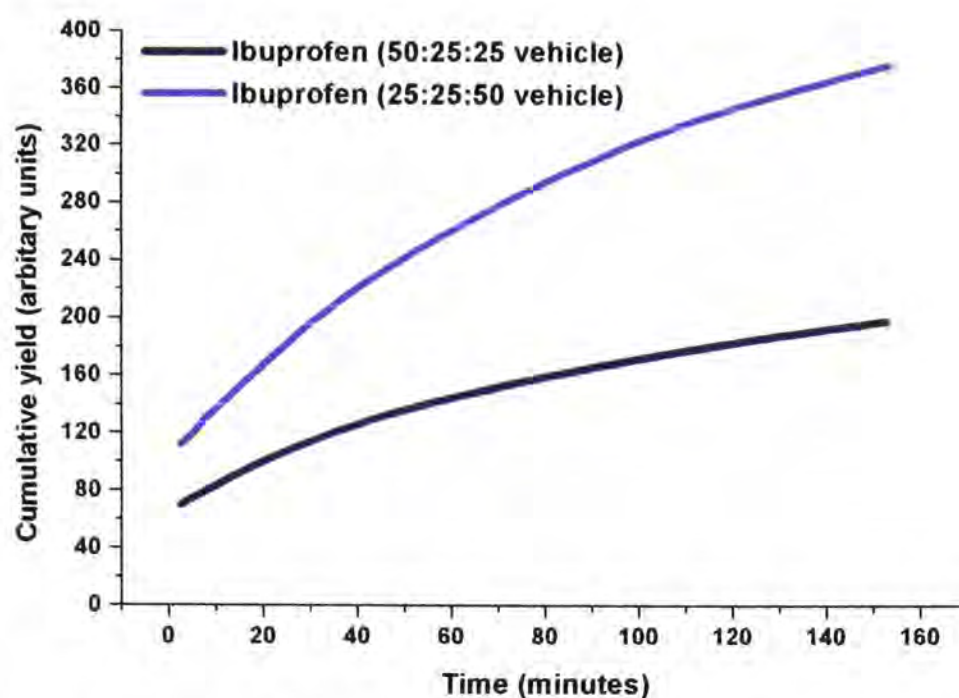


Figure 5.44. Evolution profile of ibuprofen extracted from the data for ibuprofen in ternary formulations of Transcutol, propylene glycol and water.

Figure 5.44 shows the profiles for ibuprofen in formulations containing Transcutol, propylene glycol and water. The interesting aspect of this plot is that although one would intuitively expect ibuprofen to permeate more rapidly in the formulation containing a higher proportion of Transcutol, this is not the case. On the evidence of these experiments, it seems that the formulation with less Transcutol presents a more favourable medium for delivery. If these data are compared with that obtained from traditional diffusion experiments, the mystery deepens. The results of Franz-type diffusion experiments showed that ibuprofen release was higher for the formulation containing more Transcutol (222.93 ± 6.84 and 257.08 ± 11.19 $\mu\text{g}/\text{cm}^2/\text{hr}$ respectively). However, these are single point experiments, therefore further experiments are needed to demonstrate whether this effect is reproducible.

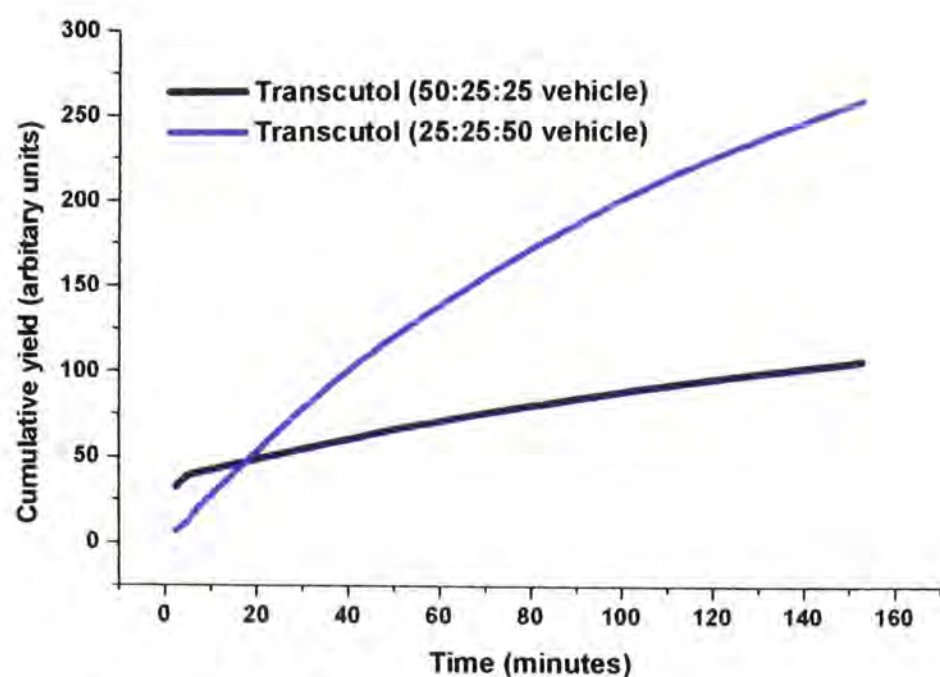


Figure 5.45. Evolution profile of Transcutol extracted from the data for ibuprofen in ternary formulations of Transcutol, propylene glycol and water.

The profiles obtained for Transcutol in the two formulations were very different when placed together. According to figure 5.45, there is a greater degree of permeation of solvent from the 25:25:50 formulation of Transcutol, propylene glycol and water. This does seem strange when there is more Transcutol available to permeate in the formulation containing 50:25:25 Transcutol, propylene glycol and water. It does not seem likely that it is the water component of the vehicle which is aiding the permeation of Transcutol, for there would be very little uptake of water by the membrane because of its hydrophobicity. The other consideration is to once again consider the findings of Boháčik, who found a similar phenomenon when investigating the permeation of DG, and this appears to be borne out by the data presented in figure 5.45.

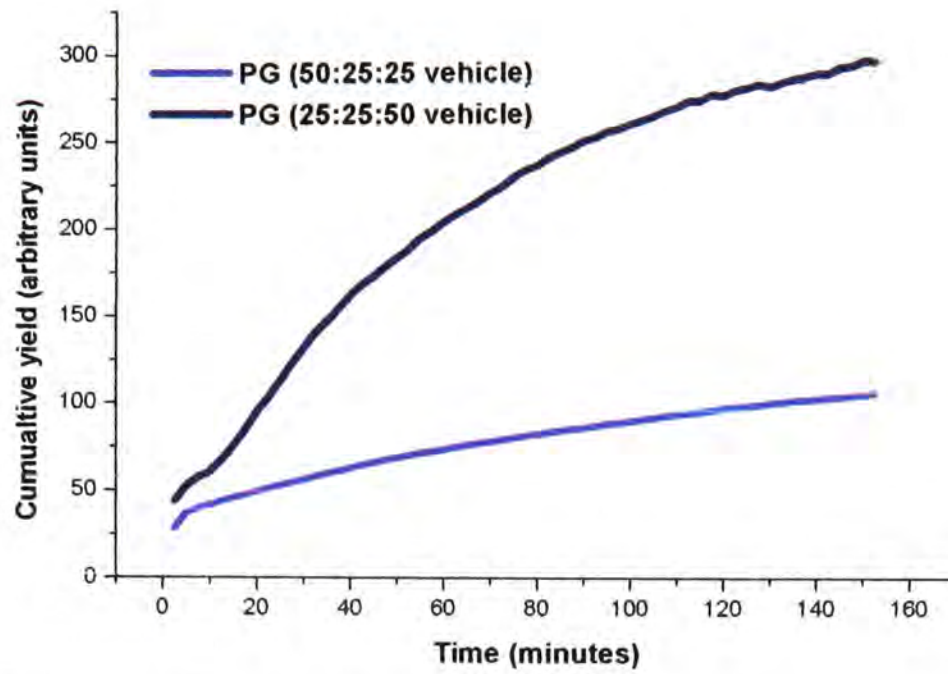


Figure 5.46. Evolution profile of propylene glycol extracted from the data for ibuprofen in ternary formulations of Transcutol, propylene glycol and water.

The shape of the profiles of propylene glycol extracted from the data show that, as for all the other components, there is higher permeation from the formulation containing less Transcutol.

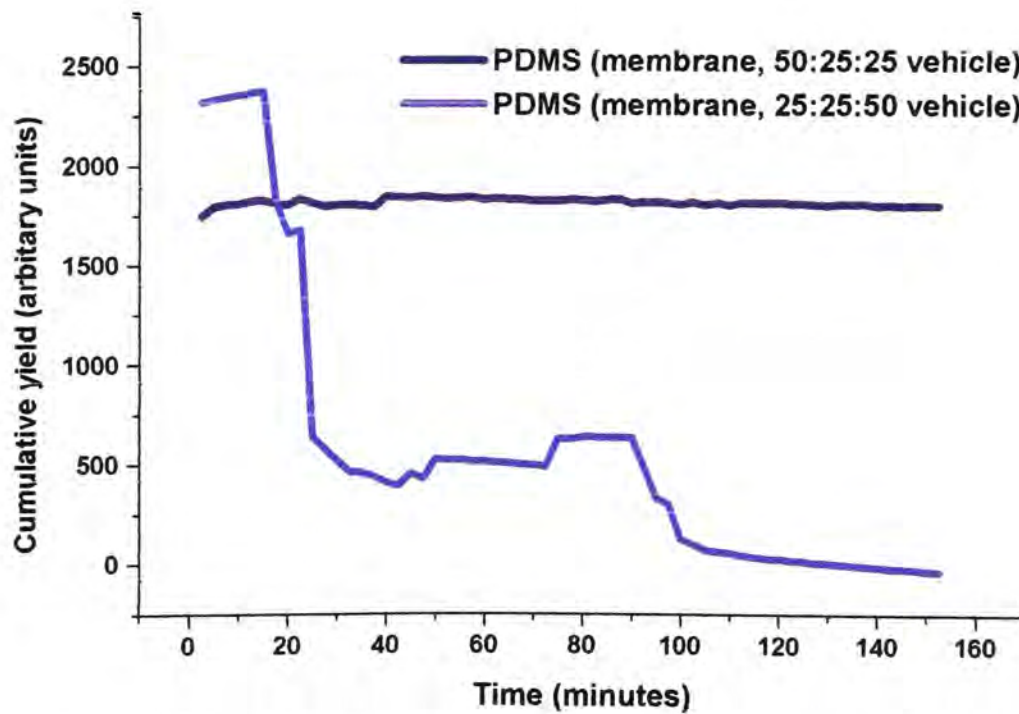


Figure 5.47. Evolution profile of PDMS membrane extracted from the data for ibuprofen in ternary formulations of Transcutol, propylene glycol and water.

The profiles for the PDMS membrane in each experiment show dramatic differences which could account for the permeation behaviour of the other components. There is very little change in the profile of the membrane during the first experiment (50:25:25 TC:PG:Water) which suggests that the solvents did not interact in any way with the membrane. However, for the next experiment (25:25:50 TC:PG:Water), the profiles shows a reduction in the signal of the membrane as the experiment goes on. It seems likely that it is this change in the membrane accounts for the higher permeation of the other components. Based upon the data obtained, this is the only change which could possibly cause the results seen in figures 5.43 - 5.46.

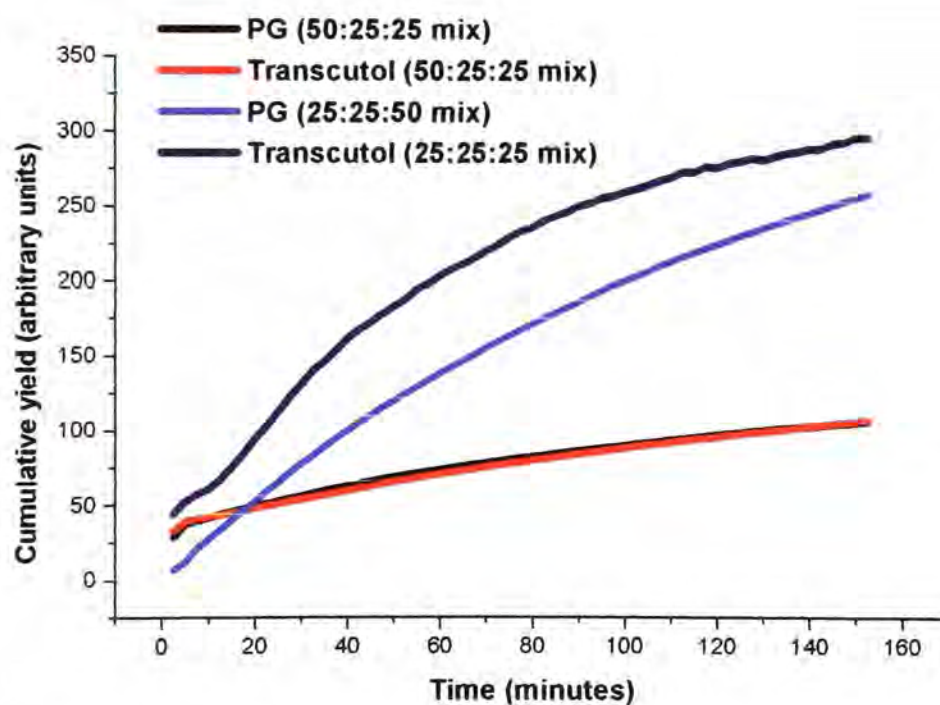


Figure 5.48. Evolution profile of Transcutol and propylene glycol extracted from the data for ibuprofen in ternary formulations of Transcutol, propylene glycol and water.

Bearing in mind the profiles for the membrane, the profiles seen in figure 5.48 make more sense. The key indication is the way that both solvents are affected by the change to the same extent. Without further

experiments it is very difficult to judge whether this effect is an experimental artefact, or that there is some interaction between the solvents and the membrane when used in certain proportions.

5.5. Conclusions

ATR-FTIR has been successfully used in the past to determine the mode of action of various enhancers on human skin and silicone membrane. In this study a different approach to the analysis of data obtained in these type of diffusion experiment was used to follow the progress of components of a formulation during permeation across silicone membrane. To this end, this part of the project was successful, and applying chemometric analysis to raw data enabled complex spectra to be deconvoluted, and each component identified. Up to five component systems were investigated, demonstrating the power of the technique and its applicability to multi-component formulations. Although 'real' formulations were not evaluated, there seems no reason why, with valid references, it would not be possible to investigate such systems. Perhaps the most valuable result of this part of work was being able to monitor the membrane during a diffusion experiment. When conducting a Franz-type diffusion experiment, the membrane can be examined before and after the experiment, but not during, and it has been exciting to see the type of changes which are occurring as solvents pass across. These experiments have shown that rather than being a passive part of the formulation, propylene glycol actually does cause some change in silicone membrane, reducing its signal during the course of an experiment. This is not the only solvent to bring about such a change, for most of the solvents used in this study produced a similar effect. The only truly non-interacting solvent is water, and it would be pertinent to conduct further experiments to investigate to what extent the solvents are able to interact.

5.6. References

L. Boháčik, V. Koprda, F. Falson-Rieg and J. Hadgraft. Penetration studies using the monoethyl-ether of diethylene glycol. In: *Prediction of Percutaneous Penetration*, Eds K. R. Brain, V. J. James and K. A. Walters. Vol. 4b. STS Publishing, Cardiff. pp133-134 (1996).

M. M. Dias. Facilitated percutaneous penetration. PhD Thesis, Cardiff University (2001).

M. M. Dias, S. L. Raghavan and J. Hadgraft. ATR-FTIR spectroscopic investigations on the permeation of benzoic acid and salicylic acid through silicone membranes. *Int. J. Pharm.* **216**, 51-59 (2001).

A. C. Watkinson, D. M. Green, J. Hadgraft and K. Brain. The relative effect of azone and Transcutol on permeant diffusivity and solubility in human stratum corneum. *Pharm. Res.* **13**, 542-546 (1996).

- Chapter Six -

Diffusion Studies Through Human Skin

6.1. Introduction

The use of different solvent combinations in formulations to obtain penetration enhancement has been demonstrated in Chapter Four using synthetic membranes. Membranes such as silicone provide a way of comparing the permeation characteristics of different formulations, without the inherent complexity and variability associated with the use of biological barriers. However, experiments using synthetic membranes can only give an indication of what may happen when a biological membrane such as skin is used. The aim of this Chapter was to determine whether the results of studies using PDMS membranes would be reflected in human skin.

The validity of using in-vitro experiments for predicting in-vivo skin permeation has often been questioned. Franz (1975) found that the total amount absorbed for a series of compounds was greater from the in-vitro studies, but the order of permeability was in good agreement with the in-vivo data. Therefore, with respect to the permeability of different formulations, in vitro human skin experiments can provide valuable information for in-vivo absorption.

Because of the low availability of human skin, the data presented in this Chapter are limited. However, it does demonstrate that in terms of modelling the permeation of drugs the most appropriate membrane to use is that which most closely resembles the in-vivo situation, the skin.

6.2. Methods

The methods and analysis used in this Chapter are described in Chapter Three.

6.3. Experimental

The following experiment were conducted using human skin:

Permeation of ibuprofen from saturated solutions

- Propylene glycol
- Propylene glycol and water 25/75 (v/v) formulation
- Propylene glycol and water 50/50 (v/v) formulation
- Water
- Mineral oil
- Mineral oil and miglyol 50/50 (v/v) formulation
- Miglyol
- Ethanol
- Ethanol and water 25/75 (v/v) formulation
- Ethanol and water 50/50 (v/v) formulation
- Ethanol and water 75/25 (v/v) formulation

Permeation of ibuprofen from ternary solvent formulations

- Ethanol/propylene glycol/water 25/25/50 (v/v)
- Ethanol/propylene glycol/water 50/25/25 (v/v)

For each experiment 1mL of a saturated solution of ibuprofen was used as the donor phase.

6.4. Results and Discussion

In order to understand the effect of selected vehicles on the skin, the diffusion of ibuprofen from several formulations through human epidermis was evaluated. Steady state fluxes were calculated by monitoring the cumulative amount of drug diffused and measuring the slope of the graph once steady state diffusion was reached. All time points were used to measure the slope of the graph. Kinetic and thermodynamic parameters were determined using a curve fitting procedure employing the appropriate solution to Fick's second law of diffusion (refer to section 4.2). Tables 6.1 - 6.4 list the flux values with associated standard deviations, the kinetic parameter β (D/h^2), the thermodynamic parameter α ($K \cdot h$) and the permeability coefficient, k_p .

6.4.1. Mineral oil and miglyol formulations

Table 6.1. Steady state fluxes, thermodynamic and kinetic parameters, permeability coefficients for the permeation of ibuprofen from saturated formulations containing mineral oil and miglyol through human epidermis (mean \pm SD, n=5).

Vehicle (v/v)	J ($\mu\text{g}/\text{cm}^2/\text{hr}$) \pm SD	K*h (cm) \pm SD	D/h ² (s) \pm SD	k _p (cm/s) \pm SD
100/0	83.1 \pm 9.23	1.74 $\times 10^{-2}$ \pm 7.10 $\times 10^{-3}$	6.95 $\times 10^{-5}$ \pm 3.68 $\times 10^{-5}$	1.03 $\times 10^{-6}$ \pm 8.37 $\times 10^{-8}$
50/50	64.5 \pm 15.16	4.22 $\times 10^{-3}$ \pm 2.66 $\times 10^{-3}$	6.46 $\times 10^{-5}$ \pm 3.02 $\times 10^{-5}$	2.04 $\times 10^{-7}$ \pm 5.03 $\times 10^{-8}$
0/100	93.6 \pm 19.11	1.30 $\times 10^{-3}$ \pm 8.95 $\times 10^{-4}$	1.56 $\times 10^{-4}$ \pm 8.41 $\times 10^{-5}$	5.57 $\times 10^{-7}$ \pm 8.22 $\times 10^{-7}$

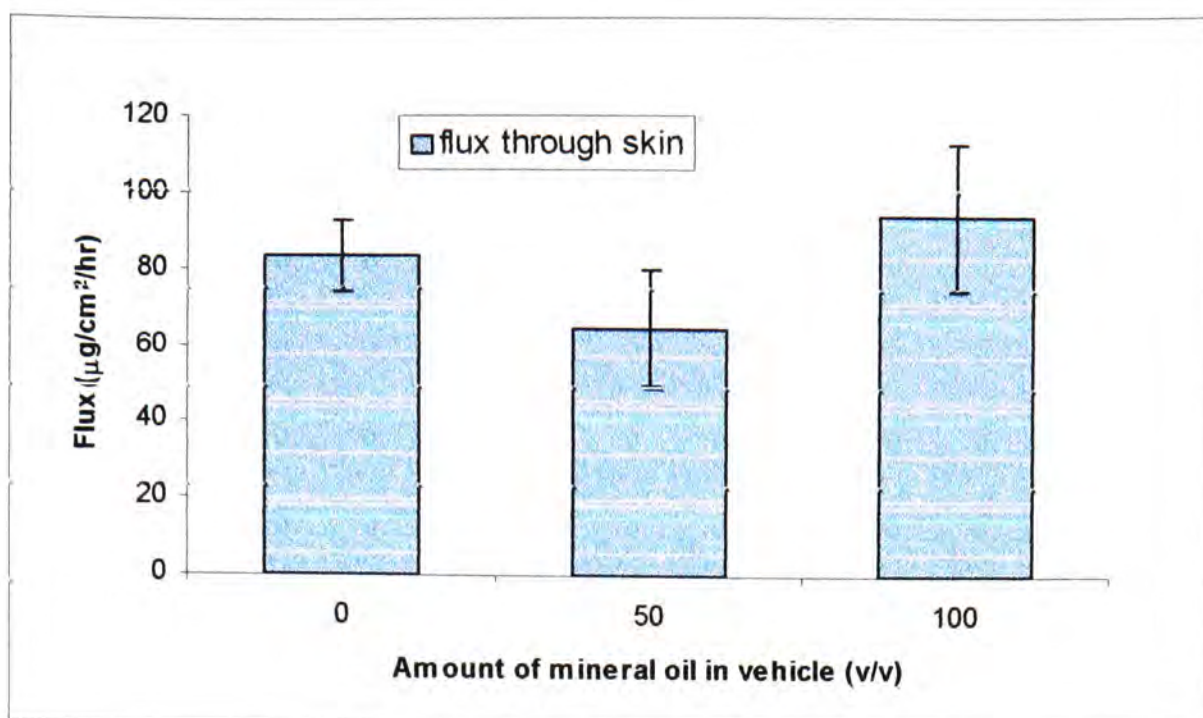


Figure 6.1. Steady-state flux values for the permeation of ibuprofen from saturated formulations containing mineral oil and miglyol.

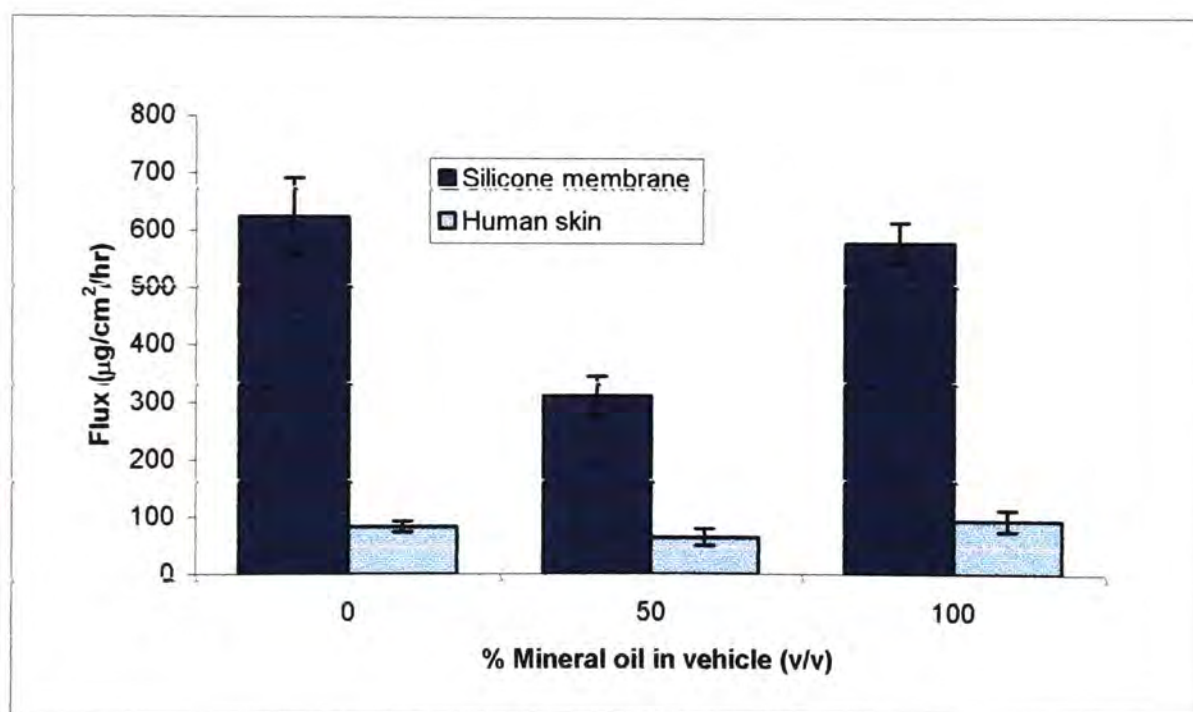


Figure 6.2. Comparison of the Steady-state flux values for the permeation of ibuprofen from saturated formulations containing mineral oil and miglyol, through silicone membrane and human skin.

There was no significant difference between the permeation rates of ibuprofen through human skin, from mineral oil and miglyol vehicles. The flux is however, very much lower than for the corresponding systems

through silicone membrane. This may be expected, since as stated in Chapter One, the skin presents a more challenging barrier to the passage of drugs than silicone membrane.

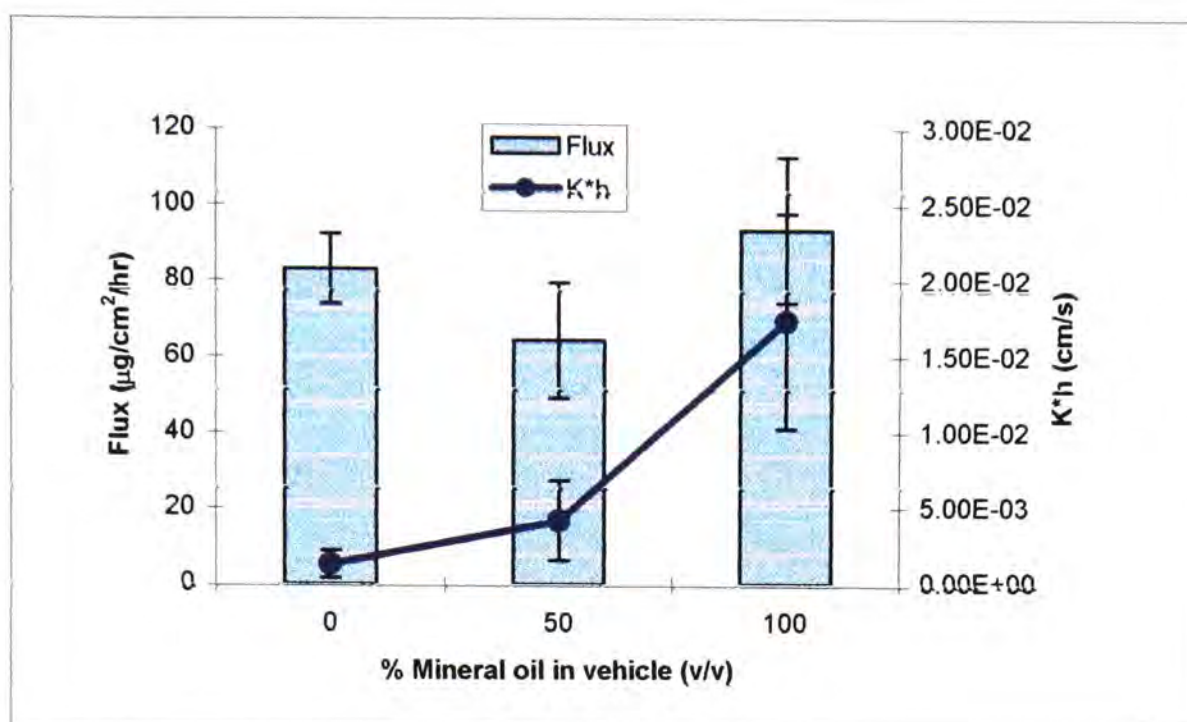


Figure 6.3. Steady state flux and K^*h values for the permeation of ibuprofen from saturated formulations containing mineral oil and miglyol.

The log K^*h values obtained from curve fitting show a decrease as the amount of mineral oil in the vehicle increases. This means that the skin-vehicle partition coefficient decreases between miglyol and mineral oil.

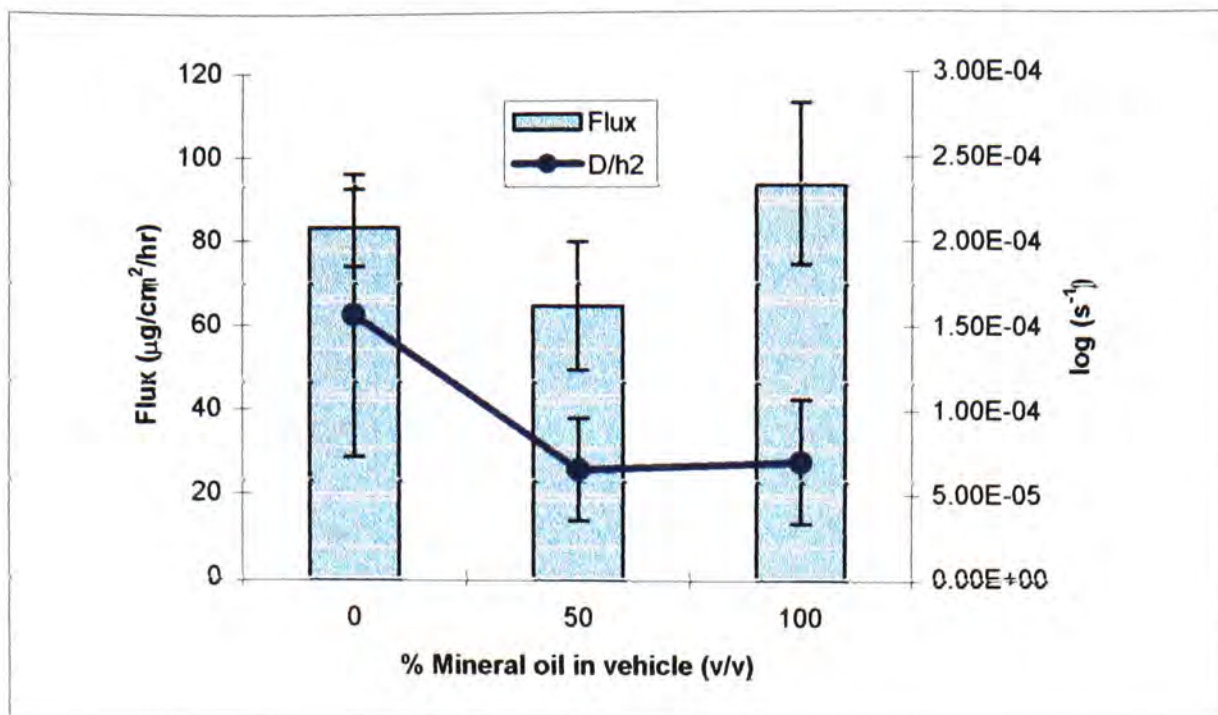


Figure 6.4. Steady state flux and D/h^2 values for the permeation of ibuprofen from saturated formulations containing mineral oil and miglyol.

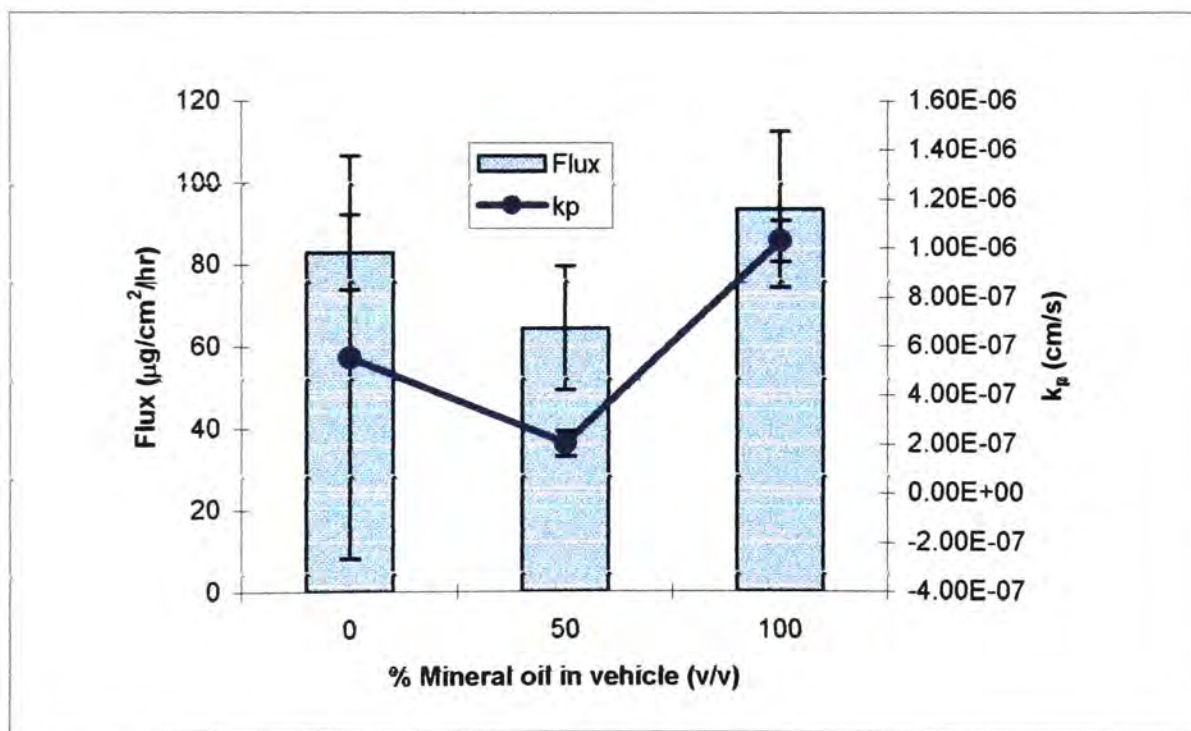


Figure 6.5. Steady state flux values and permeability coefficients for the permeation of ibuprofen from saturated formulations containing mineral oil and miglyol.

Along with the K^*h values obtained from the curve fitting experiments, the diffusion parameter also provides some information regarding the way in

which mineral oil acts as a vehicle. Figure 6.4 shows how the diffusion parameter increases slightly across the range from miglyol to mineral oil. This change in diffusion behaviour is unlikely to contribute greatly to the overall flux, as they are all of the same order of magnitude, and so it seems that mineral oil vehicles work by altering the partitioning behaviour of ibuprofen. This is most likely to be the result of increased solubility within the skin, though it is not a significant enough effect to significantly increase the flux between the formulations used.

6.4.2. Propylene glycol and water formulations

Table 6.2. Steady-state fluxes, thermodynamic and kinetic parameters, permeability coefficients for the permeation of ibuprofen from saturated formulations containing propylene glycol and water through human epidermis (mean \pm SD, n=5).

Vehicle (v/v)	J ($\mu\text{g}/\text{cm}^2/\text{hr}$) \pm SD	K*h (cm)	D/h ² (s)	k _p (cm/s)
0/100	24.4 \pm 2.69	0.79 \pm 0.50	2.14 \times 10 ⁻⁴ \pm 7.44 \times 10 ⁻⁵	2.32 \times 10 ⁻⁴ \pm 1.15 \times 10 ⁻⁴
25/75	35.5 \pm 9.77	0.46 \pm 0.26	1.92 \times 10 ⁻⁴ \pm 7.85 \times 10 ⁻⁵	7.33 \times 10 ⁻⁵ \pm 2.31 \times 10 ⁻⁵
50/50	99.1 \pm 22.77	0.28 \pm 0.17	1.05 \times 10 ⁻⁴ \pm 2.91 \times 10 ⁻⁵	2.66 \times 10 ⁻⁵ \pm 1.35 \times 10 ⁻⁵
100/0	133.8 \pm 36.11	1.01 \times 10 ⁻² \pm 1.65 \times 10 ⁻²	1.68 \times 10 ⁻⁴ \pm 1.01 \times 10 ⁻⁴	1.29 \times 10 ⁻⁷ \pm 1.18 \times 10 ⁻⁷

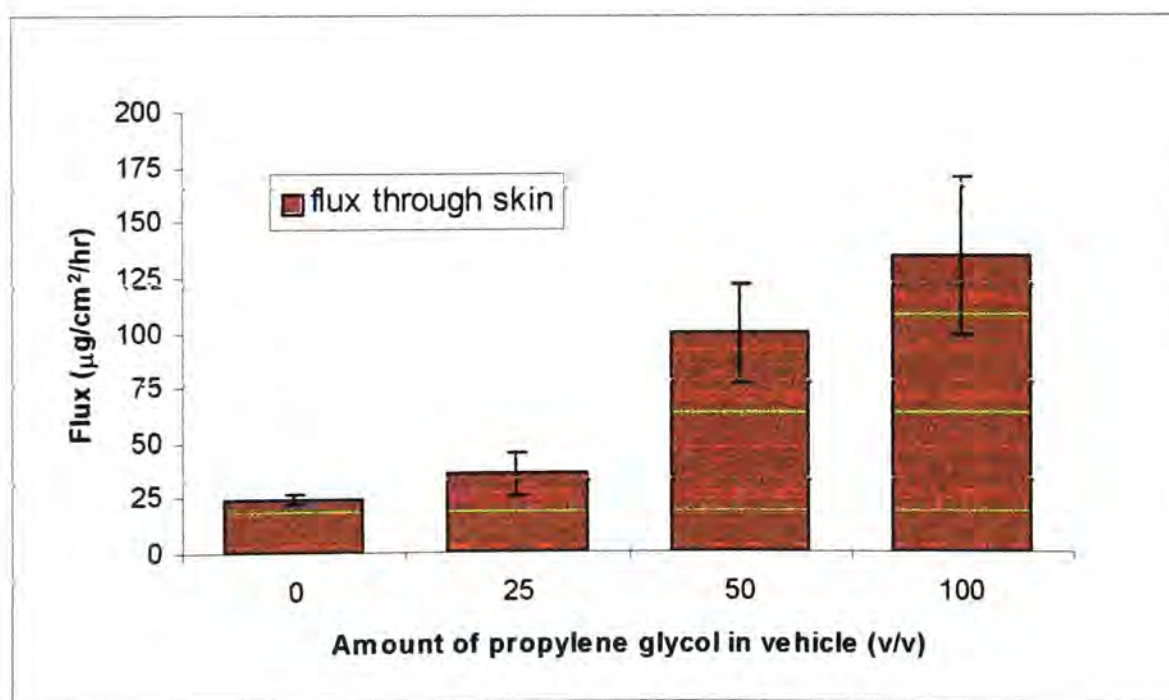


Figure 6.6. Steady-state flux values for the permeation of ibuprofen from saturated formulations containing propylene glycol and water.

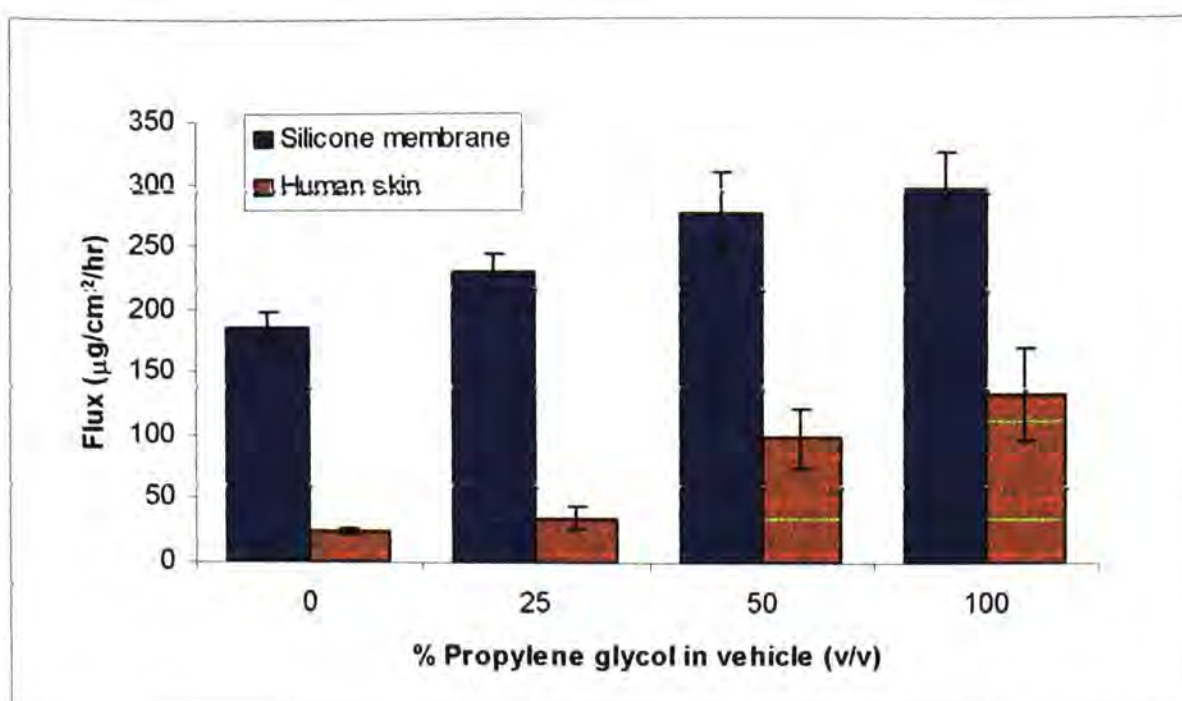


Figure 6.6. Comparison of the steady-state flux values for the permeation of ibuprofen from saturated formulations containing propylene glycol and water, through silicone membrane and human skin.

The flux values for ibuprofen permeating through human skin are again, considerably lower than for the corresponding formulations through silicone membrane. Unlike the formulations containing mineral oil and miglyol, there is a clear difference between the flux values for propylene glycol and water vehicles. As the amount of propylene glycol in the formulation increases, so does the permeation rate. The flux increase is particularly noticeable between 25-50% propylene glycol. This strongly suggests that propylene glycol, at higher concentrations is able to enhance the permeation of ibuprofen. There is no significant difference between the permeation rate of ibuprofen in a 50% formulation of propylene glycol and water, and pure propylene glycol.

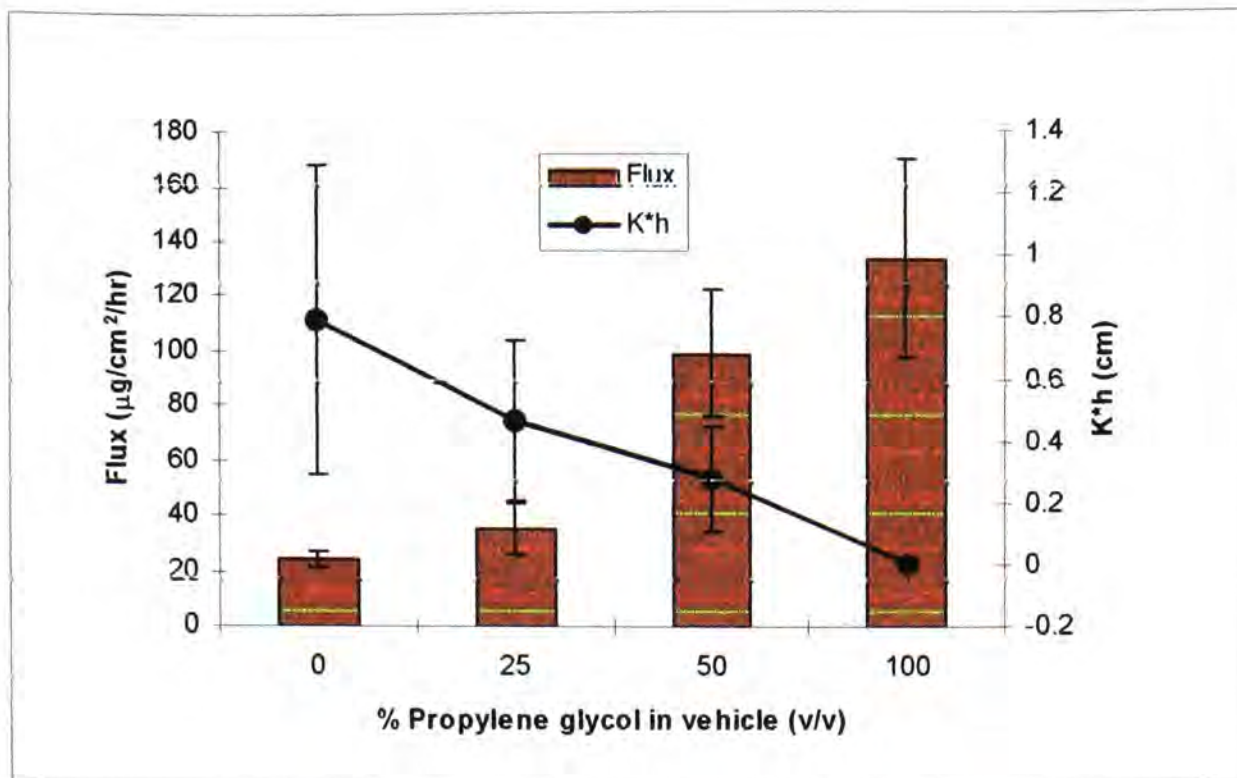


Figure 6.7. Steady state fluxes and K^*h values for the permeation of ibuprofen from saturated formulations containing propylene glycol and water.

There is not a significant difference in the partition parameters of formulation containing between 0-50% propylene glycol. There is a significant difference in partition parameter between 50% propylene glycol and the pure solvent. The data support previous experiments that suggest the action of propylene glycol is related to its diffusion into the membrane, altering the solubility of a permeant within that membrane, in this case, human skin.

The diffusional parameter does not alter significantly across the range of formulations used in the study. Both these findings imply that propylene glycol increases permeation by altering the partitioning behaviour of ibuprofen.

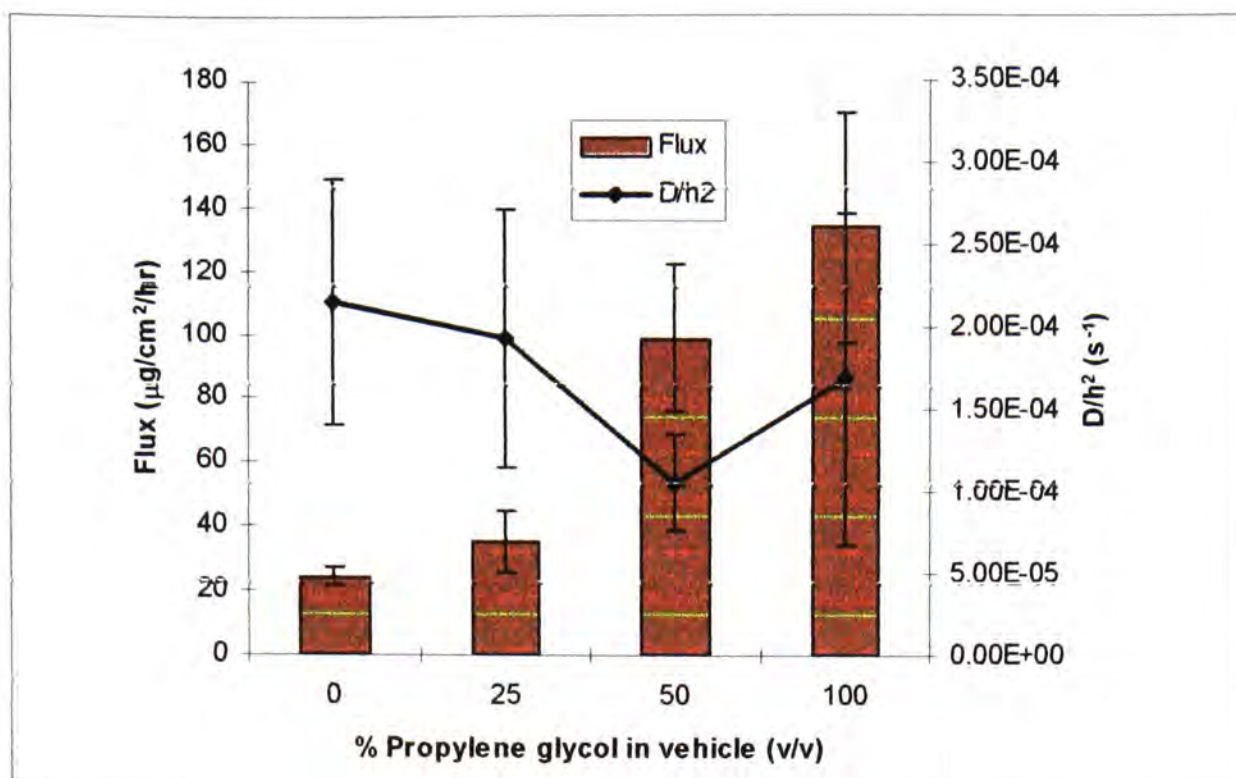


Figure 6.8. Steady state flux and D/h^2 vales for the permeation of ibuprofen from saturated formulations containing propylene glycol and water.

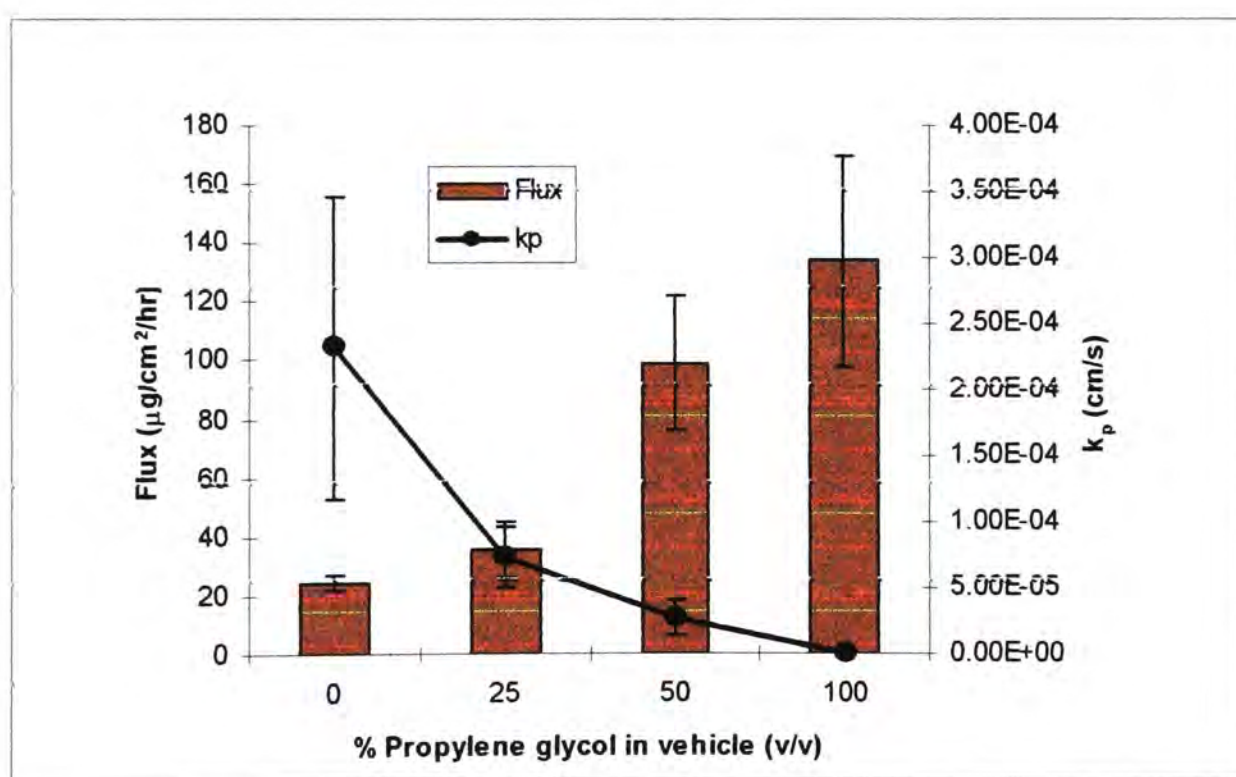


Figure 6.9. Steady state fluxes and permeability coefficients for the permeation of ibuprofen from saturated formulations containing propylene glycol and water.

The permeability coefficients for ibuprofen in propylene glycol and water formulations are statistically the same until the vehicle contains more than 50% propylene glycol. These data show a similar pattern to the K^*h values.

6.4.3. Ethanol and water formulations

Table 6.3. Steady-state fluxes, thermodynamic and kinetic parameters, permeability coefficients for the permeation of ibuprofen from saturated formulations containing ethanol and water through human epidermis (mean \pm SD, n=5).

Vehicle (v/v)	J ($\mu\text{g}/\text{cm}^2/\text{hr}$) \pm SD	K^*h (cm) \pm SD	D/h ² (s) \pm SD	k_p (cm/s) \pm SD
0/100	24.4 \pm 2.69	1.32 \pm 0.65	7.49 $\times 10^{-5}$ \pm 2.83 $\times 10^{-5}$	6.38 $\times 10^{-5}$ \pm 2.95 $\times 10^{-5}$
25/75	48 \pm 19.34	3.89 $\times 10^{-4}$ \pm 2.51 $\times 10^{-4}$	3.02 $\times 10^{-3}$ \pm 6.59 $\times 10^{-3}$	3.94 $\times 10^{-8}$ \pm 1.55 $\times 10^{-8}$
50/50	273.8 \pm 32.71	9.67 $\times 10^{-4}$ \pm 2.15 $\times 10^{-3}$	0.147 \pm 0.22	1.46 $\times 10^{-7}$ \pm 7.28 $\times 10^{-8}$
75/25	293.3 \pm 23.63	1.76 $\times 10^{-3}$ \pm 7.82 $\times 10^{-4}$	1.22 $\times 10^{-4}$ \pm 8.40 $\times 10^{-5}$	1.67 $\times 10^{-7}$ \pm 1.32 $\times 10^{-8}$
100/0	59.8 \pm 23.93	6.83 $\times 10^{-3}$ \pm 5.85 $\times 10^{-3}$	1.88 $\times 10^{-5}$ \pm 7.19 $\times 10^{-6}$	1.04 $\times 10^{-7}$ \pm 7.43 $\times 10^{-8}$

Figure 6.10 shows the steady-state flux values for the permeation of ibuprofen through human skin from formulations containing ethanol and water. The flux of ibuprofen from these vehicles is lower than for the same systems tested using silicone membrane.

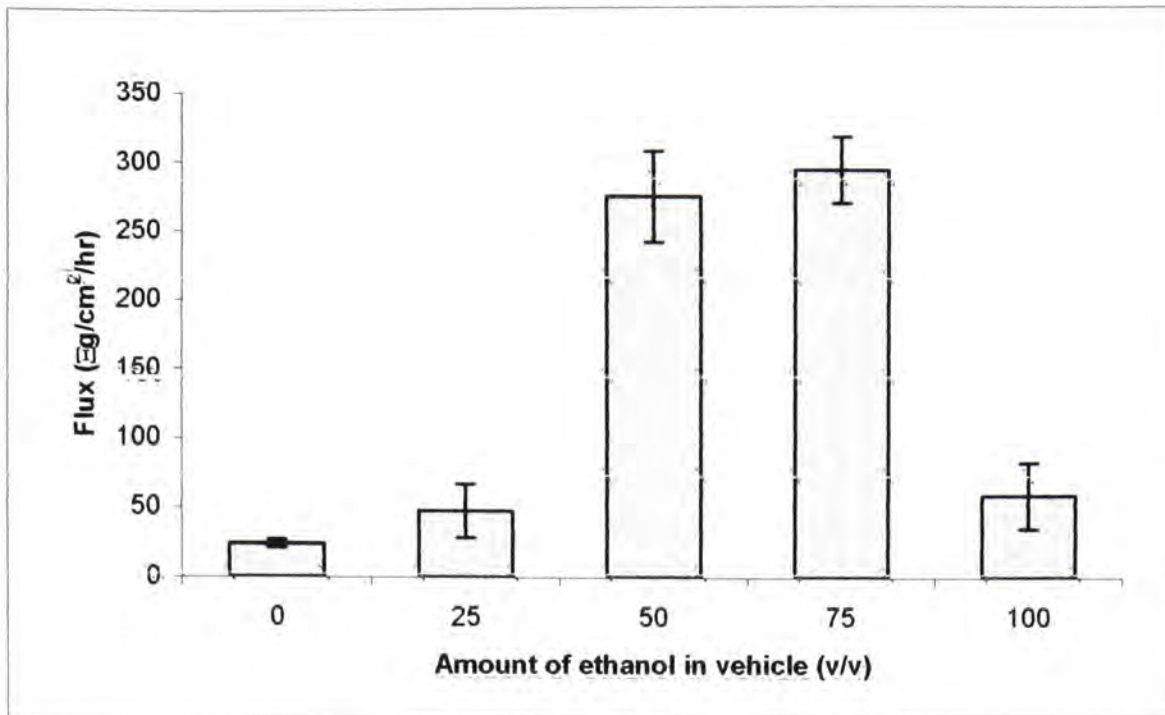


Figure 6.10. Steady-state flux values for the permeation of ibuprofen from saturated formulations containing ethanol and water.

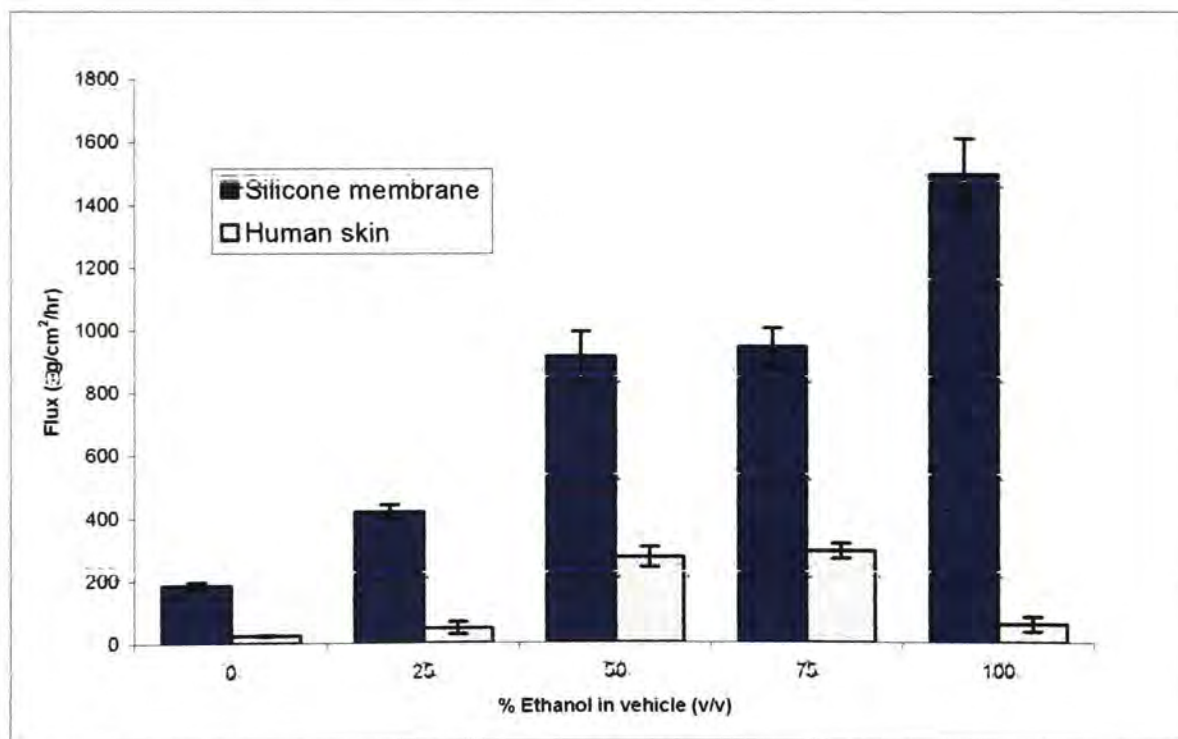


Figure 6.11. Comparison of the steady-state flux values for the permeation of ibuprofen from saturated formulations containing ethanol and water, through silicone membrane and human skin.

Figure 6.11 compares the flux through silicone membrane and human skin. The permeation rate displays a similar pattern to that seen for silicone

membrane permeation studies. The flux increases in a stepwise manner as the amount of ethanol in the formulation increases. The low flux value for a pure ethanol solution can be attributed to two possible events: evaporation of ethanol during the experiment, or dehydration of the stratum corneum. The evaporation left very little liquid in the donor chamber of the diffusion cell, causing the drug to crystallise out of solution, the large crystals which formed may have prevented permeation occurring, leading to significantly lowered flux.

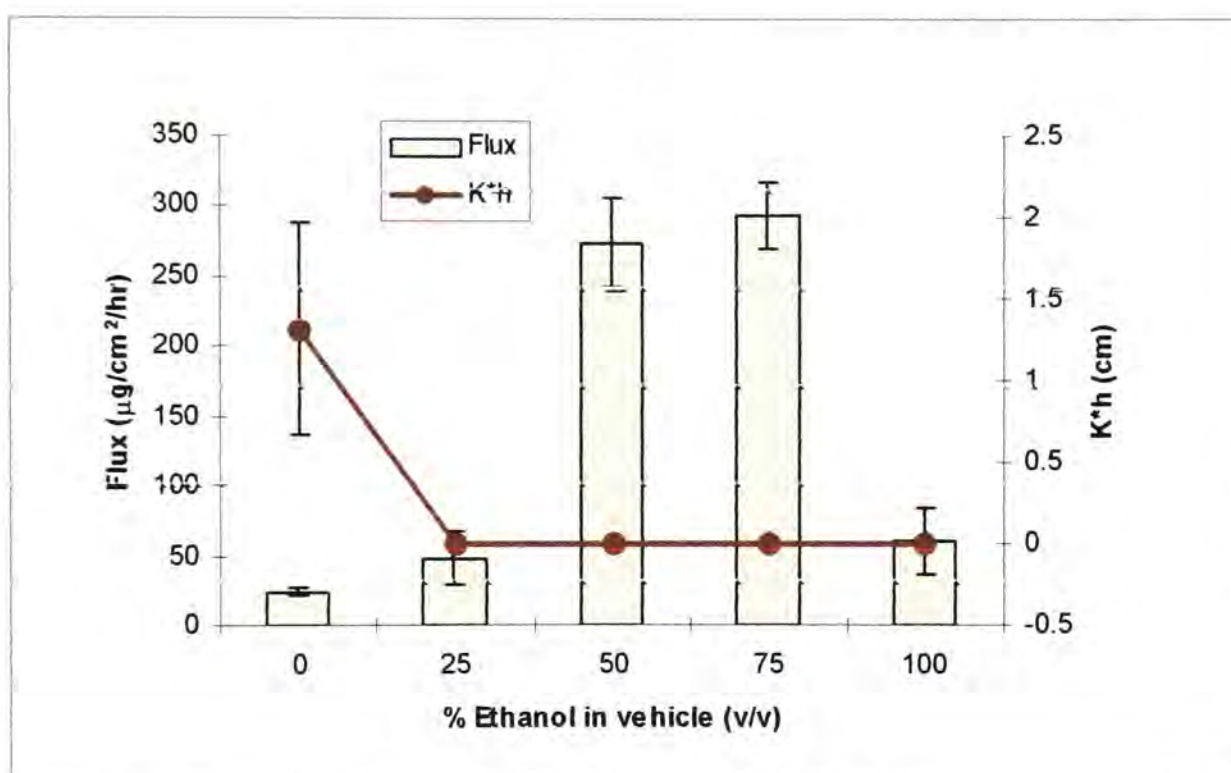


Figure 6.12. Steady state fluxes and K^*h values for the permeation of ibuprofen from saturated formulations containing ethanol and water.

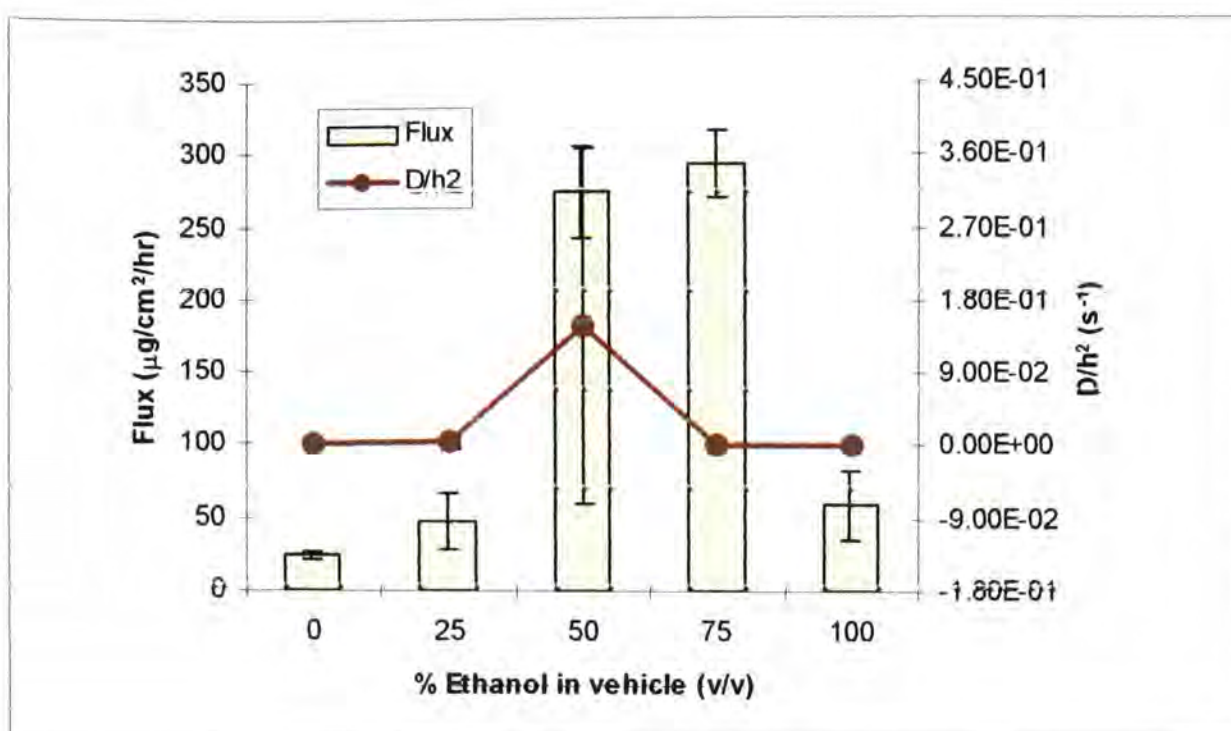


Figure 6.13. Steady state flux and D/h^2 values for the permeation of ibuprofen from saturated formulations containing ethanol and water.

There is no difference in the partition parameters between 25% and 100% ethanol. There is a significant difference between the pure water formulation and the next in the series which contains 25% ethanol. This does suggest that ethanol alters the way in which ibuprofen partitions into skin, increasing the flux. For this experiment, using human skin the effect is not as dramatic as that seen for the corresponding system tested using silicone as a membrane. This could be a result of the inherent complexity of skin as a membrane and serves to demonstrate why it is important to conduct preliminary experiments using silicone membrane. This sort of thermodynamic effect is easier to investigate, mechanistically when a simple membrane is used as a model. Diffusion parameters for ethanol and water formulations do not vary, suggesting that the diffusional parameter does not play a significant part in the enhancement of permeation.

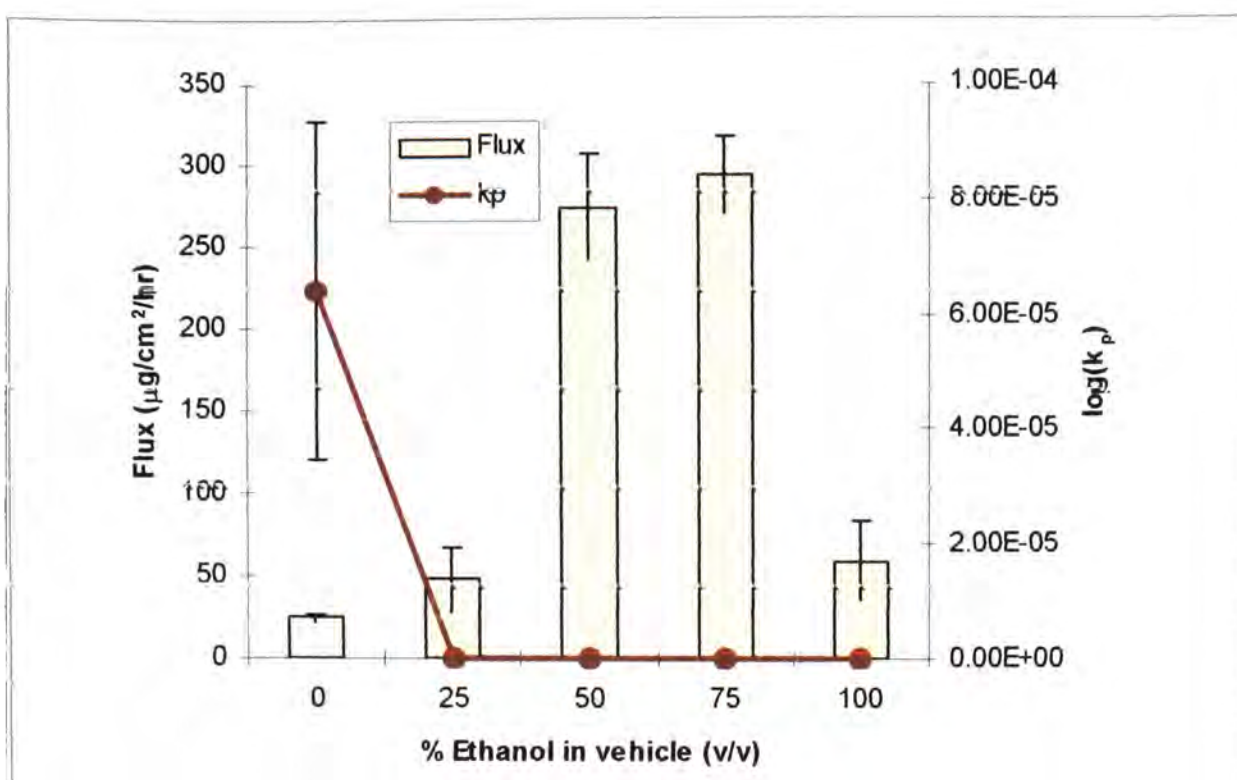


Figure 6.14. Steady state fluxes and permeability coefficients for the permeation of ibuprofen from saturated formulations containing ethanol and water.

6.4.4. Ternary solvent formulations

Table 6.4. Steady state fluxes, thermodynamic and kinetic parameters, permeability coefficients for the permeation of ibuprofen from saturated formulations containing ethanol, propylene glycol and water through human epidermis (mean \pm SD, $n=5$).

Vehicle (v/v)	J ($\mu\text{g}/\text{cm}^2/\text{hr}$) \pm SD	K*h (cm) \pm SD	D/h ² (s) \pm SD	k _p (cm/s) \pm SD
25/25/50	77.6 \pm 9.04	8.73 $\times 10^{-4}$ \pm 1.01 $\times 10^{-3}$	4.65 $\times 10^{-2}$ \pm 0.10	3.28 $\times 10^{-7}$ \pm 2.73 $\times 10^{-7}$
50/25/25	203.5 \pm 36.24	2.79 $\times 10^{-3}$ \pm 2.95 $\times 10^{-4}$	4.71 $\times 10^{-5}$ \pm 3.59 $\times 10^{-5}$	1.97 $\times 10^{-7}$ \pm 3.44 $\times 10^{-8}$

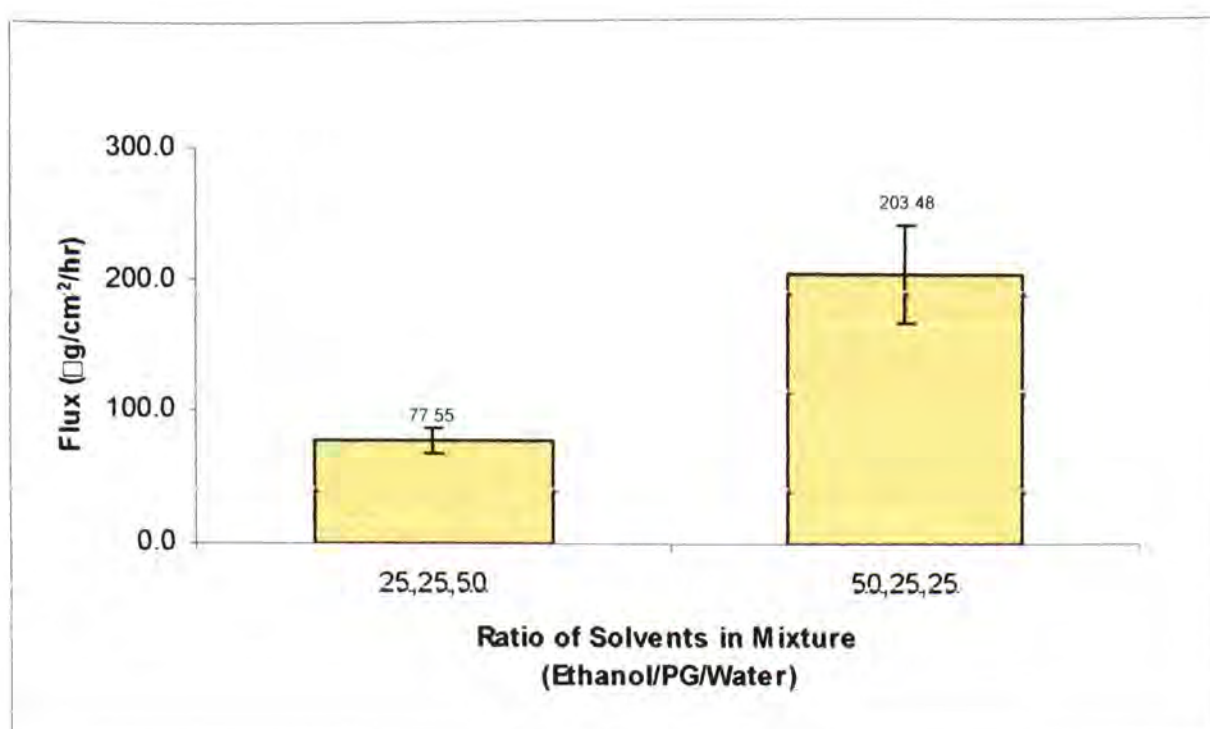


Figure 6.15. Steady-state flux values for the permeation of ibuprofen in ternary vehicles containing ethanol, propylene glycol and water.

Figure 6.15 shows the results of permeation studies using ternary solvent formulations. The flux was highest for the formulations containing more ethanol. Increasing the proportion of ethanol in the vehicle brings about a 2-fold improvement in the flux. This improvement in flux is more than that seen for permeation studies using silicone membrane. This could be because of the different interactions that ethanol would have with skin, compared with those in silicone membrane. Ethanol is known to extract skin lipids (Bommannan et al. 1991), and this effect if it occurred in vitro would improve the flux. In-vivo this extraction of lipids is offset by the skin having its own defences - it recognises that its barrier function has been compromised and in response produces more lipids in an attempt to restore its barrier. The steady state flux of ethanol through human skin has been measured to be approximately $1\text{mg}/\text{cm}^2/\text{hr}$ (Friend and Heller, 1993; Berner et al, 1989). In a formulation with a small amount of ethanol this rapid flux may be offset by the slower flux of the other components,

however, in the formulation containing 50% ethanol this would have a dramatic effect upon the flux, as seen in figure 6.15.

The flux is lower than for the silicone membrane studies, which follows a general trend seen for all the formulations investigated in this Chapter.

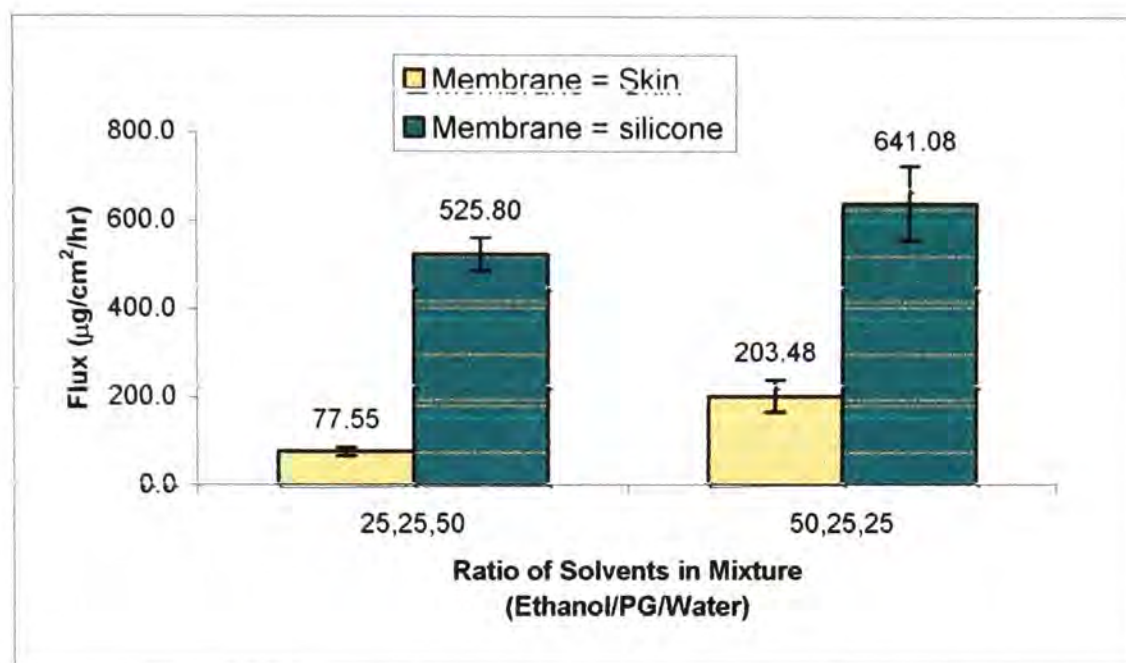


Figure 6.15. Comparison of the steady-state flux values for the permeation of ibuprofen in ternary vehicles containing ethanol, propylene glycol and water through silicone membrane and human skin.

There is no significant difference between $K \cdot h$ values for the two systems, suggesting that the partitioning behaviour of ibuprofen in the two formulations is the same.

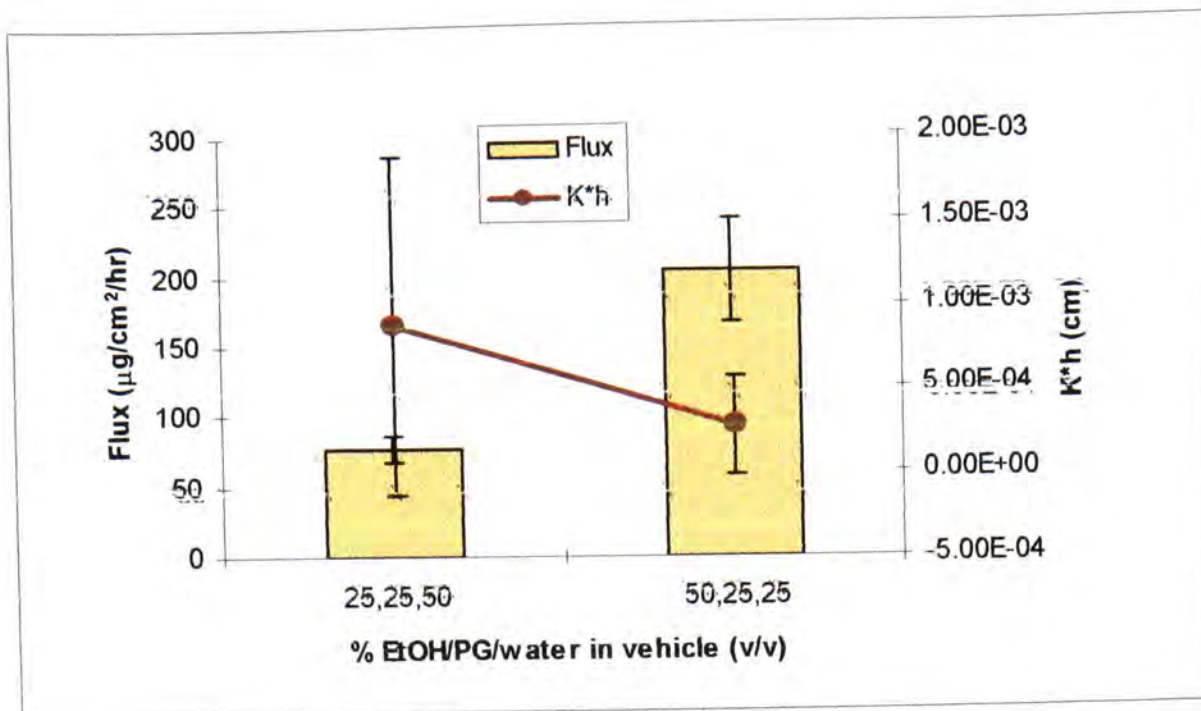


Figure 6.17. Steady state fluxes and $K \cdot h$ values for the permeation of ibuprofen from saturated formulations containing ethanol, propylene glycol and water.

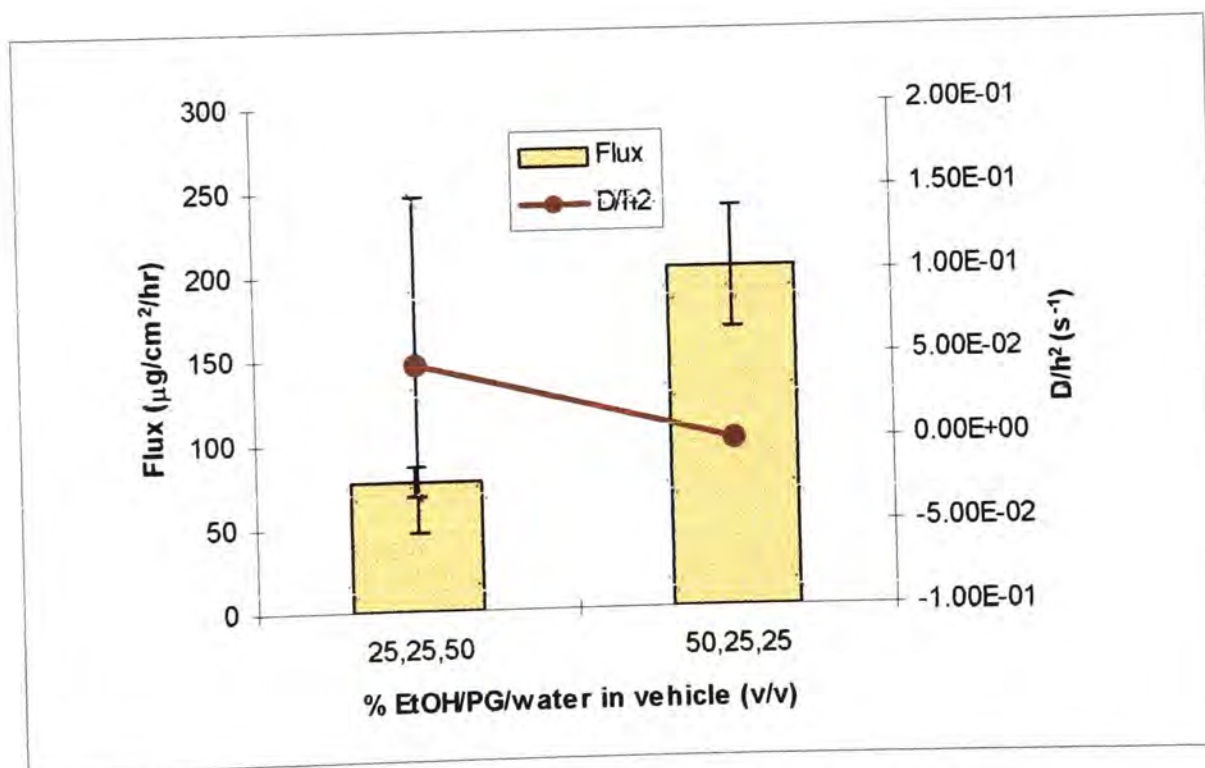


Figure 6.18. Steady state flux and D/h^2 values for the permeation of ibuprofen from saturated formulations containing ethanol, propylene glycol and water.

In terms of the diffusion coefficients, once again there is no significant difference between the two formulations.

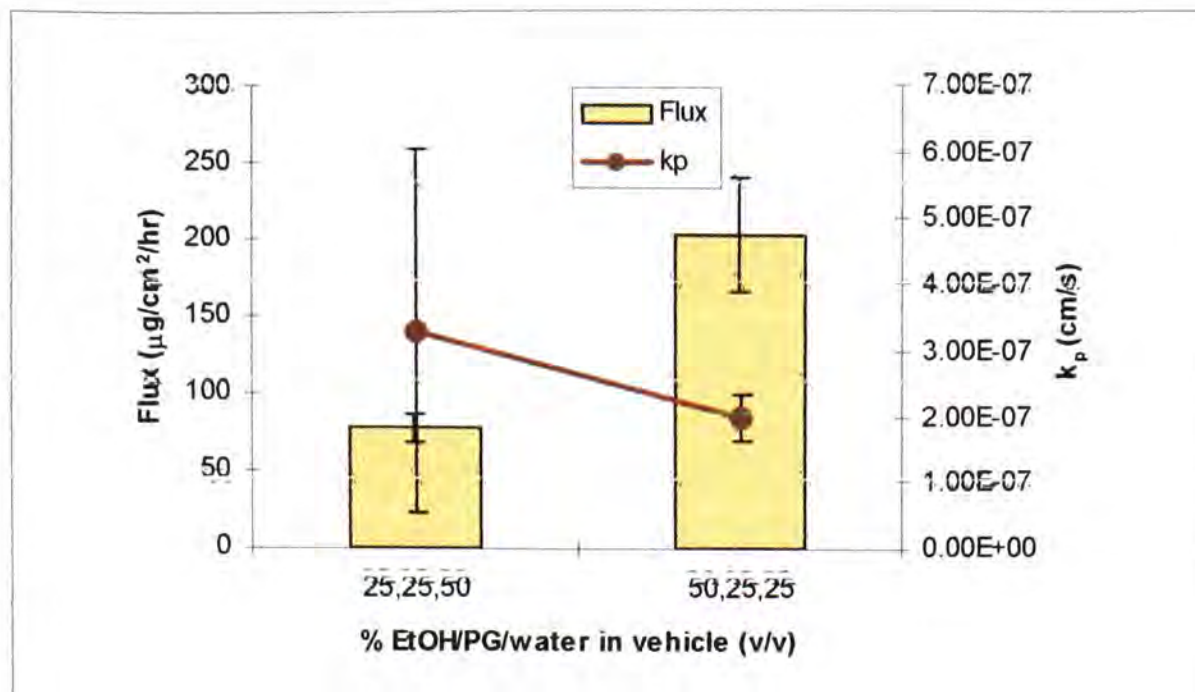


Figure 6.19. Steady state fluxes and permeability coefficients for the permeation of ibuprofen from saturated formulations containing ethanol, propylene glycol and water.

As with the other parameters obtained from curve fitting, there is no difference in the permeability coefficients when more Transcutol is added to the formulation. It should be stated that there is large error associated with all the parameters obtained from fitting the diffusion curves of the formulation composed of 25% Transcutol. This is most likely a result of the variability of skin samples used in the study (which came from different subjects and regions of the body) and does not mean that there is no alteration in any of the parameters. More experiments are needed, with skin samples from the same site and subject, to thoroughly investigate the mechanism of enhancement, as there is clearly an effect upon flux if the amount of Transcutol is increased.

6.5. Conclusions

The studies described in this Chapter have demonstrated that the permeation of ibuprofen can be enhanced by the vehicles chosen. Mineral oil and miglyol formulations were investigated because of the high flux values seen in the silicone membrane permeation studies. However, these solvents proved somewhat disappointing when using human skin with permeation rates being amongst the lowest of all the formulations investigated. For this reason, no ternary solvent formulations were tested using lipophilic vehicles. For hydrophilic vehicles the results were much better. For propylene glycol and water formulations the flux values were lower than those for the corresponding formulations tested using silicone membrane, but the flux did increase as the amount of propylene glycol in the vehicle increased. This is similar to the effect seen in silicone membrane studies and suggests that this effect could be manipulated to develop a good vehicle for ibuprofen permeation.

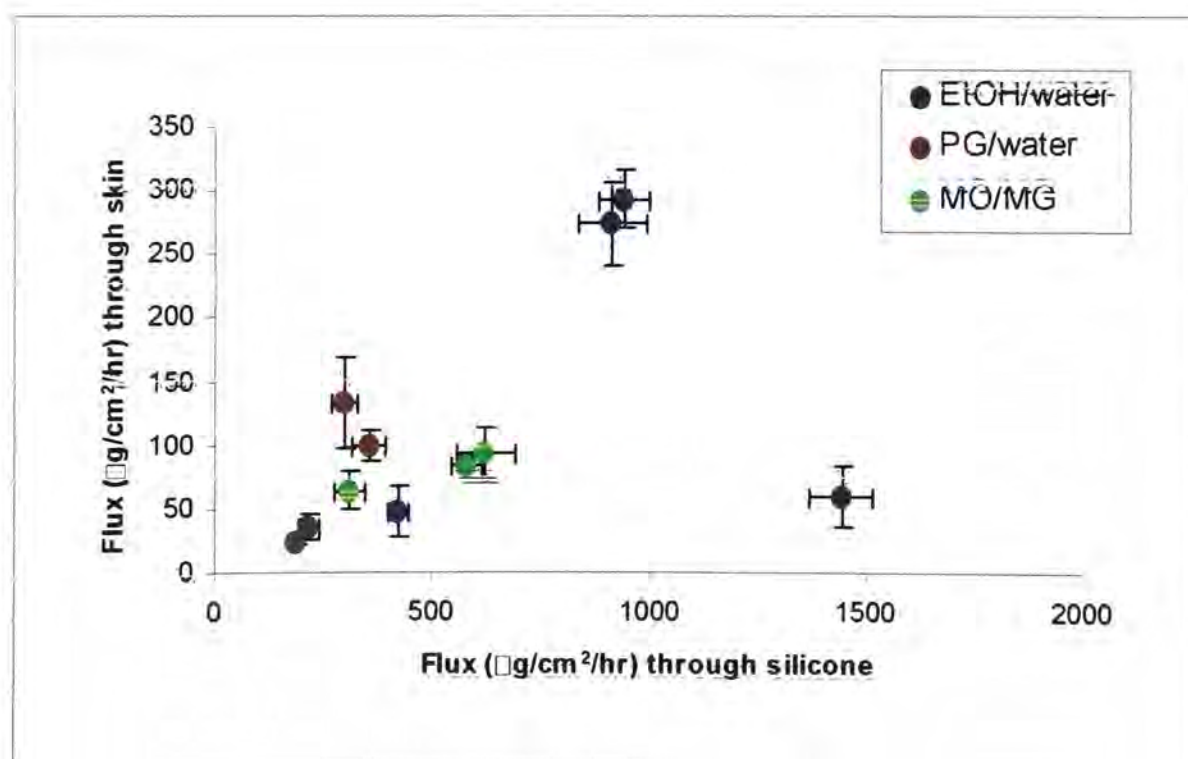


Figure 6.20. Relationship between flux through silicone membrane and flux through human skin.

Figure 6.20 shows the relationship between flux through silicone and through human skin. There are too few data points to conclude that there is a correlation between the two in vitro methods. The data demonstrate why silicone membrane studies should serve only as a guide to formulation design as there will always be interactions with the skin that cannot be accounted for. Ethanol and water formulations had the highest flux values, and this could be attributed to the way in which ethanol interacts with the skin. This is different to the way in which a solvent such as propylene glycol interacts. Propylene glycol improves flux by increasing the solubility of the permeant in the membrane. Ethanol has been shown to extract skin lipids, assisting permeation by removing the very lipophilic channel along which drug molecules permeate. The reason that this effect is not as pronounced as expected (D/h^2 values not greatly affected) could be a result of the lipophilicity of ibuprofen. If a more hydrophilic permeant had been used for this study (such as acetaminophen, $\log P = 0.46$) a greater degree of enhancement may have been seen, and reflected in a marked variation in D/h^2 values. An improvement in flux was seen for the ternary solvent formulations. Compared with water, these systems showed a 3-fold and 8-fold increase respectively (25/25/50 and 50/25/25 EtOH/PG/water).

Although all the vehicles in this study affected both diffusion and partition, it seems that partitioning of the drug in the skin is generally dominant. The caveat is that to test this it is important to also investigate vehicles that are *known* to alter the diffusion coefficient. In this study of the permeation of ibuprofen through human skin, only a select group of vehicles were tested for very specific reasons. What should also be remembered is that each vehicle used in an investigation may affect different permeants in an entirely different manner.

6.6. References

B. Berner G. C. Mazzenga, J. H. Otte, R. J. Steffens, R-H. Juang and C. D. Ebert. Ethanol: water mutually enhanced transdermal therapeutic system II: skin permeation of ethanol and nitroglycerin. *J. Pharm. Sci.* 78, 402-407 (1989).

D. Bommannan, R. O. Potts and R. H. Guy. Examination of the effect of ethanol on human stratum corneum in vivo using infrared spectroscopy. *J. Control. Release.* **16**, 299-304 (1991).

T. J. Franz. Percutaneous absorption: on the relevance of in vitro data. *J. Invest. Derm.* **64**, 190-195 (1975).

D. R. Friend and J. Heller. Simple alkyl esters as skin penetration enhancers. In: *Pharmaceutical skin penetration enhancement*. Eds. K. A. Walters and J. Hadgraft. Marcel Dekker Inc. New York. pp31-56 (1993).

- Chapter Seven -
General Discussion

7.1. General Discussion

The emphasis of the research described in this thesis has been placed on the influence of the physical and chemical properties of both the drug and the vehicle upon permeation.

NSAIDs cover many different classes of chemicals, as shown in Chapter Two, each having distinct reactions, functionalities and therefore physicochemical properties. Chapter one introduced the factors affecting permeation, with particular emphasis based upon solubility, logP and molecular size. Ibuprofen, salicylic acid and acetaminophen were selected as model drugs for the following reasons:

- All are available OTC in Europe
- Topical formulations of ibuprofen and salicylic acid are already available on the market as General Sales List medicines

The model permeants selected spanned a range of properties in an attempt to ascertain how their physicochemical properties would affect their permeation behaviour. Each drug belonged to a different class of NSAID, and as such each had slight differences in functionality. Two of the drugs; salicylic acid and ibuprofen have been successfully used in topical preparations, suggesting that they are well tolerated and have suitable characteristics for topical formulations.

It was anticipated that ibuprofen and salicylic acid could present a challenge because they are weak acids and therefore ionisation would need to be accounted for. To this end studies were conducted to characterise their ionisation behaviour, so that this could be considered when interpreting the results of diffusion experiments. These studies demonstrate that the presence of a cosolvent (in this case methanol or

ethanol) greatly modifies the dissociation of a weak acid at a given pH. This finding has implications for formulations containing propylene glycol, which is often added as a cosolvent to improve solubility of poorly soluble drugs. Though it was not possible to explore the effect of adding propylene glycol, assumptions could be made based upon the findings for the solvents methanol and ethanol.

The studies detailed in Chapter Two also demonstrate that seemingly simple systems always have a degree of complexity that has not been accounted for. A good example of this is the behaviour of acetaminophen in certain cosolvent systems. In hydrogen bonding solvents acetaminophen rapidly oxidises to p-aminophenol, a reaction that is well documented in literature. The instability of acetaminophen meant that it was a difficult substance to work with, and even simple tasks such as solubility studies were made difficult. To avoid the diversion required to explore fully this phenomenon, acetaminophen was excluded from the project at an early stage.

The next stage of the project was to determine which physicochemical properties would affect permeation in the solvents selected. Synthetic PDMS membranes were used because they offer a uniform, hydrophobic barrier to diffusion and data analysis is straightforward. The use of synthetic membranes also avoids the inherent variability associated with biological membranes.

Transport studies through PDMS membranes were useful in understanding the underlying physicochemical factors that control the diffusion process. These studies confirmed that ethanol, Transcutol and propylene glycol work as enhancers by improving the solubility of the drug within the

membrane. For single solvent formulations, the flux of ibuprofen was higher than salicylic acid. The only exceptions were Transcutol, for which both drugs had the same permeation rate, and ethanol, in which salicylic acid had higher flux. Flux values were higher for formulations containing ethanol than for corresponding formulations containing Transcutol or propylene glycol.

The data for ibuprofen and salicylic acid showed similarities which may suggest an interaction between the formulation and the membrane. Data from ATR-FTIR diffusion experiments went one step further and allowed the monitoring of the changes in the silicone membrane during the course of an experiment. ATR-FTIR data showed that both ethanol and Transcutol reduce the signal of the membrane, indicative of an interaction between the solvents and membrane. Ethanol was also shown to permeate at a faster rate than either propylene glycol or Transcutol, and this rapid permeation may account for the significantly higher flux values from this solvent compared with the others used in the study.

Ibuprofen showed the most promising results from diffusion experiments therefore this was the drug selected for studies using ternary vehicles, and for experiments using human skin.

Two types of ternary formulation were investigated: ethanol/propylene glycol/water and Transcutol/propylene glycol/water. The flux was 2.4 times higher for systems containing ethanol, which corresponds to the data from binary solvent formulations. Again, data from the ATR-FTIR diffusion experiments suggest that this improvement in flux is a result of an interaction between the vehicle and the membrane. For formulations

containing ethanol it is likely to be ethanol, rather than propylene glycol affecting the membrane.

Chapter Six details diffusion experiments using human skin. These studies demonstrated that the permeation of ibuprofen can be enhanced by the vehicles chosen. Mineral oil and miglyol formulations were investigated because of the high flux values seen in the silicone membrane permeation studies. However, these solvents proved somewhat disappointing when using human skin with permeation rates being amongst the lowest of all the formulations investigated. For this reason, no ternary solvent formulations were tested using lipophilic vehicles.

For hydrophilic vehicles the results were much better. For propylene glycol and water formulations the flux values were lower than those for the corresponding formulations tested using silicone membrane, but the flux did increase as the amount of propylene glycol in the vehicle increased. This is similar to the effect seen in silicone membrane studies and suggests that this effect could be manipulated to develop a good vehicle for ibuprofen permeation.

Ethanol and water formulations had the highest flux values, and perhaps this could be attributed to the way in which ethanol interacts with the skin. This is different to the way in which a solvent such as propylene glycol interacts. Propylene glycol improves flux by increasing the solubility of the permeant in the membrane. Ethanol has been shown to extract skin lipids, assisting permeation by removing the very lipophilic channel along which drug molecules permeate. The reason that this effect is not as pronounced as expected (D/h^2 values not greatly affected) could be a result of the lipophilicity of ibuprofen. If a more hydrophilic had been used for this study

(such as acetaminophen, $\log P = 0.46$) a greater degree of enhancement may have been seen, and reflected in a marked variation in D/h^2 values.

An improvement in flux was seen for the ternary solvent formulations. Compared with water, these systems showed a 3-fold and 8-fold increase respectively (25/25/50 and 50/25/25 EtOH/PG/water).

Although all the vehicles in this study have affected both diffusion and partition, it seems that partitioning of the drug in the skin is generally dominant. The caveat is that to test this rigorously it is important to also investigate vehicles that are *known* to alter the diffusion coefficient. In this study of the permeation of ibuprofen through human skin, only a select group of vehicles were tested, and those selected acted in a similar manner. To address this, it would be useful to investigate formulations which contain enhancers that act in different ways i.e. one which acts upon diffusion, one which acts upon partition, and perhaps a third co-solvent. Systems of this type would also allow a further exploration of the effects these solvents have upon membranes, particularly now that a technique is available that allows the membrane to be monitored.

7.2. Future Work

The factors which are most likely to influence the permeation rate are as follows:

- (a) Interactions between the drug and the components of the formulation
- (b) Interactions between the drug and the skin
- (c) Interaction between the skin and components of the formulation

In the work described in this thesis (a) has been kept constant by using saturated solutions, thereby the thermodynamic activity of the drug was maximised. (b) was not fully explored, and so the main focus of this work has been factor (c). To this end, there is a great deal of scope for further work using the drugs in this study, or for introducing a greater variety of drugs, with a wider range of physicochemical properties. As stated at the beginning of this chapter, there are numerous classes of NSAIDs, each with different properties, which provide a wealth of opportunities. A technique which could provide useful information regarding the interactions between the drugs and solvents would be molecular modelling. This is another area of research that has become increasingly sophisticated, mainly because of advances made in the hardware required to run modelling software.

Chapter Five contains the results of transport experiments using ATR-FTIR combined with chemometric analysis. This is a very new area of research, and as such presents many avenues that have yet to be explored. Further work in this area would be to run ATR-FTIR diffusion experiments using vehicles without any drug, and investigate their permeation behaviour. It may also be useful to conduct analysis in the more traditional way, by selecting certain absorbances and monitoring any shifts in the spectrum of

individual components, using chemometrics to track any changes. Another possibility is to calibrate the ATR-FTIR in order to allow quantitative as well as qualitative research to be conducted. This would also open up the possibility of measuring the flux of each component in a formulation using a simple, non-invasive technique.

There also needs to be considerable research in the way in which references for chemometric analysis are obtained and used. For the work outlined in this chapter, a single ATR-FTIR spectrum of the single component was used as a reference. This may not be the best approach to use, as it may be better to have references that are closer to the conditions of the experiment being carried out. What is meant by this is that a solid phase spectrum of the drug may not relate to the spectrum of a drug in solution, indeed in the formulation being tested. There will be all manner of interactions between the formulation components, so there is a need for a detailed examination of what constitutes a good reference state for these type of experiments. A chemometric approach to the analysis of data from ATR-FTIR diffusion experiments opens up many new avenues of research for the study of permeation of drugs across both silicone membrane and human skin, and in time it is possible that the mystery of penetration enhancers will be unlocked.

Appendix I

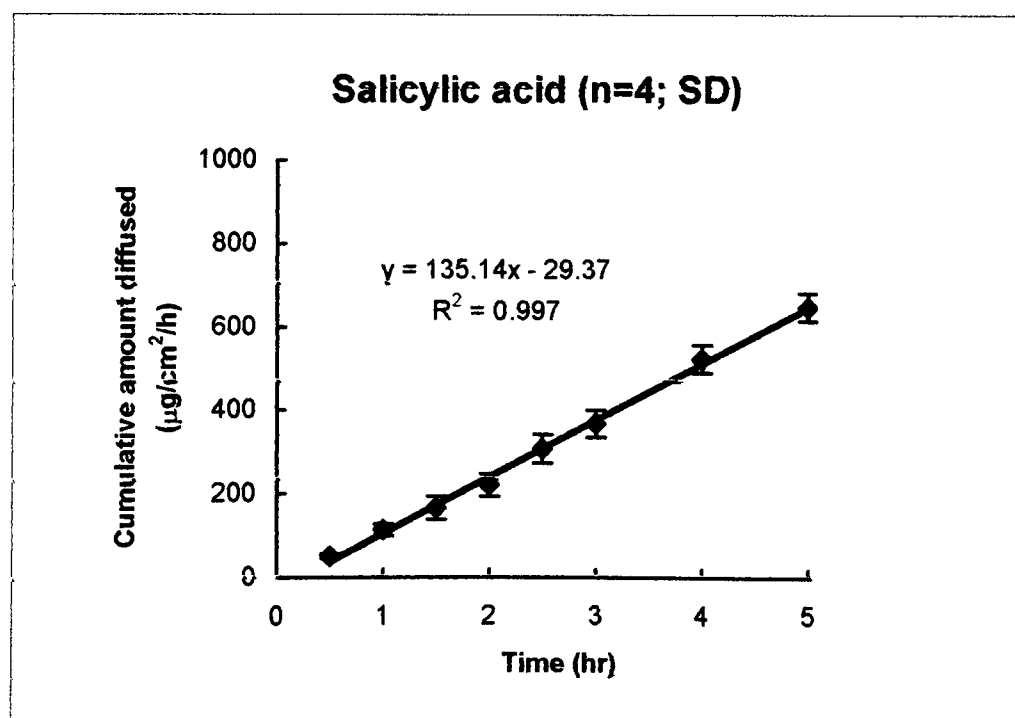
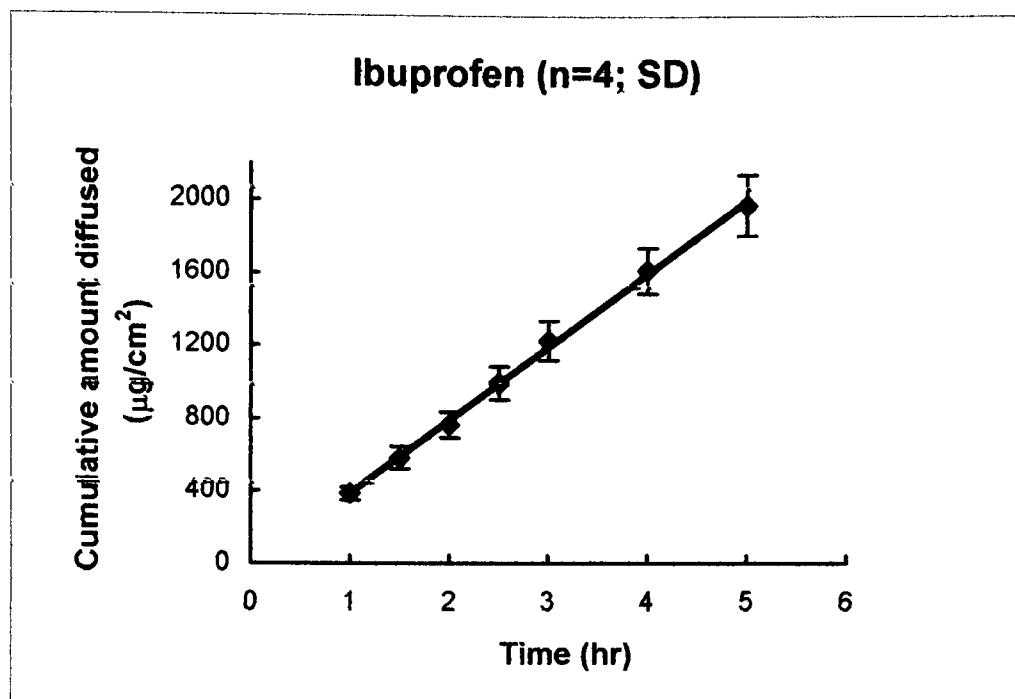
Recipe for Phosphate Buffered Saline, pH 7.4

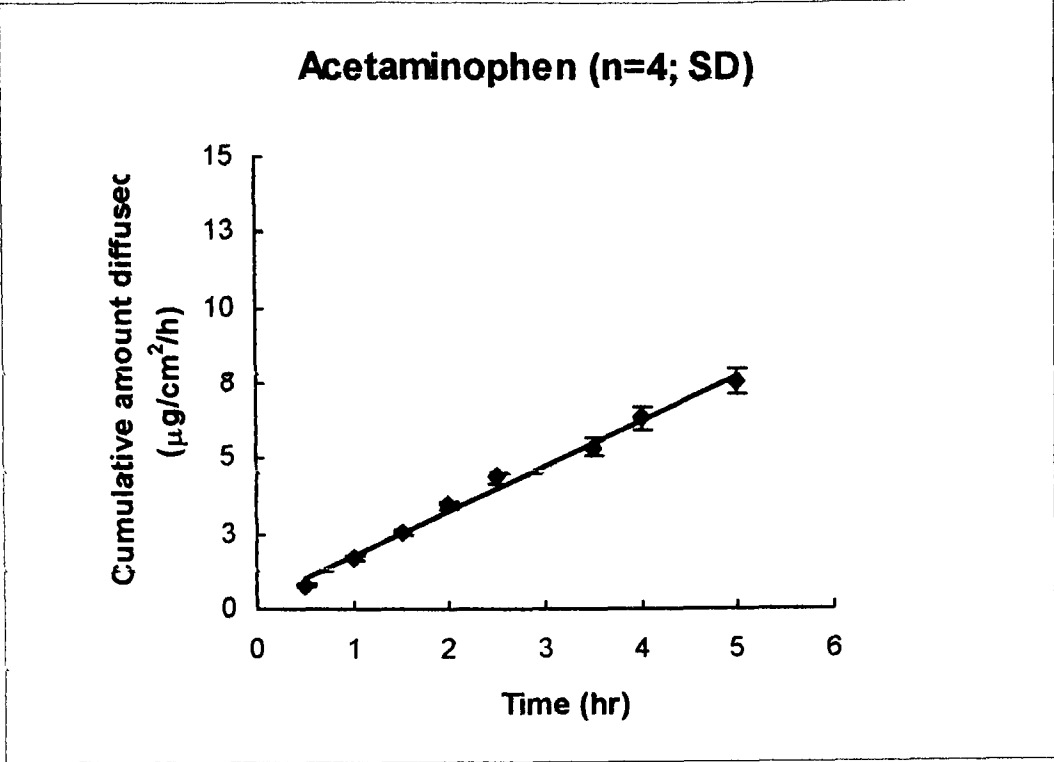
Sodium acid phosphate (NaH_2PO_4) -	2.1g/L
Sodium Chloride (NaCl) -	4.4g/L
Sodium Phosphate (Na_2HPO_4) -	9.2g/L

Appendix II

Diffusion profiles

Linearity of diffusion profiles obtained during this study, a few examples.



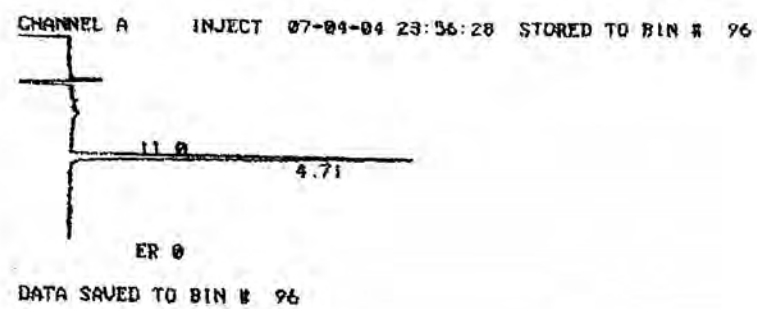


Appendix III

Chromatograms

The following chromatograms were obtained from samples of the receptor solution during the skin diffusion studies.

Ibuprofen

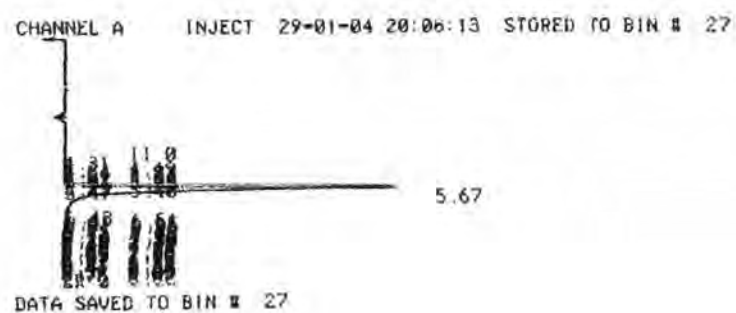


INPUT OVERRANGE AT RT= 0.01

IBU 07-04-04 23:56:28 CH= "A" PS= 1.
FILE 1. METHOD 0. RUN 96 INDEX 96 BIN 96

PEAK#	AREA%	RT	AREA BC
1	100.	4.71	69901 01
TOTAL	100.		69901

Salicylic acid



SA 29-01-04 20:06:13 CH= "A" PS= 1.
FILE 1. METHOD 0. RUN 27 INDEX 27 BIN 27

PEAK#	AREA%	RT	AREA BC
1	100.	5.67	156901 09
TOTAL	100.		156901